Designer Transcription Activator Like Effector - Chromatin Affinity Purification (dTALE-ChAP)

a novel *in planta* method to unravel the protein coverage at a promoter of choice

Dissertation

der Mathematisch-Naturwissenschaftlichen Fakultät

der Eberhard Karls Universität Tübingen

zur Erlangung des Grades eines

Doktors der Naturwissenschaften

(Dr. rer. nat.)

vorgelegt von

Stefan Markus Fischer

aus Stuttgart

Tübingen

2018

Gedruckt mit Genehmigung der Mathematisch-Naturwissenschaftlichen Fakultät der Eberhard Karls Universität Tübingen.

Tag der mündlichen Qualifikation:	25.10.2018
Dekan:	Prof. Dr. Wolfgang Rosenstiel
1. Berichterstatter:	Prof. Dr. Klaus Harter
2. Berichterstatter:	Prof. Dr. Thomas Lahaye

1. Table of Content

ABBREVATION LIST **8**

SUMMARY **10**

ZUSAMMENFASSUNG **11**

2. INTRODUCTION **12**

2.1. CHROMATIN 12

2.1.1. Transcriptional Initiation at a Core Promoter *14*

2.2. PAMP TRIGGERED IMMUNITY 15

2.2.1. Flg22 Perception at the Cell Surface by FLS2 ..... *15*

2.2.2. Activation of the MAPK Signal Cascade Pathway *16*

2.2.3. WRKYs and their Role in PTI *17*

2.3. FLG22 RESPONSIVE GENES 18

2.4. ANALYSIS OF DNA - PROTEIN INTERACTION 20

2.5. DESIGNABLE DNA BINDING PROTEINS 21

2.5.1. Zinc Finger Proteins *22*

2.5.2. Clustered Regularly Interspaced Palindromic Repeats *22*

2.5.3. TALEs *23*

2.5.4. Comparison of Zinc Finger, CRISPR and TALEs *24*

2.6. LOCUS SPECIFIC CHROMATIN PRECIPITATION 25

2.7. THE GLUCOCORTICOID RECEPTOR SYSTEM 25

2.8. AIM OF THE WORK 26

3. MATERIAL **27**

3.1. ORGANISMS 27

3.1.1. Escherichia coli strains *27*

3.1.2. Agrobacterium tumefaciens strains *27*

3.1.3. Arabidopsis thaliana lines *28*

3.1.4. Nicotiana benthamiana lines *28*

3.2. DNA 29

3.2.1. Vectors provided for the thesis *29*

3.2.2. Vectors generated during this work *29*

3.3. GENERAL CHEMICALS AND SOLUTIONS 29

3.3.1. Chemicals *29*

3.3.2. Special Chemicals used in this work *30*

3.3.3. Antibiotics *30*

3.3.4. Hormones and Elicitors *30*

3.3.5. Antibodies *30*

3.3.6. Size standards *31*
3.3.7. Enzymes and Kits *32*
3.4. BUFFERS AND SOLUTIONS FOR THE WORK WITH BACTERIA 32
3.4.1. Growth media *32*
3.4.2. Media and buffers to obtain chemically competent cells *33*
3.5. BUFFERS AND SOLUTION FOR WORK WITH PLANTS 33
3.5.1. Stable transformation of A. thaliana *34*
3.5.2. Transient expression of proteins in Nicotiana benthamiana *34*
3.6. BUFFERS AND SOLUTIONS FOR WORK WITH RNA 34
3.7. BUFFERS AND SOLUTIONS FOR WORK WITH DNA 35
3.7.1. Extraction of plasmid DNA (alkaline lysis) *35*
3.7.1.1. Extraction of genomic DNA from *Arabidopsis thaliana* seedlings 35
3.7.2. Agarose gel solutions *35*
3.7.3. Buffer for agarose gel electrophoresis *36*
3.7.4. PCR solutions *36*
3.8. BUFFERS AND SOLUTIONS FOR WORK WITH PROTEINS 36
3.8.1. Extraction buffer *36*
3.8.2. SDS-page *36*
3.8.3. Coomassie staining *37*
3.8.4. Western blot *37*
3.8.5. Immunodetection *37*
3.9. BUFFERS AND SOLUTIONS FOR X-CHIP AND DTALE-CHAP 38
3.9.1. X-ChIP *38*
3.9.2. dTALE-ChAP *38*
3.9.3. FASP Buffers *39*
3.10. PLANT GROWTH CONDITIONS 40
3.11. MACHINES 40
3.12. SOFTWARE 41
3.13. ONLINE RESOURCES 41
3.14. EXTERNAL DEVICES 41
4. METHODS 42
4.1. MOLECULAR-BIOLOGICAL METHODS 42
4.1.1. Preparation of competent cells *42*
4.1.1.1. Preparation of chemically competent *Escherichia coli* cells 42
4.1.1.2. Preparation of chemically competent *Agrobacterium tumefaciens* cells 42
4.1.2. Transformation of chemically competent cells *43*
4.1.2.1. Transformation of chemically competent *Escherichia coli* cells 43
4.1.2.2. Transformation of chemically competent *Agrobacterium tumefaciens* 43
4.1.3. Verification of the Agrobacterium tumefaciens transformation *43*

4.1.4. Generation of bacterial glycerol stocks *43*
4.1.5. Extraction of nucleic acids *44*
4.1.5.1. Extraction of plasmid DNA (alkaline lysis) 44
4.1.5.2. Extraction of plasmid DNA (midi prep) 44
4.1.5.3. Extraction of RNA from *Arabidopsis thaliana* seedlings 44
4.1.5.4. Extraction of genomic DNA from *Arabidopsis thaliana* seedlings 45
4.1.6. Restriction of plasmid DNA *45*
4.1.7. DNase digestion after RNA extraction *45*
4.1.8. Reverse transcription, generation of cDNA *46*
4.1.9. Polymerase Chain Reaction (PCR) *46*
4.1.10. Quantitative Reverse Transcriptase and quantitative PCR (qRT-PCR & qPCR) *47*
4.1.11. Cloning of dTALEs *47*
4.1.12. Cloning by homologous recombination *47*
4.1.13. Gateway™ Cloning *47*
4.1.13.1. pENTR/D-TOPO® Cloning 47
4.1.13.2. LR-Reaction 48
4.1.13.3. BP-Reaction 48
4.1.14. Denaturing extraction of nuclear proteins of A. thaliana seedlings *48*
4.2. CELL-BIOLOGICAL METHODS 49
4.2.1. Cultivation of Escherichia coli *49*
4.2.2. Cultivation of Agrobacterium tumefaciens *49*
4.2.3. Transformation of Arabidopsis thaliana plants *49*
4.2.4. Transient expression of proteins in Nicotiana benthamiana *50*
4.2.5. Fluorescence Activated Cell Sorting Analysis of Protoplasts *50*
4.2.6. Microscopy *50*
4.2.6.1. Microscopical analysis of transiently transformed Protoplasts 50
4.2.6.2. Microscopical analysis of transiently transformed tobacco leaves 51
4.2.6.3. Microscopical analysis of transgenic *Arabidopsis thaliana* roots 51
4.3. PHYSIOLOGICAL METHODS 51
4.3.1. Seed surface sterilization *51*
4.3.2. Cultivation of Arabidopsis thaliana *52*
4.3.2.1. Cultivation of *Arabidopsis thaliana* on soil 52
4.3.2.2. Cultivation of *Arabidopsis thaliana* on ½ MS plates 52
4.3.2.3. Cultivation of *Arabidopsis thaliana* in liquid media 52
4.3.3. Cultivation of Nicotiana benthamiana *53*
4.3.4. Protoplast transformation for microscopy *53*
4.3.5. Protoplast transformation for promoter reporter assays *53*
4.3.6. Promoter reporter assays *53*
4.4. BIOCHEMICAL METHODS 53
4.4.1. Agarose gel electrophoresis *53*

4.4.2. Extraction of DNA-fragments from agarose gels *54*
4.4.3. Measurement of nucleic acid concentration in solutions *54*
4.4.4. DNA-sequencing *54*
4.4.5. SDS-Polyacrylamide-Gel-Electrophoresis (SDS-PAGE) *54*
4.4.6. Coomassie staining *55*
4.4.7. Western Blot *55*
4.4.8. Immunodetection *55*
4.5. BIOINFORMATICAL METHODS 56
4.5.1. Prediction of transcription factor binding sites *56*
4.5.2. Evaluation of MS data *56*
4.5.3. Over-representation tests *56*
4.6. X-CHIP 57
4.7. DTALE-CHAP 58
4.7.1.1. Growth and treatment of *Arabidopsis thaliana* seedling 58
4.7.1.2. Formaldehyde crosslinking 58
4.7.1.3. Nuclei isolation 58
4.7.1.4. Nuclei Lysis 59
4.7.1.5. Immunoprecipitation 59
4.7.1.6. In solution trypsin digestion 60
4.7.1.7. Detergent removal and Protein Digestion by FASP 60
5. RESULTS 62
5.1. ANALYSIS OF *FRK1* REGULATION 62
5.1.1. Induction of pFRK1 with flg22 ..... *62*
5.2. THE DTALE-CHAP WORKFLOW 63
5.3. EXPERIMENTAL SETTINGS FOR THE DTALE-CHAP 66
5.3.1. Structure of the dTALEs and their binding sites in pFRK1 ..... *66*
5.3.2. Definition of the promoter area and prediction of transcription factor binding sites *68*
5.3.3. Localization of dTALEs - translocation to the nucleus *71*
5.3.3.1. Localization in *A. thaliana* protoplasts 71
5.3.3.2. Localization in *N. benthamiana* 73
5.3.3.3. Localization in transgenic *A. thaliana* lines 76
5.3.3.4. Purification of dTALE C from *A. thaliana* nuclei 79
5.3.4. Induction of pFRK1 in dTALE A. thaliana lines *81*
5.4. DNA BINDING OF DTALES 83
5.4.1. Induction of Promoter - Luciferase Reporter genes with dTALE-AD C and dTALE-AD D *83*
5.4.1.1. Induction of *pFRK1::LUC* by dTALE-AD C and dTALE-AD D 83
5.4.1.2. Induction of *pBS3 dTALE::LUC* with dTALE-AD C and dTALE-AD D 88
5.4.2. Precipitation of pFRK1 fragments with dTALEs *91*
5.4.2.1. Workflow of dTALE-based cross-linking chromatin immunoprecipitation (X-ChIP) 91
5.4.2.2. X-ChIP results 93

5.5. THE DTALE-CHAP 99
5.5.1. First trial of dTALE-ChAP with dTALE C 99
5.5.1.1. Quantification of Peptides 99
5.5.1.2. Over-representation Tests 100
5.5.2. Trial 2 repetition of the dTALE C-ChAP 106
5.5.2.1. Quantification of peptides 106
5.5.2.2. Over-representation tests dTALE C-ChAP trial 2 107
5.5.3. Trial 3 repetition of the dTALE C-ChAP 111
5.5.3.1. Quantification of Peptides dTALE-ChAP trial 3 111
5.5.3.2. Over-representation Test dTALE-ChAP Repetition 3 112
5.5.4. Overlap of dTALE-ChAP trial 1, 2 and 3 115
5.5.5. Changes in the proteome after flg22 Treatment 118
5.5.5.1. $^{14}N/^{15}N$ ratios of identified Proteins of dTALE-ChAP trial 3 118
5.5.5.2. Transcription Related Proteins found in dTALE-ChAP Repetition 3 120

6. DISCUSSION 122

6.1. *PFRK1* IS AN IDEAL PROMOTER TO ESTABLISH THE DTALE-CHAP 122
6.2. PREDICTION OF *CIS* REGULATORY ELEMENTS BY BIOINFORMATIC TOOLS IS PRONE TO FALSE POSITIVES 123
6.3. DTALES TRANSLOCATE FAST INTO THE NUCLEUS AFTER DEX TREATMENT IN *A. THALIANA* PROTOPLASTS 124
6.4. DTALES REACH THE NUCLEUS 30 MIN AFTER DEX TREATMENT IN *N. BENTHAMIANA* EPIDERMAL LEAF CELLS 125
6.5. T2 SEED POOLS ARE AN ELIGIBLE WAY TO GENERATE HIGH MASSES OF PLANT MATERIAL, CIRCUMVENT SILENCING EFFECTS AND COMPENSATE BIOLOGICAL VARIANCE 126
6.6. DTALES ACCUMULATE TO LOW LEVELS IN *ARABIDOPSIS THALIANA* 127
6.7. DTALE-AD C AND DTALE-AD D SPECIFICALLY BIND TO THEIR DNA TARGET 127
6.8. X-CHIP 129
6.8.1. Appropriate Fixation is Crucial for a Successful X-ChIP Experiment 129
6.8.2. Flg22 Treatment Opens the Chromatin and Increases dTALE Binding Site Accessibility 130
6.9. DTALE CHAP 131
6.9.1. Sample Preparation and Removal of Sample Impurities 131
6.9.2. Epigenetic Modifications at pFRK1 in Response to Flg22 132

7. CONCLUSIONS AND OUTLOOK 136

8. LITERATURE 137

9. *CURRICULUM VITAE* 150

11. SUPPLEMENT 152

11.1. SUPPLEMENTARY FIGURES 152
11.2. VECTOR MAPS 157
11.3. SUPPLEMENTARY TABLES 165

DANKSAGUNGEN 223

Abbrevation List

~	approximately
(v/v)	volume per volume
(w/v)	weight per volume
AP2	Apetala 2
APS	ammonium persulfate
ATAC-seq	Assay for Transposase Accessible Chromatin sequencing
BAK1	BRI1-Associated Receptor Kinase 1
BIR	BAK1-Interacting Receptor-Like Kinase
bp	base pairs
BRI1	Brassinosteroid-Insensitive 1
C-terminus	carboxy terminus
cDNA	complementary DNA
ChAP	Chromatin Affinity Purification
ChIP	Chromatin Immuno-precipitation
chip seq	Chromatin Immuno-precipitation - sequencing
Col-0	Columbia-0
CRISPR	Clustered Regularly Interspaced Short Palindromic Repeats
Ctd	C-terminal domain
DEX	dexamethasone
DMSO	dimethylsulfoxid
DNA	desoxyribonucleic acid
dTALE	designer Transcription Activator Like Effector
dTALE-ChAP	designer Transcription Activator Like Effector - Chromatin Affinity Purification
eGFP	enhanced Green Fluorescent Protein
EREBP	ethylene-responsive element binding protein
et al.	et alii
FAIRE-qPCR	Formaldehyde-Assisted Isolation of Regulatory Elements - quantitative Polymerase Chain Reaction
flg22	Flagellin 22
FLS2	Flagellin-sensitive 2
FRK1	Flagellin 22 induced Receptor Like Kinase 1
GR	Glucocorticoid Receptor
HD2B	*Arabidopsis* Histone Deacetylase 2
InR motif	Initiator element motif
MAMP	Microbe associated molecular pattern
MAPK	Mitogen-Activated Protein Kinase
MEKK	Mitogen-Activated Protein Kinase Kinase Kinase
MKK	Mitogen-Activated Protein Kinase Kinase
MQ	Milli-Q purified water
MS	mass spectrometry

N-terminus	amino terminus
ntd	N-terminal domain
OD	optical density
PAMP	Pathogen Associated Pattern
PCR	Polymerase Chain Reaction
pfrk1	promoter of *FRK1*
PVDF	Polyvinylidenfluorid
qPCR	quantitative PCR
RT	reverse transcriptase
SDS-PAGE	Sodium Dodecyl Sulfate Polyacrylamide Gel Electrophoresis
SOB	super optimal broth
TALE	Transcription Activator Like Effector
TEMED	tetramethylethylenediamine
TF	transcription factor
X-ChIP	ChIP followed by qPCR

Summary

The novel *in vivo* method developed in this work, allows to analyze the proteome associated with any promoter of interest and is called dTALE-ChAP. This method makes use of a set of designer Transcription Activator Like Effectors (dTALEs), designed as bait proteins for Chromatin Affinity Purification (ChAP) with subsequent mass spectrometry (MS). To demonstrate the use of the dTALE-ChAP, stable transformed dTALE-expressing *Arabidopsis thaliana* lines were used. The target of choice to establish the method was the well-known promoter of the *Flagellin22 induced Receptor Like Kinase 1* (*pFRK1*).

To establish the method, several pretests had to be performed. First, expression of the dTALEs and their dexamethasone (DEX)-inducible nuclear translocation was confirmed in transgenic *Arabidopsis thaliana* lines by microscopy. Second, it was demonstrated by promoter-reporter gene assays in *Arabidopsis* protoplasts, that dTALEs specifically bind to their DNA target sequence, derived from the *pFRK1.* Third, it was shown by Chromatin Immuno-Precipitation, that a dTALE can precipitate *pFRK1* fragments from nuclear extracts of transgenic *Arabidopsis* lines. Finally, the dTALE-ChAP was performed and several proteins including histones were identified to be associated with *pFRK1.* Thus, the dTALE-ChAP was successfully established and such a method was used for the first time in plants.

This new method allows to analyze the dynamics and post-translational modifications of DNA associated proteins over time in any organism. In future, methods like the dTALE-ChAP will help to better understand transcriptional regulation.

Zusammenfassung

In dieser Arbeit wurde der dTALE-ChAP entwickelt. Dabei handelt es sich um eine neuartige *in vivo* Methode, die es erlaubt das Proteom an einem beliebigen Promoter zu analysieren. Bei dieser Methode werden *designer Transcription Activator Like Effectors* (dTALES) genutzt, die als Ankerproteine für *Chromatin Affinity Purification* (ChAP) mit anschließender Massenspektroskopie (MS) dienen. Die dTALEs erlauben es jede beliebige DNA Region zu untersuchen. Der dTALE-ChAP wurde mittels stabil transformierten, dTALE exprimierenden *Arabidopsis thaliana* Linien etabliert. Ziel war es mit dem dTALE-ChAP Proteine, die an den Promoter des Gens *Flagellin 22 Induced Receptor Like Kinase 1* (pFRK1) binden, unvoreingenommen zu identifizieren.

Der dTALE-ChAP wurde schrittweise mittels mehrerer Vorexperimente etabliert. Zunächst wurde die Expression der dTALE-GFP Fusionsproteine und der Dexamethason-induzierbare Kernimport in transgenen *Arabidopsis thaliana* Linien mikroskopisch untersucht. Anschließend wurde in Promoter-Reportergen Versuchen gezeigt, dass in *Arabidopsis* Protoplasten dTALEs spezifisch an ihre, aus *pFRK1* abgeleitete Zielsequenz binden. Darüber hinaus wurde mittels Chromatin Immmunoprezipitation (ChIP) bestätigt, dass mit einem dTALE ein *pFRK1* Fragment aus Kernrohextrakten der transgenen *Arabidopsis* Linien aufgereinigt werden kann. Schließlich wurde der dTALE-ChAP erfolgreich durchgeführt. Es konnten mehrere Proteine identifiziert werden, die mit *pFRK1* assoziiert sind, einschließlich Histone. Somit wurde die prinzipielle Funktionsweise des dTALE-ChAPs bestätigt und eine solche Methode erstmalig in Pflanzen eingesetzt.

Diese neue Methode erlaubt es, die Dynamiken und post-translationalen Modifikationen von DNA-assoziierten Proteinen in einer zeitlichen Auflösung, unabhängig vom Organismus zu analysieren. Methoden wie der dTALE-ChAP können in Zukunft helfen, die transkriptionelle Regulierung von Genen besser zu verstehen.

2. Introduction

2.1. Chromatin

All living organisms can be divided into three kingdoms: *eukarya*, *bacteria* and *archaea* (Woese, Kandler, & Wheelis, 1990). The variety of the organisms is encoded in their desoxyribonucleic acid (DNA). Desoxyribonucleic acid (DNA) is present as a condensed macromolecule. Amongst the three kingdoms two different organizational forms of the DNA is found which is reflected in the differentiation of organisms into the *Prokaryota* and *Eukaroyta* (Woese et al., 1990). The differentiation into *prokaryotes* and *eukaryotes* was estimated 1.6 billion years ago (Wang, Kumar, & Hedges, 1999) *Prokaryotes* have their DNA organized in one circular molecule, whereas *eukaryotes* show a more complex DNA structure. The *eukaryotic* genome is organized as chromatin, comprising several linear DNA macromolecules called chromosomes, that are located in a separated organelle, the nucleus (Vellai & Vida, 1999). The fundamental packing unit of *eukaryotic* DNA is the nucleosome (Lewin, Cassimeris, Plopper, & Lingappa, 2007) (**Figure 1**). One nucleosome consists of an 11 nm diameter histone octamer, modularly built of two copies of histone protein H2a, H2b, H3 and H4 (Finch et al., 1977; Kornberg, 1974; Lewin et al., 2007; Luger, Mäder, Richmond, Sargent, & Richmond, 1997; Richmond, Finch, Rushton, Rhodes, & Klug, 1984). A 147 base pair long DNA double helix stretch is wrapped two times around the central histone core and is attached to the nucleosome by the histone protein H1 (Lewin et al., 2007). The 30 nm in diameter nucleosome - DNA string of pearls is further coiled into chromosomes.

Beside the differences in the structure of the genome, *prokaryotic* and *eukaryotic* cells differ in the regulation of transcription. *Prokaryotes* regulate several genes *via* one promoter region whereas *eukaryotes* have each gene regulated by its own promoter, at least in most cases (Martinez, 2002). It is assumed, that this complex transcriptional regulation was one of the prerequisites for evolving multicellular organisms. After developing multi cellular organisms of one cell type, organisms evolved comprising different tissues consisting of different specialized cells. The central step for developing different tissues is the differentiation from stem cells to specialized cells. Every specialized cell has an individual set of transcription factors adapted to its specific task (Kornet & Scheres, 2008). The term transcription factor subsumes DNA binding proteins that modulate transcription (Riechmann et al., 2000). In

addition to the molecular specialization by transcription factors, the specialized identity of a differentiated cell is stabilized and maintained by chromatin modifications. In its inactive condensed state (heterochromatin), the DNA is not accessible for the transcription machinery. The condensed structure needs to be actively opened to be accessible. The open chromatin structure is called euchromatin. Specialized cells differ in their pattern of euchromatin and heterochromatin pattern (Leeb & Wutz, 2012). During differentiation, the pattern of eu- and heterochromatin is established and over the time extracellular and intracellular signals are integrated (Leeb & Wutz, 2012).

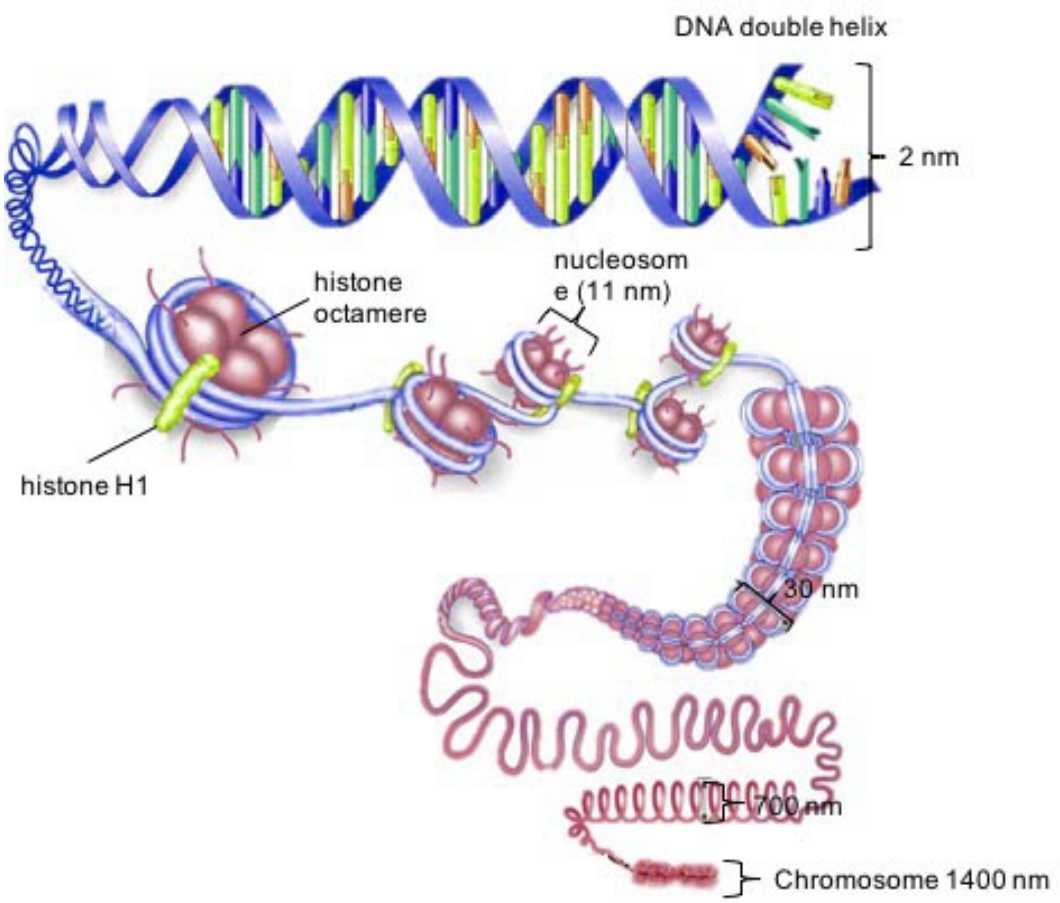

Figure 1: Packaging of eukaryotic chromatin (Sadava (2008), modified). The DNA double helix is wrapped two times around a histone octamer. The nucleosome is fixed by histone H1. The nucleosomes are connected by a DNA linker. The nucleosomes are strung like pearls on a chain and further coiled into a string that is further condensed into a chromosome.

Changes of the chromatin state are initiated by the modification of single amino acid residues of the histones. The major modifications of histones, are acetylation of lysins, methylation of lysins and arginins as well as phosphorylation of histones (Kouzarides, 2007). The silent heterochromatic state is typically associated with low levels of acetylation and high levels of methylation at histone H3 at position K9, K27 and histone H4 at position K20 (Kouzarides, 2007). Actively transcribed euchromatin has high levels of acetylation and is trimethylated at histone H3 at position K4, K36 and K79.

2.1.1. Transcriptional Initiation at a Core Promoter

An open euchromatic state itself is not sufficient for transcription initiation (Kouzarides, 2007). For the initiation of transcription initiation transcription factors bind to highly conserved *cis* regulatory elements (CREs), mainly found in the promoter region, in rare cases in introns of genes (Buck & Lieb, 2004; Deyholos & Sieburth, 2000). Transcription factors can directly influence the stability, the position and the binding of the transcription initiation complex (Berendzen, Stuber, Harter, & Wanke, 2006; Martinez, 2002) and can have activating or repressive function. In addition, they can operate indirectly as co-factor. Transcription factors often form multimeric complexes and act as multi protein complexes.

The promoter of a eukaryotic gene is usually found upstream of the translation start codon (*ATG*). Upstream of the star codon, the pyrimidine rich initiator element (InR) is found (Burley & Roeder, 1996a). In 29 % of all *Arabidopsis* promoters a highly conserved element 25-32 base pair upstream of the InR motif is observed, called *TATA* (Burley & Roeder, 1996a; Molina & Grotewold, 2005). The *TATA* marks the position of the TATA box complex during transcriptional initiation. During the initiation of polymerase II catalyzed transcription, the TATA Box complex, consisting of the general initiation factors TFIIA, TFIIB, TFII D, TFIIE and TFIIH assembles at the core promoter (Burley & Roeder, 1996b). Thereby, TFIID is the only component of this complex with site specific DNA binding ability recognizing the TATA box element (Burley & Roeder, 1996a). Binding of TFIID to the TATA box marks the beginning of the transcriptional initiation. The TATA Box complex directs further initiation factors, as well as polymerase II to the promoter, where they form the pre-initiation complex (Burley & Roeder, 1996b). After the pre-initiation complex is formed, further factors are recruited and transcription starts.

Several hundred base pairs upstream of the core promoter, with the essential binding sites for transcriptional initiation, there are further binding sites of regulatory elements. These regulatory elements are the target of *trans*-acting factors that modulate transcription. The *trans*-acting factors that modulate the transcription are mostly transcription factors, such as the members of the WRKY family

2.2. PAMP Triggered Immunity

2.2.1. Flg22 Perception at the Cell Surface by FLS2

Precise and fast regulation is a vital process, especially when plants are facing challenges like pathogen attacks. Plants are not the helpless objects they seem to be at the first sight. Although, or maybe because they are fixed to one location, they have evolved mechanisms to actively defend pathogen attacks. The first step to defend pathogen attacks is the detection of the approaching pathogens. Plants detect pathogens by highly conserved molecular structures. These molecular structures are called pathogen associated patterns (PAMPs). PAMPs are recognized by the extracellular domain of pattern recognition receptors (PRRs) that are located at the cell surface (Ronald & Beutler, 2010; Segonzac & Zipfel, 2011). The PRRs belong either to the family of receptor kinases or the receptor like protein family (Segonzac & Zipfel, 2011). The PRRs transmit the signal from the cell surface, over the plasma membrane, into the cytosol. In the cytosol further signaling steps are initiated eventually leading to an adequate immune response.

The first described example for a eubacterial PAMP is the flagellin-derived peptide flg22 (Felix, Duran, Volko, & Boller, 1999). In nearly all plant species flg22 is sensed by the flagellin sensitive 2 (FLS2) receptor (Schwessinger & Ronald, 2012). FLS2 consists of an extracellular leucine rich repeat (LRR) domain, a transmembrane domain, a juxtamembrane domain and a cytoplasmic serine/threonine kinase domain (Gomez-Gomez & Boller, 2000). Flg22 is bound by the LRR domain of FLS2.

Upon flg22 binding, FLS2 associates with the *Brassinosteroid insensitive 1*-associated kinase 1 (BAK1) (D. Chinchilla, Shan, He, de Vries, & Kemmerling, 2009; D. Chinchilla et al., 2007; Heese et al., 2007) (Figure 2). The flg22-caused heteromerization of FLS2 and BAK1 results in their

trans-phosphorylation and in the activation of the perception complex (D. Chinchilla et al., 2007; Schulze et al., 2010; Schwessinger et al., 2011). After several transphosphorylation rounds that are not completely elucidated so far, BIK1 and possibly other substrates of the FLS2-BAK1 complex get phosphorylated. The activated BIK1 is then released from the complex and is activating MAPK cascades by a yet unknown mechanism(Lu et al., 2010; J. Zhang et al., 2010).

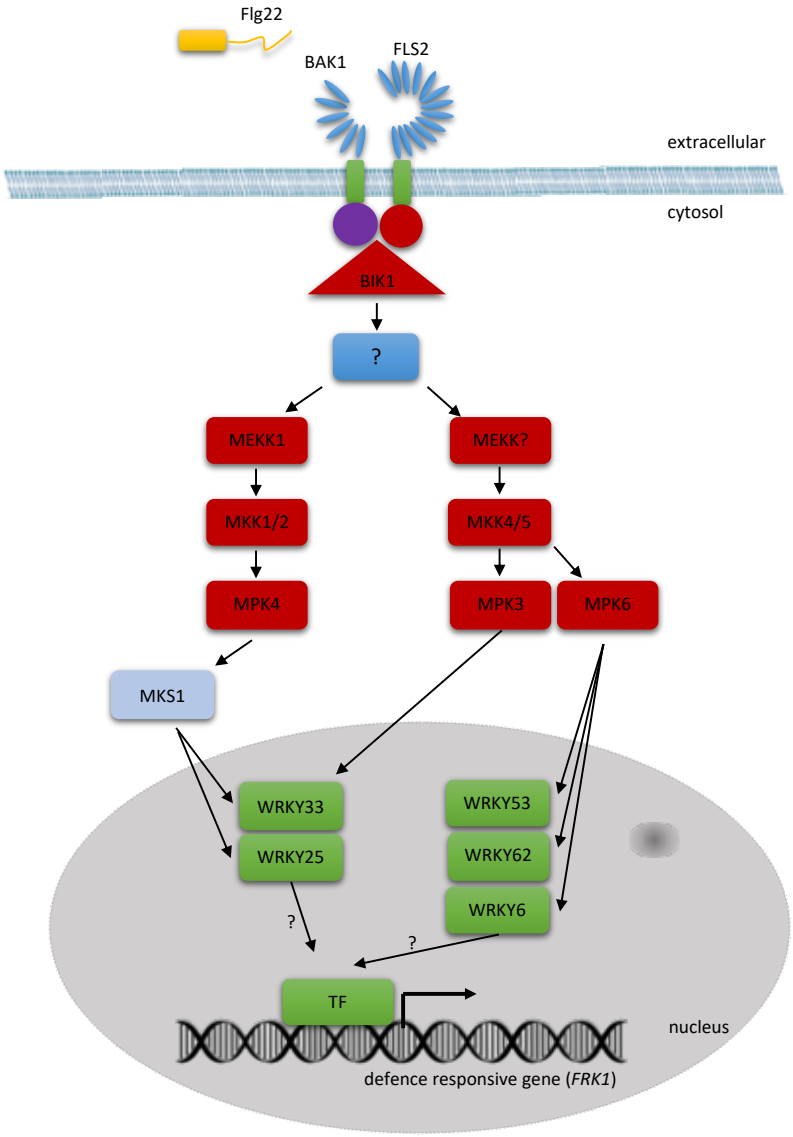

Figure 3: Signaling cascade in response to flg22 in *A. thaliana* modified after (Park, Caddell, & Ronald, 2012; Ramirez-Prado, Abulfaraj, Rayapuram, Benhamed, & Hirt, 2018; Ramirez-Prado, Piquerez, et al., 2018). After the perception of flg22 through FLS2, FLS2 and its co-receptor BAK1 are phosphorylated. On the intracellular site of the plasma membrane, BIK1 gets phosphorylated and dissociates from the BAK1-FLS2 complex. BIK1 induces two MAPK cascades. MPK4 phosphorylates MKS1 which interacts with WRKY33 and WRKY25. MPK6 phosphorylates WRKY53, WRKY62 and WRKY6. MPK3 phosphorylates WRKY33. WRKYs induce other transcription factors or function as transcription factors itself and activate defense responsive genes like *FRK1*.

2.2.2. Activation of the MAPK Signal Cascade Pathway

The central pathway that is activated during the PTI response for example after perception of flg22 is the *mitogen activated protein kinase* (MAPK) pathway (*Figure 2*).

The minimal MAPK cascade is composed of a MAPK kinase kinase (MAPKKK), a MAPK kinase (MAPKK) and a MAPK (Pitzschke, Schikora, & Hirt, 2009). In response to flg22 three MAPK kinases are strongly activated (MPK3, MPK4 and MPK6 (Asai et al., 2002; Droillard, Boudsocq, Barbier-Brygoo, & Lauriere, 2004). Asai et al. (2002) proposed, that MEKK1 (MAPKKK) is the start of the cascade, followed by MKK4/MKK5 (MAPKK) resulting in the activation of MPK3 and MPK6. The induction of MPK4 is not clearly clarified yet. The parts of the MAPK cascades are redundant and it is likely that there are parallel pathways. It was shown by Popescu et al. (2009) that in general mainly transcriptional regulators are the predominant phosphorylation targets of the MAPK cascade pathway. These include members of the largest transcription factor families of *Arabidopsis*: MYB, MYB-related, bZIPs, AP2/EREB, homeo box and WRKYs (Popescu et al., 2009).

2.2.3. WRKYs and their Role in PTI

WRKYs named after a highly conserved 60 amino acid long domain at the N-terminus starting with the sequence WRKYGQK (Eulgem, Rushton, Robatzek, & Somssich, 2000; Rushton et al., 1996), build one of the biggest transcription factor family in *Arabidopsis* with up to 100 representatives categorized in three groups (Eulgem et al., 2000). WRKYs have many different roles in *Arabidopsis* like the regulation of transcriptional responses to abiotic stress, seed development, seed dormancy, germination, plant development and senescence (Rushton, Somssich, Ringler, & Shen, 2010). Apart from the above mentioned roles, WRKYs seem to be the essential regulatory part involved in the transcriptional reprogramming during PTI (Rushton et al., 2010; Tsuda & Somssich, 2015). WRKYs preferentially bind to sites with the minimal DNA core sequence TTGACC/T, called Wbox (Ciolkowski, Wanke, Birkenbihl, & Somssich, 2008; Eulgem et al., 2000; Rushton et al., 1996). Wboxes are numerous in the *Arabidopsis* genome and equally distributed on both DNA strands (Birkenbihl, Kracher, & Somssich, 2017). The regulatory role of WRKYs during PTI is underlined by the overrepresentation of Wboxes in the promoters of flg22 induced genes (Navarro et al., 2004; Zipfel et al., 2004). This suggests that WRKYs induce PTI response genes downstream of the MAPK cascade pathways. However, because of the high number of WRKYs and their redundant roles, the identification of functional promoter-WRKY pairs is very difficult. WRKYs have many representatives that can act as homo- and heterodimers. Because of the high

number of WRKYs and their redundant roles, the identification of promoter - WRKY pairs is very difficult and largely unknown.

2.3. Flg22 Responsive Genes

As the downstream end of the flg22 induced MAPK cascade pathway early responses of the PTI are induced. While searching for early flg22 induced genes Asai et al. (2002) identified the *flg22 induced receptor like kinase 1* as one of many early flg22 induced genes. They were able to find *FRK1* transcript 30 min after flg22 treatment and showed, that the activation of *FRK1* was not dependent on *de novo* protein synthesis (Asai et al., 2002). In reporter gene studies they also demonstrated, that the induction of *FRK1* transcript accumulation was due to promoter activation. *FRK1* transcript levels are also enhanced in sepals and senescent leaves, but never in non-senescent plant tissues (Robatzek & Somssich, 2002) (*Figure 4*). Thus, since *FRK1* transcripts are not accumulated in non-senescent tissue in absence of pathogens and hardly in response to other stresses, it is commonly used as PTI primary response and marker gene. Interestingly, the function of the FRK1 protein is not yet known.

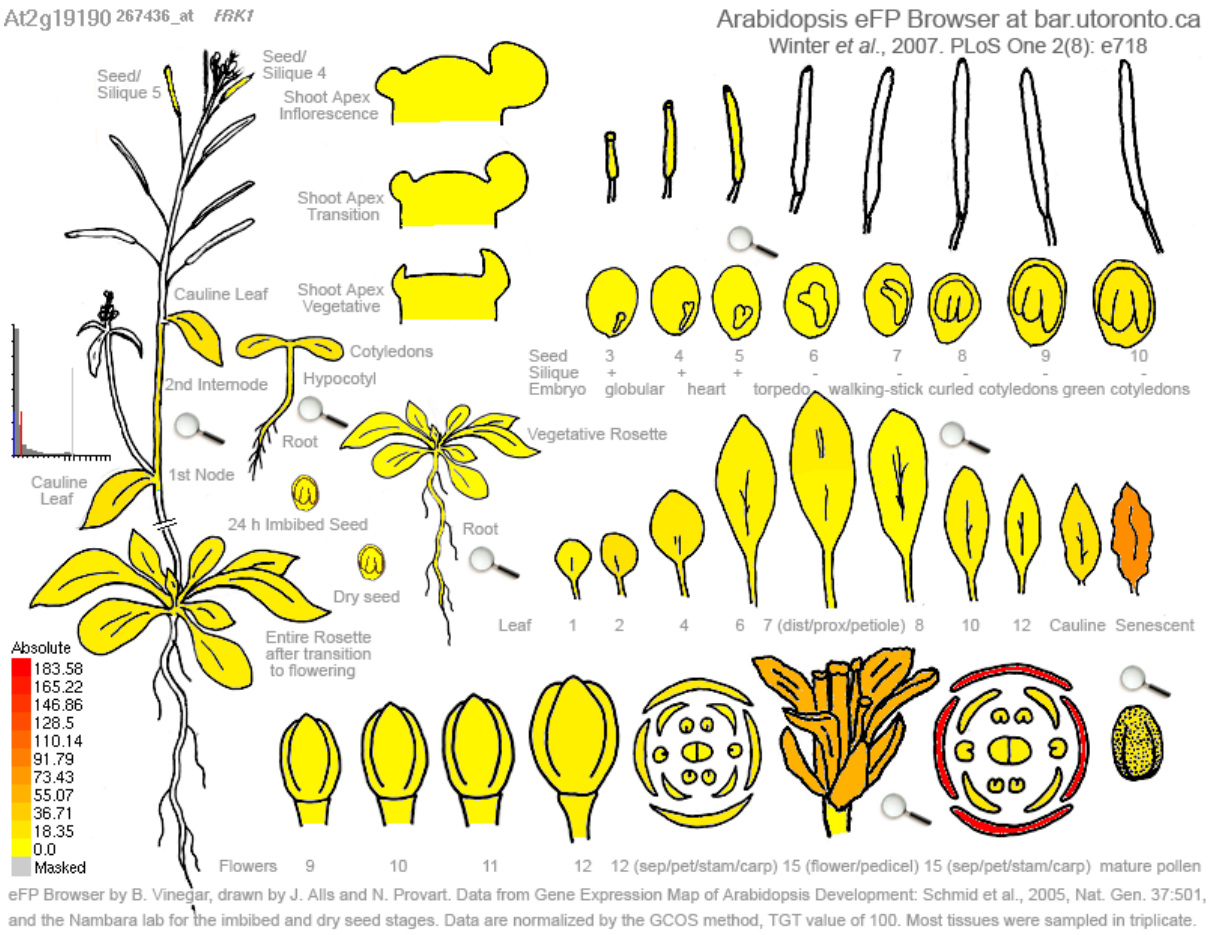

Figure 4: *FRK1* is expressed in *A. thaliana* in sepals and senescent leaves (source Winter (2007)). Shown are the expression levels of *FRK1* in *A. thaliana* in different tissues during different developmental stages and are symbolized by a color code.

It is assumed, that WRKYs play an important role in the regulation of *FRK1*. Robatzek and Somssich (2002) found nine Wboxes in the promoter of *FRK1* (*pFRK1*). Of the nine Wboxes the two proximal to the *ATG* were essential for the activation of *FRK1* (Robatzek & Somssich, 2002). Beside the presence of Wboxes, several other observations emphasize the likelihood of WRKYs to be the key regulator of *FRK1.* As already mentioned in section 2.2.3, WRKYs act downstream of the flg22 induced MAPK cascade.

Robatzek and Somssich (2002) demonstrated that WRKY6 and WRKY42 are able to activate *FRK1.* In contrast the pathogen induced WRKYs, WRKY1 and WRKY52 cannot induce *FRK1* (Robatzek & Somssich, 2002). Beside WRKY6 and WRKY42 several other WRKYs have been shown to interact with *pFRK1*. WRKY11, WRKY26 and WRKY53 have been shown to bind to *pFRK1 in vitro* (Ciolkowski et al., 2008; Miao, Laun, Zimmermann, & Zentgraf, 2004). WRKY38, WRKY26 and WRKY43 have also been shown to bind *pFRK1 in vivo* (Ciolkowski et al., 2008). In Chipseq experiments, *pFRK1* was found as a target for WRKY17, WRKY 40 and WRKY33

(Birkenbihl et al., 2017). It seems to be likely that WRKY53 binds to the distal part of *pFRK1* (Miao et al., 2004). In contrast *pFRK1* activation by WRKY6 is dependent of the interaction with the proximal part of the promoter (Robatzek & Somssich, 2002). Besides the members of the WRKY family, bZIP1 was also shown to bind to *pFRK1 in vitro* (Doidy et al., 2016). Although WRKYs were shown to interact with *pFRK1* the exact mode of regulation is not elucidated so far. Furthermore, even though *FRK1* is often used as a marker gene for the activation of PTI, the exact function of *FRK1* itself is not known so far.

2.4. Analysis of DNA - Protein Interaction

Elucidating the regulatory network of transcription factors at a promoter is often very difficult, as more than one transcription factor regulates a gene. Especially in cases like *FRK1* where possibly different members of functionally redundant transcription factor families like WRKYs are involved, the identification of the key regulator it is difficult.

The method of choice to directly analyze the *in vivo* interaction of a given protein with DNA*F*, is Chromatin Immuno Precipitation (ChIP). The ChIP methodology was established by (Orlando, Strutt, & Paro, 1997). ChIP is based on the covalent bit reversible association of proteins to DNA by formaldehyde fixation (Solomon & Varshavsky, 1985). In principle ChIP comprises the following steps (Mülhardt, 2013): 1. The tissue to be analyzed is treated with formaldehyde. The amino- and iminogroups of the proteins and the DNA are coupled covalently when they are in close proximity. 2: The cells are lysed and the nuclei are purified. 3: Ultrasonic treatment leads to cracking of the nuclei and shearing of the chromatin. 4. In the precipitation step, the protein-DNA complex is enriched using bead-coupled antibodies against the protein of interest. 5: The crosslinking is reversed and the DNA is purified after proteolytic digestion of the attached proteins with ProteinaseK. 6: The DNA is analyzed, either by sequencing, qPCR or on microarrays.

ChIP based methods can identify *in vivo* target regions of the transcription factor of interest, as well as help to understand the processes going on at the chromatin and the underlying molecular processes (Agius, Arvey, Chang, Noble, & Leslie, 2010; Buck & Lieb, 2004; Bulyk, 2006; Hoffman & Jones, 2009; Lafos et al., 2011; J. Li, Zhu, Eshaghi, Liu, & Karuturi, 2011;

MacQuarrie, Fong, Morse, & Tapscott, 2011; Massie & Mills, 2008; Rhee & Pugh, 2012; Zheng & Hearing, 2014; Zheng & Perry, 2011).

In the classical ChIP approaches the resolution limit for the mapping of target sites was the size of the DNA fragments, which is dependent on the ultrasonic treatment. Fragments under 200 base pair length are unfeasible. By the combination of ChIPseq with a subsequent exonuclease step, it became possible to map transcription factor binding sites down to single base pair resolution (Rhee & Pugh, 2011; Starick et al., 2015). To circumvent a lack of antibodies for the protein of interest, tagged versions of the bait protein in combination with antibodies against the protein tag are used (Harada & Nepveu, 2012). Drawbacks of the labor intensive ChIP approaches, especially of the ChIP-ChIP and ChIPseq are bioinformatic efforts (Szalkowski & Schmid, 2011).

Further development of ChIP was the development of Chromatin Affinity Purification (ChAP). The term ChAP is not used uniformly (Harada & Nepveu, 2012; Nikolov et al., 2011). In this work ChAP is used for experiments in which proteins shall be analyzed instead of the DNA (Nikolov et al., 2011). Proteins are purified from the protein-DNA complexes after chromatin immune precipitation. In ChAP experiments downstream of the precipitation step, the purified proteins are analyzed by western blotting or mass spectrometry. Since ChAP approaches identify DNA-bound proteins, transcription factors can be identified among other chromatin-associated factors that were known to bind to a certain DNA site. The prerequisite and concurrent weakness of ChIP and ChAP is that at least one protein that binds the DNA region of interest is needed.

2.5. Designable DNA Binding Proteins

Since a DNA binding protein is the prerequisite for ChIP or ChAP experiments, the lack of a known binder could be substituted by a designed DNA binding protein. Until now there are three different methodologies to design proteins that target specifically a DNA site of choice. The oldest methodology is to use Zinc Finger proteins (J. Miller, McLachlan, & Klug, 1985). After the code of the DNA binding domain of the Transcription Activator Like Effector (TALE) proteins, coming from *Xanthomonas* and *Ralstonia* was deciphered, they were also used to design DNA binding proteins for individual target sequences (Boch et al., 2009; Moscou &

Bogdanove, 2009). The latest method to create designable DNA binding proteins were via the clustered regularly short interspaced palindromic repeats of the CRISPR/Cas system (Bortesi & Fischer, 2015).

2.5.1. Zinc Finger Proteins

Zinc Fingers are a class of DNA binding proteins that were discovered 1985 during the analysis of a *Xenopus* transcription factor (J. Miller et al., 1985). They are named after a conserved finger like structure with a zinc ion in the center (Klug, 2010). Zinc Fingers bind as tandem or triplets to the DNA (Jamieson, Miller, & Pabo, 2003; Reynolds et al., 2003).

The structural frame work of each Zinc Finger is similar, but variation in some key amino acids encode the chemical distinctiveness (Klug, 2010). After the rules of the encoded binding specificity were encrypted, it was possible to design proteins to target a specific site by using individual specific fingers (Choo & Klug, 1994a, 1994b). The first application of a modified Zinc Finger that binds to a specific target sequence *in vitro* and *in vivo* was published in 1994 (Choo, Sanchez-Garcia, & Klug). The combination of Zinc Finger peptides with different functional domains, like activation domains, repressor domains or nucleases, enabled the design of site specific effector proteins.

2.5.2. Clustered Regularly Interspaced Palindromic Repeats

The principle of the clustered regularly interspaced palindromic repeat (CRISPR) Cas9 system differs from the Zinc Fingers and the TALEs. TALEs and Zinc Fingers are artificial proteins with an engineered DNA binding domain (Bortesi & Fischer, 2015). These engineered proteins can be coupled to different functional domains. In contrast, CRISPR is based on RNA guided engineered nucleases. CRISPR arrays were initially found by Ishino, Shinagawa, Makino, Amemura, and Nakata (1987). In 2005 it was understood, that the CRISPR arrays are part of an adaptive bacterial immune system (Bolotin, Quinquis, Sorokin, & Ehrlich, 2005; Mojica, Diez-Villasenor, Garcia-Martinez, & Soria, 2005; Pourcel, Salvignol, & Vergnaud, 2005). The discovery, that CRISPR is adjacent to Cas9 nucleases, revealed the role of CRISPR Cas9 in the immune system of bacteria and archaea (Barrangou et al., 2007).

DNA sequences can be specifically targeted with CRISPR by changing the sequence of the guide RNA (Jinek et al., 2012). Further on, also CRISPR approaches were developed, in which an inactive Cas9 (dCas) was used. The dCas can be combined with different functional domains. CRISPR dCas was used to shuttle functional domains to a specific sites. For example, there are approaches in which CRISPR dCas was combined with transcriptional repressor or activation domains, fluorescing tags and DNA methylases as reviewed by Bortesi and Fischer (2015).

2.5.3. TALEs

Transcription Activator Like Effectors (TALEs) are type III effector proteins that are released by pathogens like *Xanthomonas* and *Ralstonia* into the plant cell (Boch & Bonas, 2010; de Lange et al., 2013; L. Li et al., 2013). In the plant cell the TALE activates genes and alters the gene expression in a pathogen favorable manner. The first TALE isolated from the plant pathogen *Xanthomonas* was called avrBs3 (Kay, Hahn, Marois, Hause, & Bonas, 2007; Romer et al., 2007). AvrBS3 targets the *Bs3* disease resistance gene in *Capsicum annuum*, causing a hypersensitive response, leading to necrotic leaf lesions (Kay et al., 2007; Romer et al., 2007). Since *Bs3* is regulating the cell size, deregulation by the TALE AvrBs3 leads to, bigger cell sizes, which seemed to be favorable for the pathogen (Pennisi, 2012).

A TALE itself consists of an N-terminal domain, a central tandem repeat DNA binding domain and a C-terminal domain (Boch et al., 2009). The C-terminal domain harbors a nuclear localization signal as well as an activation domain (Boch et al., 2009). The central DNA binding domain consists of several tandem repeats. Each repeat is 34 amino acids long and is variable in position 12 and 13 (Boch et al., 2009; Moscou & Bogdanove, 2009). The variable residues are called repeat variable diresidue (RVD) (Boch et al., 2009; Moscou & Bogdanove, 2009). The basic TALE code comprises four RVDs (NI = adenine, HD = cytosine, NG = thymine NN = guanine/ adenine) (Boch et al., 2009; Moscou & Bogdanove, 2009). The decrypted TALE code was the basis to create designer TALEs (dTALEs) that bind to a target sequence of choice by re-arranging the repeats. In a screen performed by Cong, Zhou, Kuo, Cunniff, and Zhang (2012), further RVDs with different binding affinities were identified. The critical step in creating dTALEs is the assembly of the repeats. Different approaches were established to

assemble the different repeats, but mostly based on Golden Gate Cloning (Scott, Kupinski, & Boyes, 2014).

Once it was possible to create designer TALEs, first applications using dTALEs were developed. The activation domain was deleted and dTALEs were used with an added endonuclease (T. Li et al., 2011; J. C. Miller et al., 2011). This endonuclease TALE combination was used for gene editing. The endonuclease was guided to the target sequence, creating DNA breaks. Other approaches used TALEs as artificial transcriptional regulators. Therefore TALEs were combined with activation domains, like the VP64 domain, or repressor domains (L. Li et al., 2012; F. Zhang et al., 2011). TALEs as expression regulators can be applied in various organisms. They were used in yeast, plants and mammalian cells (Blount, Weenink, Vasylechko, & Ellis, 2012; Bultmann et al., 2012; Cermak et al., 2011; Y. Li, Moore, Guinn, & Bleris, 2012; Maeder et al., 2013; Morbitzer, Romer, Boch, & Lahaye, 2010; Perez-Pinera et al., 2013; Tremblay, Chapdelaine, Coulombe, & Rousseau, 2012). Besides the application as transcriptional regulator and nuclease the combination with different functional domains similar to the CRISPR/Cas system is possible. One example is the combination with a fluorescent tag to visualize chromatin dynamics (Miyanari, Ziegler-Birling, & Torres-Padilla, 2013)

2.5.4. Comparison of Zinc Finger, CRISPR and TALEs

Although the Zinc Fingers are the oldest and therefore most established system, the pitfall of Zinc fingers in comparison to CRISPR/Cas and dTALEs is the complex interaction with the DNA. In TALEs each RVD encodes for one base, in CRISPR the guide RNA encodes the target sequence. In contrast, each Zinc Finger makes contact to three bases. Therefore, Zinc Fingers are not as versatile as CRISPR and TALEs. The major advantage of CRISPR over Zinc Fingers and TALEs is the mode of target detection. Whereas with Zinc Fingers and dTALEs for a new target a new DNA binding domain needs to be designed, with CRISPR the guide RNA can be easily modified (Cano-Rodriguez & Rots, 2016).

It is difficult to compare the potency of the three methodologies. The advantage of CRISPR and dTALEs is their versatility. Reports regarding the binding capacity of dTALEs and CRISPR/Cas to chromatin are contradictory (Waryah, Moses, Arooj, & Blancafort, 2018). Therefore, it is not possible to predict whether CRISPR or dTALEs would show the higher

binding capacity to a specific target site. For these reasons, the development of both methods was drive forward in parallel.

2.6. Locus Specific Chromatin Precipitation

With the progress of the dTALE and CRISPR technology, these proteins were implemented in target site specific ChIP methods. CRISPR was successfully used to precipitate chromatin regions (Fujita & Fujii, 2013, 2014, 2015; Fujita, Yuno, & Fujii, 2016, 2018; Fujita, Yuno, Suzuki, Sugano, & Fujii, 2017). The same was true for dTALEs (Byrum, Raman, Taverna, & Tackett, 2012; Byrum, Taverna, & Tackett, 2013; Rathi, Maurer, Kubik, & Summerer, 2016).

So far the none of the developed methods have been applied in plants. In addition, in all cases the bait proteins translocate uncontrolled to the nucleus. However, it cannot be excluded that big and artificial proteins may influence the surrounding genes when they are permanently bound to the chromatin.

2.7. The Glucocorticoid Receptor System

One system to make the nuclear import of fusion proteins inducible is the attachment of the vertebrate glucocorticoid receptor (GR). In the absence of its steroid ligand, the GR is kept as a multimeric chaperone complex in the cytoplasm (Cheung & Smith, 2000; Pratt & Toft, 1997). The GR is induced by treatment with the steroid dexamethasone(DEX), a strong synthetic glucocorticoid. Upon binding of its ligand the GR is released from the chaperone complex and translocates to the nucleus (Vandevyver, Dejager, & Libert, 2012). The GR system is highly suited for the applications in plants, since plants do not have a comparable steroid receptor system, steroid treatment does not cause any pleiotropic effects. Thus, DEX treatment does also not cause major pleiotropic effects (Aoyama & Chua, 1997; Schena, Lloyd, & Davis, 1991). In this work, optimized GR-version for plants was used (Grefen et al., 2015).

2.8. Aim of the Work

This work aims to establish a new *in vivo* method, named dTALE-ChAP, with that the proteome bound at a promoter of choice can be analyzed. So far it is not possible to gain deep insight into dynamics of post-translational modifications of proteins at a single promoter. By developing the dTALE-ChAP, I aim to close this methological gap. In this work the proteome of the plant specific gene *FRK1* will be analyzed and used as proof of principle example.

Since the basis of the dTALE-ChAP are dTALEs, my first goal is the design and generation of suitable dTALE proteins against *pFRK1.* These dTALEs bind specifically to target sites in *pFRK1* and have no enzymatic activity. They were equipped with a N-terminal GR and a C-terminal GFP and HA tag, for inducible subcellular localization and precipitation.

The second goal is to test the expression of dTALEs *in planta* to verify the GR-based steroid induced nuclear import. This requires several pre-experiments including studies in transiently transformed *Arabidopsis* cell culture protoplasts and tobacco leaves. Third, in order to have material for the dTALE-ChAP, I need to generate transgenic *Arabidopsis* lines and test these for expression and localization of the dTALEs. My fourth goal is to analyze the dTALE DNA-binding capacity to different regions in *pFRK1* by Chromatin Immuno-Precipitation followed by qPCR.

My final goal is to perform the dTALE-ChAP including the identification of the proteins bound to *pFRK1* and thus to show the proof of principle of this method.

3. Material

3.1. Organisms

3.1.1. *Escherichia coli* strains

Table 1: *Escherichia coli* strains

strain	Genotype	Datasheet	Purpose
NEB 5-alpha Competent E.coli (High Efficiency) (New England Biolabs)	fhuA2 (argF-lacZ)U169 phoA glnV44 80 (lacZ)M15 gyrA96 recA1 relA1 endA1 thi-1 hsdR17	https://www.neb.com/-/media/catalog/datacards-or-manuals/c2987datasheet-lot2831402.pdf	Cloning and amplification of vector DNA
DB3.1™ (Invitrogen)	F-gyrA462 endA1 Δ(sr1-recA) mcrB hsdS20(rB–, mB–) supE44 ara-mrr 14 galK2 lacY1 proA2rpsL20(SmR) xyl-	https://assets.thermofisher.com/TFS-Assets/LSG/manuals/11782018.pdf	Amplification of Donor and Destination vectors (vectors with a ccdB cassette)

3.1.2. *Agrobacterium tumefaciens* strains

For all experiments with *Agrobacterium tumefaciens* the strain GV3101::pMP90 was used (Koncz & Schell, 1986).

3.1.3. *Arabidopsis thaliana* lines

Table 2: *Arabidopsis lines* which have been used in this work

Name	Origin	Site of insertion	Vector	Species donor	Species receiver	Resistance
Col-0 (wildtype)	Paul Verslues					
GFP	Andreas Hecker	Description in (Hecker, 2016)			*Arabidopsis thaliana* Col-0	
Fls2-SALK_062054	Markus Albert/ Birgit Kemmerling	T-DNA insertion in AT5G46330 (fls2) 1. exon	SALK_062054	*Agrobacterium tumefaciens*	*Arabidopsis thaliana* Col-0	Kanamycin
dTALE A line (seed pool of T2 generation was used)	Stefan Fischer	not known	pICH50505-35S-GR-FRK1-TALE II	*Agrobacterium tumefaciens*	*Arabidopsis thaliana* Col-0	BASTA
dTALE B line (seed pool of T2 generation was used)	Stefan Fischer	not known	pICH50505-35S-GR-FRK1-TALE III	*Agrobacterium tumefaciens*	*Arabidopsis thaliana* Col-0	BASTA
dTALE C line (seed pool of T2 generation was used)	Stefan Fischer	not known	pICH50505-35S-GR-FRK1-TALE IX +	*Agrobacterium tumefaciens*	*Arabidopsis thaliana* Col-0	BASTA
dTALE D line (seed pool of T2 generation was used)	Stefan Fischer	not known	pICH50505-35S-GR-FRK1-TALE VIII	*Agrobacterium tumefaciens*	*Arabidopsis thaliana* Col-0	BASTA
dTALE E line (seed pool of T2 generation was used)	Stefan Fischer	not known	pICH50505-35S-GR-FRK1-TALE VI	*Agrobacterium tumefaciens*	*Arabidopsis thaliana* Col-0	BASTA
dTALE F line (seed pool of T2 generation was used)	Stefan Fischer	not known	pICH50505-35S-GR-FRK1-TALE X	*Agrobacterium tumefaciens*	*Arabidopsis thaliana* Col-0	BASTA
pPGT, free GFP	Dr. Nina Jaspert	Not known	pPGT-35S-GFP	*Agrobacterium tumefaciens*	*Arabidopsis thalianana* Col-0	

3.1.4. *Nicotiana benthamiana* lines

For all experiments with tobacco *Nicotiana benthamiana* L. Samsun NN was used and transiently transformed.

3.2. DNA

3.2.1. Vectors provided for the thesis

Table 3: Vectors provided for this thesis

name	vector	Quelle/ source
pFRK1::LUC	Asai et al. (2002)	
dTALE A	pICH50505-35S-GR-FRK1-TALE II	Dr. R. Morbitzer (University of Tuebingen)
dTALE B	pICH50505-35S-GR-FRK1-TALE III	Dr. R. Morbitzer (University of Tuebingen)
dTALE E	pICH50505-35S-GR-FRK1-TALE VI	Dr. R. Morbitzer (University of Tuebingen)
dTALE F	pICH50505-35S-GR-FRK1-TALE X	Dr. R. Morbitzer (University of Tuebingen)
dTALE D	pICH50505-35S-GR-FRK1-TALE VIII	Dr. R. Morbitzer (University of Tuebingen)
dTALE C	pICH50505-35S-GR-FRK1-TALE IX +	Dr. R. Morbitzer (University of Tuebingen)
dTALE-AD A	pICH50505 TALE 364 AD	Dr. R. Morbitzer (University of Tuebingen)
dTALE-AD B	pICH50505 TALE 365 AD	Dr. R. Morbitzer (University of Tuebingen)
dTALE-AD E	pICH50505 TALE 366 AD	Dr. R. Morbitzer (University of Tuebingen)
dTALE-AD F	pICH50505 TALE 367 AD	Dr. R. Morbitzer (University of Tuebingen)
dTALE-AD D	pICH50505 TALE 368 AD	Dr. R. Morbitzer (University of Tuebingen)
dTALE-AD C	pICH50505 TALE 369 AD	Dr. R. Morbitzer (University of Tuebingen)
LHP1:RFP	(Hecker et al., 2015)	

3.2.2. Vectors generated during this work

Table 4: Vectors generated during this work

name	vector	cloning strategy
pBS3 dTALE A::LUC	pbt8	recombination
pBS3 dTALE B::LUC	pbt8	recombination
pBS3 dTALE C::LUC	pbt8	recombination
pBS3 dTALE D::LUC	pbt8	recombination
pBS3 dTALE E::LUC	pbt8	recombination
pBS3 dTALE F::LUC	pbt8	recombination

3.3. General chemicals and solutions

3.3.1. Chemicals

If not stated otherwise, all chemicals were ordered in analytical purity from Sigma-Aldrich (Since 2015 Merck, Darmstadt Germany) or Carl Roth (Karlsruhe Germany).

3.3.2. Special Chemicals used in this work

Table 5: Special chemicals used in this work

Chemical	Manufacturer	Catalogue number
Potassium Nitrate ^{15}N	Cambridge Isotope Labarotories Inc.	NLM-765-1
Ammonium Nitrate ^{15}N	Cambridge Isotope Labarotories Inc.	NLM-390-1
Sequencing Grade Modified Trypsin	Promega	V5111
Endoproteinase Lys-C Sequencing grade	Roche	11420429001
Dexamethason BioChemica	Applichem	A2143,0500

3.3.3. Antibiotics

Table 6: Concentration of antibiotics used

Antibiotic	Solvent	Company	Concentration for selection of *Agrobacterium tumefaciens*	Concentration for selection of *Escherichia coli*
Ampicillin	70 % (v/v) ethanol	Carl Roth	-	100 µg/ml
Kanamycin	H_2O	Carl Roth	50 µg/ml	50 µg/ml
Spectinomycin	H_2O	AppliChem	100 µg/ml	100 µg/ml
Rifampicin	DMSO	Sigma-Aldrich	100 µg/ml	-
Gentamycin	H_2O	Duchefa	40 µg/ml	10 µg/ml

3.3.4. Hormones and Elicitors

Dexamethasone (AppliChem) was solved in ethanol to a 10 mM Stock. The stock was stored for a maximum of two month at -20 °C.

A stock of flg22 was provided by Dr. Markus Albert (ZMBP, University of Tuebingen) and stored at -20 °C.

3.3.5. Antibodies

Table 7: Antibodies used in this work

Name	Host	Clonality	Company	Immunogen	Dilution	Used for
anti-HA	Rat	Monoclonal clone 9E10	Roche	9E10 epitope (EQKLISEEDL sequence) derived from the human c-myc protein	1:1000 in TBS-T	Western Blot

anti-GFP	Mouse	Monoclonal	Roche	partially purified recombinant Aequorea victoria GFP	1:1000 in TBS-T	Western Blot
anti-mouse-HRP	Goat		Sigma	Purified mouse IgG	1:10000 in TBS-T	Western Blot
anti-rat-HRP	Goat		Sigma	Purified rat IgG	1:10000 in TBS-T	Western Blot
anti-GFP	Rabbit	Polyclonal	Abcam	ab290	Undiluted	X-ChIP

For the dTALE-ChAP GFP-Trap®_A beads (Chromotek) were used. This are anti-GFPV_HV coupled to agarose beads.

3.3.6. Size standards

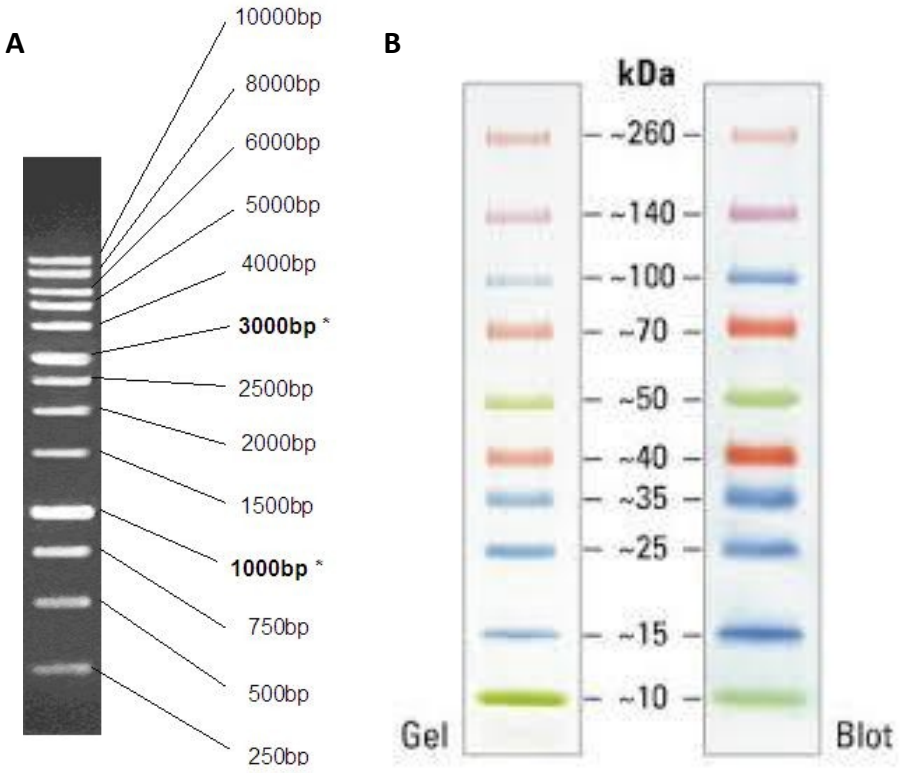

Figure 5: DNA and protein size standards. For Agarose gels the DNA size standard GenLadder 1kb (Genaxxon bioscience) was used **(A)**. For SDS-PAGE and Western Blotting the Spectra™ Multicolor Broad Range Protein Ladder (Thermo Fisher Scientific) was used **(B).**

3.3.7. Enzymes and Kits

Table 8: Enzymes and kits used in this work

Enzyme/ Kit	Manufacturer
Taq DNA Polymerase	New England Biolabs
pENTR™/D-TOPO® Cloning Kit	Thermo Fisher Scientific
Gateway® LR Clonase enzyme mix	Thermo Fisher Scientific
Gateway® BP Clonase enzyme mix	Thermo Fisher Scientific
Restriction Endonucleases	Thermo Fisher Scientific
RiboLock RNase Inhibitor	Thermo Fisher Scientific
RevertAidTM H Minus Reverse Transcriptase	Thermo Fisher Scientific
GeneJET Gel Extraction Kit	Thermo Fisher Scientific
RNeasy Plant Mini Kit	Qiagen
Sequencing Grade Modified Trypsin	Promega
Endoproteinase Lys-C Sequencing grade	Roche
Maxima® SYBR Green qPCR Master Mix (2X)	Thermo Fisher Scientific
MinElute Reaction Cleanup Kit	Qiagen
KOD Hot Start	Novagen

3.4. Buffers and solutions for the work with bacteria

3.4.1. Growth media

Luria-Bertani broth (LB)	25 g/l	LB media (liquid/ solid, premixed by Roth) ddH_2O autoclaving

For the production of plates, the autoclaved media was cooled down to a temperature below 60 °C. Then the respective antibiotics were added. The media was poured into petri dishes (8 cm, round shape, 25 ml media/dish). After the media was solid, the petri dishes were closed and stored on 4 °C.

3.4.2. Media and buffers to obtain chemically competent cells

SOB	20 g/l	Bacto tryptone
	5 g/l	Yeast extract
	0.5844 g/l	NaCl
	0.1864	KCl
	After autoclaving add filter sterilized	
	10 mM final concentration $MgCl_2$	
	10 mM final concentration $MgSO_4$	
RF1	100 mM	RbCl
	50 mM	$MnCl_2$
	30 mM	$C_2H_3KO_2$
	15 % (v/v)	Glycerol
	pH 5.8 with Acetic Acid	
	sterilize by filtration	
RF2	10 mM	MOPS
	10 mM	RbCl
	75 mM	$CaCl_2$
	pH 6.1 - 6.4 with HCl or KOH	
	sterilize by filtration	

3.5. Buffers and solution for work with plants

½ MS agar	2.15 g/l	Murashige and Skoog basal salt mixture (Sigma - Aldrich)
	pH 5.7 with KOH	
	8 g/l	Phytoagar (Duchefa)
	Autoclaving	

The media was cooled down after autoclaving to a temperature below 60 °C. Then it was supplemented with 5 µg/ml BASTA and poured into petri-dishes (12 x 12 cm, square shaped, 50 ml media/plate).

Liquid media	10 % (v/v)	10X Medium Stock Solution
	0.3 % (v/v)	1 M MES pH (5.8)
	0.5 % (w/v)	sucrose
	2 mM	KNO_3*
	1 mM	NH_4NO_3*
	1 mM	glutamine
	2 mM	K_2SO_4
	4 mM	$CaCl_2$
	1 mM	$MgSO_4$
	(5 µg/ml BASTA)	

*For ^{15}N media these ingredients were used in the heavy ^{15}N form

10X Medium Stock	0.3 % (v/v)	Microelement Stock Solution
	0.5 % (v/v)	Solution E
	375 mM	KH_2PO_4
	0.1 mM	Phosphate buffer

Microelement Stock Solution	100 mM	H_3BO_3
	100 mM	$MnSO_4$
	36 mM	$ZnSO_4$
	5 mM	KI
	1 mM	Na_2MoO_4
	0.1 mM	$CoCl_2$
	0.1 mM	$CuSO_4$

Solution E	10 mM	$FeSO_4$
	10 mM	Na_2EDTA

Phosphate Buffer	39 ml	200 mM NaH_2PO_4
	61 ml	200 mM Na_2HPO4

3.5.1. Stable transformation of *A. thaliana*

Infiltration media	5 % (w/v)	sucrose
	0.01 % (v/v)	Silwett
	0.5 g/l	$MgSO_4$

3.5.2. Transient expression of proteins in *Nicotiana benthamiana*

Infiltration media	1 % (v/v)	1M MES KOH (pH 5.6)
	0.1% (v/v)	200 mM Acetosyringon in DMSO
	0.33 % (v/v)	3 M $MgCl_2$

3.6. Buffers and solutions for work with RNA

DEPC water	0.1 % (v/v)	Diethylpyrocarbonate

	Stirred over night autoclaved 2 times to inactivate DEPC	
dNTPs	10 mM	dATP
	10 mM	dTTP
	10 mM	dGTP
	10 mM	dCTP

3.7. Buffers and solutions for work with DNA

3.7.1. Extraction of plasmid DNA (alkaline lysis)

Mini 1	50 mM	Tris/ HCl pH 8.0
	10 mM	EDTA
	After autoclaving add	
	20 mg/ml	RNAse A
Mini 2	0.2 M	NaOH
	1 %	SDS
Mini 3	29.44 % (w/v)	KCH_3COO
	11.4 (v/v)	glacial acetic acid
	final pH 5.5	

3.7.1.1. Extraction of genomic DNA from *Arabidopsis thaliana* seedlings

Edwards Buffer	200 mM	Tris/ HCl pH 7.5
	250 mM	NaCl
	25 mM	EDTA
	0.5 % (w/v)	SDS

3.7.2. Agarose gel solutions

50X TAE-buffer	2 M	Tris
	1 M	acetic acid
	0.05 M	EDTA

For TAE buffer, 50X TAE was diluted by factor 50 with MQ

3.7.3. Buffer for agarose gel electrophoresis

DNA loading buffer	50 % (v/v)	glycerol
	0.2 M	EDTA
	0.05 % (w/v)	OrangeG

3.7.4. PCR solutions

dNTPs	10 mM	dATP
	10 mM	dTTP
	10 mM	dGTP
	10 mM	dCTP

3.8. Buffers and solutions for work with proteins

3.8.1. Extraction buffer

2x SDS sample-buffer	120 mM	Tris/HCl pH 6.8
	20 % (v/v)	glycerol
	4 % (v/v)	SDS
	0.04 %	bromphenol blue
	10 % (v/v)	ß-mercaptoethanol

3.8.2. SDS-page

Bottom buffer	1 M	Tris-HCl (pH 8.8)
	0.27 % (v/v)	SDS
	Filtered to 0.45 µm filter	
Upper buffer	0.25 M	Tris-HCl pH 6.8
	0.2 % (v/v)	SDS
	Filtered through a 0.45 µm filter	
10 % running gel	2 ml	30 % acrylamide solution
	1.7 ml	H_2O
	2.25 ml	Bottom buffer
	50 µl	10 % (w/v) Ammonium persulfate
	4 µl	TEMED
4.5 % stacking gel	0.3 ml	30 % acrylamide solution
	0.7 ml	H_2O
	1 ml	Upper buffer
	10 µl	10 % (w/v) Ammonium persulfate
	2 µl	TEMED

3.8.3. Coomassie staining

Staining solution	10 % (v/v)	acetic acid
	45 % (v/v)	ethanol
	0.25 (w/v)	Coomassie brilliant blue R250
Destaining solution	10 % (v/v)	acetic acid
	30 % (v/v)	ethanol

3.8.4. Western blot

10X Running buffer	250 mM	Tris
	1.94 M	glycine
	1 % (v/v)	SDS
1X Running buffer	10 % (v/v)	10X Running Buffer
10X Transfer buffer	250 mM	Tris
	150 mM	glycine
1X Transfer buffer	10 % (v/v)	10X transfer buffer
	10 % (v/v)	ethanol

3.8.5. Immunodetection

10X TBS	0.5 M	Tris-HCl (pH 7.4)
	1.5 M	NaCl
1X TBS	10 % (v/v)	10X TBS
1X TBS-T	10 % (v/v)	10X TBS
	0.1 % (v/v)	Tween20
Blocking solution	5 % milk powder dissolved in TBS-T	

3.9. Buffers and solutions for X-ChIP and dTALE-ChAP

3.9.1. X-ChIP

Phosphate Buffer
Mixed to pH 7 in the final solution
- 200 mM NaH_2PO_4
- 200 mM Na_2HPO4

MC buffer	10 mM	phosphate buffer
	50 mM	NaCl
	100 mM	sucrose
Master-M-Buffer	10 mM	phosphate buffer
	100 mM	NaCl
	10 mM	ß-mercaptoethanol
	Roche cOmplete™Tablets EDTA free, 1 tablet/50 ml	
M1 Buffer	15 ml/130 ml	2-methy-2-4-pentanediol
	115 ml/ 130 ml	Master-M-Buffer
M2 Buffer	10 mM	$MgCl_2$
	0.5 %	Triton X-100
M3 Buffer	100% Master-M-Buffer	

3.9.2. dTALE-ChAP

HONDA buffer	20 mM	HEPES KOH pH 7.4
	10 mM	1 M $MgCl_2$
	440 mM	Sucrose
	1.25 % (w/v)	Ficoll
	2.5 % (w/v)	Dextran T40
	0.5 % (v/v)	NP40 IGEPAL CA630
	5 mM	DTT
	Roche cOmplete™Tablets EDTA free, 1 tablet/50 ml	
Nuclei Lysis buffer	50 mM	Tris-HCl pH 8
	10 mM	EDTA pH 8
	1 % (w/v)	SDS
	Roche cOmplete™Tablets EDTA free, 1 tablet/50 ml	

IP Dilution buffer	16.7 mM	Tris-HCl pH 8
	1.2 mM	EDTA pH 8
	167 mM	NaCl
	1.1 %	NP40 IGEPAL CA630
	Plant Protease Inhibitor Roche complete without EDTA (Sigma - Aldrich) 1 tablet per 50 ml	
Beads Washing buffer	20 mM	Tris-HCl pH 8
	150 mM	NaCl
	2 mM	EDTA pH 8
	1 %	NP40 IGEPAL CA630
	Plant Protease Inhibitor Roche complete without EDTA (Sigma - Aldrich) 1 tablet per 50 ml	
UTU	6 M	Urea
	2 M	Thiourea
	Solved in 10 mM Tris-HCl pH 8	
Reduction buffer	6.5 mM	DTT
Alkylation buffer	27 mM	iodoacetamide

3.9.3. FASP Buffers

UA	8 M	urea
	Solved in 0.1 M Tris-HCl pH 8.5	
UB	8 M	urea
	Solved in 0.1 M Tris-HCl pH 8	
ABC	0.05 M iodoacetamide in UA	

3.10. Plant Growth conditions

Liquid culture in Phytochamber *Arabidopsis thaliana*	constant light 22 °C, 80 rpm
½ MS plates in Percival	16 h light 22 °C
Greenhouse *Arabidopsis thaliana*	16 h light 18 °C day / 15 °C night 55 - 60 % humidity
Nicotiana benthamiana	14 h light 23 °C day / 20 °C night 60 % humidity

3.11. Machines

Thermomixer 5436	Eppendorf
Mixer Uzusio VTX 3000L	LMS
Micro Centrifuge	Carl Roth
Centrifuge 5417 R	Eppendorf
SILAMAT® S6	ivoclar vivadent®
Incubator Inova 44	New Brunswick Scientific
Centrifuge 5810 R	Eppendorf
SpeedVac	Heraeus Instruments
CFX384™ Real-Time System	Bio-Rad
PeqStar96 thermocycler	VWR
E220 evolution	Covaris
Sorvall RC6+ centrifuge	Thermo Fisher Scientific
Unimax 1010 shaker	Heidolph
Rotating wheel	LABINCO
MR Hei-Mix	Heidolph
PowerPac™ Basic	Bio-Rad
S@femate 1.2	BIOAIR
Ultrospec 3100 pro	Amersham Biosciences
NN-CS894	Panasonic
Rollordrum™	New Brunswick Scientific
Amersham Imager 600	GE
Eclipse 90 i	Nikon
TCS SP8	Leica Microsystems
Perfect Blue™ Gelsystem	Peqlab

3.12. Software

ImageJ	Wayne Rasband, National Institutes of Health
ApE - A plasmid editor	M. Wayne Davis
Microsoft Office 16.16	Microsoft Corporation
Adobe Reader IX	Adobe Systems Software Ireland Limited
Adobe Illustrator CC2018	Adobe Systems Software Ireland Limited
Leica Application Suite X	Leica Microsystems GmbH
Leica Application Suite AF Lite	Leica Microsystems GmbH

3.13. Online resources

PubMed and Blast	https://www.ncbi.nlm.nih.gov/
TAIR	https://www.arabidopsis.org/
ARAPORT	https://www.araport.org/
PlantPan2	http://plantpan2.itps.ncku.edu.tw/
PANTHER	http://go.pantherdb.org/webservices/go/overrep.jsp
COGE browser	https://genomevolution.org/coge/

3.14. External devices

GATC- Biotech (Germany)

4. Methods

4.1. Molecular-biological methods

4.1.1. Preparation of competent cells

4.1.1.1. Preparation of chemically competent *Escherichia coli* cells

Competent cells were produced based on Hanahan (1983); Hanahan, Jessee, and Bloom (1991). Cells of a glycerol stock were stroked out on a LB-plate and incubated on 37 °C over night. 5 ml of LB liquid media were inoculated with a colony of bacteria from the plate and incubated on 28 °C for 6 h. 400 ml SOB was inoculated with 1 ml of the pre-culture and kept on 25 °C until OD_{600} 0.45 - 0.55. The culture was cooled down on ice cold water for 15 min and centrifuged (2500 g, 10 min, 4 °C). The pellet was resuspended in 40 ml RF1 and kept for 1 h on ice water. After the incubation the culture was centrifuged (2500 g, 10 min, 4 °C). The pellet was resuspended in 8 ml RF2 and kept for additional 15 min on ice cold water. The cells were aliquoted in 50 µl and immediately frozen in liquid nitrogen. The cells were tested for resistance against Ampicillin, Kanamycin, Spectinomycin and Gentamycin was tested. In addition, the transformation efficiency was determined by transformation of pUC19 DNA. The cells were stored on -80°C.

4.1.1.2. Preparation of chemically competent *Agrobacterium tumefaciens* cells

Cells of a glycerol stock were stroked out on LB (Rif/Gent) and were incubated on 28 °C for 2 days. 5 ml LB (Rif/Gent) was inoculated with one colony and kept over-night at 28 °C. 150 µl of the over-night culture were transferred into 150 ml LB media and incubated on 28 °C until OD_{600} 0.5 - 0.8. The culture was cooled on ice cold water for 15 min. Afterwards it was centrifuged for 5 min (4000 g, 4°C). The pellet was resuspended in 100 ml ice cold 0.15 M $CaCl_2$ and centrifuged for 5 min (4000 g, 4°C). The pellet was resuspended in 10 ml 20 mM $CaCl_2$. The cells were distributed into 100 µl aliquots that were frozen immediately in liquid nitrogen and stored on -80°C.

4.1.2. Transformation of chemically competent cells

4.1.2.1. Transformation of chemically competent *Escherichia coli* cells

50 µl aliquots of cells was thawed on ice. 0.1 - 1 µg of DNA was added. The cells were incubated on ice for 15 min. Afterwards, a heat shock of 42 °C was applied for 1 min. After the heat shock, the cells were kept on ice for additional 10 min. 1 ml of LB was added and the cell were incubated for 1 h at 37 °C on a shaker. The cells were centrifuged (30 s, full speed). The supernatant was discarded and the pellet was resuspended in the remaining supernatant. The cells were stroked out on a LB plate with the respective antibiotics and grown over night at 37 °C.

4.1.2.2. Transformation of chemically competent *Agrobacterium tumefaciens*

1-5 µg of vector DNA was added into an aliquot of cells which was thawed on ice. After 15 min of incubation, the cells were transferred for 5 min into liquid nitrogen and 5 min on 37 °C. For recovery, the cells were kept for 5 min on ice. Then 1 ml LB media was added and the cells were placed on a rotating wheel at 28 °C for 2-4 h. The cells were pelletized for 30 s at full speed and stroked out on a LB agar plate with antibiotics. The cells were grown on 28 °C for 2 days.

4.1.3. Verification of the *Agrobacterium tumefaciens* transformation

To verify a successful transformation of *Agrobacterium tumefaciens*, the transformed vector DNA was extracted by alkaline lysis (see 4.1.5.1). 5 µl of the extracted vector DNA were re-transformed into *Escherichia coli* (see 4.1.2.1). Subsequently the vector DNA was extracted from the *Escherichia coli* cells (see 4.1.5.1) and analyzed by enzymatic restriction (see 4.1.6).

4.1.4. Generation of bacterial glycerol stocks

For long time storage of *Escherichia coli* and *Agrobacterium tumefaciens* cells glycerol stocks were generated and stored at -80 °C. For an over-night culture 3 ml of LB media was inoculated, with 300 µl of a cell culture and kept on a rotating wheel (*Agrobacterium*

tumefaciens 28 °C/ *Escherichia coli* 37 °C). The next day, 800 µl of the cell culture were mixed with 1 ml autoclaved glycerol (60 %) and immediately frozen in liquid nitrogen.

4.1.5. Extraction of nucleic acids

4.1.5.1. Extraction of plasmid DNA (alkaline lysis)

5 ml LB media with the respective antibiotics was inoculated with a bacterial colony and incubated overnight on a rotating wheel at 37 °C. 2 ml of the culture were pelletized (30 s, 14000 rpm). The supernatant was discarded and additional 2 ml of the cell culture were pelletized on top of the pellet. The pellet was resuspended in 300 µl Mini 1 solution by vortexing. 350 µl Mini 2 solution was added and the tube was inverted 4 times. 350 µl Mini 3 solution was added and the tubes were inverted for additional 4 times. The tubes were centrifuged (10 min, full speed). The supernatant was transferred into a new tube and mixed with 500 µl chloroform isoamyl alcohol (24:1) by vortexing. The tubes were centrifuged (full speed, 10 min). After centrifugation 900 µl of the upper phase was mixed with ice cold isopropanol and inverted 4 times. The tubes were incubated for 20 min at -20 °C. The precipitated DNA was pelletized (full speed, 15 min, 4 °C). The DNA pellet was washed two times with cold ethanol (70 % (v/v)). The pellet was air dried at room temperature for 15 min and resuspended in 50 µl MQ. The resuspended DNA was heat treated 65 °C for 10 min to deactivate DNase.

4.1.5.2. Extraction of plasmid DNA (midi prep)

To extract plasmid DNA in higher purity and quantity, the extraction was executed with the GeneJET Gel Extraction Kit (Thermo Fisher Scientific) according to the kits manual.

4.1.5.3. Extraction of RNA from *Arabidopsis thaliana* seedlings

The plant tissue was frozen in liquid nitrogen. 60 mg of each sample was transferred into a 1.5 ml micro reaction tube together with 2-4 heat sterilized glass beads. Each sample was placed three times on a silamat shaker for 8 s. Between the shaking, the samples were cooled in liquid

nitrogen. After sample disruption, the RNA was extracted with the RNeasy Plant Mini Kit (QIAGEN) after the manufacturer's instruction. Deviating from the manual, the elution step was done with 3 times 30 µl RNase free water.

4.1.5.4. Extraction of genomic DNA from *Arabidopsis thaliana* seedlings

150 mg of plant tissue was harvested and placed with 2-4 heat sterilized glass beads (1.25 - 1.65 mm) in 1.5 ml micro-reaction tube. The tubes were immediately placed in liquid nitrogen. The tissue was mechanically disrupted with a silamat shaker three times for 8 s. Between the shaking, the samples were cooled in liquid nitrogen. The grinded plant tissue was resuspended in 300 µl Edwards buffer and incubated on 65 °C for 10 min. The samples were centrifuged (10 min full speed). The supernatant was transferred into a new tube and the DNA was precipitated by adding of 300 µl isopropanol. The samples were inverted 4 times and centrifuged (full speed, 30 min, 4 °C). The pelletized DNA was washed 2 times with 80 % ethanol. And dissolved in 50 µl MQ. Genomic DNA was stored on -20 °C.

4.1.6. Restriction of plasmid DNA

For the restriction of plasmid DNA restriction enzymes by Thermo Fisher Scientific were used according to the manufactures manual. 1 µl of vector DNA were mixed with 0.2 µl of enzyme and 2 µl of the respective buffer. This mixture was diluted with 17.5 µl of MQ and kept on 37 °C for 1 h. The conditions for enzymatic digestions with more than one enzyme were calculated with the manufacturer's online tool:

https://www.thermofisher.com/de/de/home/brands/thermo-scientific/molecular-biology/thermo-scientific-restriction-modifying-enzymes/restriction-enzymes-thermo-scientific/double-digest-calculator-thermo-scientific.html

4.1.7. DNase digestion after RNA extraction

All steps were performed at room temperature. DNase I (Thermo Fisher Scientific) was used with the included buffer. To the 90 µl of eluted RNA, 10 µl of buffer were added. 5 units of

DNase I were added to the reaction. The samples were mixed by inverting the tube four times. The samples were incubated for 1h at 37 °C. 100 µl of isopropanol were added and the samples were stored over night at -20 °C. The next day the RNA was pelletized (30 min, full speed, 4 °C). The pellet was washed 2 times with 500 µl ethanol 80 % (diluted in DEPC water). Between the washing steps the samples were centrifuged (10 min, full speed, 4 °C). After the second washing step, the liquid was removed with a pipet tip. After an additional centrifugation of 5 min the remaining liquid was removed. The pellet was air dried for 2 min and resuspended in 30 µl preheated DEPC water (65 °C). The samples were incubated for 1 h on ice. After and 3 min incubation step on 65 °C the samples were stored at -80 °C.

4.1.8. Reverse transcription, generation of cDNA

200 - 450 ng of RNA were diluted with DEPC water to a total volume of 12.5 µl. 1 µl of oligodT primer was added. The samples were mixed and incubated for 5 min at 70 °C. After a incubation of 1-2 min on ice 6.5 µl of master mixed were added to the sample. The master mix was pre-prepared of 4 µl RT buffer (Thermo Fisher Scientific), 2 µl dNTPs (10 mM) and 0.5 µl ribonuclease inhibitor (Ribolock Thermo Fisher Scientific). The samples were mixed with the master mix and incubated for 5 min on 37 °C. After 1-2 min recovery on ice 1 µl reverse transcriptase (Thermo Fisher Scientific) was added and the samples were kept for 60 min at 42 °C and 10 min at 70 °C. The cDNA was stored at -20 °C.

4.1.9. Polymerase Chain Reaction (PCR)

According to the purpose of the PCR product different polymerases were used. For analytical PCRs the Taq Polymerase of New England Biolabs was used. For the amplification of DNA fragments that were used for cloning the KOD Hot Start DNA Polymerase (Novagen) was used due to its high fidelity. The thermocycler conditions and the composition of the reaction mix were assigned to the respective PCR reaction individually.

4.1.10. Quantitative Reverse Transcriptase and quantitative PCR (qRT-PCR & qPCR)

For all qPCR and qRT-PCR approaches the Thermo Scientific Maxima® SYBR Green Master Mix was used according to the manufacturers manual. Deviating from the instructions, the reaction volume was halved. The proportions of the components were not changed. Quality of the amplificated fragments was verified with a melting curve. The data was evaluated after the ΔΔCt method. The primer efficiencies were assessed, but not included in the calculation.

4.1.11. Cloning of dTALEs

All dTALE vectors used in this work were cloned and provided in the group of Prof. Dr. Thomas Lahaye (Dr. Robert Morbitzer, University of Tuebingen, General Genetics).

4.1.12. Cloning by homologous recombination

Cloning by recombination was done as described by Jacobus and Gross (2015). The insert was amplified by PCR with primers, that were designed to make a 20 bp overlap complementary to the backbone. A linear fragment of the backbone was amplified with primers that made a 20 bp overlap into the insert. The linear DNA fragments were purified by agarose gel electrophoresis and transformed into *Escherichia coli.*

4.1.13. Gateway™ Cloning

Gateway™ Cloning is a cloning method based on the recombination system of phage λ. The method was invented and is sold by Invitrogen. The basis of Gateway™ Cloning are the attachment sites and two proprietary enzyme mixes (LR and BP Clonase).

4.1.13.1. pENTR/D-TOPO® Cloning

The pENTR reaction was done to generate an entry vector for Gateway™ Cloning. The insert, that should be implemented into the entry vector, was amplified in a PCR. The primers were designed to attach a CACC sequence to the 5’ end of the insert. The pENTR reaction was done

as described by the manufacturer. 1 µl of the PCR mix was mixed with 0.5 µl of salt solution and 0.5 µl pENTR/D-TOPO® cloning mix. The complete reaction was incubated at room temperature and subsequently placed on ice. The complete reaction was transformed into *Escherichia coli* as described in 4.1.2.1.

4.1.13.2. LR-Reaction

The LR-Reaction was used to generate an expression clone based on an entry clone. The reaction was done as described in the manufacturer's manual, only the volumina were scaled down. 0.5 µl of Entry clone, destination vector, buffer, Tris/HCl (10 mM, pH 8) and LR Clonase were mixed and incubated over night at room temperature. The complete reaction was transformed into *Escherichia coli* as described in 4.1.2.1.

4.1.13.3. BP-Reaction

The reaction was done as described in the manufacturer's manual, only the voluminal were scaled. 2 µl of PCR product, 1 µl pDONR Vector, 2 µl BP Clonase Buffer and 3 µl TE Buffer (pH8) were mixed and incubated over night at room temperature. The reaction was heat treated for 10 min at 60 °C. 5 µl of the reaction were transformed into *Escherichia coli* as described in 4.1.2.1.

4.1.14. Denaturing extraction of nuclear proteins of *A. thaliana* seedlings

Proteins were purified from nuclei as described in in the dTALE-ChAP protocol. The GFP-tagged proteins were precipitated with a GFP-Trap®_A. The proteins were eluted as described in the manufacturer's instructions:

(https://www.chromotek.com/fileadmin/user_upload/pdfs/Manuals/GFP-Trap_A__manual_.pdf).

The extracted proteins were subsequently analyzed by Western blot.

4.2. Cell-biological methods

4.2.1. Cultivation of *Escherichia coli*

For the cultivation on LB plates, *Escherichia coli* cells in solution were stroked out either with glass beads or a pipet tip. Solid LB media was used with the respective antibiotic. The plates were incubated on 37 °C over-night. The next day, the plates were stored at 4 °C for a maximum of 14 days.

For the cultivation in liquid LB media, a single colony, 5 µl of cells in liquid culture or a part of a glycerol stock in the size of a half pea, was transferred into a glass tube with 5 ml LB with the respective antibiotics. The glass tube was kept overnight on 37 °C on a rotating wheel. The next day, the glass tubes were transferred on 4 °C for short time storage.

4.2.2. Cultivation of *Agrobacterium tumefaciens*

For the cultivation on LB plates, *Agrobacterium tumefaciens* cells in solution were stroked out either with glass beads or a pipet tip on solid LB plates with the respective antibiotics. The plates were incubated for 2 days on 28 °C. After the incubation, the plates were stored at 4 °C for a maximum of 14 days.

For the cultivation in liquid LB media, a single colony, 10 µl of cells in liquid culture, or a pea-sized part of a glycerol stock was transferred into 5 ml of LB media. The cultures were incubated over-night on 28 °C on a rotating wheel. The next day, the tubes were transferred on 4 °C for short time storage.

4.2.3. Transformation of *Arabidopsis thaliana* plants

5 ml LB with the respective antibiotics were inoculated with *Agrobacterium tumefaciens.* The culture was incubated over-night at 28 °C on a rotating wheel. 400 µl of this pre-culture was transferred into 200 ml of LB media. For the 200 ml culture, the antibiotic concentration was reduced by half. The next day, the big culture was centrifuged (4000 g, 20 min, 4 °C). The pellets were resuspended in infiltration media. Flowers of *Arabidopsis thaliana* were dipped into the bacterial solution and kept in a tray with a hood over-night. Plants were dipped 3

times with of seven days in between. The seeds of the transformed plants were collected and sawed for BASTA selection. BASTA applied by spraying on 10 days old seedlings. BASTA was applied 3 times with a recovery phase of three days in between the treatments.

4.2.4. Transient expression of proteins in *Nicotiana benthamiana*

5 ml selective LB media was inoculated with *Agrobacterium tumefaciens.* The culture was incubated over-night at 28 °C. The next day *Nicotiana benthamiana* plants were watered and kept in a tray with a hood 2-4 h prior to the infiltration. 0.5 ml of the pre-culture was used, to inoculate 3 ml of LB media. The culture was kept for 4 h at 28 °C. The cells were pelletized (15 min, 4000 g, 4°C). The pellets were resuspended in 1ml pre-cooled infiltration media. The resuspended cells were mixed with the same volume of p19, in case of co-transfection the cells were mixed in equal volumes. The infiltration solutions were kept for at least 1 h on ice. 500 µl of *Agrobacterium tumefaciens* infiltration solution was infiltrated into a *Nicotiana benthamiana* leaf. Protein expression was analyzed by fluorescent confocal microscopy after 2 - 3 days.

4.2.5. Fluorescence Activated Cell Sorting Analysis of Protoplasts

Protoplasts were removed of the 96 well plate after promoter reporter assays and collected in in 1.5 ml micro reaction tube. The proportion of fluorescing protoplasts in 5000 - 10000 total cells was counted in a CytoFLEX (Becton Dickinson) FACS machine.

4.2.6. Microscopy

4.2.6.1. Microscopical analysis of transiently transformed Protoplasts

The transiently transformed protoplasts were pipetted with a cut pipet tip onto a microscope slide. For DEX-treatment, 10 µM DEX, solved in 0.1 % ethanol was added before cover slip was placed carefully on the sample. The samples were analyzed on a Nikon Eclipse 90i fluorescence microscope.

4.2.6.2. Microscopical analysis of transiently transformed tobacco leaves

Leave disks were extracted with the backside of a 5 ml pipet tip of transiently tobacco leaves a placed on a microscope slide. Either 10 µM DEX solution or MQ for mock treatment was dropped onto the leave. The sample was covered with a coverslip and excessive air was removed by pressing the coverslip onto the leave. By pressing the coverslip, the DEX solution was infiltrated into the intercellular space. Pictures were taken with a Leica TCS SP8 confocal microscope.

4.2.6.3. Microscopical analysis of transgenic *Arabidopsis thaliana* roots

The seedlings were grown on ½ MS plates. The seedlings were carefully removed from the plate after 10 - 14 days. The seedlings were placed into a 1.5 ml micro-reaction tube with 10 µM DEX solution (0.1 % Ethanol). After the incubation time of 1 h, the seedlings were transferred on a microscopical slide. The roots were cut and the rest of the seedling was discarded. Pictures were taken with a Leica TCS SP8 confocal microscope.

4.3. Physiological methods

4.3.1. Seed surface sterilization

Seeds were placed in a 1.5 ml micro reaction tube. The tube was placed in an exicator with an open lid. In the exicator, 50 ml of 12 % sodium hypochlorite was mixed with 1.5 ml of hydrochloric acid (37 %). The seeds were exposed to chloric gas for 6 h. The valve of the exicator was opened. The next day, the lid of the reaction tubes was closed.

4.3.2. Cultivation of *Arabidopsis thaliana*

4.3.2.1. Cultivation of *Arabidopsis thaliana* on soil

The seeds were resuspended in 0.1 % (w/v) phytoagar and stratified at 4 °C for 24 h. The next day the seeds were transferred with a pipet on soil. The trays were covered with a hood for the first week. The *Arabidopsis thaliana* plants were sowed on soil were all grown in the green house.

4.3.2.2. Cultivation of *Arabidopsis thaliana* on ½ MS plates

The surface sterilized seeds were transferred with an autoclaved tooth pick on ½ MS plates. The media contained 5 µg/ml BASTA for selection purposes. The plates were placed for 24 h on 4 °C in darkness. The next day the plates were transferred into a plant incubator (22 °C, 16 h light). After 10 - 14 days, the plants were used for further experiments.

4.3.2.3. Cultivation of *Arabidopsis thaliana* in liquid media

Arabidopsis thaliana seedlings were grown in liquid media to be labeled with $^{14}N/^{15}N$. The experimental procedure was adapted from Dautel (2016); Dautel, Wu, Heunemann, Schulze, and Harter (2016); Kierszniowska, Seiwert, and Schulze (2009). Surface sterilized seeds, were placed in 1 ml of liquid media, either containing ^{14}N or ^{15}N as nitrogen source. The tubes were kept over-night on 4 °C. The next day, the seeds were resuspended and transferred in a 250 ml Erlenmeyer flask with 50 ml liquid media with the corresponding nitrogen isotope. BASTA was added to a final concentration of 5 µg/ml. The seedlings were kept on a shaker (80 rpm) in constant light 22 °C. After 10 days, the media was exchanged into media without BASTA. Every treatment/ sample was labeled reciprocally. Unlabeled approaches were performed the same way, simply ^{14}N was used as nitrogen source.

4.3.3. Cultivation of *Nicotiana benthamiana*

Seeds were grown on soil for 14 days. The 14 day old seedlings were separated into single pots. The *Nicotiana benthamiana* plants were grown for 2 -3 additional weeks in the green house. The conditions for tobacco were set to 23 °C day, 20 °C night, 14h light, 60 % humidity.

4.3.4. Protoplast transformation for microscopy

Protoplast transformation for microscopy was executed by the transformation unit of the ZMBP as described in Schutze, Harter, and Chaban (2009).

4.3.5. Protoplast transformation for promoter reporter assays

Arabidopsis thaliana cell culture protoplasts were provided by the plant transformation unit of the ZMBP (University of Tuebingen). The protoplast transformation was done as described in Mehlhorn, Wallmeroth, Berendzen, and Grefen (2018).

4.3.6. Promoter reporter assays

The promoter-reporter assays were performed as described in Wallmeroth, Anastasia, Harter, Berendzen, and Mira-Rodado (2017). For the treatments, 10 mM DEX was solubilized in 100 % ethanol and diluted with MQ to 10 µM/ 100 µM treatment solution. As control, 0.1% or 1 % ethanol solution was used. Flg22 was diluted in MQ (100 nM).

4.4. Biochemical methods

4.4.1. Agarose gel electrophoresis

1.5 % of agarose was diluted in 1x TAE buffer. The solution was cooked in a microwave. After the gel was cooled down to approximately 60 °C, it was poured into a gel chamber.

4.4.2. Extraction of DNA-fragments from agarose gels

For the extraction of DNA-fragments from agarose gels, the GeneJET Gel Extraction Kit (Thermo Fisher Scientific) was used according to the manufacturer's instructions.

4.4.3. Measurement of nucleic acid concentration in solutions

The concentration of nucleic acids in solution was measured with a NanoDrop 1000 Spectrophotometer (Thermo Scientific). For that, the NanoDrop was initialized with 1.5 µl of MQ and subsequently blanked with the buffer, in which the nucleic acids were dissolved. Each sample was measured three times. The average was used for calculations. The 260/280 nm ratio was used to check for protein impurifications (values should be over 1.8 (DNA) and 2.0 (RNA)). The 260/230 nm ratio was used to check for impurification of solvents, salts or carbohydrates (values should be > 2).

4.4.4. DNA-sequencing

Sequencing of vector DNA was done by GATC Biotech AG. The samples were prepared as requested by the service provider.

4.4.5. SDS-Polyacrylamide-Gel-Electrophoresis (SDS-PAGE)

SDS-PAGE was used to separate proteins according to their size in denatured conditions. The SDS-PAGE system of Bio-Rad was used to pour SDS gels of 1 mm thickness. The gels were placed in the running chamber. After the chamber was filled with SDS Running Buffer, the pockets were washed with a syringe. The samples were loaded with a Hamilton syringe. 5 µl of Spectra^{TM} Multicolor Broad Range protein ladder (Thermo Scientific) was used as size standard. The gels were run for 30 min at 100 V until the running band has reached the separation gel. Then the power was increased to 120 V.

4.4.6. Coomassie staining

To stain total protein the SDS-gels were stained with Coomassie brilliant blue R250. The gels were placed in staining solution on a shaker (30 min, room temperature). The staining solution was removed and the gels were incubated in destaining solution until the protein bands got visible. The destainer solution was exchanged three times. After destaining the gels were placed between two layers of Cellophan (Roth) and tried in a hood. Finally, the gels were scanned. Complete transfer of the proteins onto the membrane in the Western Blot (4.4.7) was verified by Coomassie staining of the gel after blotting.

4.4.7. Western Blot

The proteins were transferred by a wet blot onto a PVDF membrane (Immobilon-P®, Merck). This was done in the Bio-Rad western blot chamber. The membrane was initialized with methanol and paced with the gel, sandwiched between a layer of Whatman paper (GE-healthcare) between two sponges. The transfer was executed at 4 °C, either at 300 mA for 1.5 h or 65 mA overnight.

4.4.8. Immunodetection

The transferred proteins were detected with specific antibodies via luminometric measurements on the membrane. The membrane was blocked with 5 % milk powder dissolved in TBS-T. The blocking was done at 4 °C overnight on a shaker. After blocking the membrane was washed three times with TBS-T for 10 min. Then the first antibody was incubated for 1 h at 4 °C on the shaker. The antibody was removed and the membrane washed three times with TBS-T for 10 min. The second antibody was applied for 1 h at 4 °C on a shaker. The membrane was washed three times with TBS-T for 10 min. Then the membrane was stored in TBS-T at 4 °C until detection. Detection was done using the Amersham™ ECL™ Prime Western Blotting Detection Reagent (GE-Healthcare) according to the manufacturer's instructions in a CCD camera. Exposure in the camera was set to 1 min.

4.5. Bioinformatical methods

4.5.1. Prediction of transcription factor binding sites

PlantPan2 was accessed at http://plantpan2.itps.ncku.edu.tw/. The genomic sequence of the promoter was downloaded from https://www.arabidopsis.org/ and pasted into the online search tool.

4.5.2. Evaluation of MS data

MS data was evaluated by Prof. Dr. Waltraud Schulze (University of Hohenheim) as described in Pertl-Obermeyer et al. (2016).

4.5.3. Over-representation tests

For GO Term enrichment analysis, the online tool was accessed at: https://www.arabidopsis.org/tools/go_term_enrichment.jsp

The GO Term enrichment tool takes the genes, associated to the peptides that were identified in the dTALE-ChAP and compares the frequency of GO terms in the sample set, with the frequency of the same set of GO terms in the reference set. As reference set the *Arabidopsis thaliana* whole genome set is used. By this comparison it is possible to identify over- or underrepresented terms in the sample set.

4.6. X-ChIP

The *Arabidopsis thaliana* seedlings were treated directly in the media. DEX 10 µM (final concentration), mock (0.1 % ethanol final concentration) and/ or flg22 (100 nM final concentration) were used. The seedlings were kept in the Erlenmeyer flasks on a shaker at 80 rpm. After 1 h the seedlings were removed from the media and washed 2 times in MQ. Excessive water was removed by gently squeezing the seedling balls on a paper towel. The further procedure was performed as described in Hecker (2016). The tissue was fixed with 1 % formaldehyde in MC buffer. Vacuum was applied for 3x 1 min and 1 x 50 min. After fixation the tissue was frozen in liquid nitrogen. Tissue was grinded and ran through Miracloth (Merck Millipore) for 3 times. The pellet was washed several times. Chromatin was sheared to 200 - 500 bp fragments with a S220 focused-ultrasonicator (Covaris). An aliquot of every sample was saved on -80 °C before the precipitation was done. The dTALE-Chromatin complexes were precipitated with 2.5 µl a anti GFP antibody (Ab290, Abcam). To capture the precipitated proteins 40 µl of protein Agarose beads (Santa Cruz Biotechnology sc-2001) were incubated in the sample for 6 h. After proteolytic digestion with ProteinaseK over night, the Precipitated DNA was recovered with the Mini Elute PCR Purification Kit (Qiagen). DNA was also recovered from the input samples that were aliquoted prior to precipitation. Except the volume of ERC buffer that was adapted to higher sample volume, the kit was used as described in the manufacturer's instructions. The recovered DNA was eluted in 35 µl of elution buffer. The *pFRK1* levels were determined by qPCR. The qPCR data was evaluated as % of input.

4.7. dTALE-ChAP

The dTALE-ChAP protocol is based on protocol for nuclei protein isolation provided by Prof. Dr. Gordon Simpson (University of Dundee). It was further optimized for the dTALE-ChAP and used as described below. The protocol for sample preparation for MS was kindly provided by Prof. Dr. Waltraud Schulze (University of Hohenheim).

4.7.1.1. Growth and treatment of *Arabidopsis thaliana* seedling

The seedlings were grown as described in 4.3.2.3. For dTALE-ChAP trial 1 just ^{14}N media was used. For trial 2 and 3 ^{14}N and ^{15}N was used reciprocally as described. In trial 1 treatments were done as described in the X-ChIP protocol. In trial 2 and 3 the DEX treatment was done as described in the X-ChIP and with 30 min delay flg22/ mock was added into the media (1 h DEX treatment, 30 min flg22 treatment).

4.7.1.2. Formaldehyde crosslinking

After the treatment the seedlings were washed three times in MQ and the vacuum infiltrated with 1 % formaldehyde in MC buffer. The vacuum was applied 3 x for 1 min and 20 min continuously. The vacuum was gently removed and the cross-linking reaction was quenched by adding 2 M Glycine solution to the final concentration 0.125 M and application of vacuum for further 5 min. The formaldehyde treated seedlings were washed in water in a big beaker and, after removing the excess of water, were frozen in liquid nitrogen. Seedlings were ground in liquid nitrogen into fine powder and stored at -80°C until nuclei isolation.

4.7.1.3. Nuclei isolation

Flg22 treated and non-treated tissue was mixed in equal proportions (except for trial 1 were no labeling was done). ^{14}N labeled, flg22 treated tissue was mixed with non-treated tissue labeled with ^{15}N and *vice versa.* The grinded seedlings were distributed into 50 ml Falcon tubes. The Falcons were filled with seedling powder with 7.5 - 10 ml. The seedling powder was kept frozen all time until completely thawed in HONDA buffer. Three Falcon tubes were processed in parallel, the rest was stored in liquid nitrogen. The Falcon tubes with the resuspended seedling powder were stored on ice. After all Falcons tubes were processed, the

samples were ran through 2 layers of Miracloth (Merck Millipore) through a glass funnel into a new falcon. The Miracloth was equilibrated with HONDA buffer before it was placed in the funnel. The Miracloth was squeezed gently and rinsed in a 100 ml beaker with 50 ml of fresh HONDA buffer on ice. The extract of the beaker was rinsed through new two layers of Miracloth (pre-equilibrated with HONDA buffer). The Miracloth was squeezed gently on top of the funnel. The filtrates were distributed equally to six Falcon tubes. The Falcons tubes were filled up to 40 ml with HONDA buffer and inverted 4 times. The Falcons tubes were centrifuged (2000 g, 17 min, 4 °C). The supernatant was removed and the pellet resuspended in 2 - 5 ml HONDA buffer. The six pellets of one sample were pooled into a new 50 ml Falcon tubes. The Falcon tube was filled with new 40 ml of HONDA buffer. The Falcon tube was inverted four times and centrifuged (1500 g, 15 min, 4 °C). The washing step was repeated 2-3 times, until all green color of the pellet was removed.

4.7.1.4. Nuclei Lysis

The washed pellet was resuspended to a total volume of 4 ml with lysis buffer (including the pellet). The suspension was distributed to four milliTUBE 1ml AFA Fiber (Covaris). The chromatin was sheared in a S220 focused-ultrasonicator (Covaris). (PIP120, Duty 5, cycle burst 200, duration 150). After the sonification Protein LowBind tubes (Eppendorf) were used. The samples were transferred into the 1.5 ml tubes and centrifuged (16100 g, 15 min, 4 °C). The supernatants were pooled together into 15 ml Falcon tubes. The samples were diluted to 15 ml total volume by adding ChIP Dilution Buffer.

4.7.1.5. Immunoprecipitation

20 µl of GFP-Trap®_A was added per sample. (Beads pre-washed 3 times with Beads Washing Buffer). The beads were incubated in the sample over-night on 4 °C on a rotating wheel. The next day, the beads were pelletized by centrifugation (141 g, 3 min, 4 °C). It is important not to exceed centrifugal forces of 500 g, because the agarose beads can be damaged. The supernatant was carefully removed. The beads were resuspended in supernatant remains and pooled into a 15 ml falcon. The beads were washed 2 times with bead washing buffer and 2 times with bead washing buffer (without SDS). Between wash steps the beads were collected

by centrifugation (400 g, 2 min, 4 °C). After the last washing step, as much supernatant as possible was removed with a pipet tip without removing the beads.

4.7.1.6. In solution trypsin digestion

The protocol for in solution trypsin digestion was provided by Prof. Dr. W. Schulze (University of Hohenheim). It was used in dTALE-ChAP trial 1 and 2.

All steps were done at room temperature to reduce unwanted derivatization of amino acid side-chains by denaturants. The samples were dissolved in a small volume of UTU. The smallest volume possible for the complete resuspension of the beads was used. The pH of the solution was verified to be pH 8. The samples were incubated at room temperature for 30 min. Then they were sonicated in a water bath sonicater for 10 min. The beads were removed after centrifugation (12000 g, 10 min, room temperature). 2 µl of reduction buffer were added. Then 2 µl of alkylation buffer were added and the samples were incubated for 3 h at room temperature. 2 µl (1 µg) of Lys C were added and the samples were incubated for additional 3 h at room temperature. 0.8 µg of trypsin was added and the samples were incubated over night at 37 °C. The samples were centrifuged the next morning (12000 g, 10 min, room temperature), to remove any insoluble material. The samples were acidified with 2 % trifluoroacetic acid (approximately 1/10 volume) until pH 2 was reached. The samples were lyophilized in a Speed Vac (3-4 h) without heating. The samples were resolubilized, desalted with C_{18} stage tips and analyzed by Prof. Dr. Waltraud Schulze & Dr. Xuna Wu (University of Hohenheim) via mass spectrometry as described in Pertl-Obermeyer et al. (2016).

4.7.1.7. Detergent removal and Protein Digestion by FASP

For dTALE-ChAP trial 3, the samples were purified by FASP. The FASP protocol was based on the publication of Wisniewski, Zougman, Nagaraj, and Mann (2009) and was modified by Liangcui Chu (Labratory of Prof. Dr. Waltraud Schulze, University of Hohenheim). After Immunoprecipitation the proteins were eluted from the beads as described in the manufacturer's instructions:

(https://www.chromotek.com/fileadmin/user_upload/pdfs/Manuals/GFP-Trap_A__manual_.pdf).

Aberrant to the manufacturer's instructions, no bromphenol-blue was used in the buffer. 250 µl of buffer was used per sample to elute the proteins. The 250 µl were diluted with 2 ml of UA. The samples were ran over the size exclusion column in portions of 200 µl. Between the steps, the columns were centrifuged with 15 min at 14,000 g. After the complete sample was applied on the column, the column was washed two times with 250 µl UA. 150 µl of IAA solution was pipetted on the column. Columns were subsequently shaked with 600 rpm on a thermos-mixer for 1 min. Afterwards they were incubated in darkness for 30 min at room temperature. The column was washed two times with 150 µl UA. Following it was washed 3 times with 150 µl ABC. Between washing it was centrifuged (14,000 g, 15 min). The column was transferred on a new collection tube. 50 µl ABC was added (including 1.7 µl Trypsin). The columns were incubated over-night at room-temperature. The next day, the peptides were eluted 2 times with 40 µl ABC (centrifugation 14,000 g, 10 min). The Sample was acidified with 5-6 µl of trifluoroacetic acid (10 %) until pH 2 was reached. The eluted samples were desalted with C_{18} Stage Tips. Desalting was done as described in Szymanski, Kierszniowska, and Schulze (2013). MS analysis of the samples was done by Prof. Dr. Waltraud Schulze and Dr. Xuna Wu (University of Hohenheim) as described in Pertl-Obermeyer et al. (2016).

5. Results

5.1. Analysis of *FRK1* Regulation

5.1.1. Induction of *pFRK1* with flg22

FRK1 is strongly induced in response to MAMPs like flg22. Flg22 is perceived via the receptor FLS2 which is located in the plasma membrane (Delphine Chinchilla, Bauer, Regenass, Boller, & Felix, 2006). The flg22 signal is transduced via a MAP Kinase cascade into the nucleus and transcription of *FRK1* is activated. Since *FRK1* induction can be easily modulated by extracellular flg22 application and *FRK1* is not expressed in the absence of flg22, *FRK1* is an ideal gene to establish a method like the dTALE-ChAP. To determine the timepoint of the transcription start, when the transcription factors should be bound to the *FRK1* promoter (*pFRK1*), the time from flg22 treatment till transcription activation was tested in a qPCR experiment. *Arabidopsis* seedlings were treated with flg22 and transcript levels were measured via qPCR with *FRK1* and *Actin2* specific primers (Figure 6).

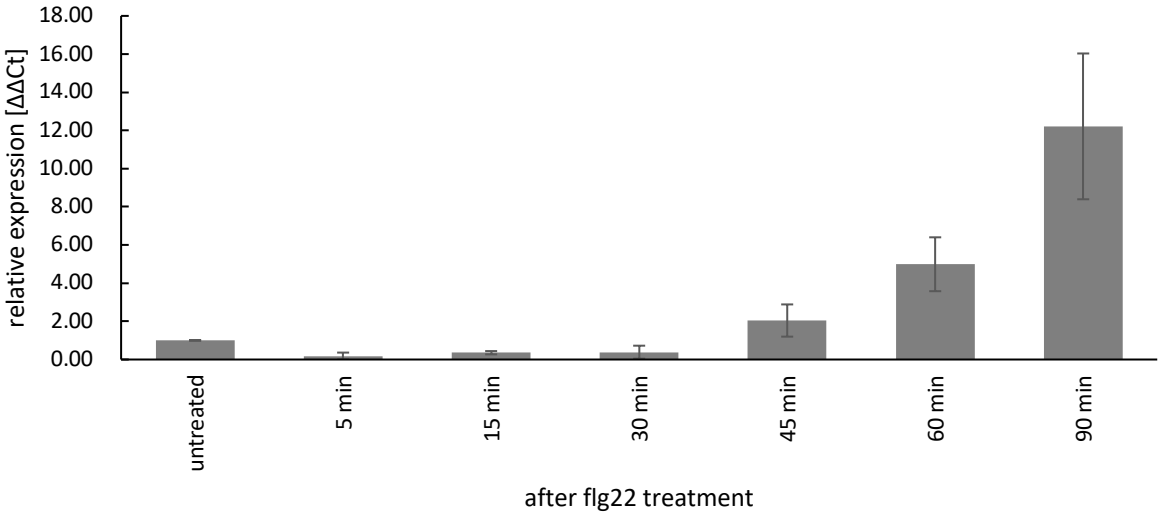

Figure 6: Transcript accumulation of *FRK1* is induced within 45 min after DEX treatment
Transcript levels of *FRK1* were detected in *A. thaliana* seedlings after DEX treatment over time. *Actin2* transcript levels were used for normalization. Error bars represent the standard deviation of three biological replicates.

It was possible to detect an elevated level of *FRK1* transcript 45 min after flg22 treatment. The detected transcript levels further increased until 60 min and 90 min. Mock treatment could not induce *FRK1* expression. In addition, induction was not possible in *fls2 Arabidopsis* lines **(**Supplementary figure 3 B**).** Minor differences between the qPCR runs, constant Ct values for the reference primers and primer efficiencies between 84 - 97 % in all three bio replicates validate the quality of the qPCR (Supplementary table 2 & Supplementary figure 3).

Therefore, I estimated the time point of transcription initiation between 30 min and 45 min after the flg22 treatment.

5.2. The dTALE-ChAP Workflow

The main goal of the thesis was the development of a method, by which proteins can be identified, that differentially bind to *pFRK1* in response to flg22. In the previous section it was determined how long the transcriptional activation of *FRK1* by an extracellular flg22 signal took. In this section the workflow of the dTALE-ChAP is explained. This new *in vivo* method will be applied for the first time in higher eukaryotes such as plants.

By Chromatin Immuno-Precipitation (ChIP) approaches, it is assayed whether a protein binds to a target DNA sequence. Backward analysis to identify the proteome bound to a DNA sequence is not possible by ChIP. For this kind of analysis Chromatin Affinity Purification (ChAP) would be the method of choice. By ChAP, chromatin fragments are precipitated and the chromatin-bound proteins are analyzed by mass spectrometry. The pitfall of ChAP approaches is the need of a bait protein that is known to bind to area of interest. However, this is not always the case. The designer TALE-ChAP (dTALE-ChAP) is independent of a known binding protein (Figure 7).

For the dTALE-ChAP, dTALEs are used to precipitate the DNA region of interest. The dTALEs were designed to bind to *pFRK1* and expressed in transgenic *A. thaliana* lines (Figure 7 1). The seedlings are grown in media containing ^{14}N or ^{15}N nitrogen isotopes. Because of an N-terminal attached GR-receptor, the dTALEs are localized in the cytosol in the absence of DEX. *pFRK1* is activated by flg22 treatment. The proteins that should be identified in the end, should be differentially associated with *pFRK1* upon flg22 treatment (Figure 7 1 cyan dots). In the control the proteins should not be present or at least to lower amounts. Upon DEX treatment

the dTALEs translocate into the nucleus and bind to *pFRK1.* After flg22 and DEX treatment, the plant tissue is fixed with formaldehyde (Figure 7 2). The tissue with the activated promoter, grown on ^{14}N containing media and the tissue of the control plants, grown on ^{15}N containing media, are mixed. The nuclei are purified and the chromatin is sheared using ultra sound (Figure 7 3). The dTALE - *pFRK1* - protein complexes are precipitated using a GFP-trap® (Figure 7 4). The proteins are released from the precipitate and analyzed by mass spectrometry (Figure 7 5). Because the plants were grown on either ^{14}N or ^{15}N containing media, in the MS analysis the origin of the identified proteins can be discriminated. By this metabolic nitrogen labeling, the qualitative and quantitative difference in the *pFRK1* associated proteome in its activated and inactivated states becomes visible.

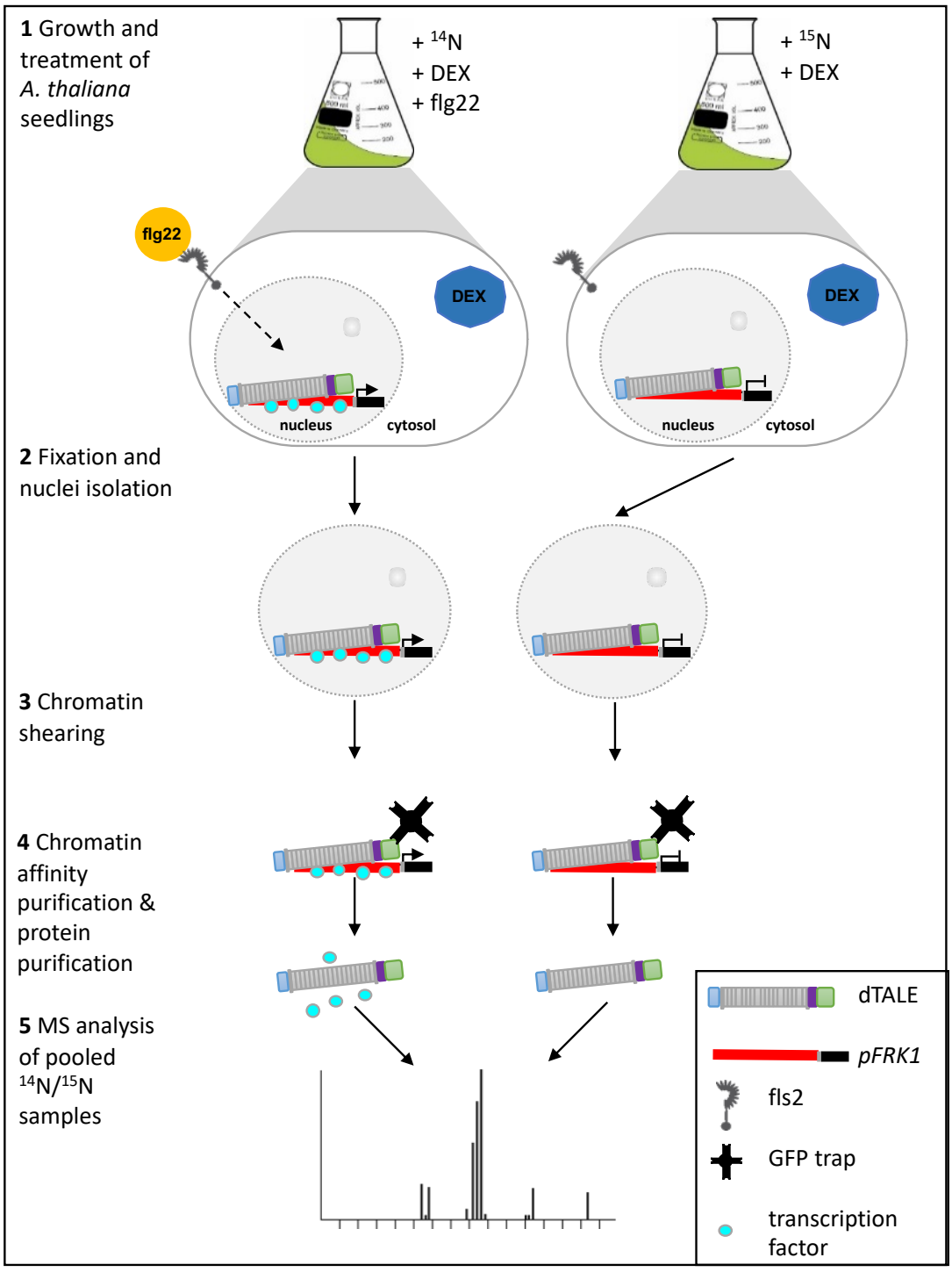

Figure 7: Workflow of the dTALE-ChAP approach

A. thaliana seedlings were grown in liquid media containing either ^{14}N or ^{15}N as nitrogen source **(1)**. The ^{14}N labeled seedlings are treated with flg22 and DEX. The ^{15}N labeled control seedlings are treated with DEX only. Flg22 treatment activates *pFRK1* and proteins that may differentially bind to the promoter (cyan dots). DEX treatment induces the translocation of the dTALEs from the cytosol to the nucleus and their binding to *pFRK1.* The plant tissue is fixed with formaldehyde and the ^{14}N and ^{15}N labeled samples are mixed **(2)**. The nuclei are purified and the chromatin is sheared **(3)**. The dTALE - *pFRK1* - protein complexes are precipitated with a GFP-trap® **(4)**. The proteins are purified analyzed by MS (5). Due to the nitrogen labeling, proteins associated with the inactive *pFRK1* can be discriminated in a quantitative manner from those associated with the flg22-activated *pFRK1.*

5.3. Experimental Settings for the dTALE-ChAP

5.3.1. Structure of the dTALEs and their binding sites in *pFRK1*

For the dTALE-ChAP, *pFRK1* specific dTALEs were designed (Figure 8 A). The backbone of the used dTALE is its DNA binding domain (TALE domain) (Figure 8 A grey). The TALE domain is assembled of tandem repeats, which define the TALE's target sequence (Boch et al., 2009; Moscou & Bogdanove, 2009). By reassembling the repeats, a dTALE can be designed to bind to a target sequence of choice (Morbitzer, Elsaesser, Hausner, & Lahaye, 2011). Six different dTALEs were designed for six binding sites in *pFRK1* and *FRK1*, respectively (Figure 8 B Supplementary figure 1): Two positions approximately 1 kb upstream of the transcription start (position A and B), two 0,5 kb upstream of the transcription start (B and C) and two 77 base pairs downstream of the transcription start (E and F) (Figure 8 B and Supplementary figure 1). The pairwise distribution of the six binding sites was intended to backup for the case, that one binding site might not be accessible for a dTALE, due to steric effects, chromatin status or other proteins that are already bound to the DNA. Although only fragments are precipitated, by distributing the dTALE binding sites over the complete promoter, a full coverage of the promoter was intended to be achieved (Figure 8 B).

The dTALE domain is bordered by different N- and C-terminal tags (Figure 8 A). A glucocorticoid receptor (GR) was fused to the N-terminus (Figure 8 A blue). The GR receptor was expected to retain the dTALE in the cytosol. Upon DEX treatment the dTALE should translocate into the nucleus. A 3xHA tag, as well as an eGFP were attached to the C-terminus of the dTALE domain (Figure 8 A purple and green). The 3xHA and the eGFP tag were intended to be used for Western Blot analysis, fluorescence microscopy and protein precipitation, respectively.

The natural activation domain of the dTALEs was removed. Consequently, the dTALEs should bind to DNA, without inductive transcriptional effects. Of all six dTALEs a second variant was designed. The second variant has a VP64 activation domain between the TALE domain and the 3xHA tag (dTALE-AD) (Figure 8 A yellow). The dTALE-AD variants should have an activating effect on *pFRK1*. They are going to be used for pre-experiments in promoter reporter assays.

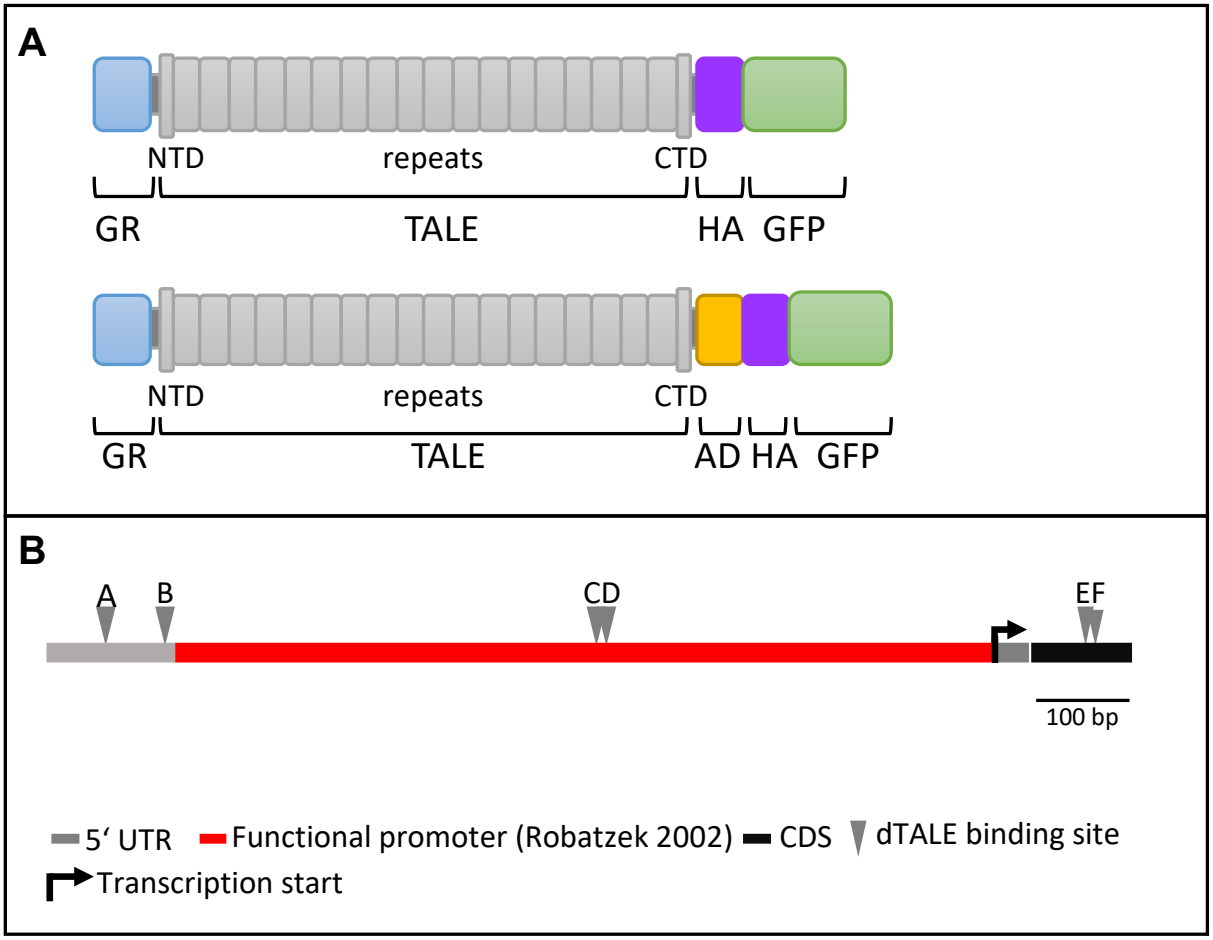

Figure 8: Domain Structure of the dTALEs and their binding sites in *pFRK1* and *FRK1*
Domain structure of dTALE and dTALE-AD variants **(A)**. A GR receptor was fused to the N-terminus of the TALE repeat domain, followed by C-terminal 3xHA and eGFP tags. The dTALE repeat domain is flanked by an N-terminal (NTD) and a C-terminal domain (CTD) of the original TALE. The generated dTALEs with different repeat domains target six different sites in *pFRK1*. Scheme of *pFRK1* with the binding sites of dTALE A-F and dTALE-AD A-F **(B)**. The dTALE binding sites where chosen in distance to the clusters of putative transcription factor binding sites to reduce the possibility of blocking them.

5.3.2. Definition of the promoter area and prediction of transcription factor binding sites

As demonstrated in the section 5.1.1, *FRK1* transcript accumulation is strongly induced after flg22 perception during PAMP triggered immunity (Asai et al., 2002). The signal is transduced into the nucleus where *FRK1* expression is initiated. *Trans*-acting and *cis*-acting elements modulate the activity at the promoter of the gene. To get an insight into the regulatory mechanisms, the promoter region of *FRK1* was analyzed in detail.

The translation start, marked by the ATG codon, is found at position 8,329,893 on chromosome 2 (TAIR accession Locus 2059093). Approximately 1,300 base pair upstream of the ATG, a long non-coding RNA is annotated (AT2G07165) and marks the 5'-end of the promoter. The functional *pFRK1* was previously described by Robatzek and Somssich (2002) having a length of 1 kb. Therefore, the further promoter analysis was focused on this 1 kb upstream region. Next, this 1 kb area was analyzed for *cis*-regulatory elements.

35 bp upstream of the ATG, a TCAT initiation motif (InR motif) was found (Supplementary figure 1). This is known to constitute the transcription start site (Berendzen et al., 2006). Upstream of the transcription start a TATA box motif (TATAAA) was identified. The TATAAA motif is one of the known functional TATA box hexanucleotides that can be found in 29 % of all *Arabidopsis* core promoters (Berendzen et al., 2006; Molina & Grotewold, 2005). The TATA Box interacts with the TATA box binding protein and is responsible for the correct positioning of the transcription initiation complex. Further upstream, some TATA-like sequences were found. Since two W boxes were also identified in this area, which seems to be important for transcriptional activation, it is unlikely that the TATA box-like elements in this area are functional (Robatzek & Somssich, 2002). WRKYs bind specifically to intact DNA double strands.

Together with the *cis*-regulatory elements in the core promoter, gene expression is modulated by *trans*-acting factors that bind to specific promoter areas. With the PlantPan2 algorithm the promoter was searched for conserved binding motifs (Chang, Lee, Huang, Huang, & Pan, 2008; Chow et al., 2016).

PlantPan2 predicted 1092 putative binding sites in *pFRK1* (Supplementary table 1). A purely sequence-based prediction, like it was done, leads to an unmanageable amount of putative binding sites. It is very likely that many false positives are under the 1092 candidates found by

PlantPan2. To narrow down the number of putative candidates, the search was limited to proteins that were already known to bind to *pFRK1.*

Altogether, 15 putative transcription factor binding sites were found in *pFRK1* whose *in vitro* or *in vivo* binding was proven experimentally (Supplementary figure 2). The binding sites of the WRKYs were redundant and were counted as one. The positions of the predicted 15 binding sites are illustrated in Figure 9.

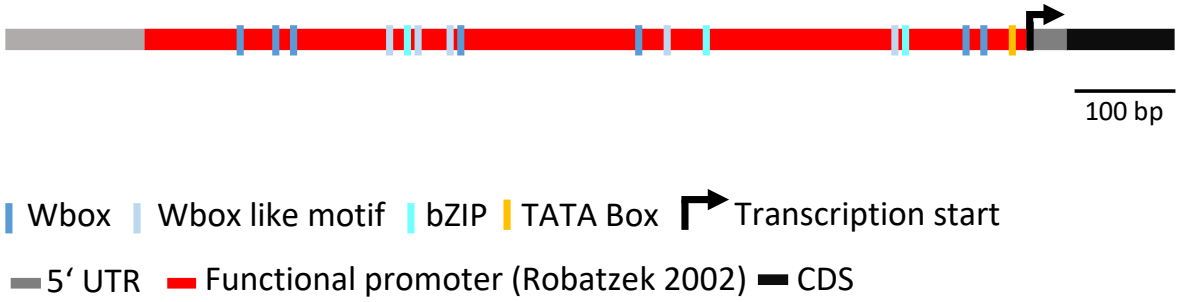

Figure 9: Fifteen putative transcription factor binding sites can be found in *pFRK1*
The positions of putative transcription factor binding sites were annotated in *pFRK1.* WRKYs (Wbox) (blue), WRKY binding sites predicted by PlantPan2, that do not show the core Wbox element were annotated as Wbox-like motif (light blue) (Brand, Fischer, Harter, Kohlbacher, & Wanke, 2013; Ciolkowski et al., 2008). bZIPs (cyan). *Cis*-regulatory elements: TATA Box (yellow) and the transcription start (black arrow). The sequence that was described as functional promoter is shown in red (Robatzek & Somssich, 2002), the 5‘UTR in grey and CDS in black.

Wboxes were the most abundant binding sites in the analysis with PlantPan2 (Figure 9 blue & light blue bars). The 12 predicted Wboxes overlap with the 12 Wboxes described by Robatzek and Somssich (2002). Five of the predicted Wboxes might not be bound by WRKYs (Figure 9 light blue bars). These Wboxes do not show the minimal core sequence of a Wbox TTGACY, like a previously described Wbox-like motif TTGACA (light blue bars) (Brand et al., 2013; Ciolkowski et al., 2008).

Since PlantPan2 did not predict any binding site for bZIP1, the sequence was searched by eye for any putative binding site. bZIP1 binds to a hexameric structure with the core motif (ACGT) (S. G. Kang, Price, Lin, Hong, & Jang, 2010). Three ACGT motifs were identified of which the middle one showed a perfect hexameric palindrome structure of AACGTT (Figure 9 orange bars & Supplementary figure 1).

The binding sites of the dTALEs were chosen near the clusters of putative transcription factor binding sites, but not directly on them. With that, the chance to pull down candidate proteins was intended to be increased, but the possibility of blocking transcription factor binding sites to be minimized (Figure 9).

5.3.3. Localization of dTALEs - translocation to the nucleus

5.3.3.1. Localization in *A. thaliana* protoplasts

In the prior section the domain structure of the dTALEs for the dTALE-ChAP approach was presented. Additionally, the workflow of the dTALE-ChAP was outlined. The basis of the dTALE-ChAP is the expression of the dTALEs in *A. thaliana* and their DEX dependent subcellular localization. To test whether the dTALEs are expressed and whether the DEX dependent translocalization into the nucleus is observable, the dTALE variant without the activation domain was expressed in *A. thaliana* protoplasts and analyzed by confocal fluorescence microscopy (Figure 10).

The observed GFP fluorescence proved, that dTALE A-F have all been expressed. The protoplasts were treated with DEX and the GFP localization was observed over time. By observing the spatial pattern of the fluorescence signal, conclusions about the subcellular localization dynamics of the dTALEs can be made.

dTALE A, B, D, E and F expressing protoplasts, showed exclusively a cytosolic GFP signal in the absence of DEX treatment (Figure 10 A, B, D - F, untreated). In dTALE C expressing protoplasts, a presumably nuclear localization of the GFP fluorescence was visible in the absence of DEX (Figure 10 C, untreated). 5 min after DEX treatment, in all six dTALE expressing protoplasts a presumably nuclear localization became visible which became more distinct over time (Figure 10 A-F, 5 min - 20 min). To see if the spatial pattern of the fluorescence signal changes after 20 min, dTALE C and dTALE F expressing protoplasts were observed over a longer time period (Figure 10 C, 45 min & 55 min, F, 25 min). Even after 55 min of DEX treatment a presumably nuclear localization was maintained. With the exception of dTALE C (Figure 10 C, untreated), the data suggest the nuclear import of the dTALEs upon DEX treatment

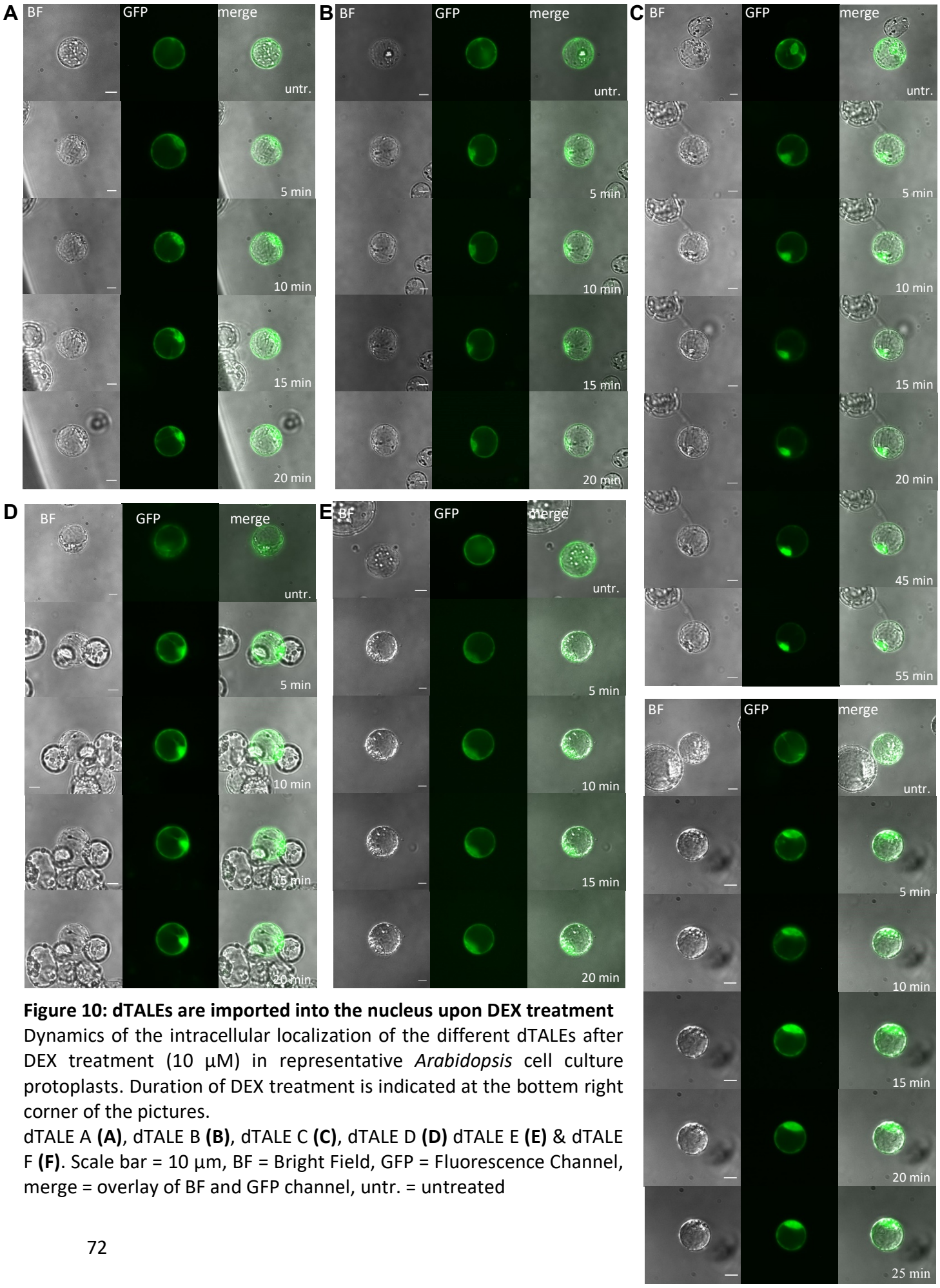

Figure 10: dTALEs are imported into the nucleus upon DEX treatment
Dynamics of the intracellular localization of the different dTALEs after DEX treatment (10 µM) in representative *Arabidopsis* cell culture protoplasts. Duration of DEX treatment is indicated at the bottem right corner of the pictures.
dTALE A **(A)**, dTALE B **(B)**, dTALE C **(C)**, dTALE D **(D)** dTALE E **(E)** & dTALE F **(F)**. Scale bar = 10 µm, BF = Bright Field, GFP = Fluorescence Channel, merge = overlay of BF and GFP channel, untr. = untreated

5.3.3.2. Localization in *N. benthamiana*

In the previous section it was shown that the dTALEs were expressed in *A. thaliana* protoplasts and that the DEX treatment interferes with their subcellular localization. Next the nuclear dTALE import was tested in an *in planta* experiment. *N. benthamiana* leaves were transfected with the dTALE A-F. For a better visualization of the nucleus, the leaves were in parallel transfected with LHP1-. The LIKE HETEROCRHOMATIN PROTEIN1 (LHP1) was previously shown to localize to the nucleus in *N. benthamiana* cells (Hecker et al., 2015).

Discs of tobacco leaves, that were transformed with the dTALEs constructs were placed in a DEX solution on a cover slip and analyzed by confocal microscopy. For each dTALE two time points were captured (Figure 11). The nucleus of the representative cell was marked with a white arrow. It was tried, to capture one cell expressing the dTALE and LHP1 as early as possible after the DEX treatment. The second picture was captured after a minimum of 60 min after DEX treatment. In Figure 11 A & B a representative cell of a dTALE A expressing leaf is shown. 6 min after DEX treatment, the GFP signal is still located in the cytosol (Figure 11 A). 60 min after DEX treatment the GFP signal was detected in the nucleus (Figure 11 B). In a representative cell expressing dTALE B, 22 min after DEX treatment a weak cytosolic GFP signal was observed (Figure 11 C). 60 min after DEX treatment the GFP signal co-localized with the RFP signal of LHP1 (Figure 11 D). The representative in which dTALE C was expressed, showed GFP signal around the nucleus 6 min after DEX treatment (Figure 11 E). It is not completely clear if the GFP signal is located around the nucleus or in the nucleus. 60 min after DEX treatment a clear nuclear GFP signal was visible (Figure 11 F). In the leaves expressing dTALE D, the earliest timepoint that was captured after DEX treatment was 30 min (Figure 11 G). At this timepoint, weak GFP fluorescence was detectable in the nucleus (Figure 11 G). 60 min after DEX treatment, GFP fluorescence was clearly detectable in the nucleus (Figure 11 H). In a representative cell expressing dTALE E 30 min after DEX treatment, it was possible to detect cytosolic signal, as well as weak nuclear GFP signal (Figure 11 I). 105 min after DEX treatment, the GFP signal co-localized with the RFP signal in the nucleus (Figure 11 J). The nucleolus was clearly visible. Due to low expression levels, the earliest timepoint, that was captured after DEX treatment in cells expressing dTALE F was 37 min after DEX treatment (Figure 11 K). Weak GFP signal was detected in the nucleus. 100 min after DEX treatment, the GFP signal was clearly visible in the nucleus (**Figure 11** L).

From the representative cells shown in Figure 11, it can be concluded, that the time period between DEX treatment until the first low level GFP fluorescence is visible in the nucleus is 30 minutes. Unfortunately, the time points between the different constructs varied greatly since, due to low transfection efficiencies it was not possible to find a dTALE expressing cell, for each construct at an early stage. The representative cell expressing dTALE A, as well as dTALE B showed no nuclear GFP signal 6 min and 22 min after DEX treatment (Figure 11 A & C). In the representative cell expressing dTALE C it was not clearly visible if GFP signal of nuclear origin or the GFP signal is located around the nucleus 6 min after DEX treatment (Figure 11 E). 30 min after DEX treatment in the representative cells expressing dTALE C- E a weak nuclear GFP fluorescence was observed (Figure 11 E, G & I). The nuclear GFP signal was clearly visible 60 min after DEX treatment or later (Figure 11 B, D, F, H, J & L). The overlay of the GFP signal of with the nuclei marker LHP1-RFP and the recess of the nucleolus in the GFP channel left no doubt, that the dTALEs were imported into the nucleus. There was no case, in which the GFP fluorescence was detected inside the nucleus without DEX treatment.

For the dTALE ChAP approach, the dTALEs appear to be present in the nucleus in a sufficient concentration. Therefore, the period for the DEX treatment was set to 60 min in the further experiments.

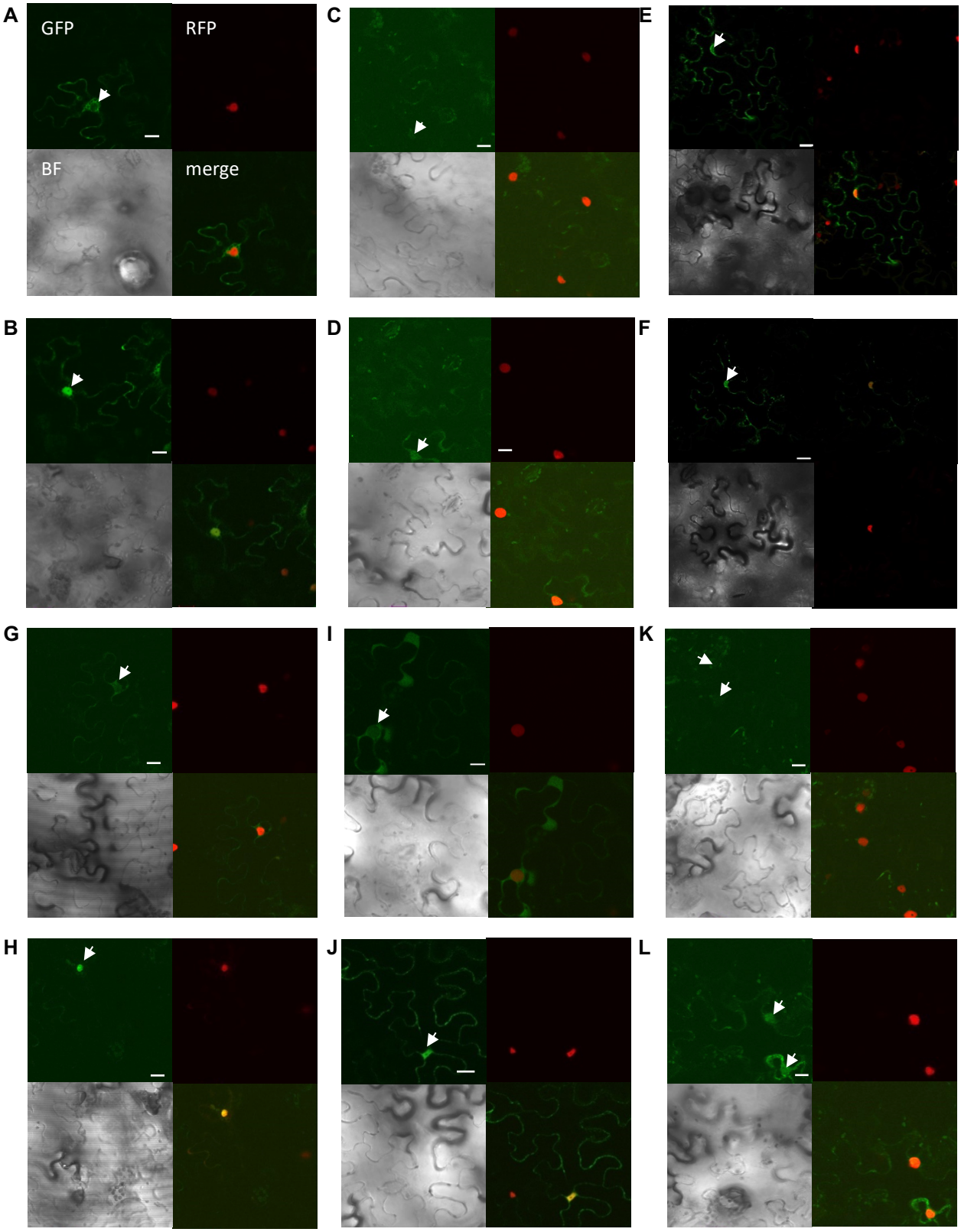

Figure 11: The dTALEs translocate in response to DEX treatment from the cytosol into the nucleus
The dTALEs translocated in response to DEX treatment from the cytosol to the nucleus. The dTALEs were co-expressed with LHP1-RFP. White arrow = representative nucleus; BF = bright field; scale bar = 20 µm dTALE-A 6 min after DEX treatment **(A),** dTALE A 81 min after DEX treatment **(B)**, dTALE B 22 min after DEX treatment **(C)**, dTALE B 60 min after DEX treatment **(D)**, dTALE C 6 min after DEX treatment **(E)**, dTALE C 60 min after DEX treatment **(F)**, dTALE D 30 min after DEX treatment **(G)**, dTALE D 60 min after DEX treatment **(H),** dTALE E 30 min after DEX treatment **(I)**, dTALE E 105 min after DEX treatment **(J)**, dTALE F 30 min after DEX treatment **(K)** and dTALE F 100 min after DEX treatment **(L)**.

5.3.3.3. Localization in transgenic *A. thaliana* lines

In the previous section the localization of the dTALEs was analyzed in *N. benthamiana* leaves. It was found that it takes approximately 30 min till the GFP fluorescence can be detected in the nucleus upon DEX treatment. In this section, the TALE domain of the plasmids was once more checked for full integrity before transformation into *Arabidopsis*.

In rare events, TALEs can lose repeats by recombination events during the cloning procedure (Weber, Gruetzner, Werner, Engler, & Marillonnet, 2011). If a complete repeat is lost, the rest of the coding sequence can still be in frame. The GFP would still be visible but the dTALE could not bind to its anticipated target sequence anymore. Therefore, the TALE domain of the dTALE and dTALE-AD constructs was amplified by PCR prior to plant transformation (Figure 12). The loss of at least one repeat would result in shortening of the TALE domain by 100 bp. Since the available DNA ladder was lacking fragments between 1500 bp and 2000 bp, four DNA fragments were amplified from the dTALE vector in the sizes 1500 bp, 1650 bp, 1750 bp and 1900 bp (Figure 12 A-D). For that, primers were designed, which amplify a part of the vector backbone in the respective size. A mixture of the amplified fragments was loaded on the gel as well (Figure 12 6^{th} lane). The TALE domain of dTALE A-F and dTALE-AD A-F should have a size of 1845 bp. Indeed, the TALE domains of all dTALEs and dTALE-ADs showed a band of the correct size (Figure 12).

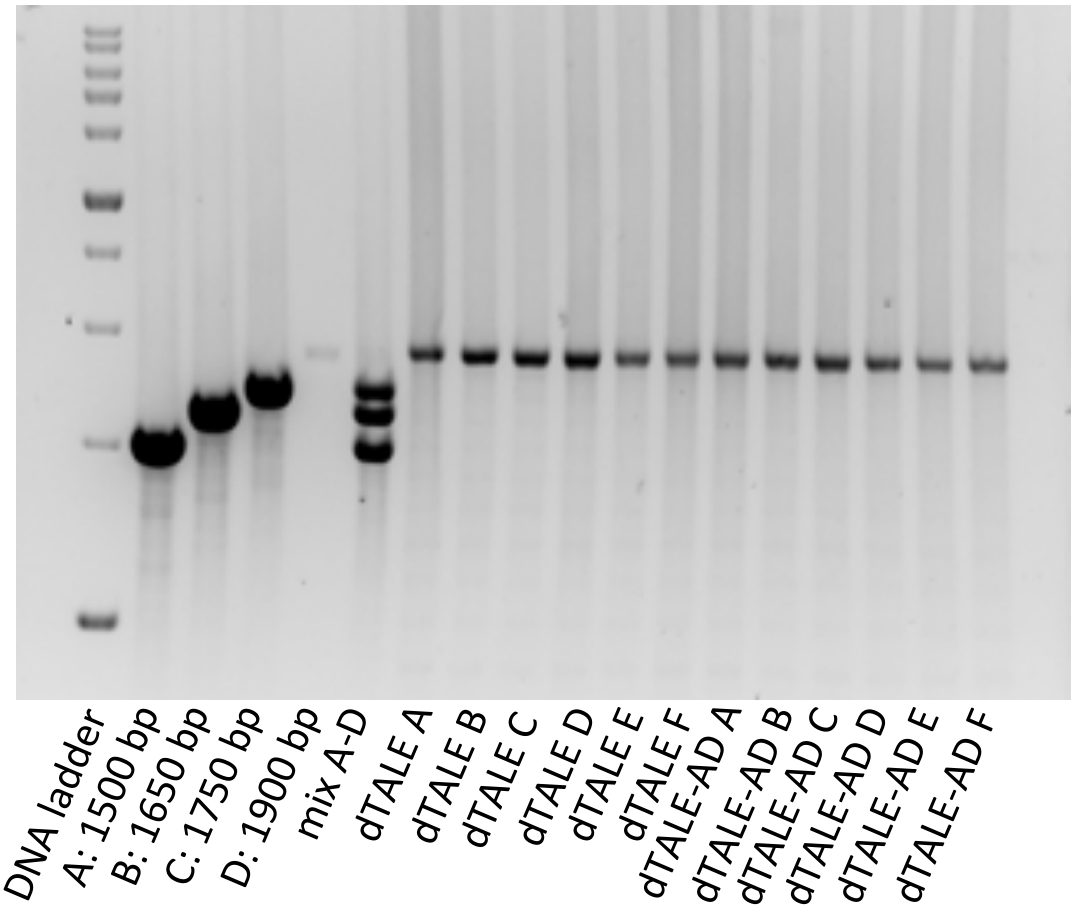

Figure 12: The DNA binding domain of all dTALEs was intact prior to plant transformation
PCR Amplification of the DNA-binding domain of dTALE and dTALE-AD plasmids, revealed the correct size of 1845 bp in every dTALE and dTALE-AD plasmid. Beside a commercial DNA ladder (Genaxxon 1 kb ladder), a 1500 bp, 1650 bp, 1750 bp and 1900 bp fragment of the dTALE vector was amplified as size standard (A-D).

After the integrity of the TALE domains was verified, the constructs were transformed into *A. thaliana.* Seeds of the transformants were propagated into the T2 generation under selective BASTA conditions. For the dTALE-ADs, in which a VP64 activation domain was included into the fusion, no positive *Arabidopsis* transformants were obtained. Either the dTALEs fluctuate into the nucleus, causing lethal effects by the activation domain, or the plasmids were degenerated prior to transformation. Of the positively selected T2 lines, 20 seeds per line were grown for 10 days on a BASTA containing MS plate. The roots were screened for GFP fluorescence by confocal microscopy. One representative root for each of the six dTALEs A-F is shown in Figure 13.

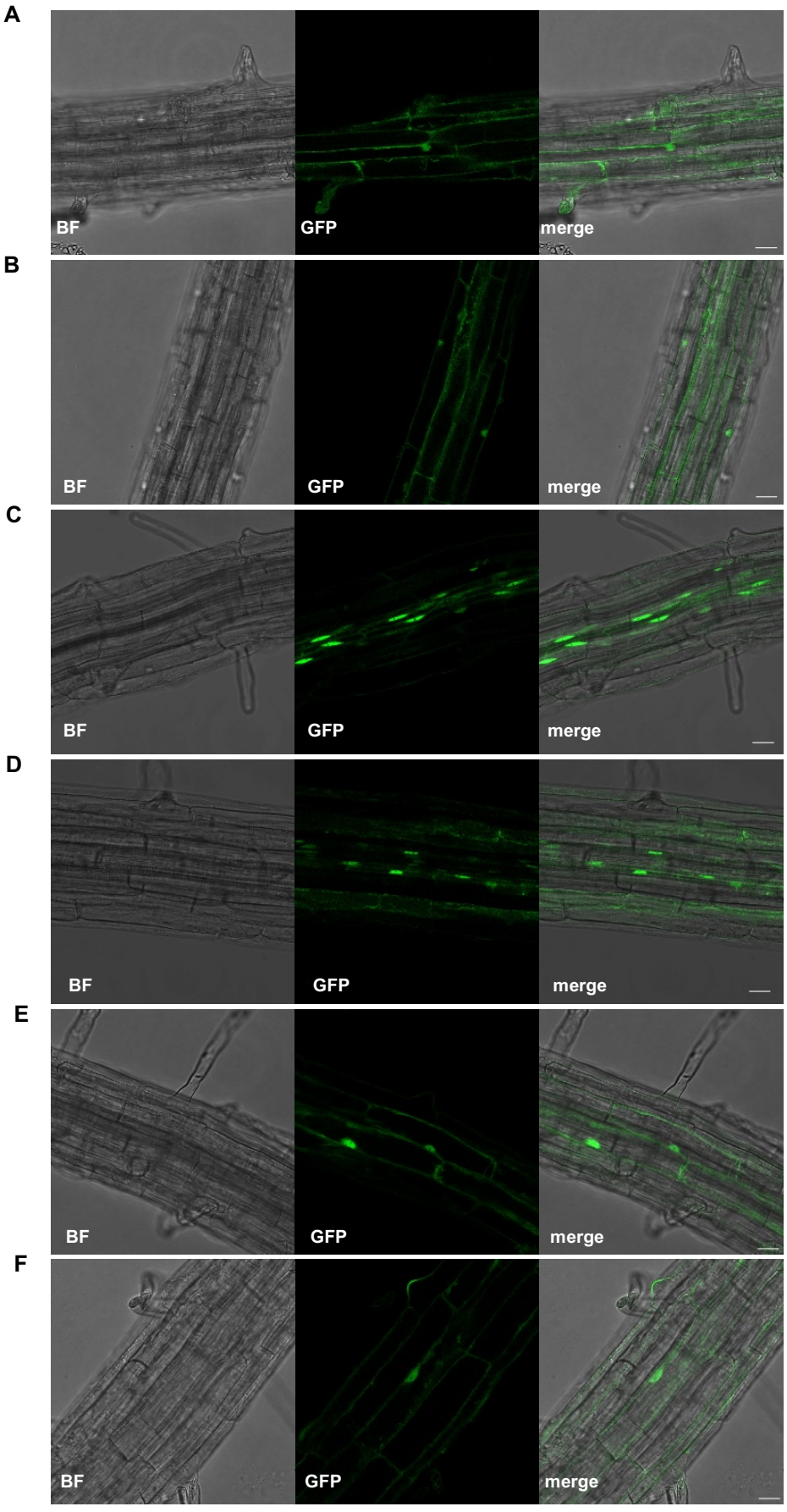

Figure 13: The dTALEs A-F localize inside the nucleus in roots of transgenic *Arabidopsis* seedings upon DEX treatment

Seedlings (T2 generation) were grown for 10 days on MS plates containing BASTA (5 µg/ml). The seedlings were treated with DEX (10 µM) for 60 min. BF = bright field, white bar = 20 µm. dTALE A **(A)** dTALE B **(B)** dTALE C **(C)** dTALE D **(D)** dTALE E **(E)** dTALE F **(F)**

Because the fluorescence intensity was generally very weak in the cytoplasm, the roots were treated with DEX before the root analysis. As shown in Figure 10, then the distinct concentrated GFP signal in the nucleus was easier to detect in comparison to the weak cytosolic signal. In total 227 BASTA selected lines were sown on the BASTA MS plates for fluorescence screening. 28 lines did not germinate and were discarded. One line germinated but did not show GFP fluorescence. The remaining lines were incorporated into pools according to the dTALE variants (Table 9).

Table 9: Number of dTALE *A. thaliana* lines that were included in the seed pools for X-ChIP and dTALE ChAP

dTALE vector	number lines included in the pool
dTALE A	n = 6
dTALE B	n = 7
dTALE C	n = 143
dTALE D	n = 13
dTALE E	n = 12
dTALE F	n = 17

The advantage of using a seed pool instead of a single stable dTALE line is that in an early transgenic generation enough seeds are available to perform the dTALE-ChAP. For the dTALE-ChAP high amounts of plant material are required. With a single dTALE line, the seeds would have been propagated to the T4 generation involving the risk of silencing effects.

The gathered seed pools were used for the further ChIP and ChAP experiments. Because the most seeds were available for the dTALE C lines, the pre-experiments were performed with the pooled dTALE C seed batch.

5.3.3.4. Purification of dTALE C from *A. thaliana* nuclei

The first steps of the dTALE-ChAP protocol to be tested were the efficiency of nuclei purification and the pulldown of dTALE proteins out of the nuclear extract. Nuclei of DEX-treated dTALE C expressing transgenic *Arabidopsis* plants were purified and opened by sonification. dTALE C was precipitated with a GFPtrap. The purified proteins were analyzed by Western Blot (Figure 14).

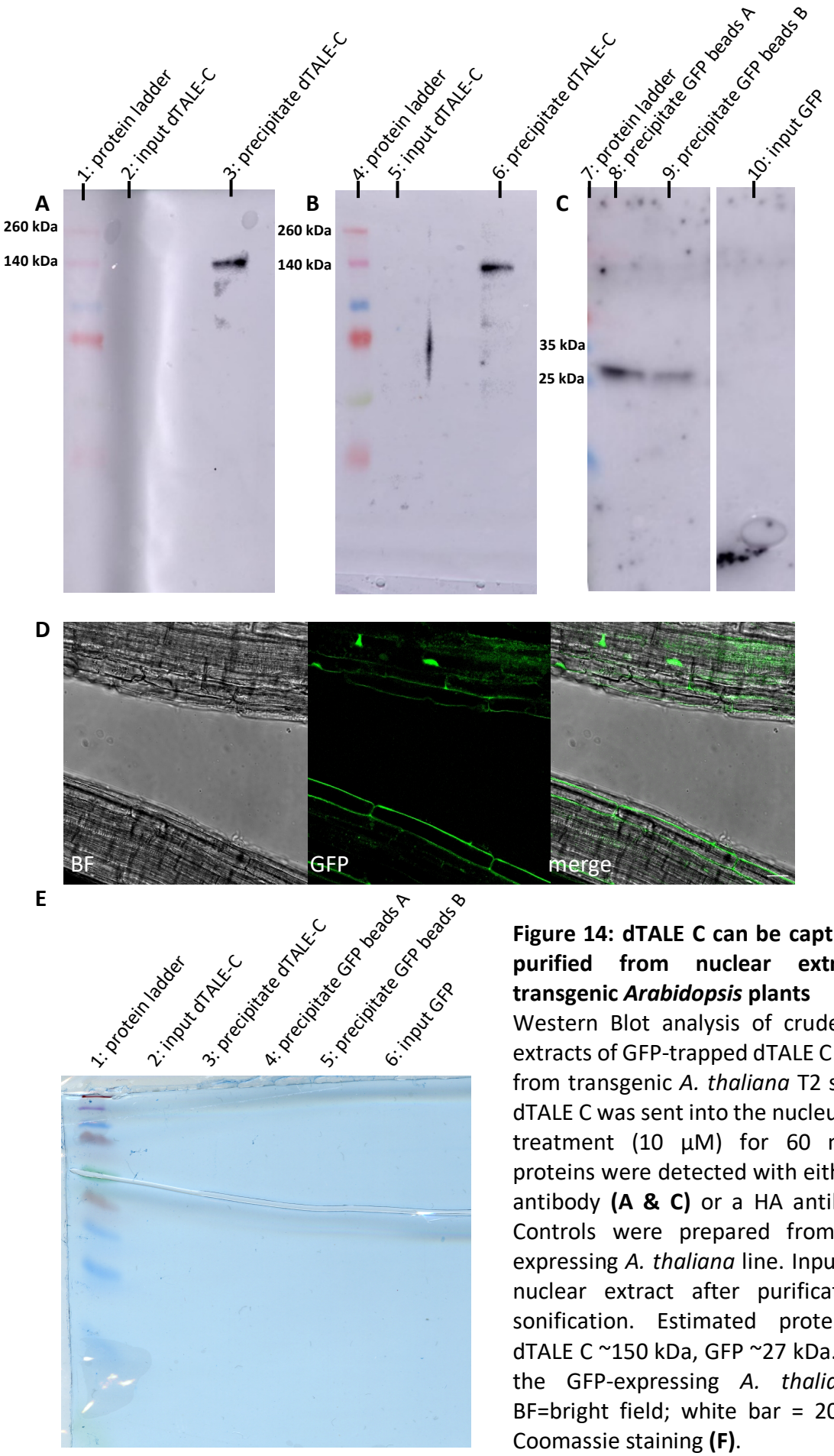

Figure 14: dTALE C can be captured and purified from nuclear extracts of transgenic *Arabidopsis* plants

Western Blot analysis of crude nuclear extracts of GFP-trapped dTALE C obtained from transgenic *A. thaliana* T2 seedlings. dTALE C was sent into the nucleus via DEX treatment (10 µM) for 60 min. The proteins were detected with either a GFP antibody **(A & C)** or a HA antibody **(B)**. Controls were prepared from a GFP-expressing *A. thaliana* line. Input = crude nuclear extract after purification and sonification. Estimated protein sizes: dTALE C ~150 kDa, GFP ~27 kDa. Roots of the GFP-expressing *A. thaliana* line. BF=bright field; white bar = 20 µm **(E)**. Coomassie staining **(F)**.

The proteins were separated by SDS PAGE and blotted on a PVDF membrane. Under the used Western Blot detection conditions, it was possible to detect proteins at ~150 kDa in the precipitated sample using an anti-GFP antibody (Figure 14 A sample 3). In the crude nuclear extract, no band was detected (Figure 14 A sample 2). The anti-HA antibody also detected a band of ~150 kDa in the precipitated sample but not in the nuclear extract (Figure 14 B sample 5 & 6). These data indicate, that the band of ~150 kDa reflects dTALE C.

As technical controls, nuclear and precipitated samples were also prepared from a transgenic *Arabidopsis* line, expressing GFP (Figure 14 C). With an anti-GFP antibody, it was possible to detect a band of the expected size of 27 kDa in the precipitate (Figure 14 C sample 8 & 9). No GFP signal was observed in the crude nuclear extract (Figure 14 C sample 10). On a Coomassie stained gel SDS-gel, no proteins were detectable (Figure 14 E).

The subcellular localization pattern of the GFP in the transgenic *Arabidopsis* line was analyzed by confocal microscopy (Figure 14 D). GFP fluorescence was detected in the cytosol, as well as in the nuclei.

From these results it can be concluded, that the GFP (fusion) proteins were highly concentrated by the precipitation procedure. The results of the Western Blot also implicate, that the protocol for the purification of the nuclei and the precipitation of the dTALE proteins from crude nuclear extracts via their GFP-tag works efficiently.

5.3.4. Induction of *pFRK1* in dTALE *A. thaliana* lines

In parallel to the DEX treatment, which causes the dTALE translocation into the nucleus, *FRK1* is induced with flg22. As described above, the dTALE binding sites are located near the predicted transcription factor binding sites in *pFRK1* (Figure 8 B & Figure 9). To exclude the possibility that *pFRK1* is no longer inducible by flg22 when a dTALE is bound, a qPCR experiment was performed. Seedlings of the dTALE C pool were grown for 14 days in liquid culture. dTALE C translocation was induced by DEX treatment (10 µM) for 30 min. Control samples were mock treated. Then the seedings were exposed to flg22 (or mock). After additional 30 min the seedlings were frozen in liquid nitrogen and the *FRK1* transcript levels were detected (**Figure 15**). In the samples treated with flg22 for 30 min, *FRK1* transcript levels were not elevated independent if the samples were treated with DEX or mock in parallel

(Figure 15 left). 60 min after flg22 treatment, a strong increase of *FRK1* transcript level was detectable (Figure 15 right). Parallel DEX treatment did not have a negative effect on the *FRK1* transcript level(Figure 15 right). DEX treatment without flg22 treatment did not induce *FRK1* expression. This is due to the lack of the activation domain in the dTALE plasmid (Figure 15 right).The control samples, that were mock treated, as well as the untreated controls did not show changes in *FRK1* transcript levels (Figure 15). The repetition of the experiment showed similar results (Supplementary figure 4).

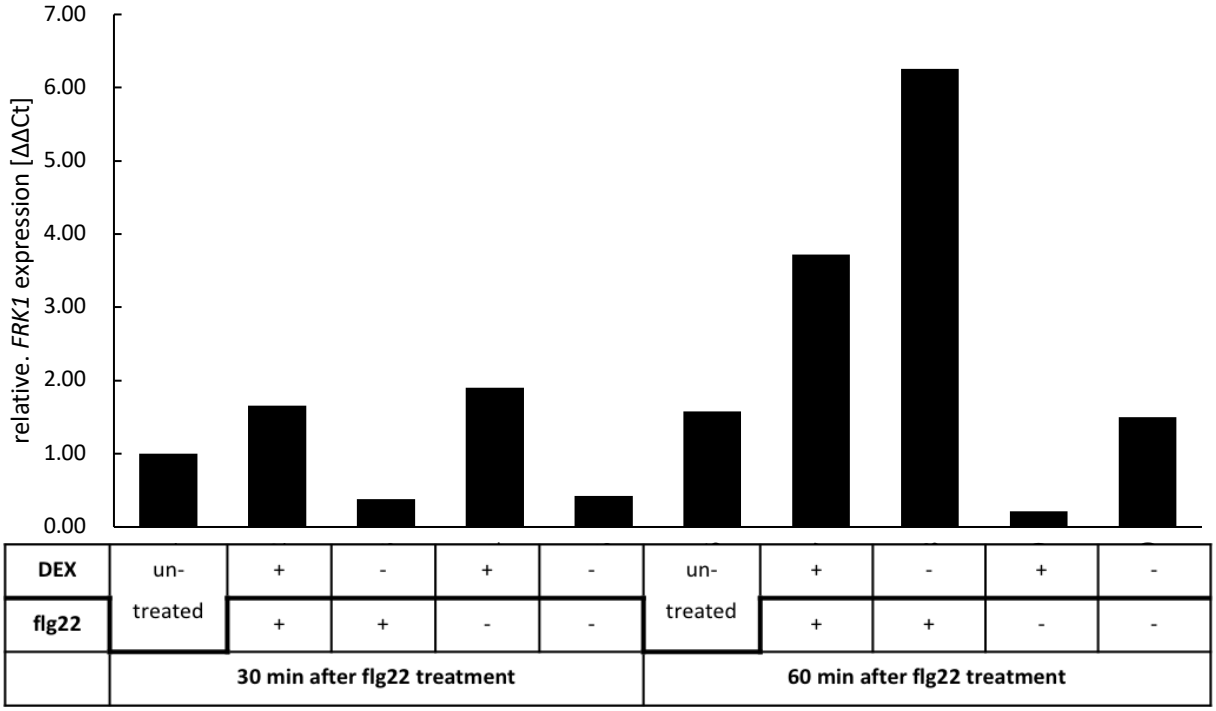

Figure 15: *FRK1* transcript accumulation is still induced by flg22 in *A. thaliana* seedlings expressing nuclear-localized dTALE C

dTALE C expressing *Arabidopsis* seedlings were treated with DEX (10 µM) or mock-treated. 30 min later the seedlings were exposed to flg22 (100 nM) or mock-exposed for 30 or 60 min. Total RNA was extracted and applied to qRT-PCR using *FRK1*-specific primers.

5.4. DNA binding of dTALEs

In the previous section it was demonstrated, that the binding of dTALE C to *pFRK1* has no significant effect on the flg22-inducibility of *FRK1* transcript accumulation in transgenic *Arabidopsis.* Further investigations were initiated to characterize the DNA-binding capacity of the dTALEs in more detail. To do so, the dTALE-AD variants were used to test if the dTALEs bind to their target sequence in promoter-reporter assays (section 5.4.1). In addition, the physical contact and capacity of the dTALEs to precipitate their target DNA *in vivo* was tested by X-ChIP (section 5.4.2).

5.4.1. Induction of Promoter - *Luciferase* Reporter genes with dTALE-AD C and dTALE-AD D

5.4.1.1. Induction of *pFRK1::LUC* by dTALE-AD C and dTALE-AD D

To test, if dTALE-AD C and dTALE AD D bind to their target sequence in *pFRK1*, *a* promoter-reporter activation assay was performed. dTALE-AD C and dTALE-AD D were co-expressed in *A. thaliana* protoplasts together with *pFRK1::Luciferase* (*LUC*). The protoplasts were treated with DEX, inducing the dTALE movement to the nucleus, where they should bind to the *pFRK1::LUC* reporter and activate LUC protein accumulation. The LUC activity is measured in a luminometric assay (Figure 16).

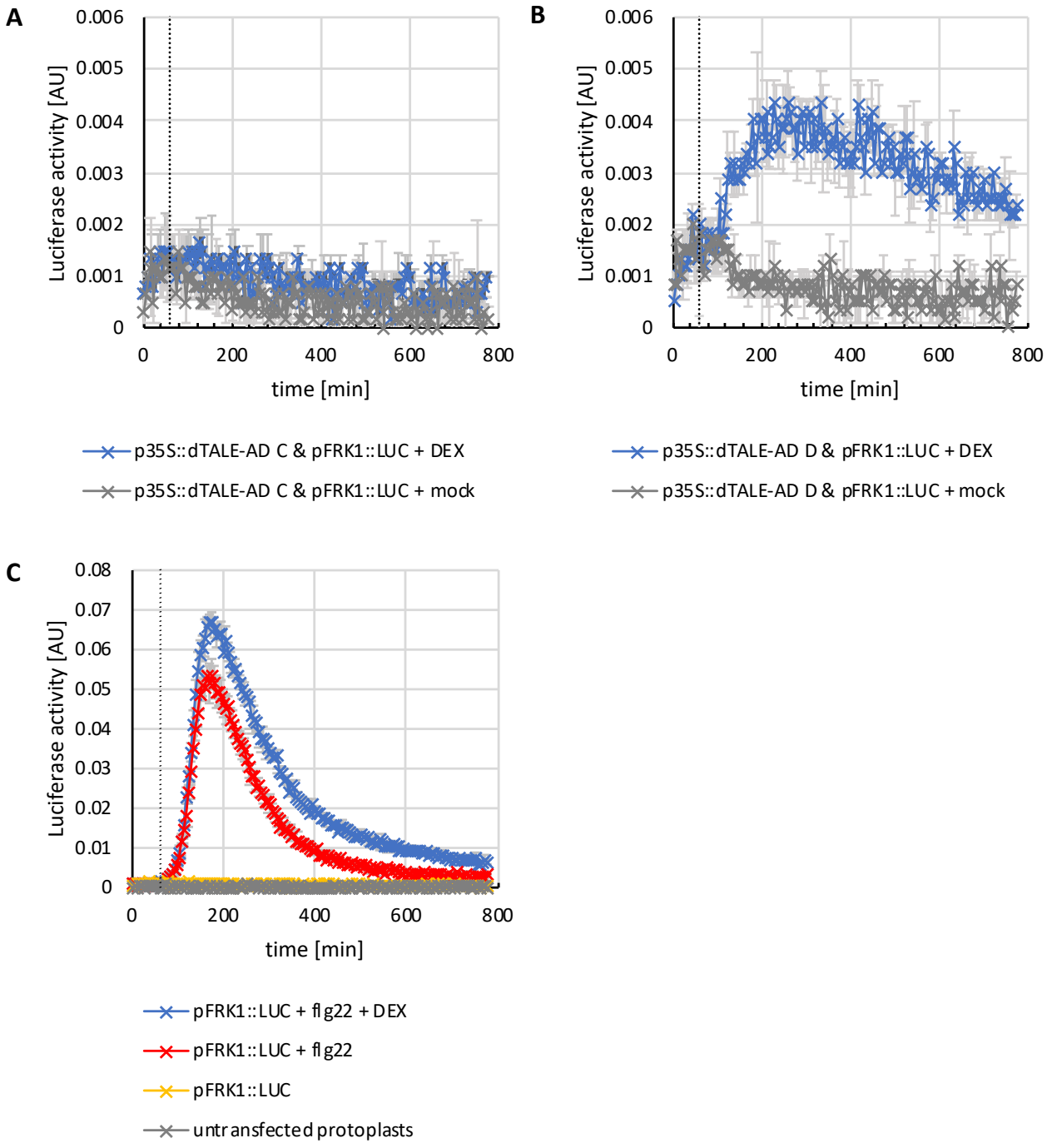

Figure 16: Transactivation of *pFRK1::LUC* by *p35S::dTALE-AD* in *A. thaliana* protoplasts over time
p35S::dTALE-AD C **(A)** and *p35S::dTALE-AD D* **(B)** were co-transformed with *pFRK1::LUC* into *Arabidopsis* cell culture protoplasts. After treatment with DEX, LUC activity was tracked over the indicated time in a luminometric assay. DEX treated samples are shown in blue, mock treated samples in grey. As a positive control, the *pFRK1::LUC* reporter was directly induced by treatment of protoplasts with 100 nM flg22 **(C)**. Flg22 treated samples are shown in red, flg22 and DEX treated samples in blue, untreated samples in yellow and untransfected protoplasts in grey. The onset of treatments is marked by a dotted vertical black line. Error bars represent the standard deviation of three independent protoplast transfections.

After transfection, the protoplasts were incubated for 6 h. After the addition of the substrate Luciferin, basal LUC activity was determined for 1 h in a 5 min intervals. Then, the protoplasts were treated with DEX or mock (Figure 16 B dotted black line). The *Luciferase* activity was measured in a 5 min interval. After 1 h the samples were treated with DEX or mock (Figure 16 dotted black line). dTALE-AD C did induce additional LUC activity response to the DEX treatment (Figure 16 A blue curve). The LUC activity stayed on the same level as in mock treated protoplasts (Figure 16 A grey). In contrast, an increase in LUC activity was observed for protoplast transfected with dTALE-AD D approximately 40 min after DEX treatment. The activity was sustainable over the complete measurement period of 12h, with a weak decrease 200 min after DEX treatment (Figure 16 B blue). The mock treated dTALE-AD D expressing protoplast did not show an effect on LUC activity (Figure 16 B grey). However, the extend of the LUC activity was 10 times lower than the induction by flg22 (Figure 16 C red curve). Parallel application of DEX and flg22 led to a slight enhancement of LUC activity (Figure 16 C blue curve). The reporter alone did not show any Luciferase activity (Figure 16 C yellow curve). The signal remained on the same level as untransfected protoplasts (Figure 16 C grey curve).

Because dTALE-AD C appeared not to activate the *pFRK1::LUC* reporter and EX treatment alone seemed to have an additive effect to the flg22 treatment (Figure 16 A & C), the experiment was repeated (Figure 17). As an additional control, the reporter was expressed alone in protoplasts and treated with DEX to exclude an inductive effect of DEX itself on the promoter.

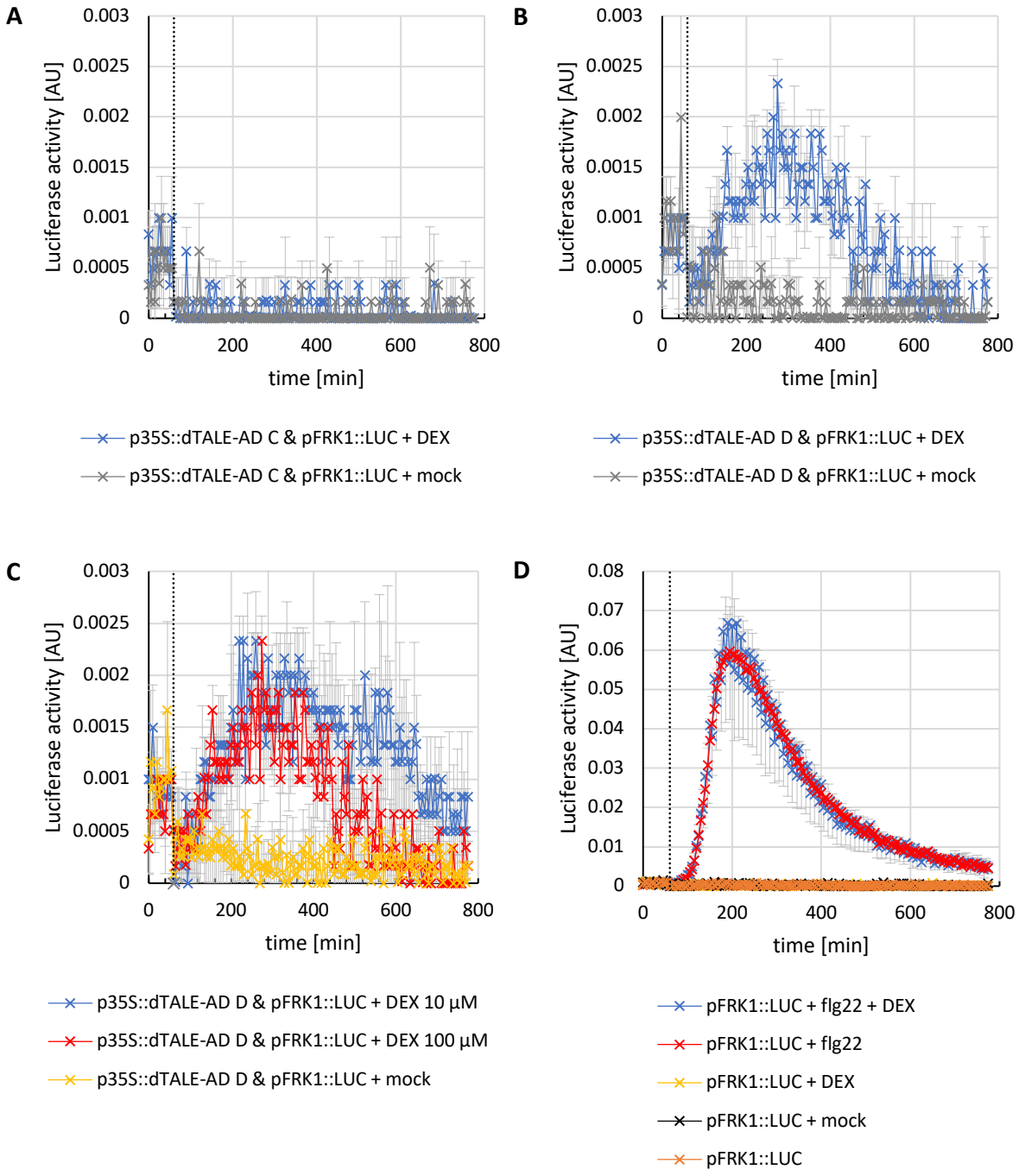

Figure 17: Transactivation of *pFRK1::LUC* by *p35S::dTALE-AD* in A. thaliana protoplasts over time *p35S::dTALE-AD C* **(A)** and *p35S::dTALE-AD D* **(B)** were co-transformed with *pFRK1::LUC* into *Arabidopsis* cell culture protoplast. After treatment with 10 µM DEX, LUC activity was tracked over the indicated time in a luminometric assay. DEX treated samples are shown in blue, mock treated samples in grey. A higher DEX concentration (100 µM) was tested with *p35S::dTALE-AD D* **(C)** As positive control the *pFRK1::LUC* reporter was directly induced, with 100 nM flg22. In addition, *pFRK1::LUC* transformed protoplasts were treated with DEX (10 µM) alone and with DEX (10 µM) in combination with flg22 (100 nM) **(D)**. Flg22 treated samples are shown in red, DEX treated samples in yellow, flg22 and DEX treated samples in blue, untreated samples in orange and non-transfected protoplasts in grey. The onset of treatments is marked by a dotted vertical black line. Error bars represent the standard deviation of three independent protoplast transfections.

Again, DEX treatment (10 µM) of the protoplasts transfected with dTALE-AD C and *pFRK1::LUC* did not show any LUC activity above background level (Figure 17 A, blue and grey curves). The results for dTALE-AD D transfected protoplasts were comparable to those of the first experimental trial, displaying an enhanced LUC activity upon DEX treatment (10 µM) (Figure 17 B blue curve and grey curves). In this trial, it was also tested, whether a 10 times increase of the DEX concentration (100 µM) would have an additional effect on dTALE-AD D induced LUC activity. As shown in Figure 17 C (blue and red curves), this was not the case. In contrast, the LUC activity decreased faster in the protoplasts treated with 100 µM than in those treated with 10 µM DEX. This negative effect could at least be partly due to either higher ethanol concentrations that comes with the higher DEX concentration, or to toxic effects caused by DEX itself.

As obvious from Figure 16 C, there was an additional inductive effect of DEX when applied in parallel to flg22. However, the repetition of this experiment did not reveal a significant additional effect of DEX on flg22-induced LUC activity (Figure 17 D). Furthermore, DEX treatment alone did not induce LUC activity above background and mock treatment level (Figure 17 D).

Since dTALE-AD C showed no inductive effect on *pFRK1::LUC* expression after DEX treatment in the reporter assays, it was tested by cytometry, to which extend dTALE-AD C and dTALE-AD D were expressed in protoplasts. Therefore, populations of 5,000 - 10,000 protoplasts per respective *dTALE-AD* construct were analyzed for GFP fluorescence (FACS) (Table 10).

Table 10:Proportion of protoplasts with GFP fluorescence
Populations of 5,000 - 10,000 protoplasts per transfected *dTALE-AD* construct and biological replicate were analyzed using fluorescence-base cytometry. Numbers show the percentage of protoplasts showing GFP fluorescence for each replicate.

sample	bio rep. 1	bio rep. 2	bio rep. 3
pFRK1:: LUC & 35S::dTALE-AD C	1.21 %	0.15 %	1.21 %
pFRK1:: LUC & 35S::dTALE-AD D	1.69 %	1.83 %	0.68 %
Control (non-transfected protoplasts)	0.05 %		

dTALE-AD C incubated protoplast showed a percentage share of 1.21 % GFP fluorescence positive cells in two independent experiments. However, the percentage share in replicate 2 was with 0.15 % much lower (Table 10). The protoplasts incubated with the *dTALE-AD D* construct showed a slightly higher percentage share of GFP fluorescence positive protoplasts in two replicates compared to *dTALE-AD C* (Table 10). However, the percentage share was lower in replicate 3 than in the other two replicates (Table 10).

Although, differences in transfection efficiency between the dTALE constructs (and independent biological replicates) have to be acknowledged, it appears that in contrast to dTALE-AD D, dTALE-AD C is not able to *trans*-activate *pFRK1 in vivo* or it binds but is not able, perhaps due to steric problems, to communicate with basal transcription initiation machinery, although it carries a VP64 activation domain (Figure 8 B).

5.4.1.2. Induction of *pBS3 dTALE::LUC* with dTALE-AD C and dTALE-AD D

In the previous experiments described above, I showed that dTALE-AD D but not dTALE-AD C can induce a *pFRK1::LUC* reporter construct. Since steric problems could not be excluded in the *pFRK1::LUC* context, the *trans*-activation capacity of both dTALEs was tested in an additional reporter system well established to test dTALEs. In this system the *pBS3* promoter originating from pepper is used (Morbitzer et al., 2010). *pBS3* is the target of a natural *Xanthomonas* derived TALE and its specific binding site within *pBS3* is spatially optimal for *trans*-activation. Importantly, the TALE binding site within *pBS3* can be changed by mutagenesis PCR to a specific target site for any (d)TALE. To perform the assay, I cloned *pBS3::LUC* versions containing either a binding site for dTALE-AD C or dTALE-AD D. The *trans*-activation capacity of both dTALEs on LUC enzymatic activity was tested in transfected *Arabidopsis* cell culture protoplasts.

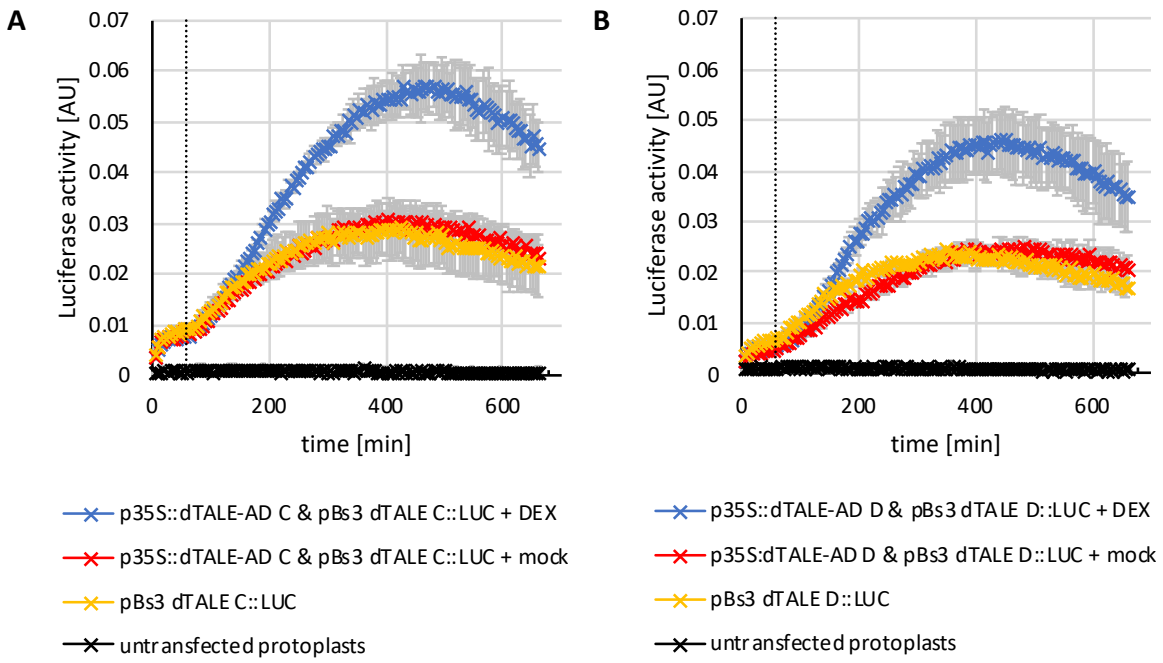

Figure 18: Transactivation of *pBS3 dTALE-AD::LUC* by *p35S::dTALE-AD* in *A. thaliana* protoplasts over time
p35S::dTALE-AD C **(A)** and *p35S::dTALE-AD D* **(B)** were co-transformed with the respective *pBS3::LUC* reporter into *Arabidopsis* protoplasts. After treatment with DEX (10 µM) LUC activity was tracked over the indicated time by a luminometric assay. DEX treated samples are shown in blue, mock treated samples in red, untreated samples in yellow and untransfected protoplasts in black. The onset of treatments is marked by a dotted vertical black line. Error bars represent the standard deviation of three independent protoplast transfections.

Treatment with DEX led to an increase of LUC activity when both dTALE-ADs were co-transfected with their corresponding *pBS3* reporter construct (Figure 18 A & B). The LUC activity was significantly higher compared to that of mock treated protoplasts or protoplasts transfected with the reporter construct alone (Figure 18 A & B). The LUC activity reached its maximum approximately 6 h after onset of DEX application but was above control activity for the entire measurement period of 10 h (Figure 18 A & B). These data demonstrate that both dTALE-ADs are capable to induce *pBS3::LUC* transcription when send to the nucleus and, thus bind to DNA, at least in protoplasts. Furthermore, both *pBS3::LUC* reporter constructs have background activity which, however is not dependent on the presence of the dTALE-ADs.

To test the specificity in the *trans*-activation and binding capability of the dTALE-ADs, the *pBS3::LUC* reporter genes were exchanged against each other (Figure 19).

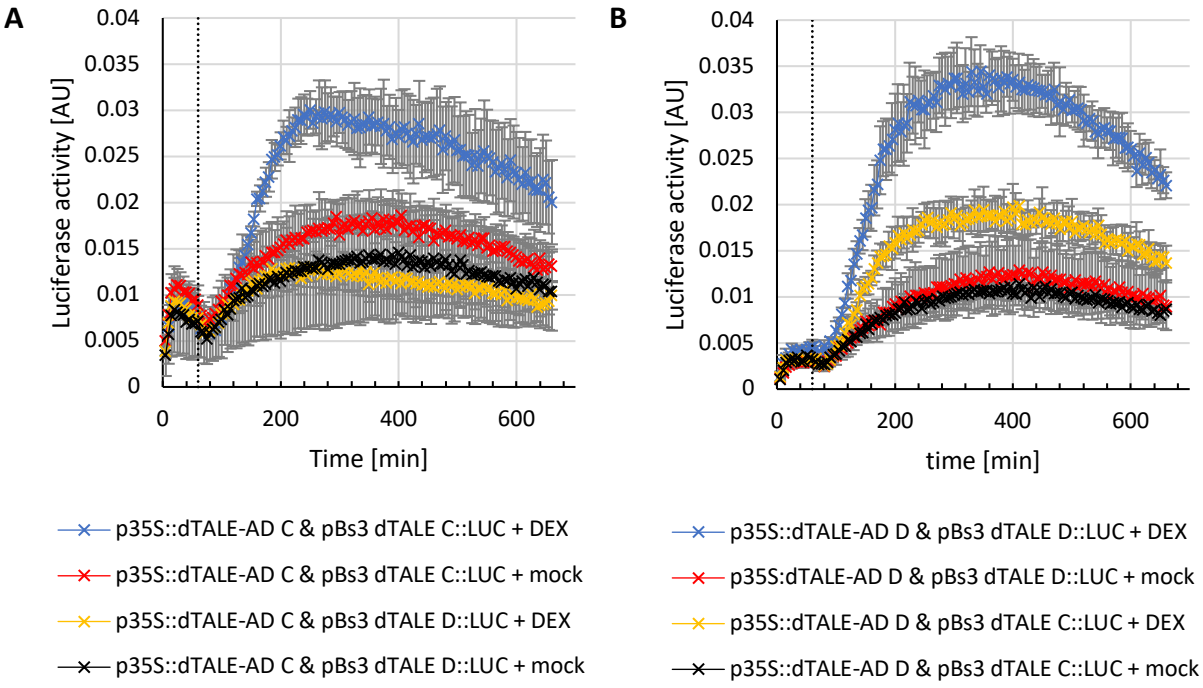

Figure 19: Transactivation of *pBS3 dTALE-AD::LUC* by p35S::dTALE-AD in *A. thaliana* protoplasts over time
p35S::dTALE-AD C **(A)** and *p35S::dTALE-AD D* **(B)** were co-transformed with the respective *pBS3::LUC* reporter into *Arabidopsis* protoplasts. In addition, the dTALE-ADs were co-transformed with the promoter with the binding site of the other dTALE-AD. After treatment with DEX (10 µM) LUC activity was tracked over the indicated time by a luminometric assay. DEX treated samples are shown in blue, mock treated samples in red, DEX treated samples in which the promoter with the binding site of the other dTALE-AD was co-transformed are shown in yellow, the respective mock treated control is shown in black. The onset of treatments is marked by a dotted vertical black line. Error bars represent the standard deviation of three independent protoplast transfections.

As shown in Figure 19 A, dTALE-AD C was only able to induce LUC activity when its cognate *pBS3 dTALE C::LUC* reporter was present in DEX treated protoplast. No activation was observed for the *pBS3 dTALE D::LUC* construct designed for dTALE-AD D (Figure 19 A). Again dTALE-AD D was able to induce LUC accumulation from its specific *pBS3 dTALE D::LUC* reporter in the presence of DEX (Figure 19 B). However, a weak LUC induction by dTALE-AD D was also observed for the non-cognate *pBS3 dTALE C::LUC* construct (Figure 19 B).

In summary it can be said, that dTALE-AD C and dTALE-AD D can bind specifically to their DNA target sequence and activate gene expression in the context of their cognate *pBS3::LUC* reporter in *Arabidopsis* protoplast. The liability of dTALE-AD C to induce LUC expression from the *pFRK1::LUC* construct is very likely due to steric hindrance that blocks the functional

interaction of dTALE-AD C with the basal transcription initiation machinery. However, “naked” DNA is used in the transient reporter gene assay in protoplasts. This raises the question whether the dTALEs are also able to bind to their cognate DNA motif in the context of “packed” chromatin in plant tissue and whether the affinity to DNA is high enough to precipitate *pFRK1* fragments.

5.4.2. Precipitation of *pFRK1* fragments with dTALEs

5.4.2.1. Workflow of dTALE-based cross-linking chromatin immunoprecipitation (X-ChIP)

To address the questions raised above, X-ChIP experiments followed by qPCR were performed using transgenic *Arabidopsis* lines independently expressing dTALEs A - F (Figure 13). The workflow for the X-ChIP approach is outlined in (Figure 20).

Seedlings of the T2 seed pools (Table 9) were grown in liquid media and were treated with flg22 and DEX (10 µM) for 60 min. Immediately after the treatments, the plant tissue was crosslinked with formaldehyde and the nuclei purified from the extracts. Afterwards the chromatin was sheared using ultrasound (Figure 20 2). In a next step the dTALE - DNA complexes were purified via GFP-antibodies coupled to agarose beads (Figure 20 3). After reversal of the crosslinking, the DNA was released from the precipitates (Figure 20 4). Using specific primers, the samples were tested for enrichment of *pFRK1* fragments by qPCR (Figure 20 5).

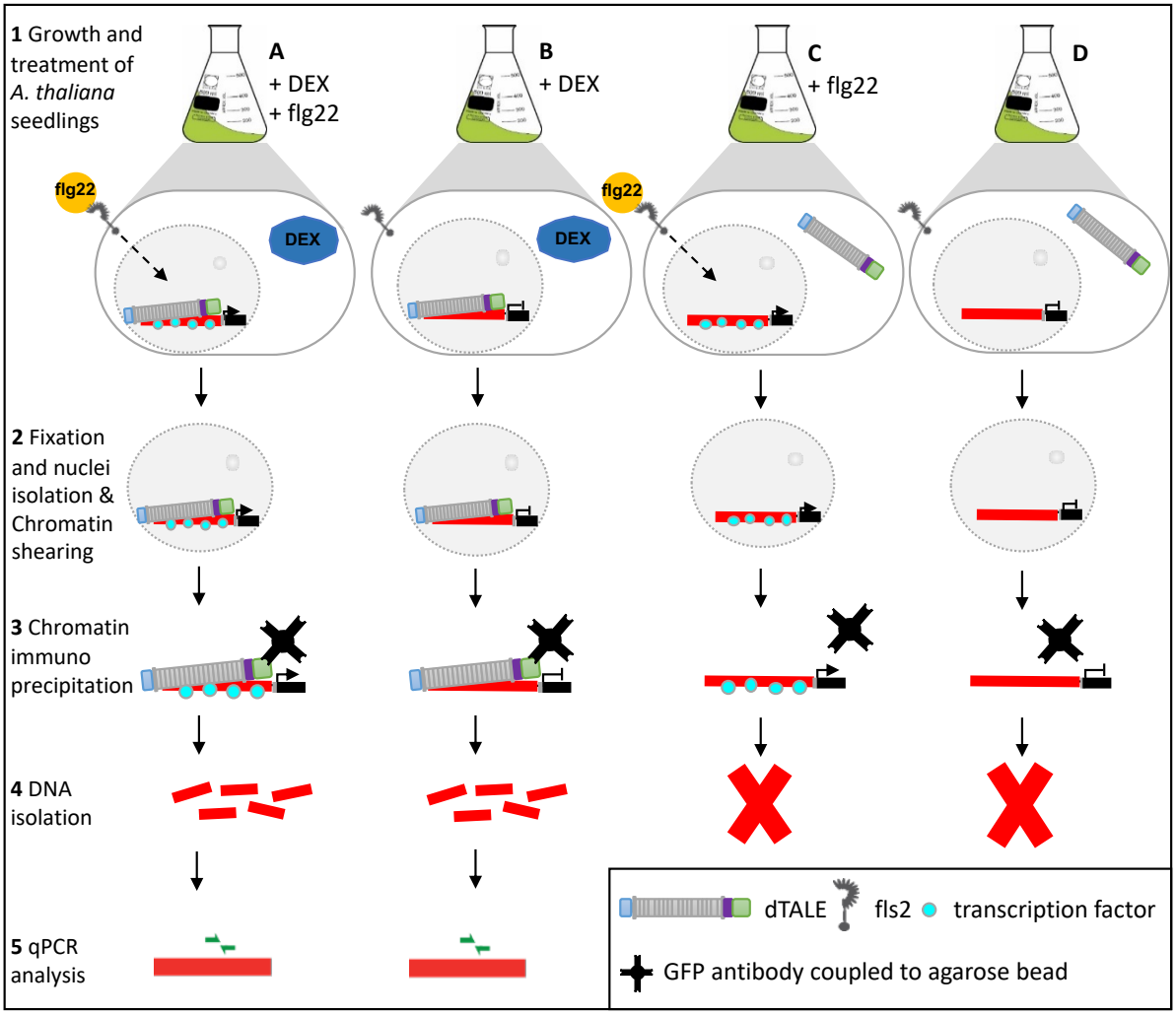

Figure 20: X-ChIP Workflow
A. thaliana seedlings are treated with DEX (10 µM) and flg22 (100 nM) **(A)**, DEX alone **(B)**, flg22 alone **(C)** or mock treated **(D)**. In response to DEX, the dTALEs move to the nucleus and should bind to their binding site in *pFRK1* (symbolized in red) **(1)**. Due to flg22 treatment transcription factors bind to *pFRK1* where they induce FRK1 expression. The plant material is fixed and the nuclei are isolated. The chromatin is sheared using ultrasound **(2)**. The dTALE-promoter-transcription factor complex is purified, using antiGFP-antibodies coupled to agarose beads **(3)**. The DNA is isolated **(4)** and quantified by qPCR using *pFRK1*-specific primers **(5)**.

Four different experimental approaches were performed: Treatment with flg22 and DEX, flg22, DEX and mock treatment (Figure 20 A-D). The DEX treatment triggers the translocation of the dTALEs into the nucleus, flg22 activates *pFRK1* (Figure 6 & Figure 13). From the theoretical point of view, it should be possible to precipitate *pFRK1* fragments from samples of nuclear extracts of DEX treated seedlings (Figure 20 A & B). In the extracts from seedlings not treated with DEX no precipitation of *pFRK1* fragments is expected, since the dTALEs should

be retained in the cytosol (Figure 20 C & D). The control samples might indicate if there is cytosolic carryover from the nuclei purification or unspecific dTALE binding.

5.4.2.2. X-ChIP results

To detect enrichment of a DNA fragment, the percentage of input was determined. For that the ΔCt values of input samples and precipitated samples where normalized to each other. Input samples were crude nuclear extracts, prior to the precipitation.

First, the dTALEs that were expected to bind 1 kb upstream of the transcription start site were tested. After the precipitation, a fragment in the region of the dTALE binding site was amplified (Figure 21 A green arrows). As control a fragment of the last exon of *FRK1* was used in the qPCR as well (Figure 21 A grey arrows).

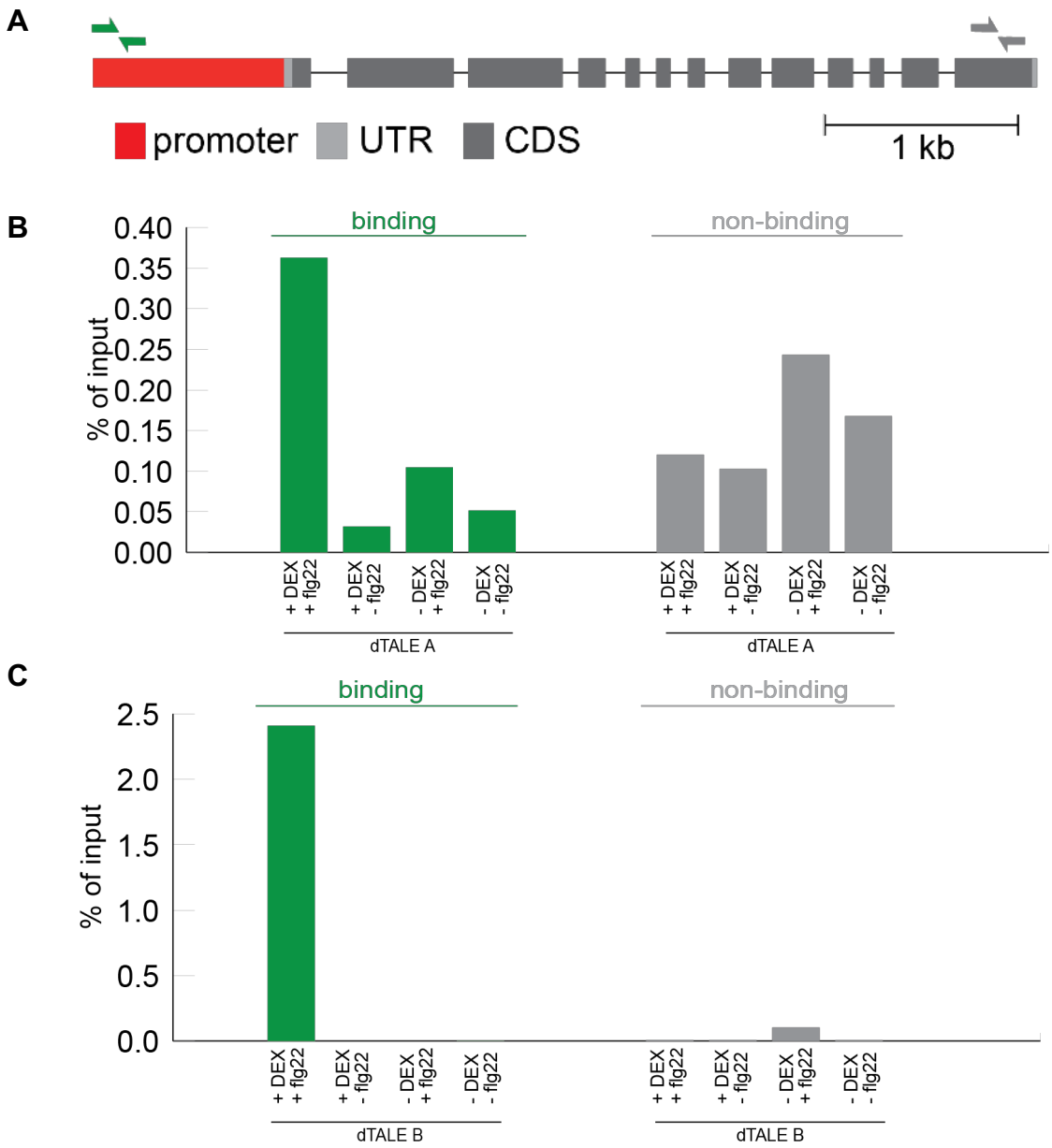

Figure 21: X-ChIP followed by qPCR of *pFRK1* fragments using dTALE A did not result in the specific enrichment of their target DNA motif, using dTALE B it did result in specific enrichment of its target DNA motif

dTALE A **(B)** and dTALE B **(C)** were used to immuno-precipitate *pFRK1* fragments. The samples were prepared from stable *A. thaliana* lines expressing dTALEs that were treated with flg22 and DEX, flg22, DEX. Precipitated DNA was quantified by qPCR with an amplicon located near the dTALE binding site (green arrows) and a control amplicon downstream in *FRK1* (grey arrows) **(A)**. The values are shown in % of input in green for the binding amplicon, grey for the non-binding amplicon.

The precipitates that were prepared from the dTALE A expressing line showed no enrichment for the non-binding amplicon in all treatment combinations (Figure 21 B grey bars). The binding amplicon was found, but all values were under 0.4 % of input in the samples prepared from the dTALE A expressing line (Figure 21 B green bars). A repetition of the experiment did

not deliver any other conclusions (Supplementary figure 5). In the X-ChIP with dTALE B no specific enrichment was found, neither for the binding amplicon nor the non-binding amplicon except in the sample that was treated with DEX and flg22(Figure 21 C). There 2.5 % of input of the binding amplicon were found. Repetition of the experiment with dTALE B it was not possible to amplify any DNA fragment.

Next the dTALEs with the binding sites 500 bp upstream of the transcription start site (dTALE C & D) were tested for their *in vivo* DNA-binding capacity by X-ChIP (Figure 22).

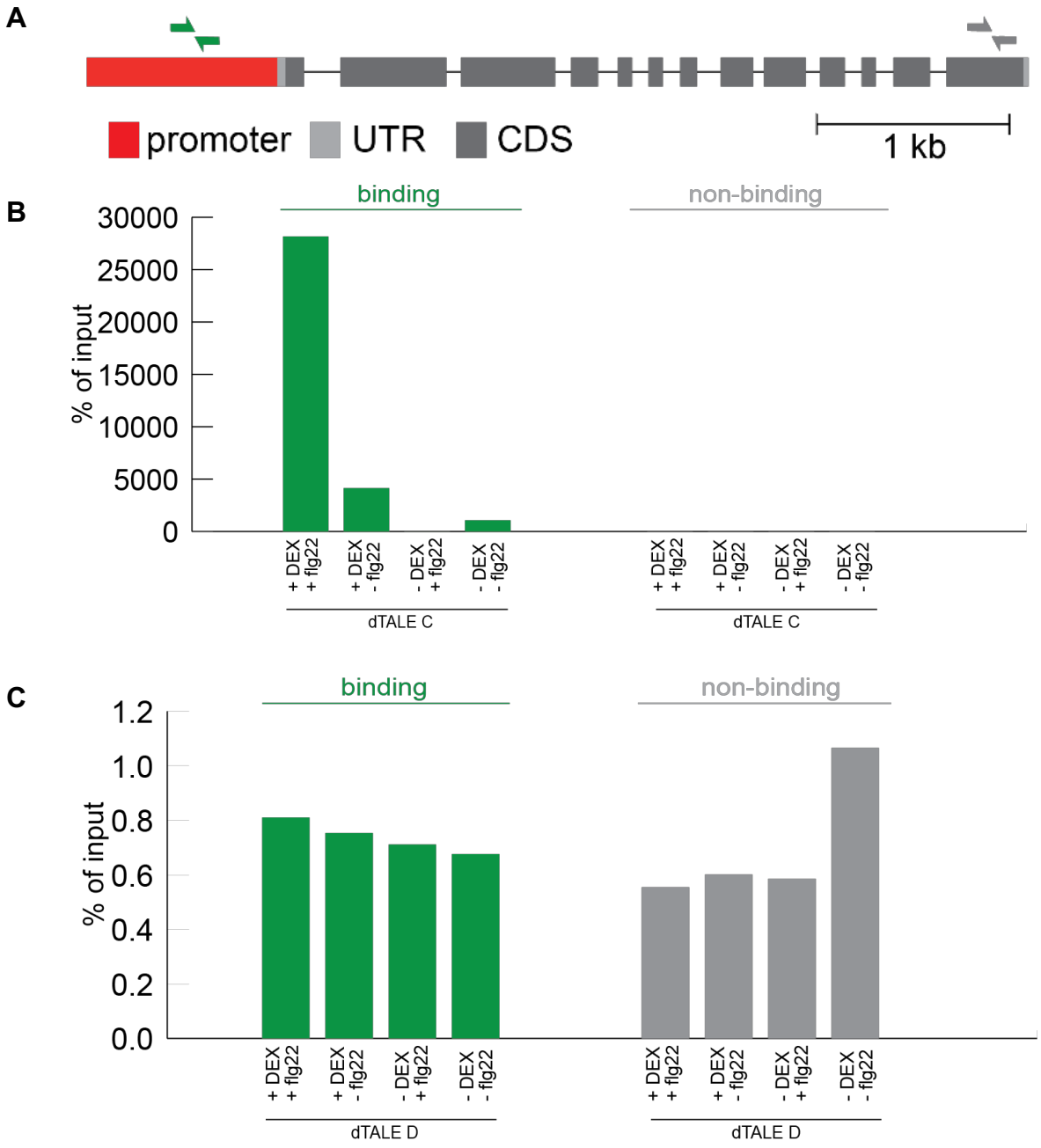

Figure 22: X-ChIP followed by qPCR of *pFRK1* fragments using dTALE C did result in specific enrichment the target DNA motif. Using dTALE D did not result in specific enrichment of the DNA motif. dTALE C **(B)** and dTALE D **(C)** were used to immuno-precipitate *pFRK1* fragments. The samples were prepared from stable *A. thaliana* lines expressing dTALEs that were treated with flg22 and DEX, flg22, DEX and mock. Precipitated DNA was quantified by qPCR with an amplicon located near the dTALE binding site (green arrows) and a control amplicon downstream in *FRK1* (grey arrows) **(A)**. The values are shown in % of input in green for the binding amplicon, grey for the non-binding amplicon.

A *pFRK1* fragment was selected near the binding site of these two dTALEs (Figure 22 A). In the first repetition with dTALE C, there was no amplification of the non-binding amplicon,

independent of the treatment (Figure 22 B grey bars). In the precipitate obtained from DEX-treated seedlings, a strong enrichment (4000% of input) was detectable for the binding amplicon (Figure 22 B green bars. The enrichment was increased 6 fold, when the seedlings were treated with DEX and flg22. Flg22 alone, as well as mock treated samples did not show any significant enrichment of the binding amplicon (Figure 22 green). A repetition of the experiment showed comparable results (Supplementary figure 5). These data suggest, that dTALE C binds tightly and specifically enough to precipitate fragments of *pFRK1*, when the dTALEs are present in the nucleus due to DEX treatment

Using dTALE D for X-CHIP, no enrichment of *pFRK1* fragments was observed (Figure 22 C green bars). All precipitates prepared from the dTALE expressing line, revealed a more or less identical level of enrichment for the binding a non-binding amplicons, independent of the treatment (Figure 22 C). The levels of enrichment were between 0.6 and 0.9% of input. The repetition of the experiment delivered comparable results (Supplementary figure 5).

At last, the dTALE E and F with the binding sites downstream of the transcription start were analyzed (Figure 23). dTALE E did not exceed enrichment levels higher than 0.15 % of input (Figure 23 B green arrows). Furthermore, no differences between the enrichment levels of the binding and non-binding amplicon was observed, independent of the seedlings' treatment. A repetition of the experiment showed comparable results (Supplementary figure 5). Subsuming the results of the X-ChIP using dTALE E, it was not possible to accomplish a specific precipitation of *pFRK1* fragments (Figure 23 B).

For the X-ChIP with dTALE F similar results were obtained as for those with dTALE E (Figure 23 C).

Derived from these results I had to conclude that it is not possible to achieve specific precipitation of *pFRK1* fragments with dTALE E and F.

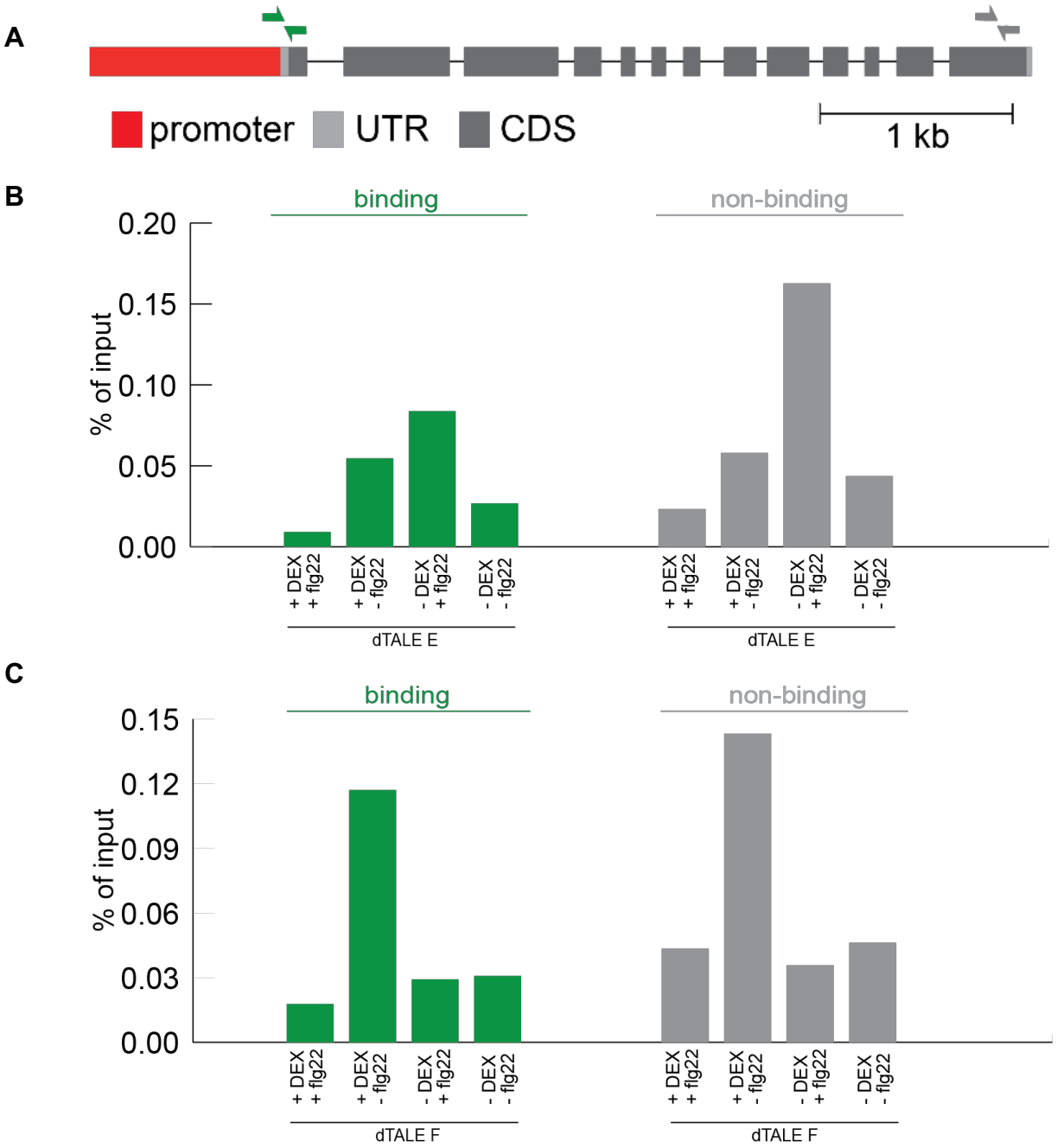

Figure 23: X-ChIP followed by qPCR of *pFRK1* fragments using dTALE E & F did not result in specific enrichment of their target DNA motif

dTALE E **(B)** and dTALE F **(C)** were used to immuno-precipitate *pFRK1* fragments. The samples were prepared from stable *A. thaliana* lines expressing dTALEs that were treated with flg22 and DEX, flg22, DEX and mock. Precipitated DNA was quantified by qPCR with an amplicon located near the dTALE binding site (green arrows) and a control amplicon downstream in *FRK1* (grey arrows) **(A)**. The values are shown in % of input in green for the binding amplicon, grey for the no binding amplicon.

Taken together, the results of the X-ChIP experiments revealed that it was only possible with dTALE B and C to precipitate *pFRK1* fragments specifically (**Figure 22** B). Since dTALE C seemed to be more suitable for *pFRK1* precipitation than dTALE B, it was chosen to perform the dTALE-ChAP approach.

5.5. The dTALE-ChAP

As shown in the previous section, *pFRK1* fragments can be precipitated with dTALE C. To identify protein factors, that bind to *pFRK1* in response to flg22 treatment, the dTALE-ChAP was performed with this dTALE. In a first trial only a limited number of samples was generated and analyzed by MS. In a second trial the procedure was optimized and a complete set of samples was processed. After further optimization, the dTALE-ChAP was done in its final optimized version, again with dTALE C.

5.5.1. First trial of dTALE-ChAP with dTALE C

5.5.1.1. Quantification of Peptides

Plants were grown from the dTALE C seed pool without metabolic labeling. One half of the population was treated with flg22 (100 nM) and DEX (10 µM), the other half was mock-treated. The plants were fixed with formaldehyde for 60 min after treatment. After Chromatin Affinity Purification with dTALE C, the precipitated proteins were analyzed via mass spectrometry. A total number of 1,240 peptides, associated to 254 different proteins was obtained (Figure 24). A list of the identified peptides and proteins, respectively, is shown in Supplementary table 3.

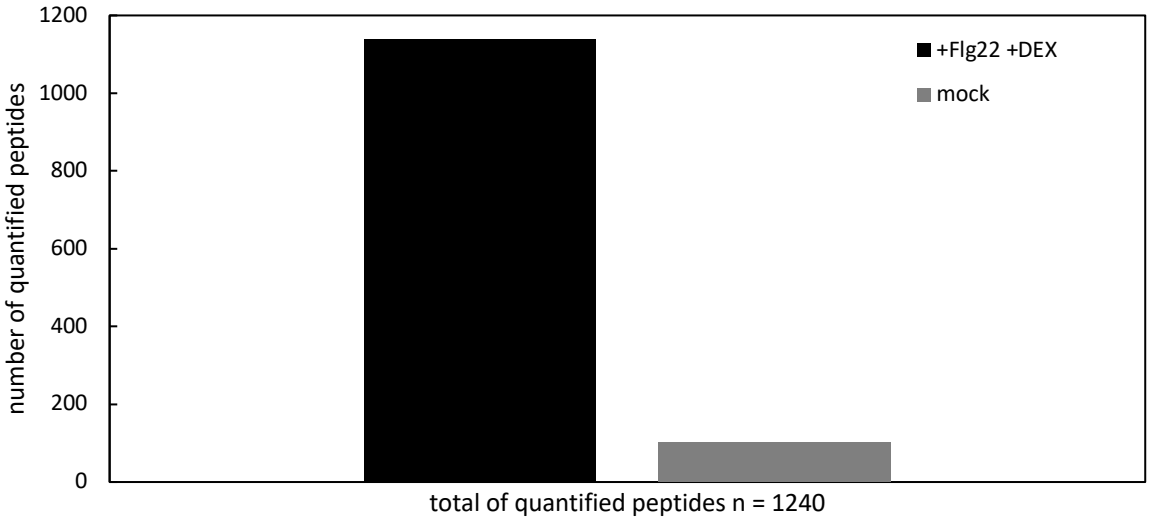

Figure 24: Protein precipitation with dTALE C relies on DEX dependent dTALE localization
dTALE C was used to precipitate *pFRK1* fragments. The associated proteins were analyzed by mass spectrometry. 1,139 peptides representing 227 different proteins in the flg22 and DEX treated sample (black bar) and 101 peptides in the mock treated sample (grey bar) were identified.

In the control sample significantly less peptides were identified than in the flg22/ DEX treated sample (Figure 24 grey & black bar). This was expected, because without DEX treatment dTALE C is retained in the cytosol. Since the dTALE and the cytosolic components and thus the dTALE are removed during the nuclei purification procedure, the difference in found proteins between the treated and the untreated sample was expected.

In the treated sample the two proteins, of which the most peptides were found *per se* and were strongly enriched in the flg22/DEX treated sample, were dTALE C itself and the elongation factor 1-alpha (AT5G60390.3) (Supplementary table 3). Elongation factor 1-alpha is a general translation elongation factor found in many eukaryotes (TAIR). The two proteins were quantified each with 105 peptides. In comparison, in the mock treated sample, the bait protein was quantified with 13 peptides.

5.5.1.2. Over-representation Tests

In the proceeding analysis the gene ontology terms (GO terms) for the found proteins were determined. With the Protein Analysis Through Evolutionary Relationship (PANTHER) tool an

over-representation test was done (Mi et al., 2017). The GO Term enrichment tool takes the genes, associated to the peptides that were identified in the dTALE-ChAP and compares the frequency of GO terms in the sample set, with the frequency of the same set of GO terms in the reference set. As reference set, the *A. thaliana* whole genome set is used. By this comparison it is possible to identify over- or under-represented terms in the sample set.

The first over-representation test was done for GO term Cellular Component (Supplementary table 4).

The strongest enriched GO terms of Cellular Components were protein members of the photosynthetic machinery. This could be caused by an unspecific carryover of chloroplast containing cellular fractions. However, the PANTHER over-representation test, does not take into account the absolute number of peptides. The list of quantified peptides revealed, that the results annotated with GO terms of chloroplastic origin, were achieved with very low peptide numbers (Supplementary table 3). Therefore, the over-representation test was repeated and all candidates were excluded from the analysis that were identified with less than five quantified peptides (Supplementary table 4). The now five strongest enriched GO-terms are shown in Table 11.

After the threshold for peptide counts was set prior to the over-representation test, photosynthetic components did not overlay the result anymore. The most over-represented cellular components were then heterochromatin, nucleosome, DNA-packaging complex, tubulin complex and U4 snRNP. The top five over-represented cellular components are all located in the nucleus.

Table 11: Nuclear components are the five strongest enriched cellular components identified in an over-representation test (Fisher exact test) amongst the dTALE-ChAP data set. The frequency of identified GO terms was compared with the *A. thaliana* reference genome. Proteins were included in the analysis that were at least represented with five peptides in the MS. Columns: GO Term, number of genes with the GO term in the reference genome, number of genes with the GO term in sample, expected number of genes of the term, over- underrepresentation, P value

GO cellular component complete	*A. thaliana* - REFLIST (27502)	Sample (n= 6)	expected	over/under represented	fold enrichment	P-value)
heterochromatin (GO:0000792)	15	3	0.03	+	85.94	9.50 E-06
nucleosome (GO:0000786)	47	9	0.11	+	82.29	7.58 E-15
DNA packaging complex (GO:0044815)	51	9	0.12	+	75.83	1.47 E-14
tubulin complex (GO:0045298)	13	2	0.03	+	66.11	5.46 E-04
U4 snRNP (GO:0005687)	13	2	0.03	+	66.11	5.46 E-04

With the PANTHER tool, proteins associated to the identified peptides were grouped into protein classes (Supplementary table 4 & Table 12). Again, the threshold was set to at least five quantified peptides, to be included in the over-representation analysis. With more than 100-fold enrichment compared to the frequency in the reference genome, the class of histone proteins was over-represented. Confirming, that DNA associated proteins were specifically precipitated by the dTALE-ChAP.

Table 12: Histones are the most over-represented protein class, identified in an over-representation test (Fisher exact test) amongst the dTALE-ChAP data set. The frequency of protein classes was compared with the *A. thaliana* reference genome. Proteins were included in the analysis that were at least represented with five peptides in the MS. Columns: PANTHER protein classes, number of genes with the protein class in the reference genome, number of genes with the protein class in the sample, expected number of genes of the respective protein class, over- underrepresentation, P value

PANTHER Protein Class	*A. thaliana* - REFLIST (27502)	Sample n = 64	Expected	Over / under represented	Fold enrichment	Raw P-value
histone (PC00118)	11	4	0.03	+	>100	3.54E-08
tubulin (PC00228)	17	2	0.04	+	50.56	8.85E-04
translation elongation factor (PC00222)	44	5	0.1	+	48.83	1.01E-07
actin and actin related protein (PC00039)	19	2	0.04	+	45.23	1.08E-03
translation initiation factor (PC00224)	96	6	0.22	+	26.86	1.39E-07
G-protein (PC00020)	95	5	0.22	+	22.62	3.65E-06
translation factor (PC00223)	138	6	0.32	+	18.68	1.07E-06
ribosomal protein (PC00202)	322	10	0.75	+	13.35	4.78E-09
RNA binding protein (PC00031)	1115	19	2.59	+	7.32	6.06E-12
nucleic acid binding (PC00171)	1771	24	4.12	+	5.82	5.75E-13
Unclassified (UNCLASSIFIED)	19939	31	46.4	-	0.67	5.75E-05

In addition, protein classes belonging to the translation machinery were enriched, such as translation elongation factors, translation initiation factors, translation factors, ribosomal proteins, RNA binding proteins. Furthermore, as expected, nucleic acid binding proteins were also found to be enriched in the flg22/ DEX treated sample.

The over-representation test was repeated three times for three GO terms: Molecular Function, Biological Processes and Reactome Pathways (Supplementary table 4 & Table 13). The strongest enrichment in the GO term Molecular Funtion was translation elongation factor

activity (Table 13 A). This is consistent with the found enrichment of translation-associated protein classes described above. Other significant hits in the GO term Molecular Functions were chlorophyll binding, structural constituent of cytoskeleton, scopolin beta-glucosidase activity and protein heterodimerization activity.

When GO terms for biological processes were tested for over-representation, the five most significant hits were found: heterochromatin organization, A-adenosylmethionine metabolic process, photosynthetic electron transport in photosystem II, chromatin silencing and negative regulation of gene expression (Table 13 B).

Table 13: Translation elongation factor is the strongest enriched molecular function (A), heterochromatin organization the strongest enriched biological process (B) and eukaryotic translation elongation the strongest enriched reactome pathway (C) identified in an over-representation test (Fisher exact test) amongst the dTALE-ChAP data set. The frequeny of identified GO terms was compared with an *A. thaliana* reference genome. Proteins were included in the analysis that were at least represented with five peptides in the MS. Columns: GO Term/ PANTHER classification, number of genes with the GO term/ PANTHER classification in the reference genome, number of genes with the GO term/ PANTHER classification in the sample, expected number of genes of the term, over- underrepresentation, P value

A	GO molecular function complete	*A. thaliana* - REFLIST (27502)	Sample = 64	expected	Over/under represented	Fold enrichment	Raw P-value
	translation elongation factor activity (GO:0003746)	55	6	0.13	+	46.88	6.19 E-09
	chlorophyll binding (GO:0016168)	36	3	0.08	+	35.81	1.03 E-04
	structural constituent of cytoskeleton (GO:0005200)	50	4	0.12	+	34.38	7.66 E-06
	scopolin beta-glucosidase activity (GO:0102483)	42	3	0.1	+	30.69	1.58 E-04
	protein heterodimerization activity (GO:0046982)	118	8	0.27	+	29.13	5.44 E-10
B	GO biological process complete	*A. thaliana* - REFLIST (27502)	Sample = 64	expected	Over/under represented	Fold enrichment	Raw P-value
	heterochromatin organization (GO:0070828)	11	3	0.03	+	100	4.27 E-06

	S-adenosylmethionine metabolic process (GO:0046500)	10	2	0.02	+	85.94	3.45 E-04
	photosynthetic electron transport in photosystem II (GO:0009772)	10	2	0.02	+	85.94	3.45 E-04
	chromatin silencing (GO:0006342)	54	6	0.13	+	47.75	5.59 E-09
	negative regulation of gene expression, epigenetic (GO:0045814)	58	6	0.13	+	44.45	8.31 E-09
C	Reactome pathways	*A. thaliana* - REFLIST (27502)	Sample = 64	expec ted	over/un der represe nted	fold enrich ment	Raw P-valu e
	Eukaryotic Translation Elongation (R-ATH-156842)	12	5	0.03	+	> 100	3.48 E-10
	Gamma carboxylation, hypusine formation and arylsulfatase activation (R-ATH-163841)	12	2	0.03	+	71.62	4.74 E-04
	Methylation (R-ATH-156581)	13	2	0.03	+	66.11	5.46 E-04
	HSF1 activation (R-ATH-3371511)	49	5	0.11	+	43.85	1.67 E-07
	Translation (R-ATH-72766)	276	14	0.64	+	21.8	4.44 E-15

Beside the data from GO terms, PANTHER implements the reactome pathway knowledgebase (Fabregat et al., 2016). The reactome pathway database is manually curated and peer reviewed and was therefore included into the analysis. As already appeared in the previous over-representation tests, the strongest enriched pathway found, compared to the *A. thaliana* reference genome, was eukaryotic translation elongation (Table 13 C). The following significant over-represented pathways were Gamma carboxylation hypusine formation and arylsulfatase activatIon, methylation, HSF1 activation and translation.

In summary, the outcome of the over-respresetation tests suggests that the principle of the dTALE-ChAP approach works in principle. Histones were precipitated as well as components of the translation machinery. Chloroplastic proteins were found with low peptide numbers, pointing to some minor contaminations. No relevant transcriptional regulator was identified in the first trial.

5.5.2. Trial 2 repetition of the dTALE C-ChAP

5.5.2.1. Quantification of peptides

As shown in the previous chapter, the dTALE-ChAP approach worked in principle. However, no transcriptional regulators were found. Instead components of the translation machinery were identified besides other DNA associated proteins like histones. It can be speculated, that the timepoint of fixation was too late to capture the transcription initiating factors. Therefore, the duration of the flg22 treatment was shortened. The plant material was fixed 30 min after flg22 treatment. The time schedule for the DEX treatment was not changed. A full set of metabolic labeled samples was prepared according to Figure 7. Plant tissue grown on ^{14}N media, in which the *pFRK1* was induced, was mixed with ^{15}N labeled, non-induced tissue an *vice versa.* Three biological replicates were made. After the precipitation with dTALE C the peptides were quantified by MS (Supplementary table 3 & Figure 25).

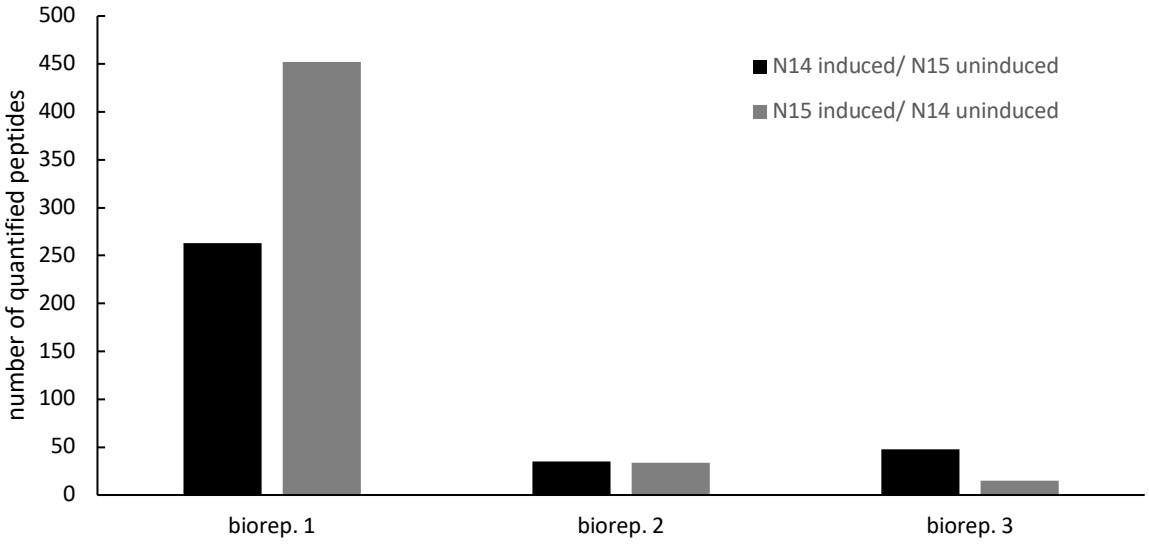

Figure 25: Detergent impurification impairs the number of quantified peptides in the dTALE-ChAP
dTALE C was used to precipitate *pFRK1* fragments with the associated proteins. Mass spectrometry identified a total of 847 peptides in the three biological replicates (biorep). The $^{14}N/^{15}N$ metabolically labeled (black and grey bars) seedlings were treated with DEX and treated with flg22 or mock. Flg22 and mock treated plant tissue was mixed prior to precipitation procedure.

The number of quantified peptides differed severely between biological replicates 1, 2 and 3 (Figure 25). During the MS analysis, contamination with detergent residues caused unexpected but severe problems. The detergents, which are necessary for the purification of

nuclei, masked peaks during the MS measurement. Bioreplicate 2 and 3 contained more residual detergents,, resulting in the lower number of quantifiable peptides (Figure 25).

Due to the impurity it was not possible to separate $^{14}N/^{15}N$ labeled peptides. At least it was possible to perform over-representation tests as in the former chapter (5.5.1.2). A complete list of the proteins associated to the quantified peptides was used for the test. It could not be discriminated in samples that were treated flg22 or mock treated since the plant tissue was mixed prior to precipitation and MS.

5.5.2.2. Over-representation tests dTALE C-ChAP trial 2

For the overrepresentation tests, the quantified peptides of the samples of all biological replicates 1, 2 and 3 were combined in one list. Tissue with induced and uninduced promoter was mixed before the precipitation. For the following analysis of this section, it has to be considered, that several peptides were not identified due to the sample contamination.

The over-representation test for cellular components showed a strong enrichment of nucleosome and DNA packaging complex (Supplementary table 4 & Table 14). Also parts of the spliceosome (U4 snRNP and U5 snRNP) and protein-DNA complex GOs were strongly enriched (Table 14).

Table 14: Nuclear components are the five strongest enriched cellular components identified in an over-representation test (Fisher exact test) amongst the dTALE-ChAP data set.
The frequency of identified GO terms was compared with an *A. thaliana* reference genome. Columns: GO Term, number of genes with the GO term in the reference genome, number of genes with the GO term in sample, expected number of genes of the term, over-underrepresentation, P value

GO cellular component complete	*A. thaliana* - REFLIST (27502)	sample n = 41	Expected	Over/ under represented	fold Enrichment	Raw P-value
nucleosome (GO:0000786)	47	8	0.07	+	> 100	1.35E-14
DNA packaging complex (GO:0044815)	51	8	0.08	+	> 100	2.45E-14

U4 snRNP (GO:0005687)	13	2	0.02	+	> 100	2.24E-04
protein-DNA complex (GO:0032993)	83	8	0.12	+	64.65	9.06E-13
U5 snRNP (GO:0005682)	21	2	0.03	+	63.88	5.36E-04

The data shown in table Table 14 demonstrate, that specifically nuclear components were purified. No chloroplastic carryover was observed in this trial compared to trial. Because of that, for the further over-representation tests no tresholds were set for absolute number of quantified peptides.

The proteins that were assigned to the identified peptides in dTALE C-ChAP trial 2 were compared to the *A. thaliana* reference genome. Histones were significantly over-represented (Supplementary table 4 Table 15). Again, protein classes associated with translation were over-represented: translation elongation factors, translation initiation factors, translation factors. Other over-represented were G-proteins, mRNA splicing, ribosomal proteins, RNA binding proteins and nucleic acid binding proteins (Table 15).

Table 15: Histones are the most over-represented protein class, identified in an over-representation test (Fisher exact test) amongst the dTALE-ChAP data set. The frequency of protein classes was compared with the *A. thaliana* reference genomes. Columns: PANTHER protein classes, number of genes with the protein classes in the reference genome, number of genes with the protein class in the sample, expected number of genes of the term, over-underrepresentation, P value

PANTHER Protein Class	*A. thaliana* - REFLIST (27502)	sample n = 41	Expected	Over/ under represented	fold Enrichment	raw P-value
histone (PC00118)	11	3	0.02	+	> 100	1.10E-06
translation elongation factor (PC00222)	44	4	0.07	+	60.98	7.84E-07
G-protein (PC00020)	95	4	0.14	+	28.24	1.44E-05
translation initiation factor (PC00224)	96	4	0.14	+	27.95	1.49E-05
translation factor (PC00223)	138	4	0.21	+	19.44	5.91E-05

mRNA splicing factor (PC00148)	150	3	0.22	+	13.42	1.53E-03
ribosomal protein (PC00202)	322	5	0.48	+	10.42	1.21E-04
RNA binding protein (PC00031)	1115	12	1.66	+	7.22	5.46E-08
nucleic acid binding (PC00171)	1771	15	2.64	+	5.68	1.80E-08

Since the over-representation of protein classes pointed in the direction of translation, the data was analyzed for over-representation of GO term Molecular Functions, Biological Processes and Reactome pathways (Supplementary table 4 & Table 16). Indeed, translation elongation factor activity was found as significantly over-represented molecular function (Table 16 A) as well as nucleosomal DNA binding. Also scopolin betaglucosidase activity, protein heterodimerization activity and betaglucosidase activity were strongly over-represented in the data set.

Table 16: Nucleosomal DNA binding is the strongest enriched GO term Molecular Function (A), Response to symbiotic fungus the strongest enriched GO term biological process (B) and Eukaryotic Translation Elongation the strongest enriched Reactome Pathways (C) (Fisher exact test) amongst the dTALE-ChAP data set. The frequency of identified GO terms was compared with an *A. thaliana* reference genome. Columns: GO Term, number of genes with the GO term in the reference genome, number of genes with the GO term in sample, expected number of genes of the term, over- underrepresentation, P value

A	GO molecular function complete	*A. thaliana* - REFLIST (27502)	sample n = 41	Expected	Over/ under represented	fold Enrichment	Raw P-value
	nucleosomal DNA binding (GO:0031492)	9	2	0.01	+	> 100	1.18E-04
	translation elongation factor activity (GO:0003746)	55	4	0.08	+	48.78	1.81E-06
	scopolin beta-glucosidase activity (GO:0102483)	42	3	0.06	+	47.91	4.16E-05
	protein heterodimerization activity (GO:0046982)	118	7	0.18	+	39.79	6.62E-10
	beta-glucosidase activity (GO:0008422)	80	3	0.12	+	25.15	2.59E-04

B	GO biological process complete	*A. thaliana* - REFLIST (27502)	sample n = 41	Expected	Over/ under represented	fold Enrichment	Raw P-value
	response to symbiotic fungus (GO:0009610)	12	2	0.02	+	> 100	1.95E-04
	response to symbiont (GO:0009608)	14	2	0.02	+	95.83	2.56E-04
	nucleosome assembly (GO:0006334)	40	4	0.06	+	67.08	5.49E-07
	chromatin assembly (GO:0031497)	48	4	0.07	+	55.9	1.09E-06
	nucleosome organization (GO:0034728)	53	4	0.08	+	50.62	1.58E-06
	chromatin assembly or disassembly (GO:0006333)	61	4	0.09	+	43.99	2.68E-06
C	Reactome pathways	*A. thaliana* - REFLIST (27502)	sample n = 41	Expected	Over/ under represented	fold Enrichment	Raw P-value
	Eukaryotic Translation Elongation (R-ATH-156842)	12	4	0.02	+	> 100	7.59E-09
	HSF1 activation (R-ATH-3371511)	49	4	0.07	+	54.76	1.17E-06
	mRNA Splicing - Minor Pathway (R-ATH-72165)	77	3	0.11	+	26.13	2.32E-04
	Cellular response to heat stress (R-ATH-3371556)	114	4	0.17	+	23.54	2.87E-05
	Translation (R-ATH-72766)	276	8	0.41	+	19.44	8.24E-09

Analysis of the GO term Biological Processes revealed that the most over-represented GO terms are related to the response to a symbiotic fungus (**Table 16 B**). Although the cultures were checked for fungal contamination prior the experiment, this could be a reaction of the *Arabidopsis* seedlings to a fungal contamination. However, these factors should be excluded due to the specific precipitation procedure. The remaining three of the five strongest enriched GO terms Biological Process were: nucleosome assembly, chromatin assembly nucleosome organization and chromatin assembly or disassembly. With regard to over-representation of GO terms in Reactome pathways were translation elongation, translation, mRNA splicing, heat stress and HSF1 activation(Table 16 C).

5.5.3. Trial 3 repetition of the dTALE C-ChAP

5.5.3.1. Quantification of Peptides dTALE-ChAP trial 3

In the previous section the dTALE-ChAP was done with the full set of plant material where ^{14}N and ^{15}N labeled probes were combined. No discrimination between the differentially N-labelled probes could be done, because detergent contamination interfered with the quality of the MS readout (see trial 2). Therefore filter-aided sample preparation (FASP) was included in the ChAP procedure. FASP is a method that combines the removal of detergents, but should not sacrifice low abundant proteins (Wisniewski et al., 2009). No remainings of detergents were found in the samples during mass spectrometry. Compared to the first two trials, the number of peptides was lower than in the last tests (Supplementary table 3 & Figure 26). A total of 113 peptides was quantified in the three biological replicates independent of the nitrogen isotope.

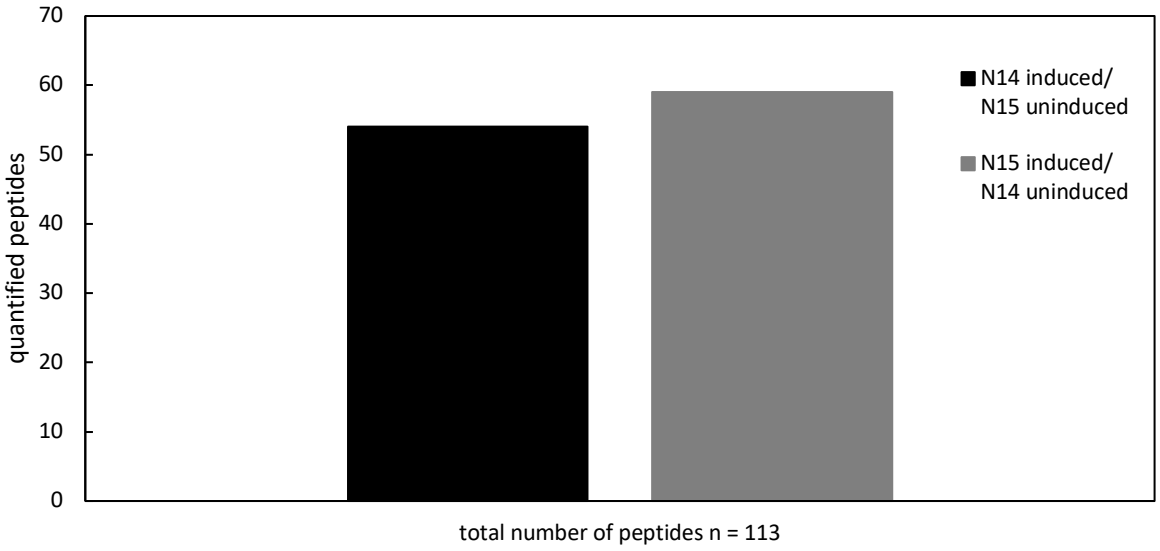

Figure 26: Number of quantified peptides in the dTALE C-ChAP is reduced when FASP is applied
dTALE C was used to precipitate *pFRK1* fragments with the associated proteins. Mass spectrometry identified an average of 113 peptides in three biological replicates. The $^{14}N/^{15}N$ metabolically labeled (black and grey bars) seedlings were treated with DEX and treated with flg22 or mock. Flg22 and mock treated plant tissue was mixed prior to precipitation procedure.

5.5.3.2. Over-representation Test dTALE-ChAP Repetition 3

The proteins were assigned to the found peptides. With the identified proteins the associated GO terms were analyzed for over-representation. Over-representation tests for GO term Cellular components delivered comparable results like in the previous trials (Supplementary table 4 & Table 17). The two most enriched GO term Cellular Components were the same as in the trial 2: Nucleosomes and DNA packaging complexes. U4snRP was not found under the enriched GO terms. Under the five most over- represented GO terms of Cellular Components were nuclear-chromatin and chromatin.

Table 17: Nuclear components are the five strongest enriched cellular components identified in an over-representation test (Fisher exact test) amongst the dTALE-ChAP data set. The frequency of identified GO terms was compared with the *A. thaliana* reference genome. Columns: GO Term, number of genes with the GO term in the reference genome, number of genes with the GO term in sample, expected number of genes of the term, over-underrepresentation, P value

GO cellular component complete	*A. thaliana* - REFLIST (27502)	Sample n = 45	expected	Over / under represented	Fold Enrichment	Raw P-value
nucleosome (GO:0000786)	47	6	0.08	+	78.02	2.91E-10
DNA packaging complex (GO:0044815)	51	6	0.08	+	71.9	4.58E-10
protein-DNA complex (GO:0032993)	83	6	0.14	+	44.18	7.05E-09
nuclear chromatin (GO:0000790)	79	3	0.13	+	23.21	3.30E-04
chromatin (GO:0000785)	170	6	0.28	+	21.57	4.14E-07

The analysis of the found protein classes revealed a strong over-representation of histones (Supplementary table 4 & Table 18). The same protein classes were enriched as in the second trial of the dTALE-ChAP (Table 15) except mRNA splicing factors and ribosomal proteins (Table 15 & Table 18)

Table 18: Histones are the most over-represented protein class, identified in an over-representation test (Fisher exact test) amongst the dTALE-ChAP data set. The frequency of identified GO terms was compared with the *A. thaliana* reference genome. Colums: PANTHER protein classes, number of genes with the protein classes in the reference genome, number

of genes with the protein class in the sample, expected number of genes of the term, over- underrepresentation, P value

PANTHER Protein Class	*A. thaliana* - REFLIST (27502)	Sample n = 45	expected	Over / under represented	Fold Enrichment	Raw P-value
histone (PC00118)	11	2	0.02	+	> 100	2.01E-04
translation elongation factor (PC00222)	44	5	0.07	+	69.45	1.67E-08
G-protein (PC00020)	95	4	0.16	+	25.73	2.09E-05
translation initiation factor (PC00224)	96	4	0.16	+	25.46	2.17E-05
translation factor (PC00223)	138	5	0.23	+	22.14	3.63E-06
RNA binding protein (PC00031)	1115	10	1.82	+	5.48	1.07E-05
nucleic acid binding (PC00171)	1771	12	2.9	+	4.14	2.02E-05

Beside histones, translation elongation factors, G-proteins, translation initation factors, translation factors, RNA proteins and nucleic acid binding proteins were significantly over-represented compared to the *A. thaliana* reference genome (Table 18).

As already done with the two previous dTALE-ChAP datasets, the identified proteins were screened for over-representation of GO terms Molecular Function, Cellular Processes and Reactome Pathways (Supplementary table 4 & Table 19).

Table 19: Nucleosomal DNA binding is the strongest enriched Molecular Function (A), translation elongation the strongest enriched Biological Process (B), and eukaryotic translation elongation the strongest enriched Reactome Pathway (C) identified in an over-representation test (Fisher exact test) amongst the dTALE-ChAP data set. The frequency of identified GO terms was compared with an *A. thaliana* reference genome. Columns: GO Term, number of genes with the GO term in the reference genome, number of genes with the GO term in sample, expected number of genes of the term, over- underrepresentation, P value

A	GO molecular function complete	*A. thaliana* - REFLIST (27502)	Sample n = 45	expected	Over / under represented	Fold Enrichment	Raw P-value
	nucleosomal DNA binding (GO:0031492)	9	2	0.01	+	> 100	1.42E-04
	translation elongation factor activity (GO:0003746)	55	4	0.09	+	44.45	2.65E-06

	protein heterodimerization activity (GO:0046982)	118	6	0.19	+	31.08	5.20E-08
	rRNA binding (GO:0019843)	156	5	0.26	+	19.59	6.48E-06
	translation factor activity, RNA binding (GO:0008135)	165	4	0.27	+	14.82	1.67E-04
B	GO biological process complete	*A. thaliana* - REFLIST (27502)	Sample n = 45	expected	Over / under represented	Fold Enrichment	Raw P-value
	translational elongation (GO:0006414)	73	4	0.12	+	33.49	7.71E-06
	response to cytokinin (GO:0009735)	251	5	0.41	+	12.17	6.01E-05
	translation (GO:0006412)	612	9	1	+	8.99	6.10E-07
	peptide biosynthetic process (GO:0043043)	617	9	1.01	+	8.91	6.52E-07
	amide biosynthetic process (GO:0043604)	693	9	1.13	+	7.94	1.68E-06
C	Reactome pathways	*A. thaliana* - REFLIST (27502)	Sample n = 45	expected	Over / under represented	Fold Enrichment	Raw P-value
	Eukaryotic Translation Elongation (R-ATH-156842)	12	4	0.02	+	> 100	1.11E-08
	HSF1 activation (R-ATH-3371511)	49	4	0.08	+	49.89	1.72E-06
	Cellular response to heat stress (R-ATH-3371556)	114	4	0.19	+	21.44	4.16E-05
	Translation (R-ATH-72766)	276	8	0.45	+	17.71	1.79E-08
	Cellular responses to stress (R-ATH-2262752)	192	4	0.31	+	12.73	2.95E-04

The two strongest enriched GO terms Molecular Functions were the same like in the dTALE ChAP data set of trial 2. Nucleosomal DNA binding was over- represented more than 100 fold, translation elongation factor activity was 44 fold over-represented (Table 19 A). Under the five strongest over-represented Molecular Functions found were: protein heterodimerization, rRNA binding and translation factor activity. Amongst the over-represented Biological

Processes the response to symbiont and symbiontic fungus as in the second trial did not appear anymore (Table 16 B & Table 19 B). Two translation related GO terms were over-represented: Translational elongation and translation (Table 19 B). In addition, the GO terms for response to cytokinin, peptide biosynthetic processes and amide biosynthetic processes were enriched. As suggested by the enrichments found for biological processes, the strongest over-represented Reactome Pathway was eukaryotic translation elongation (Table 19 C). Also translation was an enriched Reactome Pathway. Like already observed in the second data set of trial 2, the GO term Reactions to Heat Stress were enriched. Under the five strongest over-represented Reactome Pathways was cellular responses to stress.

Summarizing the results of trial 3 of the dTALE C-ChAP, FASP purification of the samples helped to get rid of the remaining detergents. Again, a transcriptional regulator was not found .

5.5.4. Overlap of dTALE-ChAP trial 1, 2 and 3

In all three dTALE C-ChAP trials, parts of histones and nucleosomes were identified. In addition, members of the translation machinery were over-represented. Therefore, it was analyzed whether there is an overlap of identified proteins between all three trials. By analyzing the overlap, rare proteins can be identified, that are masked by the background of over-represented proteins. 15 proteins were found in all of the three trials (Figure 27). Between trial 1 and 2 there was an overlap of 6 proteins, between trial 2 and 3 an overlap of 9 proteins and between trial 1 and 3 an overlap of 4 proteins (Figure 27).

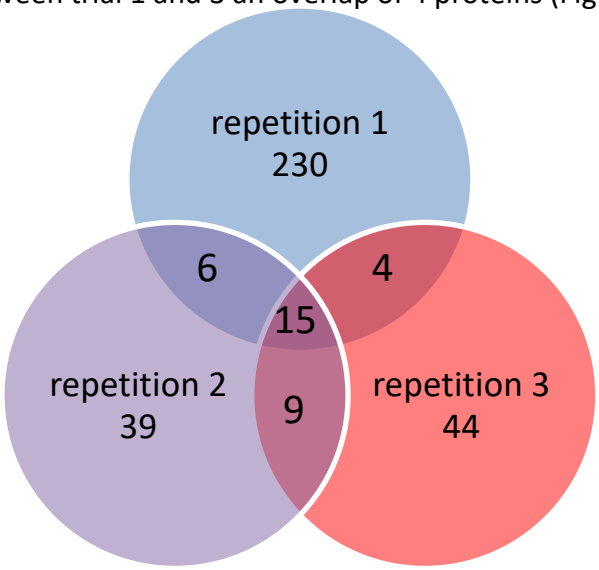

Figure 27: Fifteen identical proteins were identified in trial 1, 2 and 3 of dTALE C-ChAP. Numbers indicate different proteins associated to the identified peptides in dTALE C-ChAP detets. The quantities of found peptides are not taken into account.

The fifteen proteins that are found in all three trials are histones and ribosomal proteins (Table 20 yellow). Besides that, a Penttricopeptide repeat superfamily protein, a beta glucosidase, nucleolin protein and a splicing factor was found (Table 20). No transcriptional regulator was present in all of the three trials.

Table 20: Fifteen histone proteins were found in dTALE C-ChAP trial 1, 2 and 3. Proteins that were identified in all three dTALE-ChAP trials are listed**.** Gene descriptions were downloaded from www.arabidopsis.org Araport11, histones and ribosomal proteins are highlighted in yellow

Representative Gene Model Name	Gene Description
AT1G80550.1	Pentatricopeptide repeat (PPR) superfamily protein;(source:Araport11)
AT5G59970.1	Histone superfamily protein;(source:Araport11)
AT1G20580.1	Small nuclear ribonucleoprotein family protein;(source:Araport11)
AT3G09260.1	Encodes beta-glucosidase.The major constituent of ER bodies. One of the most abundant proteins in Arabidopsis seedlings. Exist in an soluble (inactive) and non-soluble (active) form, most probably formed in a polymerization process. Involved in the mutualistic interaction between Arabidopsis and the endophytic fungus Piriformospora indica.
AT2G41475.1	Embryo-specific protein 3, (ATS3);(source:Araport11)
AT5G65360.1	Histone superfamily protein;(source:Araport11)
AT5G10980.1	Histone superfamily protein;(source:Araport11)
AT5G27670.1	Encodes HTA7, a histone H2A protein.
AT1G52740.1	Encodes HTA9, a histone H2A protein. Loss of all H2A.Z (triple mutant with HTA8 and HTA11) results in a reduction in DNA methylation of transposons but not that of genes. Loss of H2A.Z causes misregulation of many genes involved in the response to developmental and environmental cues, and that these genes tend to have high levels of gene-body H2A.Z.
AT1G48920.1	Encodes ATNUC-L1 (NUCLEOLIN LIKE 1), the predominant form of the two nucleolin proteins found in Arabidopsis. This protein is involved in rRNA processing, ribosome biosynthesis, and vascular pattern formation. PARL1 localizes to the nucleolus and parl1 mutants accumulate elevated levels of the unspliced 35S pre-rRNA. parl1 mutants also have defects in cotyledon, leaf, sepal, and petal vein patterning and have reduced stature, reduced fertility, increased bushiness, and reduced root length. The sugar-induced expression of ribosome proteins is also reduced in parl1 mutants. The mRNA is cell-to-cell mobile.
AT5G54640.1	Isolated from T-DNA insertion line, the rat5 mutant is deficient in T-DNA integration. Encodes histone2A protein.
AT3G25520.1	Encodes ribosomal protein L5 that binds to 5S ribosomal RNA and in involved in its export from the nucleus to the cytoplasm.

	Identified in a screen for enhancers of as1. as1/pgy double mutants show defects in leaf vascular patterning and adaxial cell fate. Double mutant analysis indicates pgy genes function in the same pathway as REV, KAN1 and KAN2.
AT4G39260.1	Encodes a glycine-rich protein with RNA binding domain at the N-terminus. Protein is structurally similar to proteins induced by stress in other plants. Gene expression is induced by cold. Transcript undergoes circadian oscillations that is depressed by overexpression of AtGRP7. A substrate of the type III effector HopU1 (mono-ADP-ribosyltransferase).
AT2G24590.1	Barta et al (2010) have proposed a nomenclature for Serine/Arginine-Rich Protein Splicing Factors (SR proteins): Plant Cell. 2010, 22:2926.
AT4G09800.1	encodes a ribosomal protein S18C, a constituent of the small subunit of the ribosomal complex

5.5.5. Changes in the proteome after flg22 Treatment

5.5.5.1. $^{14}N/^{15}N$ ratios of identified Proteins of dTALE-ChAP trial 3

The peptides that were found in the third trial of the dTALE-ChAP, were analyzed if they were found in the ^{14}N as well as the ^{15}N labeled samples. For that, all precipitates of dTALE C-ChAP trial 3 were analyzed separately. As the metabolic N-labeling was performed reciprocally, six samples were available which were derived from three biolocial replicates (Table 21 2 reciprocal samples per biological replicate).

Table 21: Samples of dTALE-ChAP Repetiotion 3. Columns: Bioreplicate, sample, nitrogen isotope

		^{14}N labeled seedlings	^{15}N labeled seedlings
bioreplicate 1	sample 1	induced	uninduced
	sample 2	uninduced	induced
bioreplicate 2	sample 3	induced	uninduced
	sample 4	uninduced	induced
bioreplicate 3	sample 5	induced	uninduced
	sample 6	uninduced	induced

From when an identified protein was found in one sample in its ^{14}N and ^{15}N labeled form, a ratio was calculated based on the number of identified peptides. The proteins associated to the peptides, of which a ratio was calculated are shown in Table 22. Since distinct peaks in the MS analysis are necessary to calculate a ratio it was possible to calculate solely eleven ratios. Three ratios were found for histones: Two proteins of the histone core H3 (AT5G10980 & AT5G65360) and one of the histone core H4 (AT5G59970) (Table 22). The histone associated proteins were found more often in the flg22 induced samples, with ratios between 1.3 and 2.0 (Table 22). Unfortunately the protein with the highest ratio and therefore the biggest difference between induced and uninduced tissue was a protein of unknown function (Table 22 AT2G27830). A ratio was calculated in sample 1, sample 3 and sample 5 (Table 22). The found ratios were 2.2, 3.0 and 6.7 (Table 22). Therefore, the protein of unknown function was more abundant in the induced samples. A ratio of dTALE C was calculated in sample 1 and sample 6 (Table 22). The log2 ratio was in both cases approximately 0 (Table 22). As expected this proves that the dTALE was found in almost the same amounts independent of the flg22 treatment. In sample 5 a splicing factor was found with a ratio of 2.5 (Table 22 AT1G68470).

In sample 5 a glucosyl transferase was found in higher levels in the induced sample (Table 22 AT1G68470). The calculated ratio was 2.15. In sample 6 elevated levels, with a ratio of 0.9 of AT1G48920 was found. No ratio was found for a protein that was more abundant in the uninduced promoter.

Table 22: Histones are identified more often in the precipitates, prepared of flg22 induced *pFRK1*. Ratios of identified proteins in dTALE-ChAP trial 3. The log2 ratio was calculated based on the identified peptide numbers in dTALE C-ChAP trial 3. A high ratio indicates higher abundance at the induced promoter, a negative ratio indicate higher abundance at the uninduced promoter. Columns: sample, protein, log2 ratio, protein name, protein description.

Sample	Protein	log2 ratio	Protein Name	Protein Description
1	AT5G10980.1	1.342753147	DNA.synthesis/chromatin structure.histone.core.H3	histone H3 | chr5:3472405-3473466 REVERSE
1	AT2G27830.1	2.187138662	not assigned.unknown	FUNCTIONS IN: molecular_function unknown I chr2:11860218-11861475 FORWARD
1	dTALE C	-0.151394936		
2	AT5G59970.1	2.035000811	DNA.synthesis/chromatin structure.histone.core.H4	histone H4 | chr5:24146175-24146726 REVERSE
2	AT5G65360.1	1.37489758	DNA.synthesis/chromatin structure.histone.core.H3	histone H3 | chr5:26119859-26120581 REVERSE
3	AT2G27830.1	3.099377542	not assigned.unknown	FUNCTIONS IN: molecular_function unknown I chr2:11860218-11861475 FORWARD
3	AT2G24590.1	2.522177408	RNA.processing.splicing	splicing factor, putative | chr2:10449631-10451184 FORWARD
5	AT1G68470.1	2.159057851	misc.UDP glucosyl and glucoronyl transferases	exostosin family protein | chr1:25676395-25678288 REVERSE
5	AT2G27830.1	6.744265712	not assigned.unknown	FUNCTIONS IN: molecular_function unknown I chr2:11860218-11861475 FORWARD
6	dTALE C	-0.087631254		
6	AT1G48920.1	0.87631881	protein.synthesis.ribosome biogenesis.Pre-rRNA processing and	ATNUC-L1, PARL1 | ATNUC-L1; nucleic acid binding / nucleotide binding | chr1:18098095-18101623 FORWARD

			modifications.snoRNPs	

5.5.5.2. Transcription Related Proteins found in dTALE-ChAP Repetition 3

Amongst the ratios that were calculated in the previous section, there was no protein associated to transcription. Ratios can only be assigned automatically and thus calculated, if the ^{14}N and ^{15}N peptide peaks of the MS measurement are distinct and present in both metabolically labeled forms. However, single candidates with unclear peaks, or candidates that are identified just in one metabolically labeled form, can be analyzed manually. Therefore the list of identified peptides of trial 3 was searched for transcription-related candidates. Five proteins with a transcription-related gene description were derived (Table 23).

Table 23: Transcription Associated Genes Identified in dTALE-ChAP trial 3. Gene descriptions were accessed by Araport11 release. The MS data was screened by hand if they occur in flg22 induced or uninduced samples

Gene Name	Gene Description	More abundant in
AT5G54640.1	Isolated from T-DNA insertion line, the rat5 mutant is deficient in T-DNA integration. Encodes histone2A protein.	non-induced sample
AT3G63140.1	Encodes a protein with ribonuclease activity that is involved in plastid rRNA maturation.	induced sample
AT5G25475.4	AP2/B3-like transcriptional factor family protein;(source:Araport11)	induced sample
AT1G52740.1	Encodes HTA9, a histone H2A protein. Loss of all H2A.Z (triple mutant with HTA8 and HTA11) results in a reduction in DNA methylation of transposons but not that of genes. Loss of H2A.Z causes misregulation of many genes involved in the response to developmental and environmental cues, and that these genes tend to have high levels of gene-body H2A.Z.	exclusively found in non-induced sample
AT5G27670.1	Encodes HTA7, a histone H2A protein.	exclusively found in induced sample

Three histone proteins, an AP2/B3-like transcriptional factor family protein and a protein with ribonuclease activity were found in the protein list associated to the identified by manual analysis (Table 23). The intensities in the raw data were analyzed by hand, to check if the proteins are more abundant in the flg22 induced samples or in the non-induced controls. AT5G54640 was found more often in the non-induced samples (Table 23). AT3G63140 and

AT5G25475 were more abundant in the induced samples (Table 23). Two proteins were exlusively found in either induced or uninduced samples. AT1G52740 and AT5G27670 were only found in non-induced samples (Table 23). AT5G27670 was only present in the induced sample (Table 23).

Summarizing the results of the dTALE C-ChAP analysis, I could demonstrate the dTALE C-mediated precipitation of *pFRK1*-associated proteins from plant tissue. In three independent dTALE C-ChAP trials, an overlap of fifteen proteins was found, mainly histones and ribosomal proteins (Figure 27). Because of the metabolic labeling with two different N isotopes in trial 3, it was possible to calculate the relative amounts of dTALE C precipitated proteins in flg22/DEX treated and mock/DEX treated samples for eleven proteins (Table 22). The proteins that were identified in trial 3 and were annotated with a transcription associated gene description were analyzed manually, if they were predominately found in the flg22 induced or uninduced samples (Table 23).

Overrepresentation tests, revealed strong overrepresentation mainly of parts of the translation machinery and DNA packaging complex (Table 13, Table 16 & Table 19).

6. Discussion

The goal of this work was the establishment of a technique, the dTALE-ChAP, with which the proteome at any promoter of interest can be analyzed. The work includes a multitude of pre- and control experiments up to the full establishment of the dTALE-ChAP.

To do so, the following steps had to be carried out: Selection of a suitable promoter and DNA target sites within or next to the promoter, design of appropriate dTALE fusion proteins, analysis of the expression and inducible change of the dTALEs' intracellular localization, test of the dTALEs' *in vivo* DNA binding capacity and the implementation and optimization of the dTALE-ChAP.

These steps will be discussed in the following chapters.

6.1. *pFRK1* is an ideal Promoter to Establish the dTALE-ChAP

pFRK1 was chosen as a suitable promoter for the establishment of the dTALE-ChAP. AS proven by qRT-PCR experiment on RNA from *Arabidopsis* seedlings grown in liquid culture, it takes about 45 min after flg22 treatment until *FRK1* transcript levels increased (Figure 6).

These results are consistent with the qRT-PCR findings of Frei Dit Frey et al. (2012). They could show by endpoint determination, that *FRK1* transcript accumulation is initiated within 60 min after flg22 treatment in *Arabidopsis*. Additionally, it was shown by promoter-reporter gene assays in *Arabidopsis* protoplast that a *pFRK1::LUC* reporter gene is induced 45 min after flg22 application at earliest (Mueller et al., 2012; Pochert, 2014). Since PAMP triggered immunity is the first layer of defense response, the fast reaction of a PTI responsive gene like *FRK1*, was expected.

Due to its rapid inducibility by exogenous flg22, *pFRK1* appeared to be highly suitable for the establishment of the dTALE-ChAP.

6.2. Prediction of *cis* Regulatory Elements by Bioinformatic Tools is Prone to False Positives

To get a first insight into the regulatory proteins that might bind to *pFRK1*, the promoter sequence was analyzed *in silico* for putative transcription factor binding sites. PlantPan2 predicted 1092 putative transcription factor binding sites. After the search query was restricted to binding sites for transcription factors that were already shown to bind to *pFRK1*, twelve putative binding sites remained (Figure 9). The twelve predicted Wboxes overlap with the twelve Wboxes described by (Robatzek & Somssich, 2002). Beside the binding elements of the WRKY family three binding for bZIP1 were annotated by hand. Since *FRK1* appeared only one of three replicates of a ChIPseq experiment, it has to be further examined if *pFRK1* is a real target of bZIP1. WRKYs are plant exclusive transcription factors and are one of the largest transcription factor families (Bakshi & Oelmüller, 2014). Since WRKYs are involved in the responses to pathogens, involvement of WKRYs in the regulation of *FRK1* makes sense (Bakshi & Oelmüller, 2014).

If the dTALE-ChAP works, some members of these transcription factor families are expected to be identified.

The enormous difference in the number of predicted binding sites between the purely *in silico* based search and the search in which the query was restricted to binding sites of transcription factors that were already published to bind to *pFRK1*, indicates the weakness of *in silico* search tools. They are highly prone to false positive results. Available search tools differ in the underlying databases. PlantPan2 was chosen because it incooperates the databases TRANSFAC, PLACE, AGRIS and JASPER in one search tool (Chang et al., 2008; Chow et al., 2016). These databases are either experimentally verified, or extracted from previously published reports. Nevertheless, 1092 putative predicted binding sites in an analyzed 1 kb promoter region demonstrates, that even though high quality databases are used by PlantPan2, the list of candidates is full of potential false positives. The best trade-off between obtaining the correct regulators and controlling false positive results, is the combination of *in silico* prediction with subsequent enrichment tests like ChIP experiments.

The target sites of the dTALEs that were used for the dTALE-ChAP were chosen in the region of the transcription factor binding sites but not directly on them. It can be assumed that

because of the pure size of 150 kDa of the dTALE fusion protein, it might block binding of transcription factors. The sonification conditions in the dTALE-ChAP were adjusted to shear the chromatin in fragments of an average size of 500 bp. With three target sites in the 1 kb of *pFRK1*, full coverage of the promoter was expected. Since dTALE binding might be sensitive to chromatin modifications, for example methylation, pairs of dTALEs were designed (Kaya, Numa, Nishizawa-Yokoi, Toki, & Habu, 2017). With two dTALE target sites 1 kb upstream of the transcription start, two dTALE target sites 500 bp upstream of the transcription start and two target sites 77 bp downstream of the transcription start, lack of binding of single dTALEs can be compensated and full coverage of promoter analysis can still be reached. Since the dTALEs were planned to be used as bait protein, the natural activation domain was deleted in the construct, to prevent interference with *FRK1* expression. Of the dTALEs a second variant with an activation domain was designed, to be used in pre-experiments.

6.3. dTALEs Translocate Fast into the Nucleus after DEX Treatment in *A. thaliana* Protoplasts

After the dTALEs constructs were assembled, their expression and DEX-inducible movement from the cytoplasm to the nucleus was tested in *A. thaliana* protoplasts. All dTALEs were expressed as GFP fusion proteins. An effect of DEX treatment on nuclear accumulation of the dTALEs was visible already 5 min after application of the steroid hormone.

With regard to the very rapid nuclear accumulation of the dTALEs in response to DEX treatment in protoplasts, the lack of a cell wall has to be considered. Due to their small size and their lipophilic nature, the kinetics of cellular steroid uptake into wall containing plant cells is limited by their diffusion through the cell wall which acts as diffusion barrier (Vandevyver et al., 2012). So far, there is no study available that compared steroid diffusion rates through plasma membranes with diffusion rates through cell wall and plasma membrane in plant cells. However, the lipopolysaccharide layer of gram positive bacteria was shown to severely impair the diffusion rate of steroids into the cells (Plésiat & Nikaido, 1992). In general, the observed kinetics for the nuclear import of GR-GFP fusion proteins is faster in cells of organisms without cell walls compared to plant cells. (Brockmann et al., 2001; Ermakova et al., 1999). One could speculate that this is rather conditioned by the strong diffusion barrier

of the cell wall for steroids, than by different properties of nuclear transport in plant and non-plant cells.

In case of dTALE C, nuclear accumulation of GFP fluorescence was observed in the absence of DEX in *A. thaliana* protoplasts. This might be due to steroid independent nuclear import of dTALE C, as it was observed for other GR-GFP fusion proteins in *Arabidopsis* (Brockmann et al., 2001). Triggers for steroid independent GR activation are aberrant physiological conditions, like elevation of cytosolic pH, abiotic stresses such as chemical cues or heat (Bresnick, Dalman, Sanchez, & Pratt, 1989; Meshinchi, Matic, Hutchison, & Pratt, 1990; Sanchez, 1992). Certainly, plant protoplasts suffer under such non-physiological stress conditions. Another possibility could be the dissociation of the C-terminal GFP. Free GFP might diffuse to the nucleus.

6.4. dTALEs reach the nucleus 30 min after DEX treatment in *N. benthamiana* epidermal leaf cells

To support the protoplast results regarding the nuclear uptake of the dTALEs and to address the effect of a cell wall on the kinetics of DEX dependent dTALE translocation, the dTALEs were expressed transiently in *N. benthamiana* leaves. DEX dependent nuclear accumulation of the dTALEs into the nucleus was visible 30 mn after application. Saturating nuclear signals were achived 60 min after the onset of the treatment.

As far as it could be proven, this is the first dataset demonstrating the kinetics of DEX dependent nuclear uptake of GR-GFP fusion proteins in general and particularly of dTALE-GFP fusion in *N. benthamiana.* The nuclear uptake of the dTALEs is around five times faster in *N. benthamiana* than it was reported for GR-GFP proteins in transgenic *Arabidopsis* (Brockmann et al., 2001; Ermakova et al., 1999). This difference may be explained by the way of application of the DEX solution: Whereas the DEX solution was infiltrated into the tobacco leaves in this work, Brockmann et al. (2001) sprayed the DEX solution on the *Arabidopsis* plants. Thus, in contrast to *Arabidopsis*, the DEX had not to diffuse through the cuticula barrier in the *N. benthamiana* system. In addition, the data in this work also provide clear evidence, that the cell wall is indeed a strong diffusion barrier for steroids like DEX, as nuclear accumulation starts much earlier after DEX application in *Arabidopsis* protoplasts.

dTALE protein accumulation was surprisingly low in the *N. benthamiana* cells, although the transcription from the *dTALE* construct was driven by the *35S* promoter. Cytosolic dTALE-GFP signals were hardly detectable and distinguishable from the autofluorescence of the cell wall. A method to solve this problem from the microscopic point of view is Fluorescence Intensity Analysis Microscopy (FIDAM). FIDSAM can be used to increase the contrast between GFP and background fluorescence (Elgass et al., 2010; Schleifenbaum et al., 2010).

Although I cannot exclude the possibility that protein instability is the cause of the low dTALE accumulation, the use of alternative promoter-dTALE combinations may also increase the dTALE amounts in *N. benthamiana* cells.

6.5. T2 Seed Pools are an Eligible Way to Generate High Masses of Plant Material, Circumvent Silencing Effects and Compensate Biological Variance

Beside the expression tests in protoplasts and tobacco leaves, stable *A. thaliana* dTALE lines were generated. PCR analysis prior to plant transformation confirmed the integrity of the dTALEs' DNA sequence coding for their DNA binding domains. This verification is crucial, because of their repetitive nature, DNA sections encoding for a certain repeat of the dTALEs' DNA binding domain can be lost due to recombination events (Weber et al., 2011). The loss of such a DNA section would not cause a frame shift, but results in a dTALE, which is still visible via its GFP fluorescence, but is not longer able to bind to its target DNA. The fact, that no loss of repeats was observed, is consistent with the findings of Morbitzer et al. (2011) that the DNA assembly of the *dTALEs* with two subsequent cut ligations increases a high sequence fidelity.

The *Arabidopsis* transformants were selected and propagated under BASTA selective conditions into the T2 generation. In the T2 generation, the lines were additionally selected for GFP fluorescence before the seeds of the different dTALE lines were combined to variant specific poolsThe use of the T2 seed pools made the production of the required, high amount sof plant material for the X-ChIP and dTALE-ChAP approaches uncomplicated. It has been calculated, that single dTALE-expressing *Arabidopsis* lines would have had to be brought into the T4 generation to get enough seeds. Furthermore, the risk of transgene silencing, which increases during the propagation of transgenic plants over many generations, is minimized when T2 seed pools are used. In addition, the use of see pools level out the biological diversity

within the dTALE variant-specific lines which is caused, for instance, by their zygosity status or number of transgene insertions.

Intriguingly GFP fluorescence positive *Arabidopsis* transformants were obtained for all *dTALEs* but none for the *dTALE-AD* constructs. Perhaps, there is a basal level of import of the dTALEs and dTALE-ADs into the nucleus. Due to the activation domain, it is possible that only the dTALE-ADs cause lethal effects in *Arabidopsis.*

6.6. dTALEs accumulate to low levels in *Arabidopsis thaliana*

As far as it could be proven, this is the first report about the successful expression of GR-dTALE-GFP fusion proteins in *Arabidopsis.* However, dTALEs can hardly be observed in the cytoplasm in the absence of DEX due to their low expression. When the dTALE expressing lines were treated with DEX, the dTALEs accumulate inside the nucleus to a level which is comparable to that reported before for constitutively nuclear dTALE-GFP fusions (Fujimoto, Sugano, Kuwata, Osakabe, & Matsunaga, 2016).

Although the accumulation levels of the dTALEs are very low in the transgenic *Arabidopsis* cells, the possibility had to be excluded, that the nuclear enriched dTALEs interfere with the flg22-induction of *FRK1* expression. If such an interference is observed it implicates, that the nuclear, *pFRK1-bound* dTALEs suppress or block protein accession to the promoter required for its activation. At least for the tested dTALE C, which binds to *pFRK1* at 500 bp upstream of the transcription start, this is not the case: There is no difference in *FRK1* transcript accumulation in the transgenic *Arabidopsis* seedlings whether the dTALE C is present inside the nucleus or not. This result shows that the necessary factors for *pFRK1* activation were not hindered from binding, at least not by dTALE C, which was used in the dTALE-ChAP.

6.7. dTALE-AD C and dTALE-AD D specifically bind to their DNA target

To demonstrate the *in vivo* binding capacity of dTALEs, I perfomed reporter gene assays have been performed with two different reporter constructs in *Arabidopsis* protoplasts using dTALE-AD C and D as examples.

It was possible to induce the *pFRK1::LUC* reporter by dTALE-AD D approximately 40 min after DEX treatment. This correlates very well with the findings of the dTALEs' nuclear accumulation in tobacco, where it took approximately 30 min after DEX treatment till the GFP fluorescence got visible in the nucleus. Furthermore, the lack of LUC activity in the absence of DEX treatment demonstrates, that the tested GR-dTALEs do not leak into the nucleus to an extent required for *pFRK1::LUC* activation. The induction of *pFRK1::LUC* can be clearly assigned to the activity of dTALE-AD D. DEX treatment itself was not sufficient to induce *pFRK1::LUC*, how it was reported before for other defense-related genes (H.-G. Kang, Fang, & Singh, 1999)

Direct induction of the *pFRK1::LUC* reporter with flg22 revealed a strong increase of LUC activity 40 min after application, that fits well to the results of comparable promoter reporter assays (Mueller et al., 2012; Pochert, 2014).

However, the binding affinity of dTALEs to their target site does not necessarily correlate with their efficiency for gene induction (Bultmann et al., 2012). In that regard, the weak induction of dTALE-AD D or the lack of induction by dTALE-AD C must not represent weak or no DNA binding.

It is possible that the steric orientation of the DNA-bound dTALEs is not optimal to induce the *pFRK1::LUC* reporter like flg22 does. Furthermore, it was shown in a recent study, that genes up-regulated by TALEs (UPA) share a conserved and essential *AvrBS3* responsive element, in which a TATA-like motif is directly linked to the TALEs' binding element (Kay, Hahn, Marois, Wieduwild, & Bonas, 2009). In *pFRK1::LUC* the TATA box is located approximately 450 bp downstream of the dTALE-AD C and D binding sites. Therefore, it can be speculated, that the TATA box of *pFRK1* is not close enough to the binding site of dTALE-AD C and dTALE-AD D for the efficient activation of the reporter construct. The distance between the dTALE binding sites to the transcriptional start site was shown to possibly playing a role in gene activation in mammalian cells (Bultmann et al., 2012). Contradictory to that, Perez-Pinera et al. (2013), however were not able to show such a correlation.

To address this problem in more detail, the alternative *pBS3::LUC* reporter gene was generated and tested. *pBS3* has previously been shown to be a suitable promoter to test dTALEs (Morbitzer et al., 2010). Therefore, the respective DNA-binding sites of dTALE-AD C and dTALE-AD D were cloned into the *pBS3* promoter and transcriptionally fused to *LUC.* In contrast to the previously used ß-gucoronidase (Morbitzer et al., 2010), the LUC enzyme

activity reflects *de novo* transcription more realistic and allows a much better temporal resolution (Thompson, Hayes, & Lloyd, 1991).

dTALE-AD C and dTALE-AD D induced their respective *pBS3::LUC* reporter, but not the opposite one, demonstrating that both dTALE-ADs are able to bind to their target DNA *in vivo* in a sequence-specific manner. Thus, it has also to be assumed for these two dTALEs, that binding strength does not necessarily correlate with the induction efficiency (Bultmann et al., 2012). To get more insight into this aspect of dTALE-ADs' properties, the binding affinities can be determined by isothermal titration calorimetry or by fluorescence polarization as it was done with other TALE proteins (Bultmann et al., 2012; Stella et al., 2013).

6.8. X-ChIP

6.8.1. Appropriate Fixation is Crucial for a Successful X-ChIP Experiment

Another approach for the determination of *in vivo* binding of the dTALEs within *pFRK1* is an X-ChIP approach. If the dTALEs indeed bind to their target DNA sequence efficiently, they should precipitate *pFRK1* from crude chromatin preparations isolated from nuclear extracts of *Arabidopsis* plants.

It was not possible to specifically precipitate *pFRK1* fragments, neither with the dTALEs A and B, which should bind 1 kb upstream, with dTALEs E and F, which should bind downstream, nor with dTALE D, which binds 500 bp upstream of the transcription start site in the protoplasts assays. A specific precipitation of *pFRK1* fragments was only achieved with dTALE C.

The most sensitive part and potential source of producing unspecific background in X-ChIP in general is the fixation step, thus, the cross-linking of the bait protein (here the dTALE) to its target DNA. Especially long fixation times may result in high background signal, even in true negative controls (Baranello, Kouzine, Sanford, & Levens, 2016; Carey, Peterson, & Smale, 2009; Fan & Struhl, 2009; Marinov, Kundaje, Park, & Wold, 2014; Teytelman, Thurtle, Rine, & van Oudenaarden, 2013). In contrast to the applied 50 min of fixation, often short fixation times of 10 - 15 min were sufficient in other ChIP approaches (Ascenzi & Gantt, 1999; Bowler et al., 2004; Gendrel, Lippman, Martienssen, & Colot, 2005; Gendrel, Lippman, Yordan, Colot, & Martienssen, 2002; Haring et al., 2007; Jackson et al., 2004; Johnson, Cao, & Jacobsen,

2002). On the other hand, the application of shorter fixation times can prevent the precipitation of DNA at all (Baranello et al., 2016).

In summary, it must be said, that the optimal fixation time has to be found out individually for each dTALE, because they certainly differ in their DNA affinity, properties of interacting surfaces, spatial orientation to the target DNA. All these factors influence the cross-linking efficiency.

6.8.2. Flg22 Treatment Opens the Chromatin and Increases dTALE Binding Site Accessibility

As shown by the X-ChIP and in accordance with the data from the protoplast assays, a specific enrichment of DNA target sites deriving from *pFRK1* was achieved with dTALE C that binds 500 bp upstream of the transcription start site. Interestingly, a strong increase of fragment enrichment was detected when the plants were treated with flg22 in addition to DEX. With dTALE B a weak enrichment was achieved, only in the presence of flg22. One could discuss, that the flg22 induction leads to a change in the chromatin status of *pFRK1*, making the DNA target site more accessible for dTALE C. Although in the COGE browser no significant level of methylation in the region of *pFRK1* is annotated (E. Lyons & Freeling, 2008; Eric Lyons et al., 2008), the given interpretation fits to the unpublished observation, that according to Formaldehyde-Assisted Isolation of Regulatory Elements qPCR (FAIRE-qPCR) data, *pFRK1* gets more accessible 15 min after flg22 treatment (Behammed M. Personal communication). These results are substantiated by Assay for Transposase Accessible Chromatin sequencing (ATAC-seq) data (**Figure 28** A, Behnammed M, unpublished). In addition, the H3K27me3 methylation mark decreases 15 min after flg22 treatment (**Figure 28** A, Benhamed M, unpublished).

In conclusion, based on the data from the *Arabiopsis* protoplast assays and on the X-ChIP results obtained with transgenic *Arabidopsis* plants, the dTALE C transgenic seed pool was chosen for the implementation of dTALE-ChAP.

6.9. dTALE ChAP

The dTALE-ChAP was carried out with dTALE C in three different trials. Most importantly, all non-nuclear cellular protein contaminations have to be removed from the precipitate as much as possible by several washing steps. In the first trial chloroplastic remains were detected. In the other two trials it was possible to achieve an enrichment of the nuclear components without cholorplastic contaminations.

6.9.1. Sample Preparation and Removal of Sample Impurities

The first trial was used to test, whether the dTALE-ChAP approach worked in principle and how much non-nuclear protein contaminations were identified in the MS analysis. Indeed, a significant difference in the number of peptides between the DEX-treated and the control sample was observed in the precipitates. Thus, the dTALE-ChAP - the specific enrichment of peptides derived from promoter-associated proteins by dTALEs - worked. The contamination level with cytosolic proteins was low, but contamination with peptides derived from chloroplastic proteins was significant.

Unfortunately, remains of detergents and SDS caused problems in the MS analysis of the metabolically labeled precipitates of the second trial. For the dTALE-ChAP protocol, in-solution digestion of the precipitated proteins was chosen for MS analysis, because rare peptides were expected to be identified. However, this method carries the risk that detergents required for opening of the nuclei, contaminate the final samples and make the final MS analysis almost impossible (Wisniewski et al., 2009). Due to metabolic labeling ^{14}N and ^{15}N labeled tissue was mixed, resulting in a higher biomass per sample. Due to this higher biomass, it was necessary to use more buffer. This could explain, that total higher amount of detergent in trial 2 caused the problems. The in gel approach, which is a method more robust against impurities, was no alternative to be applied, cause it comes along with the loss of rare peptides (Wisniewski et al., 2009).

Thus, the dTALE-ChAP protocol was further optimized for the metabolically labeled precipitates of the third trial by applying Filter Aided Sample Preparation (FASP) successfully (Wisniewski et al., 2009). FASP is a size exclusion chromatography for small sample sizes, that retains high molecular weight substances like DNA and proteins on the column, whilst low

molecular weight compounds, such as detergents are washed out (Wisniewski et al., 2009). After in column digestion of the proteins, the peptides are eluted and analyzed by MS.

Since peptide overlaps were found between all three trials (excluding the control sample of trial 1), consisting mainly of histones, I propose, that the fundamental principle of the dTALE-ChAP works. A comparison of these data with the result of similar approaches is not possible so far, since dTALEs have not yet been used for *in vivo* ChAP experiments in plans. In mammalian cells, at least peptides of histone protein H2A and ribosomal protein L5 were also found in a dTALE-based ChAP approach (Fujita et al., 2013). Peptides of related plant proteins were also detected in my three dTALE-ChAP trial with *A. thaliana.*

6.9.2. Epigenetic Modifications at *pFRK1* in Response to Flg22

Independent of the metabolic labeling and the discrimination between flg22 induced und non-induced plants, the over-representation tests revealed a significant enrichment in the precipitates for peptides and thus proteins representing translation and heterochromatin related GO terms. Since heterochromatin is the inactive DNA state and opening of the chromatin in the area of *pFRK1* has already been detected already 15 min after flg22 treatment (Figure 28 A, Benhamed M, unpublished), one could speculate, that 1 after flg22 treatment translation is already ongoing and transcription is turned down. Therefore, the flg22 treatment was shortened for the second and third dTALE-ChAP trial. Again, the predominant enriched peptides in the precipitate are linked to GO terms that were not transcription related, but related to GO terms linked to nucleosome and DNA packaging complexes, as well as histones. Again, it seems like translation is still ongoing. Therefore, it is highly likely, that again the sampling time point was set too late, to precipitation the transcription initiating proteins.

In other ChAP-like approaches, followed by mass spectrometry performed with cultured mammalian cells, some proteins were identified, that are usually precipitated with chromatin (Vermeulen et al., 2010). This list of proteins, includes the ribosomal proteins L5 and L8, as well as histone H2A (Vermeulen et al., 2010). Peptides of the related *A. thaliana* proteins were found in all three dTALE-ChAP trials.

In all three dTALE-ChAP trials, peptides were significantly over-represented after flg22 treatment of the plants, that are linked to the GO term Chromatin and Nucleosome Packaging and Modellings. These results indicate a massive change in chromatin packaging after flg22 treatment. In the first trial, the tissue was fixed 1 h after flg22 application. In this data set, peptides associated with the GO term Chromatin Silencing and Methylation were enriched. After shortening the flg22 treatment in trial 2 and 3 to 30 min, chromatin re-arrangements are still going on, but chromatin silencing processes are not yet predominant. These results suggest, that chromatin silencing processes start within 1 h after flg22 treatment. Contrary to that, a significant increase of *FRK1* transcript was detected between 60 to 90 min after DEX treatment in the qPCR (Figure 6). In the promoter reporter assay, activation of *pFRK1* was sustained over the period of 12 h, after a single flg22 treatment (Figure 16 & Figure 17).

It was shown by ATAC-seq that the chromatin in the area of *pFRK1* opens within 15 min after flg22 application (Figure 28 A kindly provided by Dr. M. Benhamed; (Buenrostro, Giresi, Zaba, Chang, & Greenleaf, 2013; Buenrostro, Wu, Chang, & Greenleaf, 2015)).

The ATAC-seq data fits well to the results derived from the X-ChIP approach. Signifcantly more *pFRK1* fragments were precipitated by TALE C, 60 min after the onset of flg22 treatment compared to the non-treated control. The analysis of histone methylation revealed H3K27 next to *pFRK1* (Figure 28 B). H3K27 is linked to inactive genes and heterochromatin (Lachner, O'Sullivan, & Jenuwein, 2003). The H3K27 methylation marks are reduced upon flg22 treatment. This process may represent the activation and opening of the chromatin which enables transcription factors to bind and transcription is initiated. I could be speculated, that the peptides of proteins linked to the GO term Methylation, that were found to be over-represented in dTALE-ChAP trial 1, 1 h after flg22 treatment, are the antagonists, that are resetting the chromatin marks into the in uniduced state, by increasing methylation marks.

Beside methylation also other epigenetic modifications like deacetylation are an essential part of the immune response in *Arabidopsis* (Ramirez-Prado, Abulfaraj, et al., 2018). There is a direct link between the PAMP induced MAPK pathway and histone deacetylase HD2B (Latrasse et al., 2017). They found *pFRK1* as a target of HD2B. But the exact interaction of HD2B with *FRK1* in response to flg22 is not completely clear so far. Since HD2B is associated with downregulation of genes, the exact mechanism needs to be further elucidated.

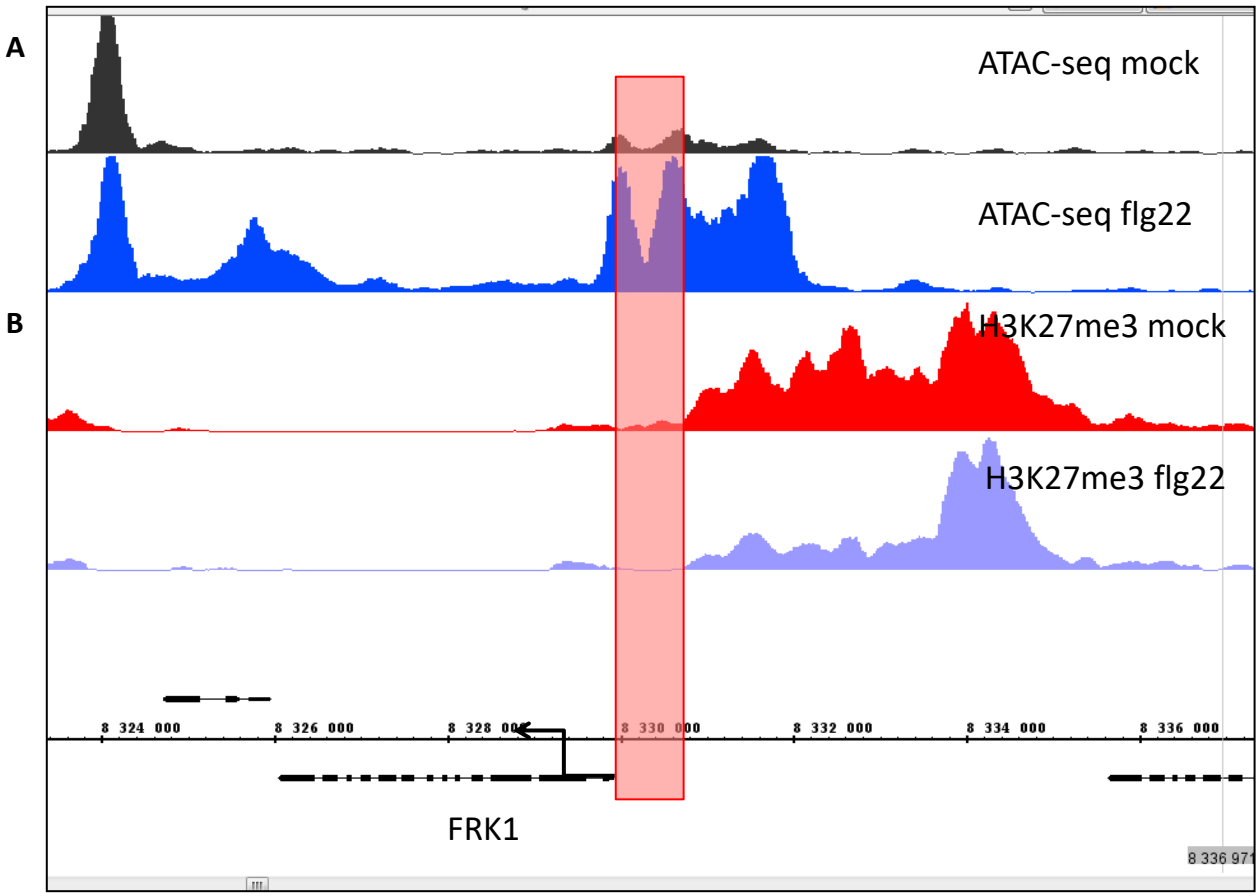

Figure 28: The chromatin status of *FRK1* changes within 15 min after flg22 application (data provided by Dr. M. Benhamed; figure modified). The graph represents the amount precipitated DNA. Samples were treated for 15 min with flg22 (blue) or mock (blue) **(A)**. Upstream of the promoter H3K27me3 marks are reduced after flg22 treatment (red) compared to mock treatment (red) **(B)**; *pFRK1* is marked with a red box

The identified peptides were compared in a quantitative manner (Table 22). By doing that, it was found that just peptides were identified, that where more abundant in the precipitates, derived from nuclei, prepared from flg22 treated plants, compared to the mock treated control. This effect might be explained by the flg22-triggered opening of the chromatin. (Figure 28 A) resulting in an enhanced accessibility for dTALE C to the *pFRK1* promoter. In turn, this enables an increased precipitation of *pFRK1* fragments as seen in the X-ChIP with dTALE C (Figure 22). This logically causes more DNA associated proteins, such as histones, in the ChAP precipitates. In further dTALE-ChAP trials, this differential precipitation of *pFRK1* fragments, as a consequence of chromatin rearrangements, has to be corrected by quantifying the precipitated amount of *pFRK1* DNA in the samples. It would be conceivable to determine the amount of precipitated *pFRK1* by qPCR, as it is done in the X-ChIP in parallel to the MS. With

this data a correction factor could be calculated. So far in no other approach a comparable correction for precipitation efficiency was done.

Unfortunately, it was not possible to identify transcriptional regulators in the three dTALE C-ChAP trials, except one member of AP2/B3-like transcriptional factor family in trial 3. The functions of this identified protein is not clear yet. However, other members of the AP2 transcription factor family are phosphorylated by MAPKs on protein microarrays (Popescu et al., 2009). Possibly, the AP2 like transcription factor found here, is phosphorylated by flg22 induced MAPKs and then binds to *pFRK1. AP2/EREBP* proteins are known to be involved in plant's responses to biotic, pathogenic and environmental stresses, as well as hormone signal transduction (Brown, Kazan, McGrath, Maclean, & Manners, 2003; Chakravarthy et al., 2003; Gutterson & Reuber, 2004; Knight, Veale, Warren, & Knight, 1999; Magome, Yamaguchi, Hanada, Kamiya, & Oda, 2004; Stockinger, Gilmour, & Thomashow, 1997; Yi et al., 2004). The finding, that a AP2/B3-like transcription factor is interacting with *pFRK1* could be the starting point of further studies.

7. Conclusions and Outlook

Taken together it was possible to demonstrate, that the principle of the dTALE-ChAP was working. Although an AP2/B3-like transcriptional factor family protein of unknown function was the only transcriptional regulator which could be identified, an insight in the chromatin changes after flg22 treatment was achievd. It could be proposed, that transcription initiation at the promoter and therefore the binding of the transcription factors happens earlier than the tested timepoints of 30 min and 60 min. Therefore, it would be promising to test earlier timepoints. The validation of found transcription factor candidates might be re-evaluated by X-ChIP experiments using the found candidates as bait proteins.

The dTALE-ChAP is an *in vivo* method that was applied in plants the first time. In contrast to the similar approaches that were developed in parallel to this work, nobody used bait proteins, with inducible cellular localization. After optimization of the protocol what includes a correction step for differences in precipitation efficiencies between activated and inactivated promoters. So far, no approach is known which includes such a correction step. Beside including a correction factor and optimizing the duration of flg22 treatment, an essential step that needs to be improved is the fixation step.

In future, the dTALE-ChAP can be a valuable *in vivo* method for analyzing transcriptional regulation. The dTALE-ChAP can be applied at any promoter, not restricted to an organism. After including the correction factor for precipitation efficiency, the dTALE-ChAP would be the only method taking Chromatin accessibility in a Chromatin Affinity Purification Step into account. So far, the dTALE-ChAP was the only approach in which a designed bait protein, with an inducible subcellular localization was used.

8. Literature

Agius, P., Arvey, A., Chang, W., Noble, W. S., & Leslie, C. (2010). High resolution models of transcription factor-DNA affinities improve in vitro and in vivo binding predictions. *PLoS Comput Biol, 6*(9). doi:10.1371/journal.pcbi.1000916

Aoyama, T., & Chua, N. H. (1997). A glucocorticoid-mediated transcriptional induction system in transgenic plants. *Plant J, 11*(3), 605-612. doi:doi:10.1046/j.1365-313X.1997.11030605.x

Asai, T., Tena, G., Plotnikova, J., Willmann, M. R., Chiu, W. L., Gomez-Gomez, L., . . . Sheen, J. (2002). MAP kinase signalling cascade in Arabidopsis innate immunity. *Nature, 415*(6875), 977-983. doi:10.1038/415977a

Ascenzi, R., & Gantt, J. S. (1999). Subnuclear distribution of the entire complement of linker histone variants in Arabidopsis thaliana. *Chromosoma, 108*(6), 345-355.

Bakshi, M., & Oelmüller, R. (2014). WRKY transcription factors: Jack of many trades in plants. *Plant Signaling & Behavior, 9*, e27700. doi:10.4161/psb.27700

Baranello, L., Kouzine, F., Sanford, S., & Levens, D. (2016). ChIP bias as a function of cross-linking time. *Chromosome Res, 24*(2), 175-181. doi:10.1007/s10577-015-9509-1

Barrangou, R., Fremaux, C., Deveau, H., Richards, M., Boyaval, P., Moineau, S., . . . Horvath, P. (2007). CRISPR provides acquired resistance against viruses in prokaryotes. *Science, 315*(5819), 1709-1712. doi:10.1126/science.1138140

Berendzen, K. W., Stuber, K., Harter, K., & Wanke, D. (2006). Cis-motifs upstream of the transcription and translation initiation sites are effectively revealed by their positional disequilibrium in eukaryote genomes using frequency distribution curves. *BMC Bioinformatics, 7*, 522. doi:10.1186/1471-2105-7-522

Birkenbihl, R. P., Kracher, B., & Somssich, I. E. (2017). Induced Genome-Wide Binding of Three Arabidopsis WRKY Transcription Factors during Early MAMP-Triggered Immunity. *Plant Cell, 29*(1), 20-38. doi:10.1105/tpc.16.00681

Blount, B. A., Weenink, T., Vasylechko, S., & Ellis, T. (2012). Rational Diversification of a Promoter Providing Fine-Tuned Expression and Orthogonal Regulation for Synthetic Biology. *PLoS One, 7*(3), e33279. doi:10.1371/journal.pone.0033279

Boch, J., & Bonas, U. (2010). Xanthomonas AvrBs3 family-type III effectors: discovery and function. *Annu Rev Phytopathol, 48*, 419-436. doi:10.1146/annurev-phyto-080508-081936

Boch, J., Scholze, H., Schornack, S., Landgraf, A., Hahn, S., Kay, S., . . . Bonas, U. (2009). Breaking the code of DNA binding specificity of TAL-type III effectors. *Science, 326*(5959), 1509-1512. doi:10.1126/science.1178811

Bolotin, A., Quinquis, B., Sorokin, A., & Ehrlich, S. D. (2005). Clustered regularly interspaced short palindrome repeats (CRISPRs) have spacers of extrachromosomal origin. *Microbiology, 151*(Pt 8), 2551-2561. doi:10.1099/mic.0.28048-0

Bortesi, L., & Fischer, R. (2015). The CRISPR/Cas9 system for plant genome editing and beyond. *Biotechnol Adv, 33*(1), 41-52. doi:10.1016/j.biotechadv.2014.12.006

Bowler, C., Benvenuto, G., Laflamme, P., Molino, D., Probst, A. V., Tariq, M., & Paszkowski, J. (2004). Chromatin techniques for plant cells. *Plant J, 39*(5), 776-789. doi:10.1111/j.1365-313X.2004.02169.x

Brand, L. H., Fischer, N. M., Harter, K., Kohlbacher, O., & Wanke, D. (2013). Elucidating the evolutionary conserved DNA-binding specificities of WRKY transcription factors by

molecular dynamics and in vitro binding assays. *Nucleic Acids Res, 41*(21), 9764-9778. doi:10.1093/nar/gkt732

Bresnick, E. H., Dalman, F. C., Sanchez, E. R., & Pratt, W. B. (1989). Evidence that the 90-kDa heat shock protein is necessary for the steroid binding conformation of the L cell glucocorticoid receptor. *J Biol Chem, 264*(9), 4992-4997.

Brockmann, B., Smith, M. W., Zaraisky, A. G., Harrison, K., Okada, K., & Kamiya, Y. (2001). Subcellular localization and targeting of glucocorticoid receptor protein fusions expressed in transgenic Arabidopsis thaliana. *Plant Cell Physiol, 42*(9), 942-951. doi:10.1093/pcp/pce120

Brown, R. L., Kazan, K., McGrath, K. C., Maclean, D. J., & Manners, J. M. (2003). A role for the GCC-box in jasmonate-mediated activation of the PDF1.2 gene of Arabidopsis. *Plant Physiol, 132*(2), 1020-1032. doi:10.1104/pp.102.017814

Buck, M. J., & Lieb, J. D. (2004). ChIP-chip: considerations for the design, analysis, and application of genome-wide chromatin immunoprecipitation experiments. *Genomics, 83*(3), 349-360.

Buenrostro, J. D., Giresi, P. G., Zaba, L. C., Chang, H. Y., & Greenleaf, W. J. (2013). Transposition of native chromatin for fast and sensitive epigenomic profiling of open chromatin, DNA-binding proteins and nucleosome position. *Nat Methods, 10*(12), 1213-1218. doi:10.1038/nmeth.2688

Buenrostro, J. D., Wu, B., Chang, H. Y., & Greenleaf, W. J. (2015). ATAC-seq: A Method for Assaying Chromatin Accessibility Genome-Wide. *Curr Protoc Mol Biol, 109*, 21 29 21-29. doi:10.1002/0471142727.mb2129s109

Bultmann, S., Morbitzer, R., Schmidt, C. S., Thanisch, K., Spada, F., Elsaesser, J., . . . Leonhardt, H. (2012). Targeted transcriptional activation of silent oct4 pluripotency gene by combining designer TALEs and inhibition of epigenetic modifiers. *Nucleic Acids Res, 40*(12), 5368-5377. doi:10.1093/nar/gks199

Bulyk, M. L. (2006). DNA microarray technologies for measuring protein-DNA interactions. *Curr Opin Biotechnol, 17*(4), 422-430. doi:10.1016/j.copbio.2006.06.015

Burley, S. K., & Roeder, R. G. (1996a). Biochemistry and structural biology of transcription factor IID (TFIID). *Annu Rev Biochem, 65*(1), 769-799. doi:10.1146/annurev.bi.65.070196.004005

Burley, S. K., & Roeder, R. G. (1996b). Biochemistry and Structural Biology of Transcription Factor IID (TFIID). *Annual Review of Biochemistry, 65*(1), 769-799. doi:10.1146/annurev.bi.65.070196.004005

Byrum, S. D., Raman, A., Taverna, S. D., & Tackett, A. J. (2012). ChAP-MS: a method for identification of proteins and histone posttranslational modifications at a single genomic locus. *Cell Rep, 2*(1), 198-205. doi:10.1016/j.celrep.2012.06.019

Byrum, S. D., Taverna, S. D., & Tackett, A. J. (2013). Purification of a specific native genomic locus for proteomic analysis. *Nucleic Acids Res, 41*(20), e195. doi:10.1093/nar/gkt822

Cano-Rodriguez, D., & Rots, M. G. (2016). Epigenetic Editing: On the Verge of Reprogramming Gene Expression at Will. *Curr Genet Med Rep, 4*(4), 170-179. doi:10.1007/s40142-016-0104-3

Carey, M. F., Peterson, C. L., & Smale, S. T. (2009). Chromatin immunoprecipitation (ChIP). *Cold Spring Harb Protoc, 2009*(9), pdb prot5279. doi:10.1101/pdb.prot5279

Cermak, T., Doyle, E. L., Christian, M., Wang, L., Zhang, Y., Schmidt, C., . . . Voytas, D. F. (2011). Efficient design and assembly of custom TALEN and other TAL effector-based constructs for DNA targeting. *Nucleic Acids Res, 39*(12), e82. doi:10.1093/nar/gkr218

Chakravarthy, S., Tuori, R. P., D'Ascenzo, M. D., Fobert, P. R., Despres, C., & Martin, G. B. (2003). The tomato transcription factor Pti4 regulates defense-related gene expression via GCC box and non-GCC box cis elements. *Plant Cell, 15*(12), 3033-3050. doi:10.1105/tpc.017574

Chang, W. C., Lee, T. Y., Huang, H. D., Huang, H. Y., & Pan, R. L. (2008). PlantPAN: Plant promoter analysis navigator, for identifying combinatorial cis-regulatory elements with distance constraint in plant gene groups. *BMC Genomics, 9*, 561. doi:10.1186/1471-2164-9-561

Cheung, J., & Smith, D. F. (2000). Molecular chaperone interactions with steroid receptors: an update. *Mol Endocrinol, 14*(7), 939-946. doi:10.1210/mend.14.7.0489

Chinchilla, D., Bauer, Z., Regenass, M., Boller, T., & Felix, G. (2006). The Arabidopsis Receptor Kinase FLS2 Binds flg22 and Determines the Specificity of Flagellin Perception. *The Plant Cell, 18*(2), 465-476. doi:10.1105/tpc.105.036574

Chinchilla, D., Shan, L., He, P., de Vries, S., & Kemmerling, B. (2009). One for all: the receptor-associated kinase BAK1. *Trends Plant Sci, 14*(10), 535-541. doi:10.1016/j.tplants.2009.08.002

Chinchilla, D., Zipfel, C., Robatzek, S., Kemmerling, B., Nurnberger, T., Jones, J. D., . . . Boller, T. (2007). A flagellin-induced complex of the receptor FLS2 and BAK1 initiates plant defence. *Nature, 448*(7152), 497-500. doi:10.1038/nature05999

Choo, Y., & Klug, A. (1994a). Selection of DNA binding sites for zinc fingers using rationally randomized DNA reveals coded interactions. *Proc Natl Acad Sci U S A, 91*(23), 11168-11172.

Choo, Y., & Klug, A. (1994b). Toward a code for the interactions of zinc fingers with DNA: selection of randomized fingers displayed on phage. *Proc Natl Acad Sci U S A, 91*(23), 11163-11167.

Choo, Y., Sanchez-Garcia, I., & Klug, A. (1994). In vivo repression by a site-specific DNA-binding protein designed against an oncogenic sequence. *Nature, 372*(6507), 642-645. doi:10.1038/372642a0

Chow, C. N., Zheng, H. Q., Wu, N. Y., Chien, C. H., Huang, H. D., Lee, T. Y., . . . Chang, W. C. (2016). PlantPAN 2.0: an update of plant promoter analysis navigator for reconstructing transcriptional regulatory networks in plants. *Nucleic Acids Res, 44*(D1), D1154-1160. doi:10.1093/nar/gkv1035

Ciolkowski, I., Wanke, D., Birkenbihl, R. P., & Somssich, I. E. (2008). Studies on DNA-binding selectivity of WRKY transcription factors lend structural clues into WRKY-domain function. *Plant Mol Biol, 68*(1-2), 81-92. doi:10.1007/s11103-008-9353-1

Cong, L., Zhou, R., Kuo, Y. C., Cunniff, M., & Zhang, F. (2012). Comprehensive interrogation of natural TALE DNA-binding modules and transcriptional repressor domains. *Nat Commun, 3*, 968. doi:10.1038/ncomms1962

Dautel, R. (2016). *MOLECULAR CHARACTERIZATION OF THE ARABIDOPSIS THALIANA HISTIDINE KINASE 1 AND TRANSITIONS FROM THE MULTISTEP PHOSPHORELAY SYSTEM TO SER/THR/TYR PHOSPHORYLATION*

. (Doktor der Naturwissenschaften Dissertation), Eberhard Karls Universität Tübingen, Tübingen.

Dautel, R., Wu, Xu N., Heunemann, M., Schulze, Waltraud X., & Harter, K. (2016). The Sensor Histidine Kinases AHK2 and AHK3 Proceed into Multiple Serine/Threonine/Tyrosine Phosphorylation Pathways in Arabidopsis thaliana. *Molecular Plant, 9*(1), 182-186. doi:10.1016/j.molp.2015.10.002

de Lange, O., Schreiber, T., Schandry, N., Radeck, J., Braun, K. H., Koszinowski, J., . . . Lahaye, T. (2013). Breaking the DNA-binding code of Ralstonia solanacearum TAL effectors provides new possibilities to generate plant resistance genes against bacterial wilt disease. *New Phytol, 199*(3), 773-786. doi:10.1111/nph.12324

Deyholos, M. K., & Sieburth, L. E. (2000). Separable whorl-specific expression and negative regulation by enhancer elements within the AGAMOUS second intron. *Plant Cell, 12*(10), 1799-1810.

Doidy, J., Li, Y., Neymotin, B., Edwards, M. B., Varala, K., Gresham, D., & Coruzzi, G. M. (2016). "Hit-and-Run" transcription: de novo transcription initiated by a transient bZIP1 "hit" persists after the "run". *BMC Genomics, 17*, 92. doi:10.1186/s12864-016-2410-2

Droillard, M. J., Boudsocq, M., Barbier-Brygoo, H., & Lauriere, C. (2004). Involvement of MPK4 in osmotic stress response pathways in cell suspensions and plantlets of Arabidopsis thaliana: activation by hypoosmolarity and negative role in hyperosmolarity tolerance. *FEBS Lett, 574*(1-3), 42-48. doi:10.1016/j.febslet.2004.08.001

Elgass, K., Caesar, K., Wanke, D., Harter, K., Meixner, A. J., & Schleifenbaum, F. (2010). Application of FLIM-FIDSAM for the in vivo analysis of hormone competence of different cell types. *Anal Bioanal Chem, 398*(5), 1919-1925. doi:10.1007/s00216-010-4127-4

Ermakova, G. V., Alexandrova, E. M., Kazanskaya, O. V., Vasiliev, O. L., Smith, M. W., & Zaraisky, A. G. (1999). The homeobox gene, Xanf-1, can control both neural differentiation and patterning in the presumptive anterior neurectoderm of the Xenopus laevis embryo. *Development, 126*(20), 4513-4523.

Eulgem, T., Rushton, P. J., Robatzek, S., & Somssich, I. E. (2000). The WRKY superfamily of plant transcription factors. *Trends Plant Sci, 5*(5), 199-206. doi:https://doi.org/10.1016/S1360-1385(00)01600-9

Fabregat, A., Sidiropoulos, K., Garapati, P., Gillespie, M., Hausmann, K., Haw, R., . . . D'Eustachio, P. (2016). The Reactome pathway Knowledgebase. *Nucleic Acids Res, 44*(D1), D481-487. doi:10.1093/nar/gkv1351

Fan, X., & Struhl, K. (2009). Where does mediator bind in vivo? *PLoS One, 4*(4), e5029. doi:10.1371/journal.pone.0005029

Felix, G., Duran, J. D., Volko, S., & Boller, T. (1999). Plants have a sensitive perception system for the most conserved domain of bacterial flagellin. *Plant Journal, 18*(3), 265-276. doi:DOI 10.1046/j.1365-313X.1999.00265.x

Finch, J. T., Lutter, L. C., Rhodes, D., Brown, R. S., Rushton, B., Levitt, M., & Klug, A. (1977). Structure of nucleosome core particles of chromatin. *Nature, 269*, 29. doi:10.1038/269029a0

Frei Dit Frey, N., Mbengue, M., Kwaaitaal, M., Nitsch, L., Altenbach, D., Häweker, H., . . . Robatzek, S. (2012). *Plasma Membrane Calcium ATPases Are Important Components of Receptor-Mediated Signaling in Plant Immune Responses and Development* (Vol. 159).

Fujimoto, S., Sugano, S. S., Kuwata, K., Osakabe, K., & Matsunaga, S. (2016). Visualization of specific repetitive genomic sequences with fluorescent TALEs in Arabidopsis thaliana. *J Exp Bot, 67*(21), 6101-6110. doi:10.1093/jxb/erw371

Fujita, T., Asano, Y., Ohtsuka, J., Takada, Y., Saito, K., Ohki, R., & Fujii, H. (2013). Identification of telomere-associated molecules by engineered DNA-binding molecule-mediated chromatin immunoprecipitation (enChIP). *Sci Rep, 3*, 3171. doi:10.1038/srep03171

Fujita, T., & Fujii, H. (2013). Efficient isolation of specific genomic regions and identification of associated proteins by engineered DNA-binding molecule-mediated chromatin

immunoprecipitation (enChIP) using CRISPR. *Biochem Biophys Res Commun, 439*(1), 132-136. doi:10.1016/j.bbrc.2013.08.013

Fujita, T., & Fujii, H. (2014). Identification of proteins associated with an IFNgamma-responsive promoter by a retroviral expression system for enChIP using CRISPR. *PLoS One, 9*(7), e103084. doi:10.1371/journal.pone.0103084

Fujita, T., & Fujii, H. (2015). Isolation of specific genomic regions and identification of associated molecules by engineered DNA-binding molecule-mediated chromatin immunoprecipitation (enChIP) using CRISPR. *Methods Mol Biol, 1288*, 43-52. doi:10.1007/978-1-4939-2474-5_4

Fujita, T., Yuno, M., & Fujii, H. (2016). Efficient sequence-specific isolation of DNA fragments and chromatin by in vitro enChIP technology using recombinant CRISPR ribonucleoproteins. *Genes Cells, 21*(4), 370-377. doi:10.1111/gtc.12341

Fujita, T., Yuno, M., & Fujii, H. (2018). enChIP systems using different CRISPR orthologues and epitope tags. *BMC Res Notes, 11*(1), 154. doi:10.1186/s13104-018-3262-4

Fujita, T., Yuno, M., Suzuki, Y., Sugano, S., & Fujii, H. (2017). Identification of physical interactions between genomic regions by enChIP-Seq. *Genes Cells, 22*(6), 506-520. doi:10.1111/gtc.12492

Gendrel, A. V., Lippman, Z., Martienssen, R., & Colot, V. (2005). Profiling histone modification patterns in plants using genomic tiling microarrays. *Nat Methods, 2*(3), 213-218. doi:10.1038/nmeth0305-213

Gendrel, A. V., Lippman, Z., Yordan, C., Colot, V., & Martienssen, R. A. (2002). Dependence of heterochromatic histone H3 methylation patterns on the Arabidopsis gene DDM1. *Science, 297*(5588), 1871-1873. doi:10.1126/science.1074950

Gomez-Gomez, L., & Boller, T. (2000). FLS2: an LRR receptor-like kinase involved in the perception of the bacterial elicitor flagellin in Arabidopsis. *Mol Cell, 5*(6), 1003-1011.

Grefen, C., Karnik, R., Larson, E., Lefoulon, C., Wang, Y., Waghmare, S., . . . Blatt, M. R. (2015). A vesicle-trafficking protein commandeers Kv channel voltage sensors for voltage-dependent secretion. *Nature Plants, 1*, 15108. doi:10.1038/nplants.2015.108

https://www.nature.com/articles/nplants2015108#supplementary-information

Gutterson, N., & Reuber, T. L. (2004). Regulation of disease resistance pathways by AP2/ERF transcription factors. *Current Opinion in Plant Biology, 7*(4), 465-471. doi:https://doi.org/10.1016/j.pbi.2004.04.007

Hanahan, D. (1983). Studies on transformation of Escherichia coli with plasmids. *J Mol Biol, 166*(4), 557-580.

Hanahan, D., Jessee, J., & Bloom, F. R. (1991). Plasmid transformation of Escherichia coli and other bacteria. *Methods Enzymol, 204*, 63-113.

Harada, R., & Nepveu, A. (2012). Chromatin affinity purification. *Methods Mol Biol, 809*, 237-253. doi:10.1007/978-1-61779-376-9_16

Haring, M., Offermann, S., Danker, T., Horst, I., Peterhansel, C., & Stam, M. (2007). Chromatin immunoprecipitation: optimization, quantitative analysis and data normalization. *Plant Methods, 3*(1), 11. doi:10.1186/1746-4811-3-11

Hecker, A. (2016). *Charakterisierung des pflanzlichen Chromatin Remodeling Komplexes um das GAGA-Bindeprotein BPC6 mittels etablierter und neu entwickelter Methoden.* (Doktor der Naturwissenschaften Dissertation), Eberhard Karls Universität Tübingen, Tübingen.

Hecker, A., Brand, L. H., Peter, S., Simoncello, N., Kilian, J., Harter, K., . . . Wanke, D. (2015). The Arabidopsis GAGA-Binding Factor BASIC PENTACYSTEINE6 Recruits the

POLYCOMB-REPRESSIVE COMPLEX1 Component LIKE HETEROCHROMATIN PROTEIN1 to GAGA DNA Motifs. *Plant Physiol, 168*(3), 1013-1024. doi:10.1104/pp.15.00409

Heese, A., Hann, D. R., Gimenez-Ibanez, S., Jones, A. M., He, K., Li, J., . . . Rathjen, J. P. (2007). The receptor-like kinase SERK3/BAK1 is a central regulator of innate immunity in plants. *Proc Natl Acad Sci U S A, 104*(29), 12217-12222. doi:10.1073/pnas.0705306104

Hoffman, B. G., & Jones, S. J. (2009). Genome-wide identification of DNA-protein interactions using chromatin immunoprecipitation coupled with flow cell sequencing. *J Endocrinol, 201*(1), 1-13. doi:10.1677/JOE-08-0526

Ishino, Y., Shinagawa, H., Makino, K., Amemura, M., & Nakata, A. (1987). Nucleotide sequence of the iap gene, responsible for alkaline phosphatase isozyme conversion in Escherichia coli, and identification of the gene product. *J Bacteriol, 169*(12), 5429-5433. doi:10.1128/jb.169.12.5429-5433.1987

Jackson, J. P., Johnson, L., Jasencakova, Z., Zhang, X., PerezBurgos, L., Singh, P. B., . . . Jacobsen, S. E. (2004). Dimethylation of histone H3 lysine 9 is a critical mark for DNA methylation and gene silencing in Arabidopsis thaliana. *Chromosoma, 112*(6), 308-315. doi:10.1007/s00412-004-0275-7

Jacobus, A. P., & Gross, J. (2015). Optimal cloning of PCR fragments by homologous recombination in Escherichia coli. *PLoS One, 10*(3), e0119221. doi:10.1371/journal.pone.0119221

Jamieson, A. C., Miller, J. C., & Pabo, C. O. (2003). Drug discovery with engineered zinc-finger proteins. *Nat Rev Drug Discov, 2*(5), 361-368. doi:10.1038/nrd1087

Jinek, M., Chylinski, K., Fonfara, I., Hauer, M., Doudna, J. A., & Charpentier, E. (2012). A programmable dual-RNA-guided DNA endonuclease in adaptive bacterial immunity. *Science, 337*(6096), 816-821. doi:10.1126/science.1225829

Johnson, L., Cao, X., & Jacobsen, S. (2002). Interplay between two epigenetic marks. DNA methylation and histone H3 lysine 9 methylation. *Curr Biol, 12*(16), 1360-1367.

Kang, H.-G., Fang, Y., & Singh, K. B. (1999). A glucocorticoid-inducible transcription system causes severe growth defects in Arabidopsis and induces defense-related genes. *The Plant Journal, 20*(1), 127-133. doi:10.1046/j.1365-313X.1999.00575.x

Kang, S. G., Price, J., Lin, P.-C., Hong, J. C., & Jang, J.-C. (2010). The Arabidopsis bZIP1 Transcription Factor Is Involved in Sugar Signaling, Protein Networking, and DNA Binding. *Molecular Plant, 3*(2), 361-373. doi:https://doi.org/10.1093/mp/ssp115

Kay, S., Hahn, S., Marois, E., Hause, G., & Bonas, U. (2007). A bacterial effector acts as a plant transcription factor and induces a cell size regulator. *Science, 318*(5850), 648-651. doi:10.1126/science.1144956

Kay, S., Hahn, S., Marois, E., Wieduwild, R., & Bonas, U. (2009). Detailed analysis of the DNA recognition motifs of the Xanthomonas type III effectors AvrBs3 and AvrBs3Deltarep16. *Plant J, 59*(6), 859-871. doi:10.1111/j.1365-313X.2009.03922.x

Kaya, H., Numa, H., Nishizawa-Yokoi, A., Toki, S., & Habu, Y. (2017). DNA Methylation Affects the Efficiency of Transcription Activator-Like Effector Nucleases-Mediated Genome Editing in Rice. *Frontiers in Plant Science, 8*, 302. doi:10.3389/fpls.2017.00302

Kierszniowska, S., Seiwert, B., & Schulze, W. X. (2009). Definition of Arabidopsis sterol-rich membrane microdomains by differential treatment with methyl-beta-cyclodextrin and quantitative proteomics. *Mol Cell Proteomics, 8*(4), 612-623. doi:10.1074/mcp.M800346-MCP200

Klug, A. (2010). The discovery of zinc fingers and their development for practical applications in gene regulation and genome manipulation. *Q Rev Biophys, 43*(1), 1-21. doi:10.1017/S0033583510000089

Knight, H., Veale, E. L., Warren, G. J., & Knight, M. R. (1999). The sfr6 mutation in Arabidopsis suppresses low-temperature induction of genes dependent on the CRT/DRE sequence motif. *Plant Cell, 11*(5), 875-886.

Koncz, C., & Schell, J. (1986). The promoter of TL-DNA gene 5 controls the tissue-specific expression of chimaeric genes carried by a novel type of Agrobacterium binary vector. *Molecular and General Genetics MGG, 204*(3), 383-396. doi:10.1007/bf00331014

Kornberg, R. D. (1974). Chromatin structure: a repeating unit of histones and DNA. *Science, 184*(4139), 868-871.

Kornet, N., & Scheres, B. (2008). Stem cell factors in plants: chromatin connections. *Cold Spring Harb Symp Quant Biol, 73*, 235-242. doi:10.1101/sqb.2008.73.043

Kouzarides, T. (2007). Chromatin Modifications and Their Function. *Cell, 128*(4), 693-705. doi:https://doi.org/10.1016/j.cell.2007.02.005

Lachner, M., O'Sullivan, R. J., & Jenuwein, T. (2003). An epigenetic road map for histone lysine methylation. *Journal of Cell Science, 116*(11), 2117-2124. doi:10.1242/jcs.00493

Lafos, M., Kroll, P., Hohenstatt, M. L., Thorpe, F. L., Clarenz, O., & Schubert, D. (2011). Dynamic regulation of H3K27 trimethylation during Arabidopsis differentiation. *PLoS Genet, 7*(4), e1002040. doi:10.1371/journal.pgen.1002040

Latrasse, D., Jegu, T., Li, H., de Zelicourt, A., Raynaud, C., Legras, S., . . . Hirt, H. (2017). MAPK-triggered chromatin reprogramming by histone deacetylase in plant innate immunity. *Genome Biol, 18*(1), 131. doi:10.1186/s13059-017-1261-8

Leeb, M., & Wutz, A. (2012). Establishment of epigenetic patterns in development. *Chromosoma, 121*(3), 251-262. doi:10.1007/s00412-012-0365-x

Lewin, B., Cassimeris, L., Plopper, G., & Lingappa, V. R. (2007). *Chromatin and chromosomes*: Jones and Bartlett Publishers.

Li, J., Zhu, L., Eshaghi, M., Liu, J., & Karuturi, K. M. (2011). Deciphering transcription factor binding patterns from genome-wide high density ChIP-chip tiling array data. *BMC Proc, 5 Suppl 2*, S8. doi:10.1186/1753-6561-5-S2-S8

Li, L., Atef, A., Piatek, A., Ali, Z., Piatek, M., Aouida, M., . . . Mahfouz, M. M. (2013). Characterization and DNA-binding specificities of Ralstonia TAL-like effectors. *Mol Plant, 6*(4), 1318-1330. doi:10.1093/mp/sst006

Li, L., Piatek, M. J., Atef, A., Piatek, A., Wibowo, A., Fang, X., . . . Mahfouz, M. M. (2012). Rapid and highly efficient construction of TALE-based transcriptional regulators and nucleases for genome modification. *Plant Mol Biol, 78*(4-5), 407-416. doi:10.1007/s11103-012-9875-4

Li, T., Huang, S., Jiang, W. Z., Wright, D., Spalding, M. H., Weeks, D. P., & Yang, B. (2011). TAL nucleases (TALNs): hybrid proteins composed of TAL effectors and FokI DNA-cleavage domain. *Nucleic Acids Res, 39*(1), 359-372. doi:10.1093/nar/gkq704

Li, Y., Moore, R., Guinn, M., & Bleris, L. (2012). Transcription activator-like effector hybrids for conditional control and rewiring of chromosomal transgene expression. *Sci Rep, 2*, 897. doi:10.1038/srep00897

Lu, D., Wu, S., Gao, X., Zhang, Y., Shan, L., & He, P. (2010). A receptor-like cytoplasmic kinase, BIK1, associates with a flagellin receptor complex to initiate plant innate immunity. *Proc Natl Acad Sci U S A, 107*(1), 496-501. doi:10.1073/pnas.0909705107

Luger, K., Mäder, A. W., Richmond, R. K., Sargent, D. F., & Richmond, T. J. (1997). Crystal structure of the nucleosome core particle at 2.8 Å resolution. *Nature, 389*, 251. doi:10.1038/38444

Lyons, E., & Freeling, M. (2008). How to usefully compare homologous plant genes and chromosomes as DNA sequences. *Plant J, 53*(4), 661-673. doi:10.1111/j.1365-313X.2007.03326.x

Lyons, E., Pedersen, B., Kane, J., Alam, M., Ming, R., Tang, H., . . . Freeling, M. (2008). Finding and Comparing Syntenic Regions among Arabidopsis and the Outgroups Papaya, Poplar, and Grape: CoGe with Rosids. *Plant Physiol, 148*(4), 1772-1781. doi:10.1104/pp.108.124867

MacQuarrie, K. L., Fong, A. P., Morse, R. H., & Tapscott, S. J. (2011). Genome-wide transcription factor binding: beyond direct target regulation. *Trends Genet, 27*(4), 141-148. doi:10.1016/j.tig.2011.01.001

Maeder, M. L., Linder, S. J., Reyon, D., Angstman, J. F., Fu, Y., Sander, J. D., & Joung, J. K. (2013). Robust, synergistic regulation of human gene expression using TALE activators. *Nat Methods, 10*(3), 243-245. doi:10.1038/nmeth.2366

Magome, H., Yamaguchi, S., Hanada, A., Kamiya, Y., & Oda, K. (2004). dwarf and delayed-flowering 1, a novel Arabidopsis mutant deficient in gibberellin biosynthesis because of overexpression of a putative AP2 transcription factor. *Plant J, 37*(5), 720-729.

Marinov, G. K., Kundaje, A., Park, P. J., & Wold, B. J. (2014). Large-scale quality analysis of published ChIP-seq data. *G3 (Bethesda), 4*(2), 209-223. doi:10.1534/g3.113.008680

Martinez, E. (2002). Multi-protein complexes in eukaryotic gene transcription. *Plant Mol Biol, 50*(6), 925-947.

Massie, C. E., & Mills, I. G. (2008). ChIPping away at gene regulation. *EMBO Rep, 9*(4), 337-343. doi:10.1038/embor.2008.44

Mehlhorn, D. G., Wallmeroth, N., Berendzen, K. W., & Grefen, C. (2018). 2in1 Vectors Improve In Planta BiFC and FRET Analyses. In C. Hawes & V. Kriechbaumer (Eds.), *The Plant Endoplasmic Reticulum : Methods and Protocols* (pp. 139-158). New York, NY: Springer New York.

Meshinchi, S., Matic, G., Hutchison, K. A., & Pratt, W. B. (1990). Selective molybdate-directed covalent modification of sulfhydryl groups in the steroid-binding versus the DNA-binding domain of the glucocorticoid receptor. *J Biol Chem, 265*(20), 11643-11649.

Mi, H., Huang, X., Muruganujan, A., Tang, H., Mills, C., Kang, D., & Thomas, P. D. (2017). PANTHER version 11: expanded annotation data from Gene Ontology and Reactome pathways, and data analysis tool enhancements. *Nucleic Acids Res, 45*(D1), D183-D189. doi:10.1093/nar/gkw1138

Miao, Y., Laun, T., Zimmermann, P., & Zentgraf, U. (2004). Targets of the WRKY53 transcription factor and its role during leaf senescence in Arabidopsis. *Plant Mol Biol, 55*(6), 853-867. doi:10.1007/s11103-004-2142-6

Miller, J., McLachlan, A. D., & Klug, A. (1985). Repetitive zinc-binding domains in the protein transcription factor IIIA from Xenopus oocytes. *EMBO J, 4*(6), 1609-1614.

Miller, J. C., Tan, S., Qiao, G., Barlow, K. A., Wang, J., Xia, D. F., . . . Rebar, E. J. (2011). A TALE nuclease architecture for efficient genome editing. *Nat Biotechnol, 29*(2), 143-148. doi:10.1038/nbt.1755

Miyanari, Y., Ziegler-Birling, C., & Torres-Padilla, M. E. (2013). Live visualization of chromatin dynamics with fluorescent TALEs. *Nat Struct Mol Biol, 20*(11), 1321-1324. doi:10.1038/nsmb.2680

Mojica, F. J., Diez-Villasenor, C., Garcia-Martinez, J., & Soria, E. (2005). Intervening sequences of regularly spaced prokaryotic repeats derive from foreign genetic elements. *J Mol Evol, 60*(2), 174-182. doi:10.1007/s00239-004-0046-3

Molina, C., & Grotewold, E. (2005). Genome wide analysis of Arabidopsis core promoters. *BMC Genomics, 6*, 25. doi:10.1186/1471-2164-6-25

Morbitzer, R., Elsaesser, J., Hausner, J., & Lahaye, T. (2011). Assembly of custom TALE-type DNA binding domains by modular cloning. *Nucleic Acids Res, 39*(13), 5790-5799. doi:10.1093/nar/gkr151

Morbitzer, R., Romer, P., Boch, J., & Lahaye, T. (2010). Regulation of selected genome loci using de novo-engineered transcription activator-like effector (TALE)-type transcription factors. *Proc Natl Acad Sci U S A, 107*(50), 21617-21622. doi:10.1073/pnas.1013133107

Moscou, M. J., & Bogdanove, A. J. (2009). A simple cipher governs DNA recognition by TAL effectors. *Science, 326*(5959), 1501. doi:10.1126/science.1178817

Mueller, K., Bittel, P., Chinchilla, D., Jehle, A. K., Albert, M., Boller, T., & Felix, G. (2012). Chimeric FLS2 receptors reveal the basis for differential flagellin perception in Arabidopsis and tomato. *Plant Cell, 24*(5), 2213-2224. doi:10.1105/tpc.112.096073

Mülhardt, C. (2013). *Der Experimentator Molekularbiologie / Genomics*: Springer Berlin Heidelberg.

Navarro, L., Zipfel, C., Rowland, O., Keller, I., Robatzek, S., Boller, T., & Jones, J. D. (2004). The transcriptional innate immune response to flg22. Interplay and overlap with Avr gene-dependent defense responses and bacterial pathogenesis. *Plant Physiol, 135*(2), 1113-1128. doi:10.1104/pp.103.036749

Nikolov, M., Stutzer, A., Mosch, K., Krasauskas, A., Soeroes, S., Stark, H., . . . Fischle, W. (2011). Chromatin affinity purification and quantitative mass spectrometry defining the interactome of histone modification patterns. *Mol Cell Proteomics, 10*(11), M110 005371. doi:10.1074/mcp.M110.005371

Orlando, V., Strutt, H., & Paro, R. (1997). Analysis of chromatin structure by in vivo formaldehyde cross-linking. *Methods, 11*(2), 205-214. doi:10.1006/meth.1996.0407

Park, C. J., Caddell, D. F., & Ronald, P. C. (2012). Protein phosphorylation in plant immunity: insights into the regulation of pattern recognition receptor-mediated signaling. *Front Plant Sci, 3*, 177. doi:10.3389/fpls.2012.00177

Pennisi, E. (2012). The tale of the TALEs. *Science, 338*(6113), 1408-1411. doi:10.1126/science.338.6113.1408

Perez-Pinera, P., Ousterout, D. G., Brunger, J. M., Farin, A. M., Glass, K. A., Guilak, F., . . . Gersbach, C. A. (2013). Synergistic and tunable human gene activation by combinations of synthetic transcription factors. *Nat Methods, 10*(3), 239-242. doi:10.1038/nmeth.2361

Pertl-Obermeyer, H., Wu, X. N., Schrodt, J., Mudsam, C., Obermeyer, G., & Schulze, W. X. (2016). Identification of Cargo for Adaptor Protein (AP) Complexes 3 and 4 by Sucrose Gradient Profiling. *Mol Cell Proteomics, 15*(9), 2877-2889. doi:10.1074/mcp.M116.060129

Pitzschke, A., Schikora, A., & Hirt, H. (2009). MAPK cascade signalling networks in plant defence. *Curr Opin Plant Biol, 12*(4), 421-426. doi:10.1016/j.pbi.2009.06.008

Plésiat, P., & Nikaido, H. (1992). Outer membranes of Gram-negative bacteria are permeable to steroid probes. *Molecular Microbiology, 6*(10), 1323-1333. doi:10.1111/j.1365-2958.1992.tb00853.x

Pochert, S. (2014). *Reportergenanalyse von transient transformierten Arabidopsis thaliana Protoplasten.* (Bachelor of Science Bachelorthesis), Eberhard Karls Universität Tübingen, Tübingen.

Popescu, S. C., Popescu, G. V., Bachan, S., Zhang, Z., Gerstein, M., Snyder, M., & Dinesh-Kumar, S. P. (2009). MAPK target networks in Arabidopsis thaliana revealed using functional protein microarrays. *Genes Dev, 23*(1), 80-92. doi:10.1101/gad.1740009

Pourcel, C., Salvignol, G., & Vergnaud, G. (2005). CRISPR elements in Yersinia pestis acquire new repeats by preferential uptake of bacteriophage DNA, and provide additional tools for evolutionary studies. *Microbiology, 151*(Pt 3), 653-663. doi:10.1099/mic.0.27437-0

Pratt, W. B., & Toft, D. O. (1997). Steroid receptor interactions with heat shock protein and immunophilin chaperones. *Endocr Rev, 18*(3), 306-360. doi:10.1210/edrv.18.3.0303

Ramirez-Prado, J. S., Abulfaraj, A. A., Rayapuram, N., Benhamed, M., & Hirt, H. (2018). Plant Immunity: From Signaling to Epigenetic Control of Defense. *Trends Plant Sci*. doi:10.1016/j.tplants.2018.06.004

Ramirez-Prado, J. S., Piquerez, S. J. M., Bendahmane, A., Hirt, H., Raynaud, C., & Benhamed, M. (2018). Modify the Histone to Win the Battle: Chromatin Dynamics in Plant-Pathogen Interactions. *Front Plant Sci, 9*(355), 355. doi:10.3389/fpls.2018.00355

Rathi, P., Maurer, S., Kubik, G., & Summerer, D. (2016). Isolation of Human Genomic DNA Sequences with Expanded Nucleobase Selectivity. *J Am Chem Soc, 138*(31), 9910-9918. doi:10.1021/jacs.6b04807

Reynolds, L., Ullman, C., Moore, M., Isalan, M., West, M. J., Clapham, P., . . . Choo, Y. (2003). Repression of the HIV-1 5' LTR promoter and inhibition of HIV-1 replication by using engineered zinc-finger transcription factors. *Proc Natl Acad Sci U S A, 100*(4), 1615-1620. doi:10.1073/pnas.252770699

Rhee, H. S., & Pugh, B. F. (2011). Comprehensive genome-wide protein-DNA interactions detected at single-nucleotide resolution. *Cell, 147*(6), 1408-1419. doi:10.1016/j.cell.2011.11.013

Rhee, H. S., & Pugh, B. F. (2012). Genome-wide structure and organization of eukaryotic pre-initiation complexes. *Nature, 483*(7389), 295-301. doi:10.1038/nature10799

Richmond, T. J., Finch, J. T., Rushton, B., Rhodes, D., & Klug, A. (1984). Structure of the nucleosome core particle at 7 Å resolution. *Nature, 311*, 532. doi:10.1038/311532a0

Riechmann, J. L., Heard, J., Martin, G., Reuber, L., Jiang, C., Keddie, J., . . . Yu, G. (2000). Arabidopsis transcription factors: genome-wide comparative analysis among eukaryotes. *Science, 290*(5499), 2105-2110.

Robatzek, S., & Somssich, I. E. (2002). Targets of AtWRKY6 regulation during plant senescence and pathogen defense. *Genes Dev, 16*(9), 1139-1149. doi:10.1101/gad.222702

Romer, P., Hahn, S., Jordan, T., Strauss, T., Bonas, U., & Lahaye, T. (2007). Plant pathogen recognition mediated by promoter activation of the pepper Bs3 resistance gene. *Science, 318*(5850), 645-648. doi:10.1126/science.1144958

Ronald, P. C., & Beutler, B. (2010). Plant and animal sensors of conserved microbial signatures. *Science, 330*(6007), 1061-1064. doi:10.1126/science.1189468

Rushton, P. J., Somssich, I. E., Ringler, P., & Shen, Q. J. (2010). WRKY transcription factors. *Trends Plant Sci, 15*(5), 247-258. doi:10.1016/j.tplants.2010.02.006

Rushton, P. J., Torres, J. T., Parniske, M., Wernert, P., Hahlbrock, K., & Somssich, I. E. (1996). Interaction of elicitor-induced DNA-binding proteins with elicitor response elements in the promoters of parsley PR1 genes. *EMBO J, 15*(20), 5690-5700.

Sadava, D. (2008). DNA is Packed into a Mitotic Chromosome. Retrieved from https://www.nature.com/scitable/content/DNA-is-Packed-into-a-Mitotic-Chromosome-3497

Sanchez, E. R. (1992). Heat shock induces translocation to the nucleus of the unliganded glucocorticoid receptor. *J Biol Chem, 267*(1), 17-20.

Schena, M., Lloyd, A. M., & Davis, R. W. (1991). A steroid-inducible gene expression system for plant cells. *Proc Natl Acad Sci U S A, 88*(23), 10421-10425.

Schleifenbaum, F., Elgass, K., Sackrow, M., Caesar, K., Berendzen, K., Meixner, A. J., & Harter, K. (2010). Fluorescence intensity decay shape analysis microscopy (FIDSAM) for quantitative and sensitive live-cell imaging: a novel technique for fluorescence microscopy of endogenously expressed fusion-proteins. *Mol Plant, 3*(3), 555-562. doi:10.1093/mp/ssp110

Schulze, B., Mentzel, T., Jehle, A. K., Mueller, K., Beeler, S., Boller, T., . . . Chinchilla, D. (2010). Rapid heteromerization and phosphorylation of ligand-activated plant transmembrane receptors and their associated kinase BAK1. *J Biol Chem, 285*(13), 9444-9451. doi:10.1074/jbc.M109.096842

Schutze, K., Harter, K., & Chaban, C. (2009). Bimolecular fluorescence complementation (BiFC) to study protein-protein interactions in living plant cells. *Methods Mol Biol, 479*, 189-202. doi:10.1007/978-1-59745-289-2_12

Schwessinger, B., & Ronald, P. C. (2012). Plant innate immunity: perception of conserved microbial signatures. *Annu Rev Plant Biol, 63*, 451-482. doi:10.1146/annurev-arplant-042811-105518

Schwessinger, B., Roux, M., Kadota, Y., Ntoukakis, V., Sklenar, J., Jones, A., & Zipfel, C. (2011). Phosphorylation-dependent differential regulation of plant growth, cell death, and innate immunity by the regulatory receptor-like kinase BAK1. *PLoS Genet, 7*(4), e1002046. doi:10.1371/journal.pgen.1002046

Scott, J. N., Kupinski, A. P., & Boyes, J. (2014). Targeted genome regulation and modification using transcription activator-like effectors. *Febs j, 281*(20), 4583-4597. doi:10.1111/febs.12973

Segonzac, C., & Zipfel, C. (2011). Activation of plant pattern-recognition receptors by bacteria. *Curr Opin Microbiol, 14*(1), 54-61. doi:10.1016/j.mib.2010.12.005

Solomon, M. J., & Varshavsky, A. (1985). Formaldehyde-mediated DNA-protein crosslinking: a probe for in vivo chromatin structures. *Proc Natl Acad Sci U S A, 82*(19), 6470-6474.

Starick, S. R., Ibn-Salem, J., Jurk, M., Hernandez, C., Love, M. I., Chung, H. R., . . . Meijsing, S. H. (2015). ChIP-exo signal associated with DNA-binding motifs provides insight into the genomic binding of the glucocorticoid receptor and cooperating transcription factors. *Genome Res, 25*(6), 825-835. doi:10.1101/gr.185157.114

Stella, S., Molina, R., Yefimenko, I., Prieto, J., Silva, G., Bertonati, C., . . . Montoya, G. (2013). Structure of the AvrBs3-DNA complex provides new insights into the initial thymine-recognition mechanism. *Acta Crystallogr D Biol Crystallogr, 69*(Pt 9), 1707-1716. doi:10.1107/s0907444913016429

Stockinger, E. J., Gilmour, S. J., & Thomashow, M. F. (1997). Arabidopsis thaliana CBF1 encodes an AP2 domain-containing transcriptional activator that binds to the C-repeat/DRE, a cis-acting DNA regulatory element that stimulates transcription in response to low temperature and water deficit. *Proc Natl Acad Sci U S A, 94*(3), 1035-1040.

Szalkowski, A. M., & Schmid, C. D. (2011). Rapid innovation in ChIP-seq peak-calling algorithms is outdistancing benchmarking efforts. *Briefings in Bioinformatics, 12*(6), 626-633. doi:10.1093/bib/bbq068

Szymanski, W. G., Kierszniowska, S., & Schulze, W. X. (2013). Metabolic labeling and membrane fractionation for comparative proteomic analysis of Arabidopsis thaliana suspension cell cultures. *J Vis Exp*(79), e50535. doi:10.3791/50535

Teytelman, L., Thurtle, D. M., Rine, J., & van Oudenaarden, A. (2013). Highly expressed loci are vulnerable to misleading ChIP localization of multiple unrelated proteins. *Proc Natl Acad Sci U S A, 110*(46), 18602-18607. doi:10.1073/pnas.1316064110

Thompson, J. F., Hayes, L. S., & Lloyd, D. B. (1991). Modulation of firefly luciferase stability and impact on studies of gene regulation. *Gene, 103*(2), 171-177. doi:https://doi.org/10.1016/0378-1119(91)90270-L

Tremblay, J. P., Chapdelaine, P., Coulombe, Z., & Rousseau, J. (2012). Transcription activator-like effector proteins induce the expression of the frataxin gene. *Hum Gene Ther, 23*(8), 883-890. doi:10.1089/hum.2012.034

Tsuda, K., & Somssich, I. E. (2015). Transcriptional networks in plant immunity. *New Phytol, 206*(3), 932-947. doi:10.1111/nph.13286

Vandevyver, S., Dejager, L., & Libert, C. (2012). On the trail of the glucocorticoid receptor: into the nucleus and back. *Traffic, 13*(3), 364-374. doi:10.1111/j.1600-0854.2011.01288.x

Vellai, T., & Vida, G. (1999). The origin of eukaryotes: the difference between prokaryotic and eukaryotic cells. *Proceedings of the Royal Society of London. Series B: Biological Sciences, 266*(1428), 1571-1577. doi:10.1098/rspb.1999.0817

Vermeulen, M., Eberl, H. C., Matarese, F., Marks, H., Denissov, S., Butter, F., . . . Mann, M. (2010). Quantitative interaction proteomics and genome-wide profiling of epigenetic histone marks and their readers. *Cell, 142*(6), 967-980. doi:10.1016/j.cell.2010.08.020

Wallmeroth, N., Anastasia, A. K., Harter, K., Berendzen, K. W., & Mira-Rodado, V. (2017). Arabidopsis response regulator 22 inhibits cytokinin-regulated gene transcription in vivo. *Protoplasma, 254*(1), 597-601. doi:10.1007/s00709-016-0944-4

Wang, D. Y., Kumar, S., & Hedges, S. B. (1999). Divergence time estimates for the early history of animal phyla and the origin of plants, animals and fungi. *Proc Biol Sci, 266*(1415), 163-171. doi:10.1098/rspb.1999.0617

Waryah, C. B., Moses, C., Arooj, M., & Blancafort, P. (2018). Zinc Fingers, TALEs, and CRISPR Systems: A Comparison of Tools for Epigenome Editing. In A. Jeltsch & M. G. Rots (Eds.), *Epigenome Editing: Methods and Protocols* (pp. 19-63). New York, NY: Springer New York.

Weber, E., Gruetzner, R., Werner, S., Engler, C., & Marillonnet, S. (2011). Assembly of designer TAL effectors by Golden Gate cloning. *PLoS One, 6*(5), e19722. doi:10.1371/journal.pone.0019722

Winter, e. a. (2007). Developmental Map AT2G19190, Arabiopsis eFP Browser at bar.utoronta.ca. Retrieved from https://www.arabidopsis.org/servlets/TairObject?id=34421&type=locus

Wisniewski, J. R., Zougman, A., Nagaraj, N., & Mann, M. (2009). Universal sample preparation method for proteome analysis. *Nat Methods, 6*(5), 359-362. doi:10.1038/nmeth.1322

Woese, C. R., Kandler, O., & Wheelis, M. L. (1990). Towards a natural system of organisms: proposal for the domains Archaea, Bacteria, and Eucarya. *Proc Natl Acad Sci U S A, 87*(12), 4576-4579.

Yi, S. Y., Kim, J.-H., Joung, Y.-H., Lee, S., Kim, W.-T., Yu, S. H., & Choi, D. (2004). The Pepper Transcription Factor CaPF1 Confers Pathogen and Freezing Tolerance in Arabidopsis. *Plant Physiol, 136*(1), 2862-2874. doi:10.1104/pp.104.042903

Zhang, F., Cong, L., Lodato, S., Kosuri, S., Church, G. M., & Arlotta, P. (2011). Efficient construction of sequence-specific TAL effectors for modulating mammalian transcription. *Nat Biotechnol, 29*(2), 149-153. doi:10.1038/nbt.1775

Zhang, J., Li, W., Xiang, T., Liu, Z., Laluk, K., Ding, X., . . . Zhou, J. M. (2010). Receptor-like cytoplasmic kinases integrate signaling from multiple plant immune receptors and are

targeted by a Pseudomonas syringae effector. *Cell Host Microbe, 7*(4), 290-301. doi:10.1016/j.chom.2010.03.007

Zheng, Y., & Hearing, P. (2014). The use of chromatin immunoprecipitation (ChIP) to study the binding of viral proteins to the adenovirus genome in vivo. *Methods Mol Biol, 1089*, 79-87. doi:10.1007/978-1-62703-679-5_6

Zheng, Y., & Perry, S. E. (2011). Chromatin immunoprecipitation to verify or to identify in vivo protein-DNA interactions. *Methods Mol Biol, 754*, 277-291. doi:10.1007/978-1-61779-154-3_16

Zipfel, C., Robatzek, S., Navarro, L., Oakeley, E. J., Jones, J. D., Felix, G., & Boller, T. (2004). Bacterial disease resistance in Arabidopsis through flagellin perception. *Nature, 428*(6984), 764-767. doi:10.1038/nature02485

9. *Curriculum Vitae*

Stefan Markus Fischer

Education

12/2013 - present	PhD Student Centre for Plant Molecular Biology, University of Tuebingen, Department of Plantphysiology
10/2011 - 10/2013	Master of Science Centre for Plant Molecular Biology, University of Tuebingen, Department of General Genetics, Grade 1,2
10/2008 - 10/2011	Bachelor of Science Centre for Plant Molecular Biology, University of Tuebingen Department of General Genetics; Grade 1,9
07/1998 - 07/2007	Abitur Otto-Hahn Gymnasium, Nagold

Awards and stipends

2016 - 2017	Doctoral fellowship, Landesgraduiertenförderung Baden-Württemberg
2015	Reinhold von Sengbusch Poster Award 2015

Publications

01/2016	**Fischer S. M.**, Böser A, Hirsch J. P. and Wanke D., *Quantitative Analysis of Protein-DNA Interaction by qDPI-ELISA,* Springer Protocols, Methods in Molecular Biology Vol. 1482 pp 49-66
09/2015	Smykowski, A., **Fischer S. M.**, and U. Zentgraf, *Phosphorylation Affects DNA-Binding oft he Senescence-Regulating bZIP Transcription Factor GBF1,* Plants, 2015. **4**(3): p. 691

Conferences

07/2017	3rd Summer academy in Plant Molecular Biology 2017, Bad Heiligenkreuztal, Poster Presentation
04/2017	9th Regio Plant Science Meeting 2017, Tübingen, Poster Presentation

02/2017	30. Tagung Molekularbiologie der Pflanzen 2017, Dabringhausen, Poster Presentation
07/2016	2nd PhD Symposium 2016, Tübingen, Talk
07/2015	2nd Summer Academy in Plant Molecular Biology Freudenstadt, Poster Presentation
02/2015	28. Tagung Molekularbiologie der Pflanzen, Dabringhausen, Poster Presentation (Awarded with R.v.S. Poster Award)
02/2015	8th Regio Plant Science Meeting 2015, Ulm, Poster Presentation
09/2013	Botanikertagung 2013, Tübingen

11. Supplement

11.1. Supplementary figures

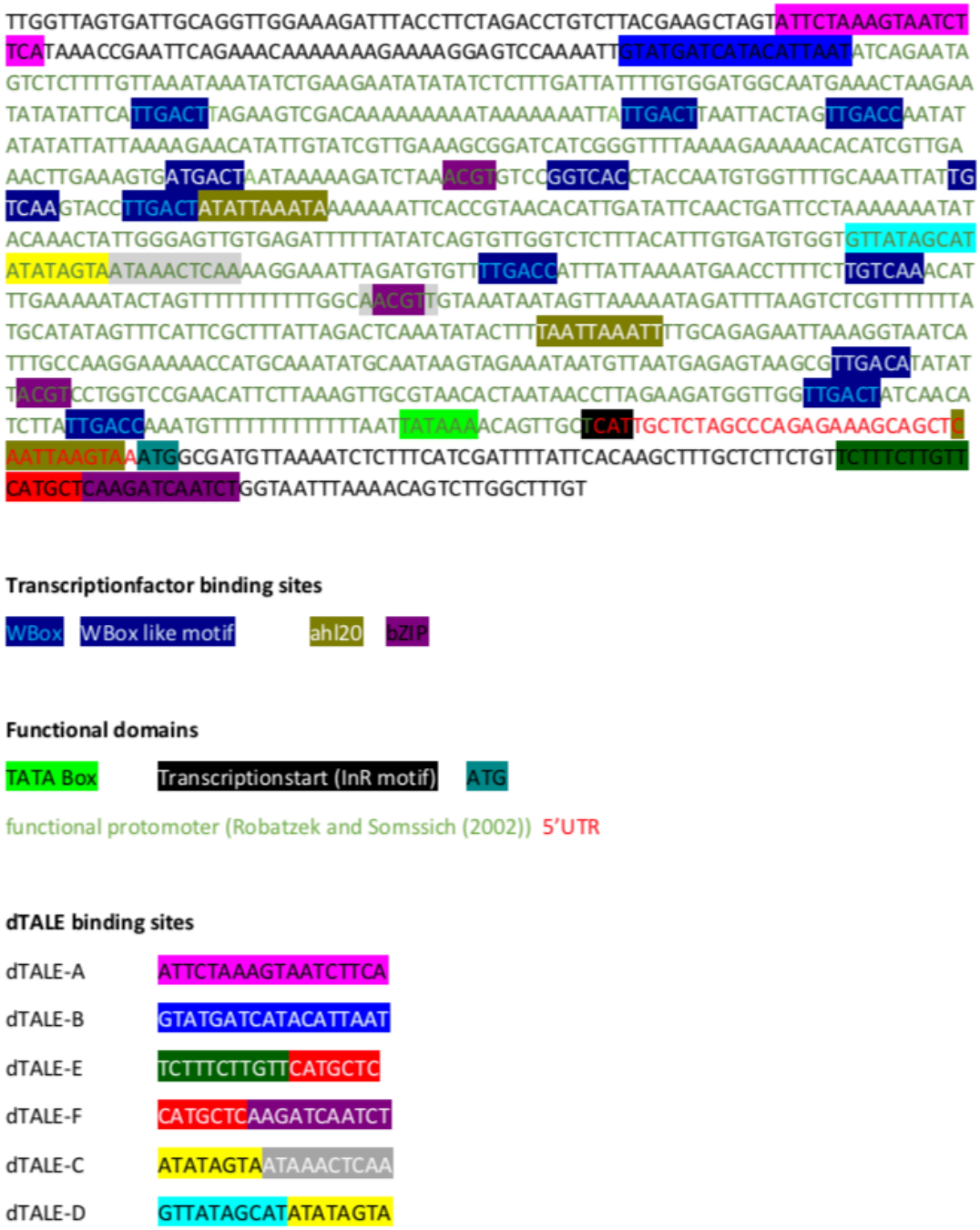

Supplementary figure 1: Overview of pFRK1 with *cis*-regulatory elements and putative binding sites of transcription factors and the dTALEs in pFRK1
Sequence 1051 bp up- and 108 bp downstream of the annotated ATG is shown.

Supplementary figure 2: PlantPan2 output. Search query 1 kb upstream of TSS and 100 bp downstream.

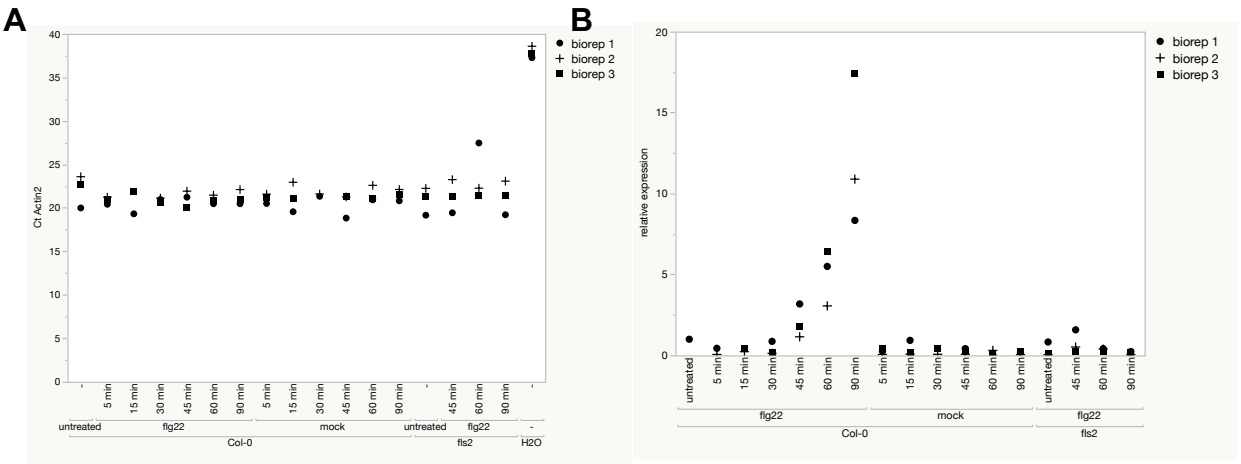

Supplementary figure 3: qPCR after flg22 treatment of *A. thaliana* seedlings
A Ct values of the Actin2 reference primers
B Relative *FRK1* expression [ΔΔCt] of the bio replicates shown separately. *FRK1* was induced within 45 min by flg22 treatment. Mock treatment did not have an effect. *fls2* plants did not express *FRK1* RNA after flg22 treatment. *Actin2* was used as reference gene.

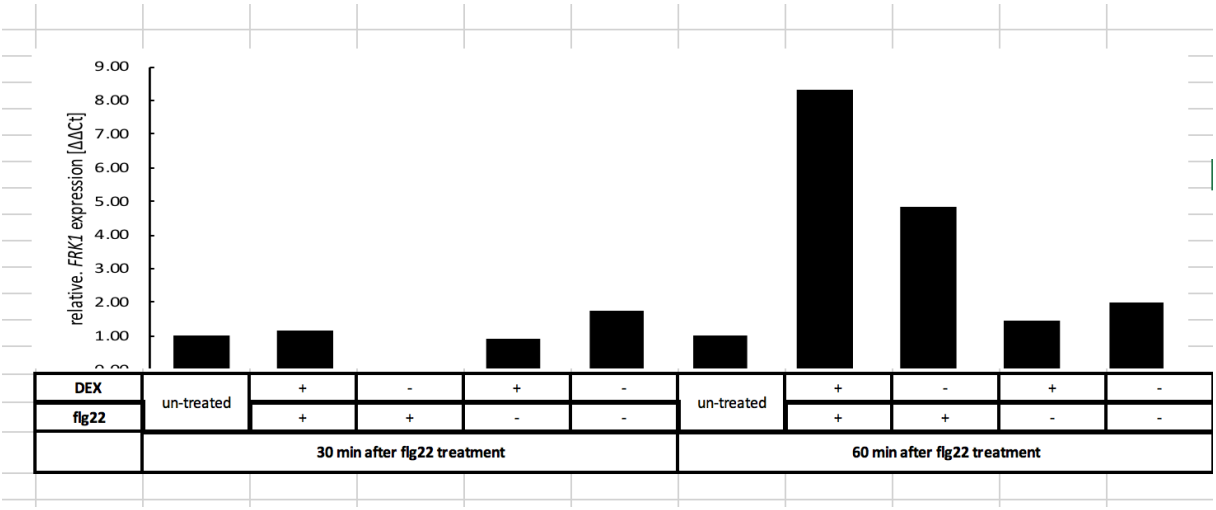

Supplementary figure 4: *FRK1* transcript accumulation is still induced by flg22 in *A. thaliana* seedlings expressing nuclear-localized dTALE C (bioreplicate 2)

dTALE C expressing Arabidopsis seedlings were treated with DEX (10 µM) or mock-treated. 30 min later the seedlings were exposed to flg22 (100 nM) or mock-exposed for 30 or 60 min. Total RNA was extracted and applied to qRT-PCR using FRK1-specific primers.

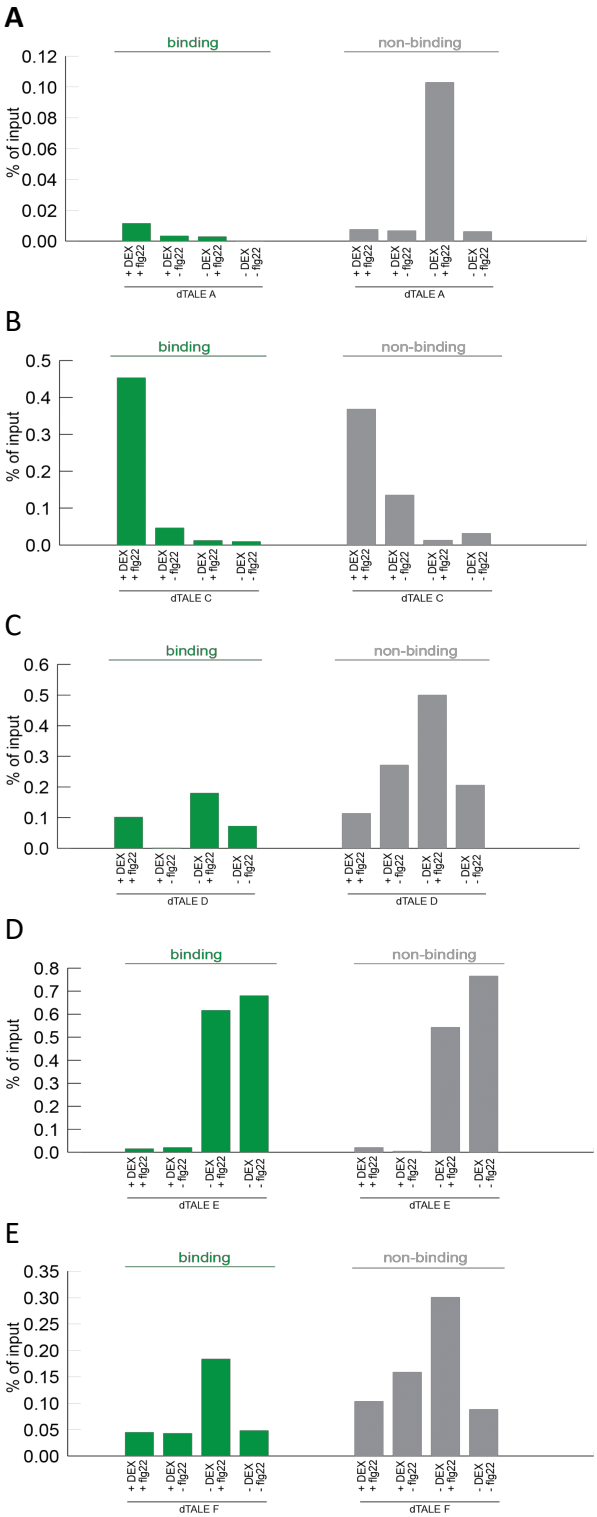

Supplementary figure 5: Repetition of X-ChIP followed by qPCR of *pFRK1* fragments using dTALEs. dTALE A **(A)**, dTALE C **(B)**, dTALE D **(C)**, dTALE E **(D)** and dTALE F **(E)** were used to immuno-precipitate pFRK1 fragments. The samples were prepared from stable A. thaliana lines expressing dTALEs that were treated with flg22 and DEX, flg22, DEX and mock. Precipitated DNA was quantified by qPCR. The values are shown in % of input in green for the binding amplicon, grey for the no binding amplicon.

11.2. Vector Maps

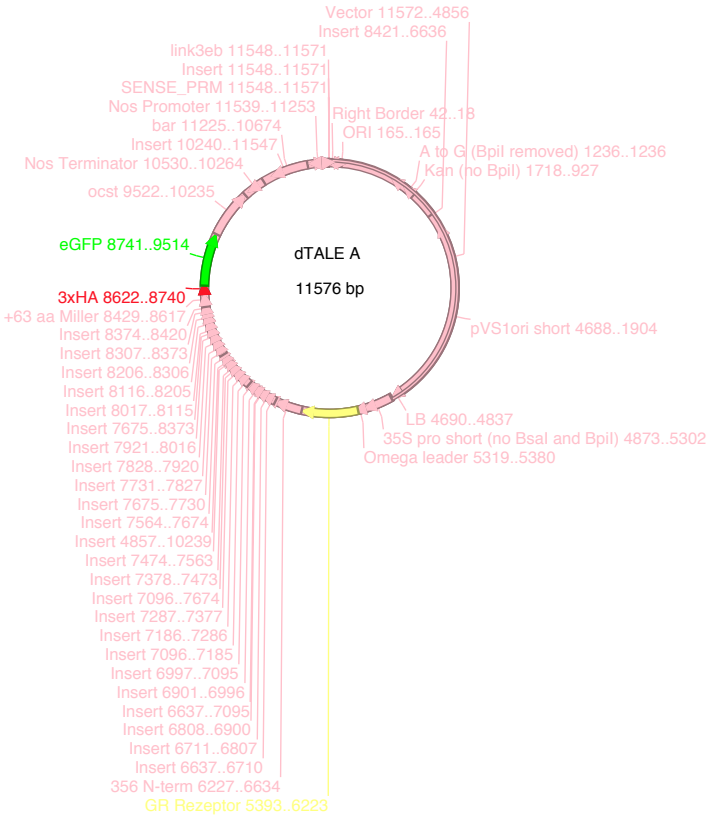

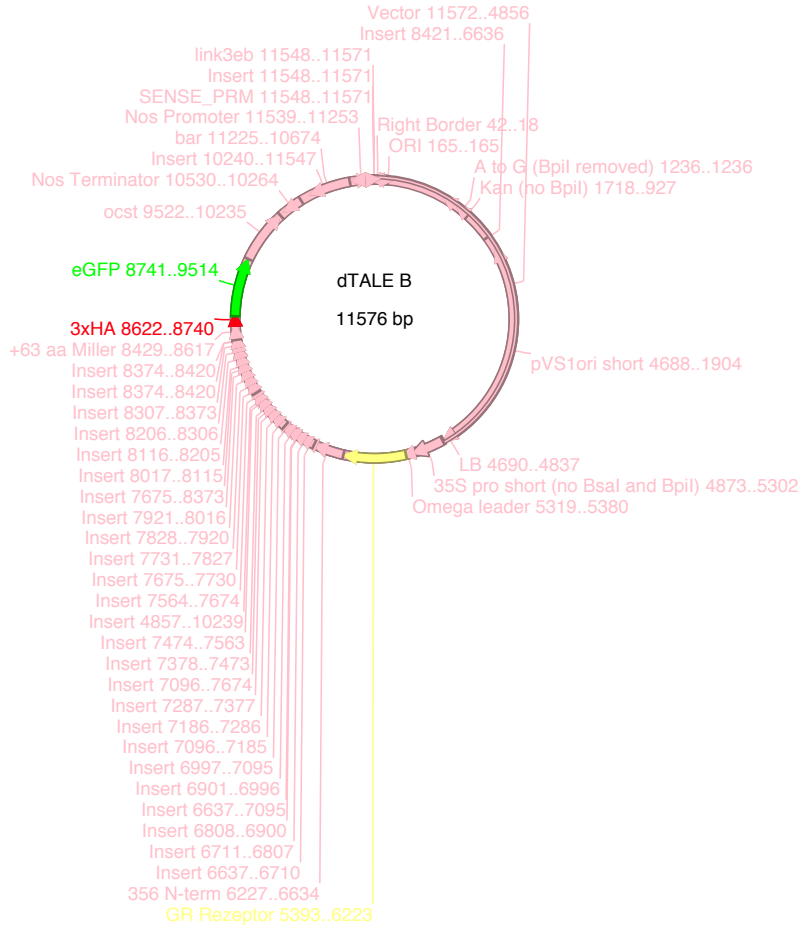

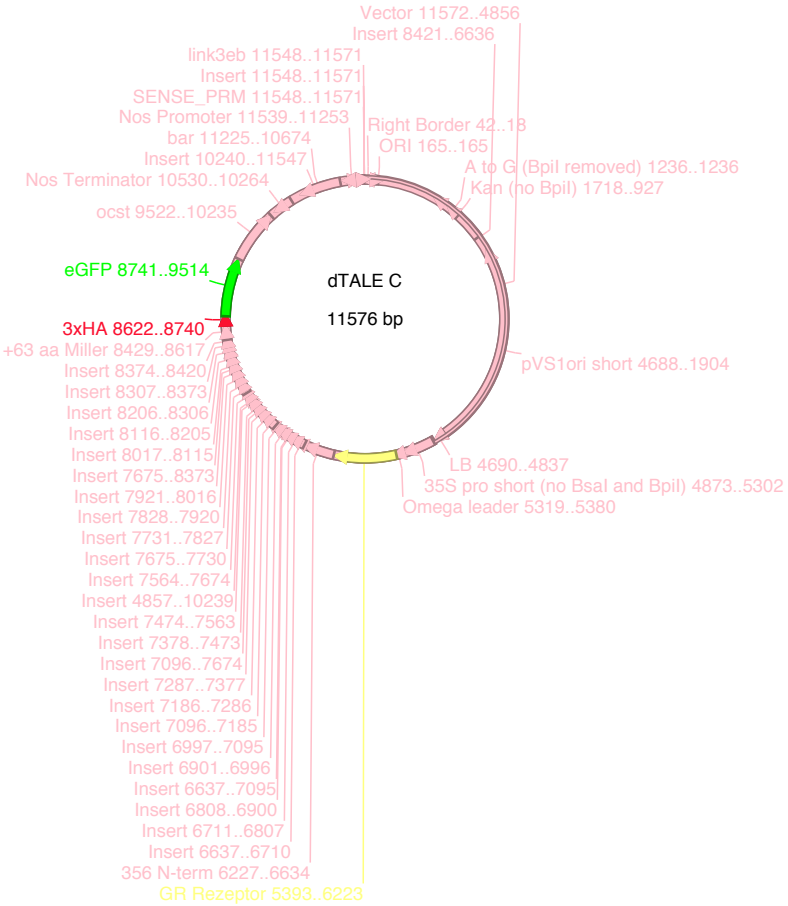
Vector 11572..4856
Insert 8421..6636
link3eb 11548..11571
Insert 11548..11571
SENSE_PRM 11548..11571
Nos Promoter 11539..11253
bar 11225..10674
Insert 10240..11547
Nos Terminator 10530..10264
ocst 9522..10235
eGFP 8741..9514
3xHA 8622..8740
+63 aa Miller 8429..8617
Insert 8374..8420
Insert 8307..8373
Insert 8206..8306
Insert 8116..8205
Insert 8017..8115
Insert 7675..8373
Insert 7921..8016
Insert 7828..7920
Insert 7731..7827
Insert 7675..7730
Insert 7564..7674
Insert 4857..10239
Insert 7474..7563
Insert 7378..7473
Insert 7096..7674
Insert 7287..7377
Insert 7186..7286
Insert 7096..7185
Insert 6997..7095
Insert 6901..6996
Insert 6637..7095
Insert 6808..6900
Insert 6711..6807
Insert 6637..6710
356 N-term 6227..6634
GR Rezeptor 5393..6223
Right Border 42..18
ORI 165..165
A to G (BpiI removed) 1236..1236
Kan (no BpiI) 1718..927
pVS1ori short 4688..1904
LB 4690..4837
35S pro short (no BsaI and BpiI) 4873..5302
Omega leader 5319..5380
dTALE C
11576 bp

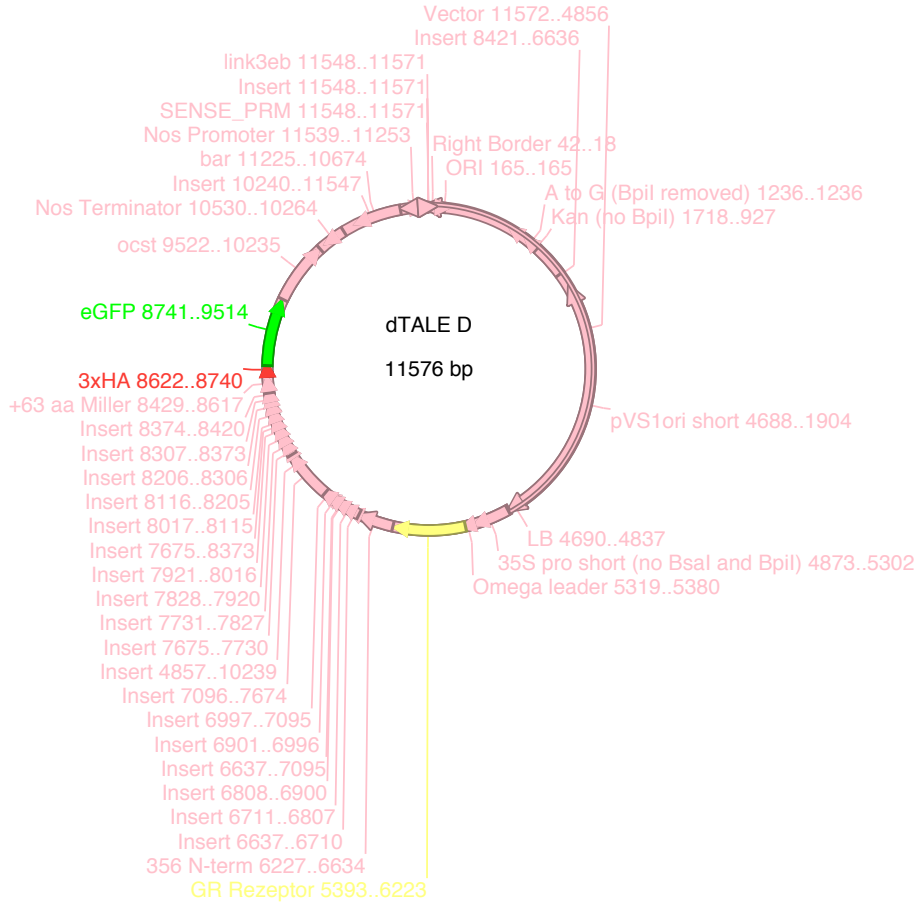
Vector 11572..4856
Insert 8421..6636
link3eb 11548..11571
Insert 11548..11571
SENSE_PRM 11548..11571
Nos Promoter 11539..11253
bar 11225..10674
Insert 10240..11547
Nos Terminator 10530..10264
ocst 9522..10235
eGFP 8741..9514
3xHA 8622..8740
+63 aa Miller 8429..8617
Insert 8374..8420
Insert 8307..8373
Insert 8206..8306
Insert 8116..8205
Insert 8017..8115
Insert 7675..8373
Insert 7921..8016
Insert 7828..7920
Insert 7731..7827
Insert 7675..7730
Insert 4857..10239
Insert 7096..7674
Insert 6997..7095
Insert 6901..6996
Insert 6637..7095
Insert 6808..6900
Insert 6711..6807
Insert 6637..6710
356 N-term 6227..6634
GR Rezeptor 5393..6223
Right Border 42..18
ORI 165..165
A to G (BpiI removed) 1236..1236
Kan (no BpiI) 1718..927
pVS1ori short 4688..1904
LB 4690..4837
35S pro short (no BsaI and BpiI) 4873..5302
Omega leader 5319..5380
dTALE D
11576 bp

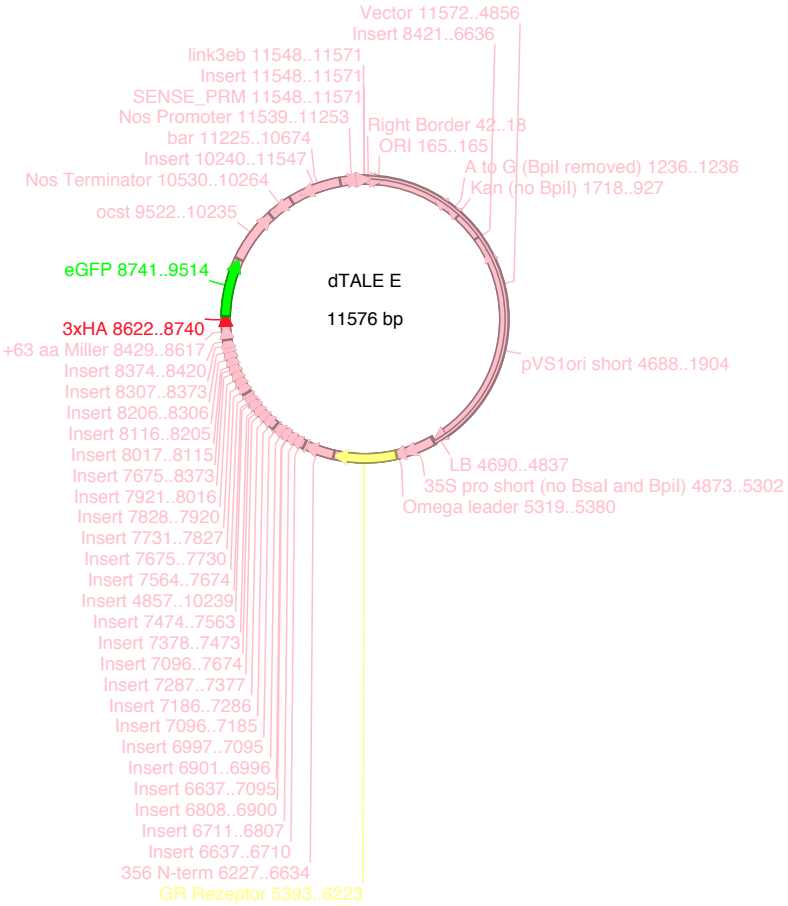
Vector 11572..4856
Insert 8421..6636
link3eb 11548..11571
Insert 11548..11571
SENSE_PRM 11548..11571
Nos Promoter 11539..11253
bar 11225..10674
Insert 10240..11547
Nos Terminator 10530..10264
ocst 9522..10235
eGFP 8741..9514
3xHA 8622..8740
+63 aa Miller 8429..8617
Insert 8374..8420
Insert 8307..8373
Insert 8206..8306
Insert 8116..8205
Insert 8017..8115
Insert 7675..8373
Insert 7921..8016
Insert 7828..7920
Insert 7731..7827
Insert 7675..7730
Insert 7564..7674
Insert 4857..10239
Insert 7474..7563
Insert 7378..7473
Insert 7096..7674
Insert 7287..7377
Insert 7186..7286
Insert 7096..7185
Insert 6997..7095
Insert 6901..6996
Insert 6637..7095
Insert 6808..6900
Insert 6711..6807
Insert 6637..6710
356 N-term 6227..6634
GR Rezeptor 5393..6223
Right Border 42..18
ORI 165..165
A to G (BpiI removed) 1236..1236
Kan (no BpiI) 1718..927
pVS1ori short 4688..1904
LB 4690..4837
35S pro short (no BsaI and BpiI) 4873..5302
Omega leader 5319..5380
dTALE E
11576 bp

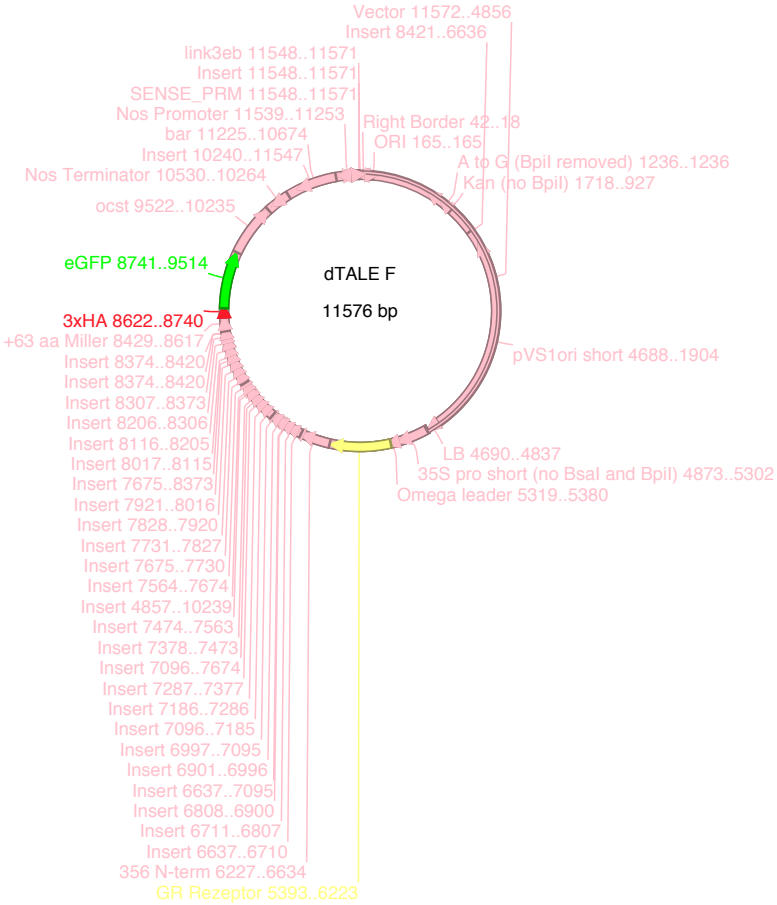
Vector 11572..4856
Insert 8421..6636
link3eb 11548..11571
Insert 11548..11571
SENSE_PRM 11548..11571
Nos Promoter 11539..11253
bar 11225..10674
Insert 10240..11547
Nos Terminator 10530..10264
ocst 9522..10235
eGFP 8741..9514
3xHA 8622..8740
+63 aa Miller 8429..8617
Insert 8374..8420
Insert 8374..8420
Insert 8307..8373
Insert 8206..8306
Insert 8116..8205
Insert 8017..8115
Insert 7675..8373
Insert 7921..8016
Insert 7828..7920
Insert 7731..7827
Insert 7675..7730
Insert 7564..7674
Insert 4857..10239
Insert 7474..7563
Insert 7378..7473
Insert 7096..7674
Insert 7287..7377
Insert 7186..7286
Insert 7096..7185
Insert 6997..7095
Insert 6901..6996
Insert 6637..7095
Insert 6808..6900
Insert 6711..6807
Insert 6637..6710
356 N-term 6227..6634
GR Rezeptor 5393..6223
Right Border 42..18
ORI 165..165
A to G (BpiI removed) 1236..1236
Kan (no BpiI) 1718..927
pVS1ori short 4688..1904
LB 4690..4837
35S pro short (no BsaI and BpiI) 4873..5302
Omega leader 5319..5380
dTALE F
11576 bp

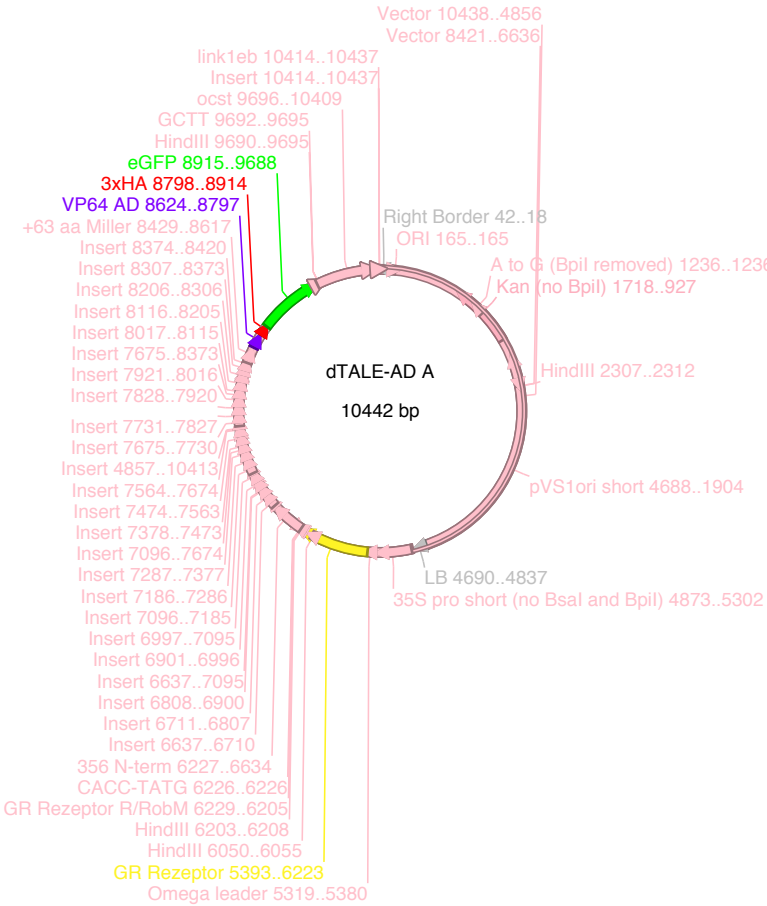
Vector 10438..4856
Vector 8421..6636
link1eb 10414..10437
Insert 10414..10437
ocst 9696..10409
GCTT 9692..9695
HindIII 9690..9695
eGFP 8915..9688
3xHA 8798..8914
VP64 AD 8624..8797
+63 aa Miller 8429..8617
Insert 8374..8420
Insert 8307..8373
Insert 8206..8306
Insert 8116..8205
Insert 8017..8115
Insert 7675..8373
Insert 7921..8016
Insert 7828..7920
Insert 7731..7827
Insert 7675..7730
Insert 4857..10413
Insert 7564..7674
Insert 7474..7563
Insert 7378..7473
Insert 7096..7674
Insert 7287..7377
Insert 7186..7286
Insert 7096..7185
Insert 6997..7095
Insert 6901..6996
Insert 6637..7095
Insert 6808..6900
Insert 6711..6807
Insert 6637..6710
356 N-term 6227..6634
CACC-TATG 6226..6226
GR Rezeptor R/RobM 6229..6205
HindIII 6203..6208
HindIII 6050..6055
GR Rezeptor 5393..6223
Omega leader 5319..5380
Right Border 42..18
ORI 165..165
A to G (BpiI removed) 1236..1236
Kan (no BpiI) 1718..927
HindIII 2307..2312
pVS1ori short 4688..1904
LB 4690..4837
35S pro short (no BsaI and BpiI) 4873..5302
dTALE-AD A
10442 bp

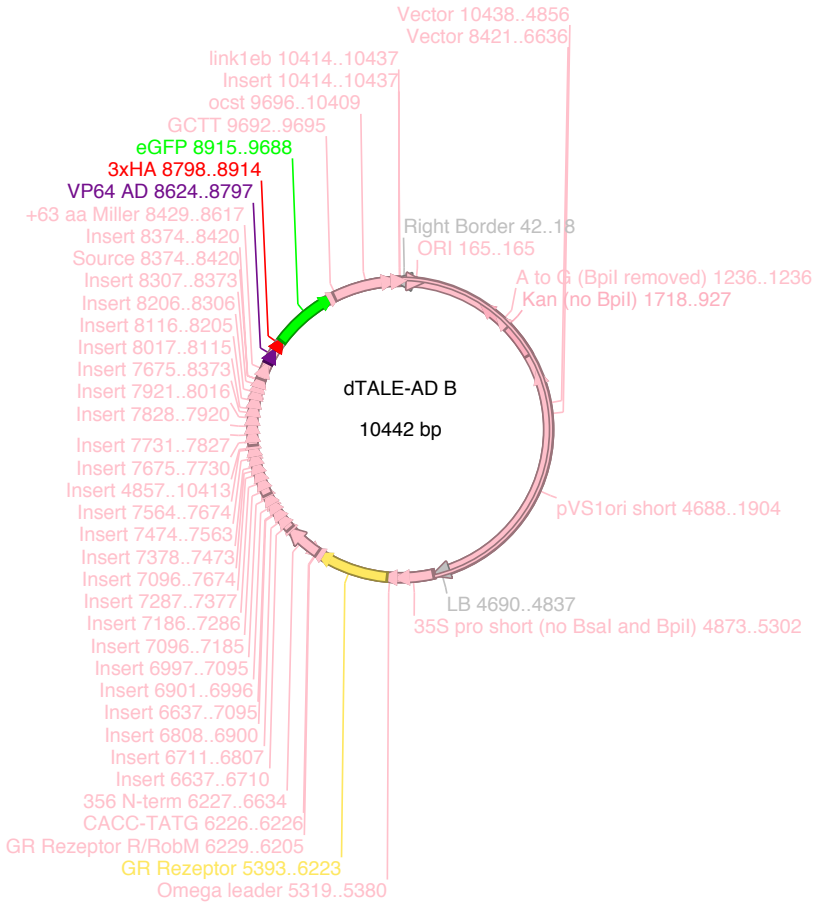
Vector 10438..4856
Vector 8421..6636
link1eb 10414..10437
Insert 10414..10437
ocst 9696..10409
GCTT 9692..9695
eGFP 8915..9688
3xHA 8798..8914
VP64 AD 8624..8797
+63 aa Miller 8429..8617
Insert 8374..8420
Source 8374..8420
Insert 8307..8373
Insert 8206..8306
Insert 8116..8205
Insert 8017..8115
Insert 7675..8373
Insert 7921..8016
Insert 7828..7920
Insert 7731..7827
Insert 7675..7730
Insert 4857..10413
Insert 7564..7674
Insert 7474..7563
Insert 7378..7473
Insert 7096..7674
Insert 7287..7377
Insert 7186..7286
Insert 7096..7185
Insert 6997..7095
Insert 6901..6996
Insert 6637..7095
Insert 6808..6900
Insert 6711..6807
Insert 6637..6710
356 N-term 6227..6634
CACC-TATG 6226..6226
GR Rezeptor R/RobM 6229..6205
GR Rezeptor 5393..6223
Omega leader 5319..5380
Right Border 42..18
ORI 165..165
A to G (BpiI removed) 1236..1236
Kan (no BpiI) 1718..927
pVS1ori short 4688..1904
LB 4690..4837
35S pro short (no BsaI and BpiI) 4873..5302
dTALE-AD B
10442 bp

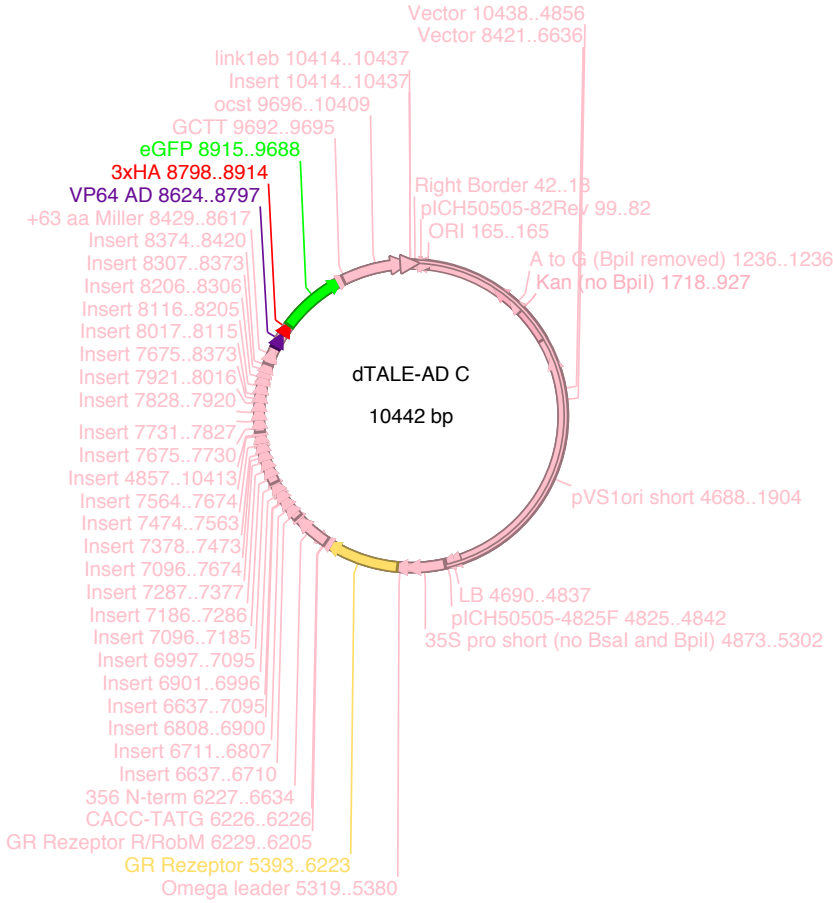
Vector 10438..4856
Vector 8421..6636
link1eb 10414..10437
Insert 10414..10437
ocst 9696..10409
GCTT 9692..9695
eGFP 8915..9688
3xHA 8798..8914
VP64 AD 8624..8797
+63 aa Miller 8429..8617
Insert 8374..8420
Insert 8307..8373
Insert 8206..8306
Insert 8116..8205
Insert 8017..8115
Insert 7675..8373
Insert 7921..8016
Insert 7828..7920
Insert 7731..7827
Insert 7675..7730
Insert 4857..10413
Insert 7564..7674
Insert 7474..7563
Insert 7378..7473
Insert 7096..7674
Insert 7287..7377
Insert 7186..7286
Insert 7096..7185
Insert 6997..7095
Insert 6901..6996
Insert 6637..7095
Insert 6808..6900
Insert 6711..6807
Insert 6637..6710
356 N-term 6227..6634
CACC-TATG 6226..6226
GR Rezeptor R/RobM 6229..6205
GR Rezeptor 5393..6223
Omega leader 5319..5380
Right Border 42..13
pICH50505-82Rev 99..82
ORI 165..165
A to G (BpiI removed) 1236..1236
Kan (no BpiI) 1718..927
dTALE-AD C
10442 bp
pVS1ori short 4688..1904
LB 4690..4837
pICH50505-4825F 4825..4842
35S pro short (no BsaI and BpiI) 4873..5302

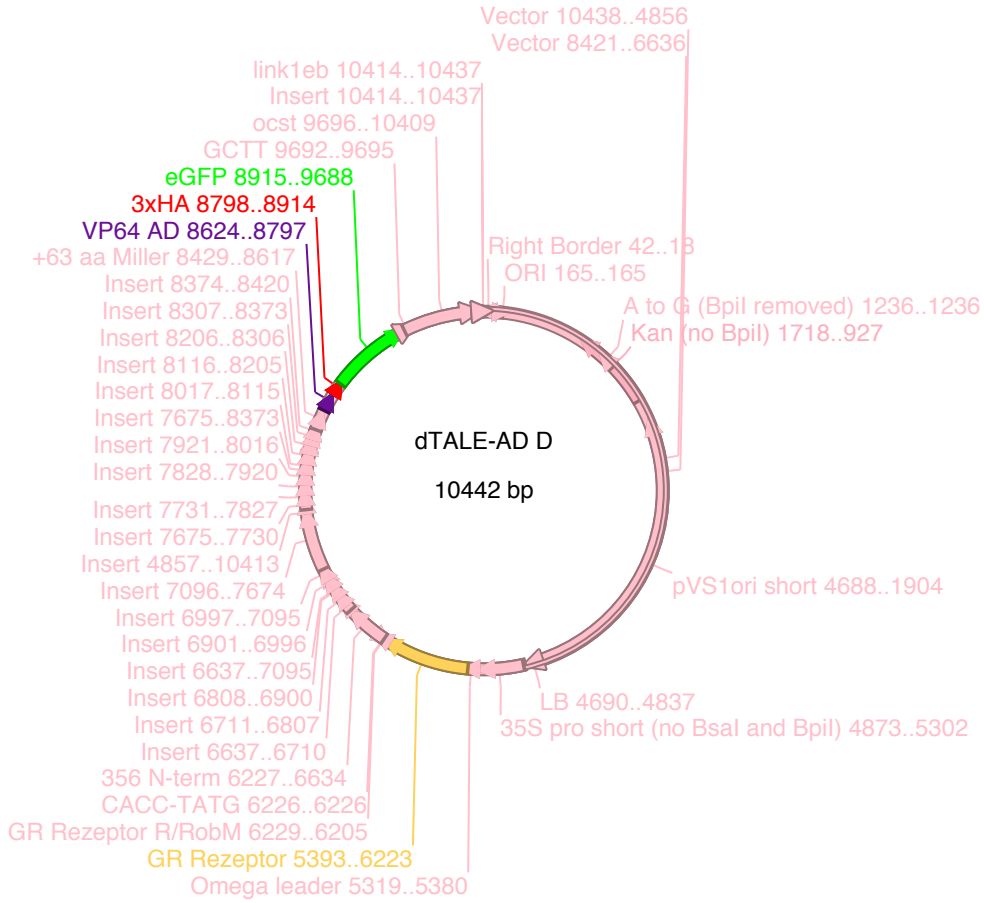
Vector 10438..4856
Vector 8421..6636
link1eb 10414..10437
Insert 10414..10437
ocst 9696..10409
GCTT 9692..9695
eGFP 8915..9688
3xHA 8798..8914
VP64 AD 8624..8797
+63 aa Miller 8429..8617
Insert 8374..8420
Insert 8307..8373
Insert 8206..8306
Insert 8116..8205
Insert 8017..8115
Insert 7675..8373
Insert 7921..8016
Insert 7828..7920
Insert 7731..7827
Insert 7675..7730
Insert 4857..10413
Insert 7096..7674
Insert 6997..7095
Insert 6901..6996
Insert 6637..7095
Insert 6808..6900
Insert 6711..6807
Insert 6637..6710
356 N-term 6227..6634
CACC-TATG 6226..6226
GR Rezeptor R/RobM 6229..6205
GR Rezeptor 5393..6223
Omega leader 5319..5380
Right Border 42..13
ORI 165..165
A to G (BpiI removed) 1236..1236
Kan (no BpiI) 1718..927
dTALE-AD D
10442 bp
pVS1ori short 4688..1904
LB 4690..4837
35S pro short (no BsaI and BpiI) 4873..5302

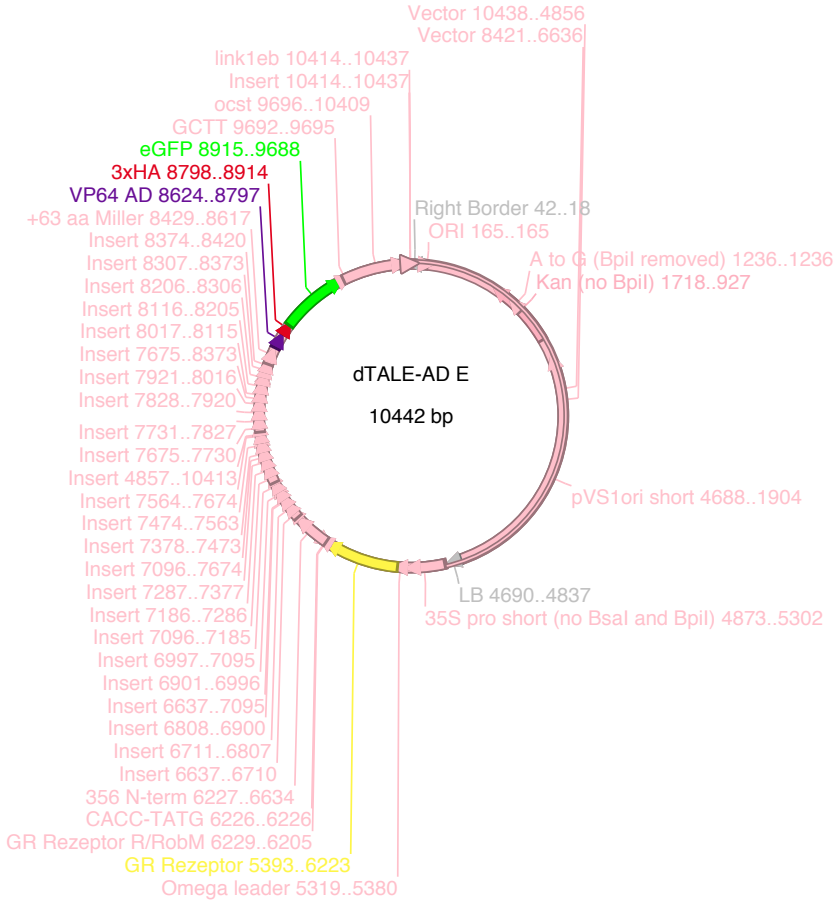
Vector 10438..4856
Vector 8421..6636
link1eb 10414..10437
Insert 10414..10437
ocst 9696..10409
GCTT 9692..9695
eGFP 8915..9688
3xHA 8798..8914
VP64 AD 8624..8797
+63 aa Miller 8429..8617
Insert 8374..8420
Insert 8307..8373
Insert 8206..8306
Insert 8116..8205
Insert 8017..8115
Insert 7675..8373
Insert 7921..8016
Insert 7828..7920
Insert 7731..7827
Insert 7675..7730
Insert 4857..10413
Insert 7564..7674
Insert 7474..7563
Insert 7378..7473
Insert 7096..7674
Insert 7287..7377
Insert 7186..7286
Insert 7096..7185
Insert 6997..7095
Insert 6901..6996
Insert 6637..7095
Insert 6808..6900
Insert 6711..6807
Insert 6637..6710
356 N-term 6227..6634
CACC-TATG 6226..6226
GR Rezeptor R/RobM 6229..6205
GR Rezeptor 5393..6223
Omega leader 5319..5380
Right Border 42..18
ORI 165..165
A to G (BpiI removed) 1236..1236
Kan (no BpiI) 1718..927
pVS1ori short 4688..1904
LB 4690..4837
35S pro short (no BsaI and BpiI) 4873..5302
dTALE-AD E
10442 bp

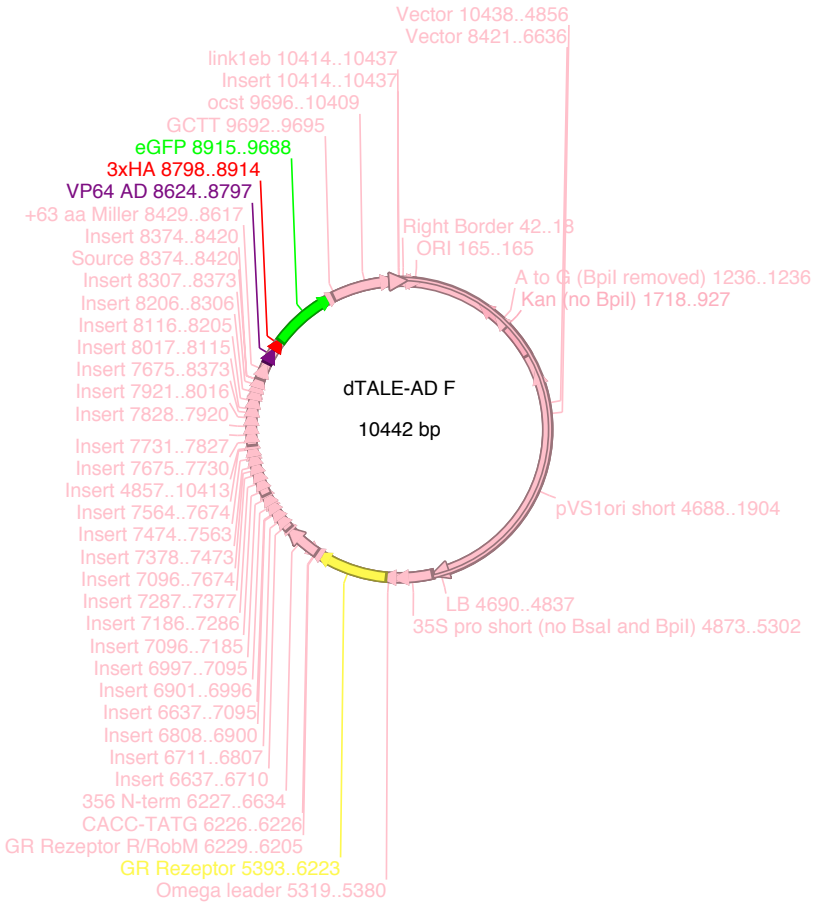
Vector 10438..4856
Vector 8421..6636
link1eb 10414..10437
Insert 10414..10437
ocst 9696..10409
GCTT 9692..9695
eGFP 8915..9688
3xHA 8798..8914
VP64 AD 8624..8797
+63 aa Miller 8429..8617
Insert 8374..8420
Source 8374..8420
Insert 8307..8373
Insert 8206..8306
Insert 8116..8205
Insert 8017..8115
Insert 7675..8373
Insert 7921..8016
Insert 7828..7920
Insert 7731..7827
Insert 7675..7730
Insert 4857..10413
Insert 7564..7674
Insert 7474..7563
Insert 7378..7473
Insert 7096..7674
Insert 7287..7377
Insert 7186..7286
Insert 7096..7185
Insert 6997..7095
Insert 6901..6996
Insert 6637..7095
Insert 6808..6900
Insert 6711..6807
Insert 6637..6710
356 N-term 6227..6634
CACC-TATG 6226..6226
GR Rezeptor R/RobM 6229..6205
GR Rezeptor 5393..6223
Omega leader 5319..5380
Right Border 42..18
ORI 165..165
A to G (BpiI removed) 1236..1236
Kan (no BpiI) 1718..927
pVS1ori short 4688..1904
LB 4690..4837
35S pro short (no BsaI and BpiI) 4873..5302
dTALE-AD F
10442 bp

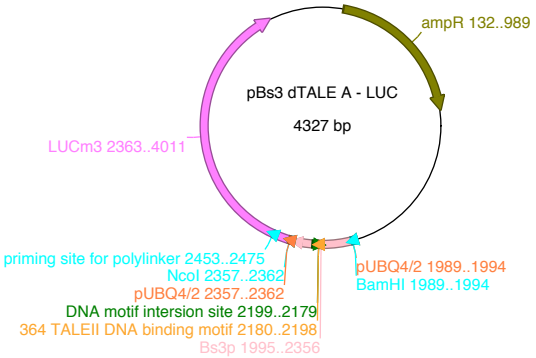
ampR 132..989
pBs3 dTALE A - LUC
4327 bp
LUCm3 2363..4011
priming site for polylinker 2453..2475
NcoI 2357..2362
pUBQ4/2 2357..2362
DNA motif intersion site 2199..2179
364 TALEII DNA binding motif 2180..2198
Bs3p 1995..2356
pUBQ4/2 1989..1994
BamHI 1989..1994

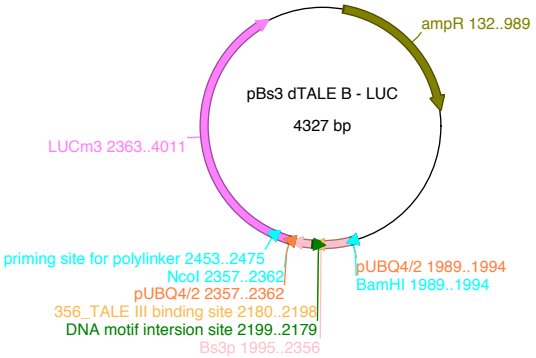
ampR 132..989
pBs3 dTALE B - LUC
4327 bp
LUCm3 2363..4011
priming site for polylinker 2453..2475
NcoI 2357..2362
pUBQ4/2 2357..2362
356_TALE III binding site 2180..2198
DNA motif intersion site 2199..2179
Bs3p 1995..2356
pUBQ4/2 1989..1994
BamHI 1989..1994

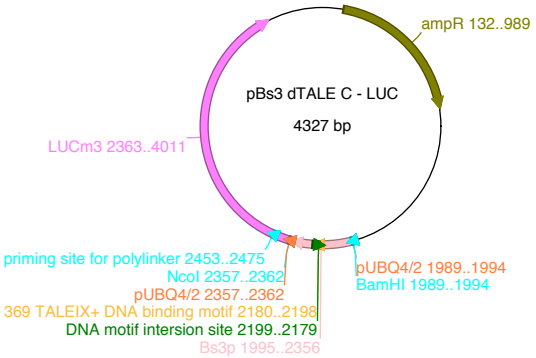
ampR 132..989
pBs3 dTALE C - LUC
4327 bp
LUCm3 2363..4011
priming site for polylinker 2453..2475
NcoI 2357..2362
pUBQ4/2 2357..2362
369 TALEIX+ DNA binding motif 2180..2198
DNA motif intersion site 2199..2179
Bs3p 1995..2356
pUBQ4/2 1989..1994
BamHI 1989..1994

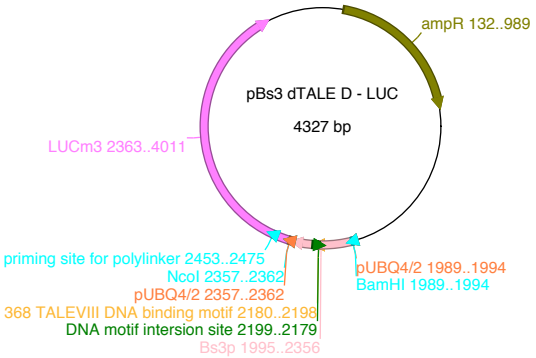
ampR 132..989
pBs3 dTALE D - LUC
4327 bp
LUCm3 2363..4011
priming site for polylinker 2453..2475
NcoI 2357..2362
pUBQ4/2 2357..2362
368 TALEVIII DNA binding motif 2180..2198
DNA motif intersion site 2199..2179
Bs3p 1995..2356
pUBQ4/2 1989..1994
BamHI 1989..1994

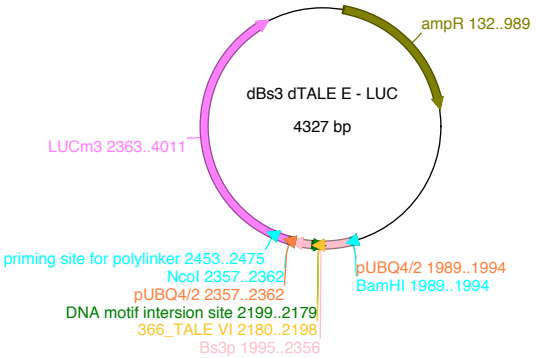
ampR 132..989
dBs3 dTALE E - LUC
4327 bp
LUCm3 2363..4011
priming site for polylinker 2453..2475
NcoI 2357..2362
pUBQ4/2 2357..2362
DNA motif intersion site 2199..2179
366_TALE VI 2180..2198
Bs3p 1995..2356
pUBQ4/2 1989..1994
BamHI 1989..1994

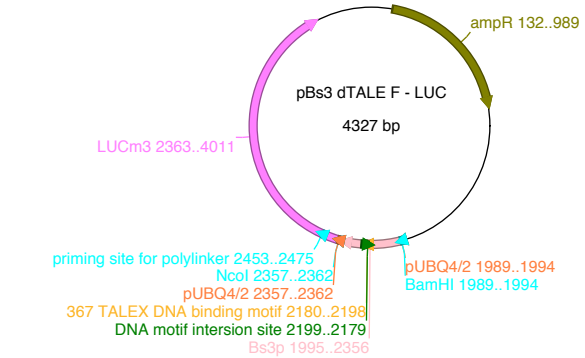
ampR 132..989
pBs3 dTALE F - LUC
4327 bp
LUCm3 2363..4011
priming site for polylinker 2453..2475
NcoI 2357..2362
pUBQ4/2 2357..2362
367 TALEX DNA binding motif 2180..2198
DNA motif intersion site 2199..2179
Bs3p 1995..2356
pUBQ4/2 1989..1994
BamHI 1989..1994

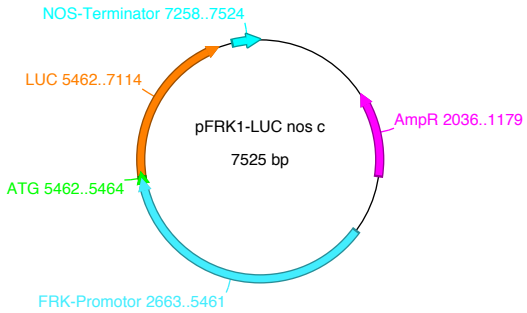
NOS-Terminator 7258..7524
LUC 5462..7114
pFRK1-LUC nos c
7525 bp
AmpR 2036..1179
ATG 5462..5464
FRK-Promotor 2663..5461

11.3. Supplementary tables

Supplementary table 1: Predicted transcription factor binding sites in *pFRK1*

Position	Matrix ID	Family	Strand	Similar Score	Hit Sequence	TF ID or Motif name
2	TF_motif_seq_0341	(Motif sequence only)	-	1	TGGTTa	MYB1AT
2	TF_motif_seq_0366	(Motif sequence only)	-	1	tgGTTAG	MYBATRD22
4	TF_motif_seq_0267	Trihelix	+	0.8	GTTAG	AT5G01380
4	TF_motif_seq_0373	(Motif sequence only)	+	0.86	GTTAGtg	MYB1LEPR
6	TFmatrixID_0283	Homeodomain;HD-ZIP	+	0.96	tagTGATTgc	AT2G22800;AT2G44910;AT4G16780;AT4G37790;AT5G06710;AT5G47370
6	TFmatrixID_0284	Homeodomain;HD-ZIP	+	0.93	tagTGATTgc	AT2G46680
8	TFmatrixID_0286	Homeodomain;HD-ZIP	+	0.99	gTGATTgc	AT2G22800;AT3G60390;AT4G16780;AT4G37790;AT5G06710;AT5G47370
8	TFmatrixID_0299	Homeodomain;WOX	+	0.98	gTGATTgc	AT1G20700;AT1G20710
8	TF_motif_seq_0435	(Motif sequence only)	+	0.75	GTGATtgc	PIATGAPB
9	TF_motif_seq_0237	GATA;tify	+	1	TGATT	AT1G51600;AT2G45050;AT3G06740;AT3G16870;AT3G21175;AT3G24050;AT3G54810;AT3G60530;AT4G17570;AT4G24470;AT4G26150;AT4G32890;AT4G34680;AT5G25830;AT5G26930;AT5G56860;AT5G66320;AT2G18380;AT3G50870;AT4G36620
9	TF_motif_seq_0268	(Motif sequence only)	+	1	TGATT	ARR1AT
11	TF_motif_seq_0257	NF-YB;NF-YA;NF-YC	-	0.8	ATTGC	AT1G09030;AT1G17590;AT1G21970;AT1G30500;AT1G54160;AT1G54830;AT1G56170;AT1G72830;AT2G38880;AT2G47810;AT3G05690;AT3G14020;AT3G20910;AT3G53340;AT4G14540;AT5G06510;AT5G12840;AT5G27910;AT5G38140;AT5G47640;AT5G47670;AT5G50470;AT5G50480
15	TF_motif_seq_0249	(Motif sequence only)	-	0.8	CAGGT	ABRELATERD1
18	TF_motif_seq_0257	NF-YB;NF-YA;NF-YC	-	0.8	GTTGG	AT1G09030;AT1G17590;AT1G21970;AT1G30500;AT1G54160;AT1G54830;AT1G56170;AT1G72830;AT2G38880;AT2G47810;AT3G05690;AT3G14020;AT3G20910;AT3G53340;AT4G14540;AT5G06510;AT5G12840;AT5G27910;AT5G38140;AT5G47640;AT5G47670;AT5G50470;AT5G50480
18	TF_motif_seq_0258	Dehydrin	-	0.8	GTTGG	U01377
18	TF_motif_seq_0455	(Motif sequence only)	-	0.75	gttGGAAA	E2FANTRNR
23	TF_motif_seq_0239	Dof	+	1	AAAGA	AT1G29160;AT1G64620;AT2G37590;AT3G21270;AT3G45610;AT3G47500;AT4G38000;AT5G39660;AT5G60200;AT5G60850;AT5G62940;AT2G46590;AT1G07640;AT1G21340;AT1G26790;AT1G47655;AT1G51700;AT1G69570;AT2G28510;AT2G28810;AT2G34140;AT3G50410;AT3G55370;AT3G61850;AT4G00940;AT4G21050;AT4G21080;AT4G24060;AT5G02460;AT5G62430;AT5G65590;AT5G66940
24	TF_motif_seq_0254	AP2;ERF	-	0.8	AAGAT	AT3G14230
25	TF_motif_seq_0237	GATA;tify	+	1	AGATT	AT1G51600;AT2G45050;AT3G06740;AT3G16870;AT3G21175;AT3G24050;AT3G54810;AT3G60530;AT4G17570;AT4G24470;AT4G26150;AT4G32890;AT4G34680;AT5G25830;AT5G26930;AT5G56860;AT5G66320;AT2G18380;AT3G50870;AT4G36620
25	TF_motif_seq_0252	Myb/SANT;MYB;ARR-B	+	1	AGATT	AT2G01760;AT3G16857;AT4G16110;AT4G18020;AT4G31920;AT5G58080;AT1G67710;AT1G49190;AT2G25180;AT5G49240
25	TF_motif_seq_0268	(Motif sequence only)	+	1	AGATT	ARR1AT
27	TF_motif_seq_0254	AP2;ERF	+	0.8	ATTTA	AT3G14230
28	TF_motif_seq_0267	Trihelix	+	0.8	TTTAC	AT5G01380
28	TF_motif_seq_0319	Trihelix	-	1	tTTACC	AT1G33240
28	TF_motif_seq_0275	(Motif sequence only)	+	0.8	TTTAC	WBOXATNPR1
28	TF_motif_seq_0321	(Motif sequence only)	-	1	tTTACC	GT1CONSENSUS
31	TF_motif_seq_0239	Dof	-	1	ACCTT	AT1G29160;AT1G64620;AT2G37590;AT3G21270;AT3G45610;AT3G47500;AT4G38000;AT5G39660;AT5G60200;AT5G60850;AT5G62940;AT2G46590;AT1G07640;AT1G21340;AT1G26790;AT1G47655;AT1G51700;AT1G69570;AT2G28510;AT2G28810;AT2G34140;AT3G50410;AT3G55370;AT3G61850;AT4G00940;AT4G21050;AT4G21080;AT4G24060;AT5G02460;AT5G62430;AT5G65590;AT5G66940
34	TF_motif_seq_0254	AP2;ERF	+	0.8	TTCTA	AT3G14230
37	TF_motif_seq_0254	AP2;ERF	-	0.8	TAGAC	AT3G14230
37	TF_motif_seq_0261	(Motif sequence only)	+	0.8	TAGAC	SURECOREATSULTR11
37	TF_motif_s	(Motif sequence only)	+	0.8	TAGAC	WBOXATNPR1

	eq_0275					
38	TFmatrixID_0188	bZIP	-	0.96	agacCTGTCt	AT1G06070;AT2G31370;AT2G40620
38	TFmatrixID_0193	bZIP	-	0.75	agaCCTGT	AT3G19290;AT4G34000
40	TF_motif_seq_0249	(Motif sequence only)	+	0.8	ACCTG	ABRELATERD1
44	TF_motif_seq_0261	(Motif sequence only)	-	0.8	GTCTT	SURECOREATSULTR11
45	TF_motif_seq_0508	SBP	-	0.75	tcTTACGaa	AT1G20980;AT1G27360;AT1G27370;AT1G53160;AT1G69170;AT1G76580;AT2G33810;AT2G42200;AT2G47070;AT3G15270;AT3G57920;AT3G60030;AT5G18830;AT5G43270
46	TF_motif_seq_0267	Trihelix	+	0.8	CTTAC	AT5G01380
47	TF_motif_seq_0271	bZIP	+	0.8	TTACG	AT1G77920;AT3G12250;AT5G06950;AT5G06960;AT5G10030;AT5G65210;AT1G22070
53	TF_motif_seq_0254	AP2;ERF	+	0.8	AGCTA	AT3G14230
61	TF_motif_seq_0254	AP2;ERF	+	0.8	TTCTA	AT3G14230
64	TFmatrixID_0384	NAC;NAM	-	0.89	taaAGTAAt	AT1G33060;AT3G49530;AT4G35580;AT5G24590
65	TF_motif_seq_0239	Dof	+	1	AAAGT	AT1G29160;AT1G64620;AT2G37590;AT3G21270;AT3G45610;AT3G47500;AT4G38000;AT5G39660;AT5G60200;AT5G60850;AT5G62940;AT2G46590;AT1G07640;AT1G21340;AT1G26790;AT1G47655;AT1G51700;AT1G69570;AT2G28510;AT2G28810;AT2G34140;AT3G50410;AT3G55370;AT3G61850;AT4G00940;AT4G21050;AT4G21080;AT4G24060;AT5G02460;AT5G62430;AT5G65590;AT5G66940
66	TFmatrixID_0349	Myb/SANT;ARR-B	+	0.99	aagtAATCTt	AT4G18020
68	TF_motif_seq_0241	ZF-HD	-	1	GTAAT	AT1G75240
68	TF_motif_seq_0267	Trihelix	-	0.8	GTAAT	AT5G01380
70	TF_motif_seq_0237	GATA;tify	-	1	AATCT	AT1G51600;AT2G45050;AT3G06740;AT3G16870;AT3G21175;AT3G24050;AT3G54810;AT3G60530;AT4G17570;AT4G24470;AT4G26150;AT4G32890;AT4G34680;AT5G25830;AT5G26930;AT5G56860;AT5G66320;AT2G18380;AT3G50870;AT4G36620
70	TF_motif_seq_0252	Myb/SANT;MYB;ARR-B	-	1	AATCT	AT2G01760;AT3G16857;AT4G16110;AT4G18020;AT4G31920;AT5G58080;AT1G67710;AT1G49190;AT2G25180;AT5G49240
70	TF_motif_seq_0268	(Motif sequence only)	-	1	AATCT	ARR1AT
71	TF_motif_seq_0254	AP2;ERF	+	0.8	ATCTT	AT3G14230
73	TF_motif_seq_0271	bZIP	-	0.8	CTTCA	AT1G77920;AT3G12250;AT5G06950;AT5G06960;AT5G10030;AT5G65210;AT1G22070
80	TF_motif_seq_0248	(Motif sequence only)	+	0.8	AACCG	MYBCOREATCYCB1
82	TF_motif_seq_0258	Dehydrin	+	0.8	CCGAA	U01377
83	TF_motif_seq_0257	NF-YB;NF-YA;NF-YC	+	0.8	CGAAT	AT1G09030;AT1G17590;AT1G21970;AT1G30500;AT1G54160;AT1G54830;AT1G56170;AT1G72830;AT2G38880;AT2G47810;AT3G05690;AT3G14020;AT3G20910;AT3G53340;AT4G14540;AT5G06510;AT5G12840;AT5G27910;AT5G38140;AT5G47640;AT5G47670;AT5G50470;AT5G50480
89	TFmatrixID_0503	MADS box;MIKC	+	0.92	cagaaacaaaaaaAGAAAagg	AT4G22950;AT5G10140;AT5G65050;AT5G65060;AT5G65070;AT5G65080;AT1G77080;AT2G45650;AT3G57390;AT4G11880
91	TFmatrixID_0134	AT-Hook	+	0.98	gaaacAAAAA	AT4G21895;AT5G62260
91	TF_motif_seq_0267	Trihelix	-	0.8	GAAAC	AT5G01380
91	TF_motif_seq_0261	(Motif sequence only)	+	0.8	GAAAC	SURECOREATSULTR11
92	TFmatrixID_0274	MADS box;MIKC	-	0.88	aaacAAAAAaagaaaaggagt	AT2G45660
92	TFmatrixID_0499	MADS box;MIKC	+	0.88	aaacAAAAAaagaaaaggagt	AT4G22950;AT4G24540;AT4G37940;AT5G51860;AT5G51870;AT5G60910;AT5G62165;AT1G26310;AT2G14210;AT2G22630;AT2G45650;AT2G45660;AT3G30260;AT3G57230;AT3G57390;AT3G61120;AT4G09960;AT4G11880
92	TFmatrixID_0501	MADS box;MIKC	+	0.87	aaaCAAAAAaagaaa	AT5G51870;AT2G45650;AT3G54340
92	TF_motif_seq_0343	(Motif sequence only)	+	1	AAACAaa	ANAERO1CONSENSUS
94	TFmatrixID_0508	MADS box;MIKC	+	0.9	aCAAAAaaaga	AT4G22950;AT4G24540;AT5G51860;AT5G60910;AT5G62165;AT1G24260;AT1G26310;AT2G45650;AT3G30260;AT3G57230;AT3G57390;AT3G61120;AT4G09960;AT4G11880
94	TF_motif_seq_0404	(Motif sequence only)	+	0.88	ACAAAaaa	XYLAT
100	TF_motif_seq_0239	Dof	+	1	AAAGA	AT1G29160;AT1G64620;AT2G37590;AT3G21270;AT3G45610;AT3G47500;AT4G38000;AT5G39660;AT5G60200;AT5G60850;AT5G62940;AT2G46590;AT1G07640;AT1G21340;AT1G26790;AT1G47655;AT1G51700;AT1G69570;AT2G28510;AT2G28810;AT2G34140;AT3G50410;AT3G55370;AT3G61850;AT4G00940;AT4G21050;AT4G21080;AT4G24060;AT5G02460;AT5G62430;AT5G65590;AT5G66940
105	TF_motif_s	Dof	+	1	AAAGG	AT1G29160;AT1G64620;AT2G37590;AT3G21270;AT3G45610;AT3G47500;AT4G38000;AT5G39660;AT5G60200;AT5G60850;AT5G62940;AT2G46590;AT1G07640;AT1G21340;AT1G26790;AT1G47655;AT1G51700;AT1G69570;AT2G28510;AT2G28810;AT2G34140;AT3G50410;AT3G55370;AT3G61850;AT4G00940;AT4G21050;AT4G21080;AT4G24060;AT5G02460;AT5G62430;AT5G65590;AT5G66940

	eq_0239					
105	TF_motif_seq_0248	(Motif sequence only)	+	0.8	AAAGG	MYBCOREATCYCB1
106	TF_motif_seq_0239	Dof	+	1	AAGGA	AT1G29160;AT1G64620;AT2G37590;AT3G21270;AT3G45610;AT3G47500;AT4G38000;AT5G39660;AT5G60200;AT5G60850;AT5G62940;AT2G46590;AT1G07640;AT1G21340;AT1G26790;AT1G47655;AT1G51700;AT1G69570;AT2G28510;AT2G28810;AT2G34140;AT3G50410;AT3G55370;AT3G61850;AT4G00940;AT4G21050;AT4G21080;AT4G24060;AT5G02460;AT5G62430;AT5G65590;AT5G66940
109	TF_motif_seq_0261	(Motif sequence only)	+	0.8	GAGTC	SURECOREATSULTR11
111	TF_motif_seq_0275	(Motif sequence only)	-	0.8	GTCCA	WBOXATNPR1
113	TFmatrixID_0508	MADS box;MIKC	+	0.89	cCAAAAttgta	AT4G22950;AT4G24540;AT5G51860;AT5G60910;AT5G62165;AT1G24260;AT1G26310;AT2G45650;AT3G30260;AT3G57230;AT3G57390;AT3G61120;AT4G09960;AT4G11880
113	TF_motif_seq_0257	NF-YB;NF-YA;NF-YC	+	0.8	CCAAA	AT1G09030;AT1G17590;AT1G21970;AT1G30500;AT1G54160;AT1G54830;AT1G56170;AT1G72830;AT2G38880;AT2G47810;AT3G05690;AT3G14020;AT3G20910;AT3G53340;AT4G14540;AT5G06510;AT5G12840;AT5G27910;AT5G38140;AT5G47640;AT5G47670;AT5G50470;AT5G50480
118	TF_motif_seq_0257	NF-YB;NF-YA;NF-YC	-	0.8	ATTGT	AT1G09030;AT1G17590;AT1G21970;AT1G30500;AT1G54160;AT1G54830;AT1G56170;AT1G72830;AT2G38880;AT2G47810;AT3G05690;AT3G14020;AT3G20910;AT3G53340;AT4G14540;AT5G06510;AT5G12840;AT5G27910;AT5G38140;AT5G47640;AT5G47670;AT5G50470;AT5G50480
119	TF_motif_seq_0508	SBP	-	0.75	ttGTATGat	AT1G20980;AT1G27360;AT1G27370;AT1G53160;AT1G69170;AT1G76580;AT2G33810;AT2G42200;AT2G47070;AT3G15270;AT3G57920;AT3G60030;AT5G18830;AT5G43270
122	TFmatrixID_0262	GATA	+	1	taTGATCat	AT3G06740;AT3G16870;AT4G16141;AT4G26150;AT5G26930;AT5G49300;AT5G56860
123	TFmatrixID_0262	GATA	-	1	atGATCAta	AT3G06740;AT3G16870;AT4G16141;AT4G26150;AT5G26930;AT5G49300;AT5G56860
124	TF_motif_seq_0237	GATA;tify	+	1	TGATC	AT1G51600;AT2G45050;AT3G06740;AT3G16870;AT3G21175;AT3G24050;AT3G54810;AT3G60530;AT4G17570;AT4G24470;AT4G26150;AT4G32890;AT4G34680;AT5G25830;AT5G26930;AT5G56860;AT5G66320;AT2G18380;AT3G50870;AT4G36620
125	TF_motif_seq_0237	GATA;tify	-	1	GATCA	AT1G51600;AT2G45050;AT3G06740;AT3G16870;AT3G21175;AT3G24050;AT3G54810;AT3G60530;AT4G17570;AT4G24470;AT4G26150;AT4G32890;AT4G34680;AT5G25830;AT5G26930;AT5G56860;AT5G66320;AT2G18380;AT3G50870;AT4G36620
130	TFmatrixID_0290	Homeodomain;HD-ZIP	-	0.98	tacATTAAta	AT1G05230;AT1G17920;AT2G32370;AT3G61150;AT4G21750;AT5G46880
130	TF_motif_seq_0254	AP2;ERF	-	0.8	TACAT	AT3G14230
131	TFmatrixID_0280	Homeodomain;HD-ZIP	-	0.95	acATTAAtat	AT1G05230;AT1G17920;AT1G73360;AT1G79840;AT3G03260;AT3G61150;AT5G46880
131	TFmatrixID_0288	Homeodomain;HD-ZIP	+	0.95	acaTTAATatc	AT1G05230;AT1G17920;AT3G61150;AT4G00730;AT5G46880
132	TFmatrixID_0144	AT-Hook	-	0.98	catTAATAtcag	AT4G21895;AT5G62260
133	TF_motif_seq_0241	ZF-HD	+	1	ATTAA	AT1G75240
134	TFmatrixID_0334	Myb/SANT;MYB-related	+	0.97	ttaATATCa	AT1G18330;AT3G10113
134	TF_motif_seq_0241	ZF-HD	-	1	TTAAT	AT1G75240
135	TFmatrixID_0320	Myb/SANT;MYB-related	-	0.86	taATATCag	AT1G01520;AT3G09600;AT4G01280;AT5G02840;AT5G52660
135	TFmatrixID_0610	MYB-related	+	0.95	taATATCaga	AT5G17300
137	TF_motif_seq_0243	GATA;tify	-	1	ATATC	AT1G51600;AT2G45050;AT3G06740;AT3G16870;AT3G21175;AT3G24050;AT3G54810;AT3G60530;AT4G17570;AT4G24470;AT4G26150;AT4G32890;AT4G34680;AT5G25830;AT5G26930;AT5G56860;AT5G66320;AT2G18380;AT3G50870;AT4G36620
138	TF_motif_seq_0237	GATA;tify	-	1	TATCA	AT1G51600;AT2G45050;AT3G06740;AT3G16870;AT3G21175;AT3G24050;AT3G54810;AT3G60530;AT4G17570;AT4G24470;AT4G26150;AT4G32890;AT4G34680;AT5G25830;AT5G26930;AT5G56860;AT5G66320;AT2G18380;AT3G50870;AT4G36620
141	TFmatrixID_0050	Myb/SANT;MYB;G2-like	-	0.92	caGAATAgtc	AT5G42630
142	TFmatrixID_0049	Myb/SANT;MYB;G2-like	+	0.88	aGAATAgtct	AT5G42630
142	TF_motif_seq_0010	HSF	+	0.88	AGAATagtct	AT3G24520;AT1G32330;AT1G46264;AT1G67970;AT2G26150;AT2G41690;AT3G02990;AT3G22830;AT3G51910;AT3G63350;AT4G11660;AT4G13980;AT4G17750;AT4G18880;AT5G03720;AT5G16820;AT5G43840;AT5G45710;AT5G54070;AT5G62020
143	TF_motif_seq_0434	(Motif sequence only)	+	0.83	GAATAgtc	P1BS
148	TFmatrixID_0638	Dof	-	0.99	gtcTCTTTtg	AT5G65590
148	TF_motif_seq_0261	(Motif sequence only)	-	1	GTCTC	SURECOREATSULTR11
151	TF_motif_seq_0239	Dof	-	1	TCTTT	AT1G29160;AT1G64620;AT2G37590;AT3G21270;AT3G45610;AT3G47500;AT4G38000;AT5G39660;AT5G60200;AT5G60850;AT5G62940;AT2G46590;AT1G07640;AT1G21340;AT1G26790;AT1G47655;AT1G51700;AT1G69570;AT2G28510;AT2G28810;AT2G34140;AT3G50410;AT3G55370;AT3G61850;AT4G00940;AT4G21050;AT4G21080;AT4G24060;AT5G02460;AT5G62430;AT5G65590;AT5G66940
154	TF_motif_seq_0377	(Motif sequence only)	-	1	ttTGTTA	GAREAT
157	TF_motif_seq_0267	Trihelix	+	0.8	GTTAA	AT5G01380
157	TF_motif_s	(Motif sequence only)	-	0.8	GTTAA	WBOXATNPR1

	eq_0275					
159	TF_motif_seq_0254	AP2;ERF	-	0.8	TAAAT	AT3G14230
160	TFmatrixID_0009	AT-Hook	-	0.98	aAATAAatat	AT4G35390
160	TFmatrixID_0142	AT-Hook	+	1	AAATAaat	AT4G21895;AT5G62260
161	TFmatrixID_0571	TBP	+	0.96	aATAAAta	AT1G55520;AT3G13445
163	TFmatrixID_0029	MYB-related	+	0.98	taaATATCtg	AT2G46830
163	TFmatrixID_0334	Myb/SANT;MYB-related	+	1	taaATATCt	AT1G18330;AT3G10113
163	TFmatrixID_0609	MYB-related	+	0.98	taaATATCtg	AT5G17300
163	TF_motif_seq_0254	AP2;ERF	-	0.8	TAAAT	AT3G14230
164	TFmatrixID_0320	Myb/SANT;MYB-related	-	1	aaATATCtg	AT1G01520;AT3G09600;AT4G01280;AT5G02840;AT5G52660
164	TFmatrixID_0364	Myb/SANT;MYB-related	+	1	aaATATCt	AT3G09600;AT4G01280
164	TFmatrixID_0369	Myb/SANT;MYB-related	+	1	aaATATCtg	AT1G01060;AT5G37260
164	TFmatrixID_0610	MYB-related	+	0.96	aaATATCtga	AT5G17300
166	TF_motif_seq_0243	GATA;tify	-	1	ATATC	AT1G51600;AT2G45050;AT3G06740;AT3G16870;AT3G21175;AT3G24050;AT3G54810;AT3G60530;AT4G17570;AT4G24470;AT4G26150;AT4G32890;AT4G34680;AT5G25830;AT5G26930;AT5G56860;AT5G66320;AT2G18380;AT3G50870;AT4G36620
167	TF_motif_seq_0237	GATA;tify	-	1	TATCT	AT1G51600;AT2G45050;AT3G06740;AT3G16870;AT3G21175;AT3G24050;AT3G54810;AT3G60530;AT4G17570;AT4G24470;AT4G26150;AT4G32890;AT4G34680;AT5G25830;AT5G26930;AT5G56860;AT5G66320;AT2G18380;AT3G50870;AT4G36620
168	TF_motif_seq_0254	AP2;ERF	+	0.8	ATCTG	AT3G14230
169	TFmatrixID_0491	TBP	+	0.94	tctgaagaaTATATatctctt	AT1G55520;AT3G13445
169	TFmatrixID_0572	TBP	+	0.94	tctgaagaaTATATatctctt	AT1G55520;AT3G13445
170	TF_motif_seq_0069	(Motif sequence only)	+	0.82	CTGAAgaatat	TL1ATSAR
171	TF_motif_seq_0271	bZIP	+	0.8	TGAAG	AT1G77920;AT3G12250;AT5G06950;AT5G06960;AT5G10030;AT5G65210;AT1G22070
172	TFmatrixID_0491	TBP	-	0.97	gaagaatATATAtctctttga	AT1G55520;AT3G13445
172	TFmatrixID_0572	TBP	-	0.97	gaagaatATATAtctctttga	AT1G55520;AT3G13445
173	TF_motif_seq_0281	bZIP	+	1	AAGAAt	AT1G68640
174	TFmatrixID_0048	Myb/SANT;MYB;G2-like	-	0.99	aGAATAtata	AT5G16560
175	TF_motif_seq_0434	(Motif sequence only)	+	0.83	GAATAtat	P1BS
176	TFmatrixID_0003	AT-Hook	+	0.98	aATATAtatc	AT1G63480
176	TFmatrixID_0003	AT-Hook	-	0.99	aataTATAtc	AT1G63480
176	TFmatrixID_0419	TBP	+	1	aaTATAT	AT1G55520;AT3G13445
177	TF_motif_seq_0254	AP2;ERF	+	0.8	ATATA	AT3G14230
178	TFmatrixID_0030	MYB-related	-	0.99	tataTATCtc	AT2G46830
178	TFmatrixID_0334	Myb/SANT;MYB-related	+	0.95	tatATATCt	AT1G18330;AT3G10113
178	TF_motif_seq_0254	AP2;ERF	-	0.8	TATAT	AT3G14230
179	TFmatrixID_0369	Myb/SANT;MYB-related	+	0.98	atATATCtc	AT1G01060;AT5G37260
179	TF_motif_seq_0254	AP2;ERF	+	0.8	ATATA	AT3G14230
180	TF_motif_s	AP2;ERF	-	0.8	TATAT	AT3G14230

	eq_0254					
181	TF_motif_seq_0243	GATA;tify	-	1	ATATC	AT1G51600;AT2G45050;AT3G06740;AT3G16870;AT3G21175;AT3G24050;AT3G54810;AT3G60530;AT4G17570;AT4G24470;AT4G26150;AT4G32890;AT4G34680;AT5G25830;AT5G26930;AT5G56860;AT5G66320;AT2G18380;AT3G50870;AT4G36620
182	TF_motif_seq_0237	GATA;tify	-	1	TATCT	AT1G51600;AT2G45050;AT3G06740;AT3G16870;AT3G21175;AT3G24050;AT3G54810;AT3G60530;AT4G17570;AT4G24470;AT4G26150;AT4G32890;AT4G34680;AT5G25830;AT5G26930;AT5G56860;AT5G66320;AT2G18380;AT3G50870;AT4G36620
183	TF_motif_seq_0254	AP2;ERF	+	0.8	ATCTC	AT3G14230
183	TF_motif_seq_0261	(Motif sequence only)	-	0.8	ATCTC	SURECOREATSULTR11
186	TF_motif_seq_0239	Dof	-	1	TCTTT	AT1G29160;AT1G64620;AT2G37590;AT3G21270;AT3G45610;AT3G47500;AT4G38000;AT5G39660;AT5G60200;AT5G60850;AT5G62940;AT2G46590;AT1G07640;AT1G21340;AT1G26790;AT1G47655;AT1G51700;AT1G69570;AT2G28510;AT2G28810;AT2G34140;AT3G50410;AT3G55370;AT3G61850;AT4G00940;AT4G21050;AT4G21080;AT4G24060;AT5G02460;AT5G62430;AT5G65590;AT5G66940
188	TF_motif_seq_0399	(Motif sequence only)	+	0.84	TTTGAtt	WBBOXPCWRKY1
189	TF_motif_seq_0254	AP2;ERF	-	0.8	TTGAT	AT3G14230
189	TF_motif_seq_0275	(Motif sequence only)	+	0.8	TTGAT	WBOXATNPR1
190	TF_motif_seq_0237	GATA;tify	+	1	TGATT	AT1G51600;AT2G45050;AT3G06740;AT3G16870;AT3G21175;AT3G24050;AT3G54810;AT3G60530;AT4G17570;AT4G24470;AT4G26150;AT4G32890;AT4G34680;AT5G25830;AT5G26930;AT5G56860;AT5G66320;AT2G18380;AT3G50870;AT4G36620
190	TF_motif_seq_0268	(Motif sequence only)	+	1	TGATT	ARR1AT
192	TFmatrixID_0146	AT-Hook	-	1	ATTATttg	AT4G21895;AT5G62260
192	TFmatrixID_0154	AT-Hook	-	1	atTATTTt	AT4G21895;AT5G62260
192	TF_motif_seq_0241	ZF-HD	+	1	ATTAT	AT1G75240
193	TFmatrixID_0132	AT-Hook	-	1	TTATTttgt	AT4G21895;AT5G62260
200	TF_motif_seq_0263	(Motif sequence only)	-	0.8	GTGGA	SORLIP1AT
201	TF_motif_seq_0254	AP2;ERF	-	0.8	TGGAT	AT3G14230
202	TF_motif_seq_0237	GATA;tify	+	1	GGATG	AT1G51600;AT2G45050;AT3G06740;AT3G16870;AT3G21175;AT3G24050;AT3G54810;AT3G60530;AT4G17570;AT4G24470;AT4G26150;AT4G32890;AT4G34680;AT5G25830;AT5G26930;AT5G56860;AT5G66320;AT2G18380;AT3G50870;AT4G36620
204	TF_motif_seq_0263	(Motif sequence only)	-	0.8	ATGGC	SORLIP1AT
206	TF_motif_seq_0275	(Motif sequence only)	-	0.8	GGCAA	WBOXATNPR1
207	TF_motif_seq_0257	NF-YB;NF-YA;NF-YC	+	0.8	GCAAT	AT1G09030;AT1G17590;AT1G21970;AT1G30500;AT1G54160;AT1G54830;AT1G56170;AT1G72830;AT2G38880;AT2G47810;AT3G05690;AT3G14020;AT3G20910;AT3G53340;AT4G14540;AT5G06510;AT5G12840;AT5G27910;AT5G38140;AT5G47640;AT5G47670;AT5G50470;AT5G50480
212	TF_motif_seq_0267	Trihelix	-	0.8	GAAAC	AT5G01380
212	TF_motif_seq_0261	(Motif sequence only)	+	0.8	GAAAC	SURECOREATSULTR11
214	TFmatrixID_0491	TBP	+	0.96	aactaagaaTATATattcatt	AT1G55520;AT3G13445
214	TFmatrixID_0572	TBP	+	0.96	aactaagaaTATATattcatt	AT1G55520;AT3G13445
214	TF_motif_seq_0254	AP2;ERF	+	0.8	AACTA	AT3G14230
217	TFmatrixID_0491	TBP	-	0.95	taagaatATATAttcattgac	AT1G55520;AT3G13445
217	TFmatrixID_0572	TBP	-	0.95	taagaatATATAttcattgac	AT1G55520;AT3G13445
218	TF_motif_seq_0281	bZIP	+	1	AAGAAt	AT1G68640
219	TFmatrixID_0048	Myb/SANT;MYB;G2-like	-	0.99	aGAATAtata	AT5G16560
220	TF_motif_seq_0434	(Motif sequence only)	+	0.83	GAATAtat	P1BS
221	TFmatrixID_0003	AT-Hook	+	1	aATATAtatt	AT1G63480
221	TFmatrixID_0003	AT-Hook	-	1	aataTATAt	AT1G63480
221	TFmatrixID_0419	TBP	+	1	aaTATAT	AT1G55520;AT3G13445
222	TF_motif_s	AP2;ERF	+	0.8	ATATA	AT3G14230

	eq_0254					
223	TF_motif_seq_0254	AP2;ERF	-	0.8	TATAT	AT3G14230
224	TFmatrixID_0419	TBP	-	1	ATATAtt	AT1G55520;AT3G13445
224	TF_motif_seq_0254	AP2;ERF	+	0.8	ATATA	AT3G14230
224	TF_motif_seq_0434	(Motif sequence only)	-	0.83	ataTATTC	P1BS
225	TF_motif_seq_0254	AP2;ERF	-	0.8	TATAT	AT3G14230
230	TFmatrixID_0452	WRKY	-	0.99	tcaTTGACtt	AT1G18860;AT1G29280;AT1G29860;AT1G55600;AT1G62300;AT1G64000;AT1G66550;AT1G66560;AT1G68150;AT1G69810;AT2G21900;AT2G34830;AT2G40740;AT2G40750;AT2G44745;AT2G46130;AT2G46400;AT3G01970;AT3G04670;AT3G56400;AT3G58710;AT3G62340;AT4G00450;AT4G11070;AT4G18170;AT4G22070;AT4G23810;AT4G24240;AT4G39410;AT5G15130;AT5G22570;AT5G26170;AT5G28650;AT5G41570;AT5G43290;AT5G45050;AT5G45260
230	TFmatrixID_0455	WRKY	-	0.92	tcaTTGACtta	AT1G18860;AT1G29280;AT1G29860;AT1G55600;AT1G62300;AT1G64000;AT1G66550;AT1G66560;AT1G68150;AT1G69810;AT2G21900;AT2G34830;AT2G40740;AT2G44745;AT2G46400;AT3G01970;AT3G04670;AT3G56400;AT3G58710;AT3G62340;AT4G01720;AT4G04450;AT4G11070;AT4G18170;AT4G22070;AT4G23810;AT4G24240;AT4G39410;AT5G15130;AT5G26170;AT5G28650;AT5G41570;AT5G43290;AT5G45050;AT5G45260
230	TFmatrixID_0457	WRKY	-	0.97	tcaTTGACtt	AT1G18860;AT1G29280;AT1G29860;AT1G55600;AT1G62300;AT1G64000;AT1G66560;AT1G68150;AT1G69810;AT2G21900;AT2G34830;AT2G40740;AT2G44745;AT2G46400;AT3G01970;AT3G04670;AT3G56400;AT3G58710;AT3G62340;AT4G04450;AT4G11070;AT4G18170;AT4G22070;AT4G23810;AT4G24240;AT4G31550;AT4G39410;AT5G15130;AT5G22570;AT5G26170;AT5G28650;AT5G41570;AT5G43290;AT5G45050;AT5G45260
230	TF_motif_seq_0009	(Motif sequence only)	-	0.7	tcattGACTT	LS7ATPR1
231	TFmatrixID_0382	NAC;NAM	-	1	caTTGACtt	AT1G01720;AT1G52880;AT1G52890;AT1G69490;AT3G04070;AT3G15500;AT3G15510;AT4G27410
231	TFmatrixID_0444	WRKY	-	0.98	caTTGACtta	AT1G18860;AT1G29280;AT1G29860;AT1G55600;AT1G62300;AT1G64000;AT1G66550;AT1G66560;AT1G68150;AT1G69310;AT1G69810;AT1G80590;AT2G21900;AT2G34830;AT2G40740;AT2G44745;AT2G46400;AT3G01970;AT3G04670;AT3G56400;AT3G58710;AT3G62340;AT4G04450;AT4G11070;AT4G18170;AT4G22070;AT4G23810;AT4G24240;AT4G39410;AT5G15130;AT5G22570;AT5G26170;AT5G28650;AT5G41570;AT5G43290;AT5G45050
231	TFmatrixID_0453	WRKY	-	0.91	caTTGACt	AT1G18860;AT1G29280;AT1G29860;AT1G55600;AT1G62300;AT1G64000;AT1G66550;AT1G66560;AT1G68150;AT1G69810;AT1G80590;AT2G21900;AT2G34830;AT2G40740;AT2G40750;AT2G44745;AT2G46400;AT2G47260;AT3G01970;AT3G04670;AT3G56400;AT3G58710;AT3G62340;AT4G04450;AT4G11070;AT4G18170;AT4G22070;AT4G23810;AT4G24240;AT4G39410;AT5G15130;AT5G22570;AT5G26170;AT5G28650;AT5G41570;AT5G43290;AT5G45050
232	TFmatrixID_0445	WRKY	-	1	aTTGACtt	AT1G18860;AT1G29280;AT1G29860;AT1G55600;AT1G62300;AT1G64000;AT1G68150;AT1G69810;AT1G80840;AT2G21900;AT2G34830;AT2G44745;AT3G01970;AT3G04670;AT3G58710;AT3G62340;AT4G04450;AT4G18170;AT4G22070;AT4G24240;AT4G39410;AT5G15130;AT5G26170;AT5G28650;AT5G41570;AT5G43290;AT5G45050;AT5G45260
232	TF_motif_seq_0257	NF-YB;NF-YA;NF-YC	-	0.8	ATTGA	AT1G09030;AT1G17590;AT1G21970;AT1G30500;AT1G54160;AT1G54830;AT1G56170;AT1G72830;AT2G38880;AT2G47810;AT3G05690;AT3G14020;AT3G20910;AT3G53340;AT4G14540;AT5G06510;AT5G12840;AT5G27910;AT5G38140;AT5G47640;AT5G47670;AT5G50470;AT5G50480
233	TF_motif_seq_0339	WRKY	+	1	TTGACt	AT1G13960;AT1G18860;AT1G29280;AT1G29860;AT1G30650;AT1G55600;AT1G62300;AT1G64000;AT1G66550;AT1G68150;AT1G69310;AT1G69810;AT1G80590;AT1G80840;AT2G03340;AT2G23320;AT2G24570;AT2G25000;AT2G30250;AT2G30590;AT2G34830;AT2G37260;AT2G38470;AT2G40740;AT2G40750;AT2G44745;AT2G46130;AT2G46400;AT2G47260;AT3G01080;AT3G01970;AT3G04670;AT3G56400;AT3G58710;AT4G01250;AT4G01720;AT4G04450;AT4G12020;AT4G18170;AT4G22070;AT4G23810;AT4G24240;AT4G26440;AT4G26640;AT4G30935;AT4G31550;AT4G31800;AT4G39410;AT5G07100;AT5G13080;AT5G15130;AT5G22570;AT5G24110;AT5G28650;AT5G45050;AT5G45260;AT5G46350;AT5G49520;AT5G52830;AT5G56270
233	TF_motif_seq_0275	(Motif sequence only)	+	1	TTGAC	WBOXATNPR1
234	TF_motif_seq_0246	Homeodomain;TALE	+	1	TGACT	AT1G23380;AT1G62360;AT1G70510;AT4G08150
234	TF_motif_seq_0270	WRKY	+	1	TGACT	AT1G13960;AT1G18860;AT1G29280;AT1G29860;AT1G30650;AT1G55600;AT1G62300;AT1G64000;AT1G66550;AT1G68150;AT1G69310;AT1G69810;AT1G80590;AT1G80840;AT2G03340;AT2G23320;AT2G24570;AT2G25000;AT2G30250;AT2G30590;AT2G34830;AT2G37260;AT2G38470;AT2G40740;AT2G40750;AT2G44745;AT2G46130;AT2G46400;AT2G47260;AT3G01080;AT3G01970;AT3G04670;AT3G56400;AT3G58710;AT4G01250;AT4G01720;AT4G04450;AT4G12020;AT4G18170;AT4G22070;AT4G23810;AT4G24240;AT4G26440;AT4G26640;AT4G30935;AT4G31550;AT4G31800;AT4G39410;AT5G07100;AT5G13080;AT5G15130;AT5G22570;AT5G24110;AT5G28650;AT5G45050;AT5G45260;AT5G46350;AT5G49520;AT5G52830;AT5G56270
234	TF_motif_seq_0271	bZIP	+	0.8	TGACT	AT1G77920;AT3G12250;AT5G06950;AT5G06960;AT5G10030;AT5G65210;AT1G22070
239	TF_motif_seq_0254	AP2;ERF	-	0.8	TAGAA	AT3G14230
242	TFmatrixID_0041	B3;ARF	+	0.92	aaGTCGAcaa	AT2G33860
242	TFmatrixID_0041	B3;ARF	-	0.92	aagTCGACaa	AT2G33860
244	TFmatrixID_0156	B3;ARF;	+	0.96	gtCGACAaa	AT1G19220;AT1G19850;AT1G30330;AT5G20730;AT5G37020;AT5G60450
244	TF_motif_seq_0258	Dehydrin	-	0.8	GTCGA	U01377
244	TF_motif_seq_0275	(Motif sequence only)	-	0.8	GTCGA	WBOXATNPR1
245	TF_motif_seq_0258	Dehydrin	+	0.8	TCGAC	U01377
245	TF_motif_seq_0275	(Motif sequence only)	+	0.8	TCGAC	WBOXATNPR1
246	TFmatrixID_0274	MADS box;MIKC	-	0.94	cgacAAAAAaataaaaaaa	AT2G45660
246	TFmatrixID_0499	MADS box;MIKC	+	0.94	cgacAAAAAaataaaaaaa	AT4G22950;AT4G24540;AT4G37940;AT5G51860;AT5G51870;AT5G60910;AT5G62165;AT1G26310;AT2G14210;AT2G22630;AT2G45650;AT2G45660;AT3G30260;AT3G57230;AT3G57390;AT3G61120;AT4G09960;AT4G11880
246	TF_motif_seq_0271	bZIP	-	0.8	CGACA	AT1G77920;AT3G12250;AT5G06950;AT5G06960;AT5G10030;AT5G65210;AT1G22070
247	TFmatrixID_0134	AT-Hook	+	0.97	gacaaAAAAA	AT4G21895;AT5G62260
247	TF_motif_seq_0275	(Motif sequence only)	-	0.8	GACAA	WBOXATNPR1
248	TFmatrixID_0274	MADS box;MIKC	-	0.89	acaaAAAAaataaaaaaatt	AT2G45660
248	TFmatrixID	MADS box;MIKC	+	0.89	acaaAAAAaat	AT4G22950;AT4G24540;AT4G37940;AT5G51860;AT5G51870;AT5G60910;AT5G62165;AT1G26310;AT2G14210;AT2G22630;AT2G45650;AT2G45660;AT3G30260;AT3G57230;AT3G57390;AT3G61120;AT4G09960;AT4G11880

	_0499				aaaaaaatt	
248	TF_motif_seq_0404	(Motif sequence only)	+	0.88	ACAAAaaa	XYLAT
250	TFmatrixID_0476	AT-Hook	+	0.93	aaaaaaaaatAAAAAa	AT1G48610
251	TFmatrixID_0476	AT-Hook	+	0.92	aaaaaaaataAAAAAa	AT1G48610
252	TFmatrixID_0140	AT-Hook	+	1	aaaAAAAT	AT4G21895;AT5G62260
252	TFmatrixID_0476	AT-Hook	+	0.95	aaaaaaataAAAAAt	AT1G48610
253	TFmatrixID_0148	AT-Hook	+	1	aaAAAATa	AT1G19485;AT1G48610
254	TFmatrixID_0131	AT-Hook	+	1	aaaaATAAA	AT1G19485;AT1G48610
255	TFmatrixID_0136	AT-Hook	+	1	aaaATAAA	AT4G21895;AT5G62260
255	TFmatrixID_0138	AT-Hook	+	1	aAAATAaa	AT4G21895;AT5G62260
257	TFmatrixID_0222	CSD	+	1	aATAAAaa	AT2G21060;AT4G38680
260	TFmatrixID_0129	AT-Hook	+	1	aaaaAAATT	AT1G14900;AT1G48610
260	TFmatrixID_0140	AT-Hook	+	1	aaaAAAAT	AT4G21895;AT5G62260
260	TFmatrixID_0484	Homeodomain;HD-ZIP;bZIP	-	0.9	aaaaaaaTTATTg	AT1G26960;AT1G69780;AT3G01220;AT5G15150;AT5G65310
261	TFmatrixID_0058	Homeodomain;bZIP;HD-ZIP	+	0.96	aaaaaATTATTgac	AT3G01470
261	TFmatrixID_0148	AT-Hook	+	1	aaAAAATt	AT1G19485;AT1G48610
261	TFmatrixID_0540	Homeodomain;HD-ZIP;bZIP	-	0.95	aaaaaaTTATTgac	AT1G69780;AT3G01220;AT3G01470;AT5G15150
262	TFmatrixID_0002	AT-Hook	-	0.97	aaaAATTAtt	AT1G63480
262	TFmatrixID_0152	AT-Hook	+	1	aaAAATT	AT1G19485;AT1G48610
262	TFmatrixID_0517	Homeodomain;HD-ZIP;bZIP	-	0.96	aaaaaTTATTga	AT1G69780;AT3G01220;AT3G01470;AT5G15150
264	TFmatrixID_0026	bZIP;Homeodomain;HD-ZIP	+	1	aaATTATtga	AT5G03790
264	TFmatrixID_0116	Homeodomain;bZIP;HD-ZIP	+	0.93	aaaTTATTg	AT5G65310
264	TFmatrixID_0471	Homeodomain;HD-ZIP;bZIP	-	0.99	aaATTATt	AT1G69780;AT3G01220;AT3G01470;AT5G15150
264	TFmatrixID_0541	Homeodomain;HD-ZIP;bZIP	-	0.94	aaaTTATTg	AT1G26960;AT1G69780;AT3G01220;AT5G15150;AT5G65310
264	TF_motif_seq_0472	Homeodomain;bZIP;HD-ZIP	-	0.88	aaatTATTG	AT5G65310
265	TFmatrixID_0281	Homeodomain;HD-ZIP	+	1	aaTTATTga	AT1G26960;AT1G69780;AT2G22430;AT3G01220;AT5G15150
265	TFmatrixID_0292	Homeodomain;HD-ZIP	+	0.96	aATTATtg	AT1G26960;AT1G69780;AT3G01220;AT4G40060;AT5G15150
266	TF_motif_seq_0241	ZF-HD	+	1	ATTAT	AT1G75240
267	TFmatrixID_0452	WRKY	-	0.99	ttaTTGACtt	AT1G18860;AT1G29280;AT1G29860;AT1G55600;AT1G62300;AT1G64000;AT1G66550;AT1G66560;AT1G68150;AT1G69810;AT2G21900;AT2G34830;AT2G40740;AT2G40750;AT2G44745;AT2G46130;AT2G46400;AT3G01970;AT3G04670;AT3G56400;AT3G58710;AT3G62340;AT4G04450;AT4G11070;AT4G18170;AT4G22070;AT4G23810;AT4G24240;AT4G39410;AT5G15130;AT5G22570;AT5G26170;AT5G28650;AT5G41570;AT5G43290;AT5G45050;AT5G45260
268	TFmatrixID_0382	NAC;NAM	-	1	taTTGACtt	AT1G01720;AT1G52880;AT1G52890;AT1G69490;AT3G04070;AT3G15500;AT3G15510;AT4G27410
269	TFmatrixID_0445	WRKY	-	1	aTTGACtt	AT1G18860;AT1G29280;AT1G29860;AT1G55600;AT1G62300;AT1G64000;AT1G68150;AT1G69810;AT1G80840;AT2G21900;AT2G34830;AT2G44745;AT3G01970;AT3G04670;AT3G58710;AT3G62340;AT4G04450;AT4G18170;AT4G22070;AT4G24240;AT4G39410;AT5G15130;AT5G26170;AT5G28650;AT5G41570;AT5G43290;AT5G45050;AT5G45260
269	TF_motif_seq_0257	NF-YB;NF-YA;NF-YC	-	0.8	ATTGA	AT1G09030;AT1G17590;AT1G21970;AT1G30500;AT1G54160;AT1G54830;AT1G56170;AT1G72830;AT2G38880;AT2G47810;AT3G05690;AT3G14020;AT3G20910;AT3G53340;AT4G14540;AT5G06510;AT5G12840;AT5G27910;AT5G38140;AT5G47640;AT5G47670;AT5G50470;AT5G50480
270	TF_motif_seq_0339	WRKY	+	1	TTGACt	AT1G13960;AT1G18860;AT1G29280;AT1G29860;AT1G30650;AT1G55600;AT1G62300;AT1G64000;AT1G66550;AT1G68150;AT1G69310;AT1G69810;AT1G80590;AT1G80840;AT2G03340;AT2G23320;AT2G24570;AT2G25000;AT2G30250;AT2G30590;AT2G34830;AT2G37260;AT2G38470;AT2G40740;AT2G40750;AT2G44745;AT2G46130;AT2G46400;AT2G47260;AT3G01080;AT3G01970;AT3G04670;AT3G56400;AT3G58710;AT4G01250;AT4G01720;AT4G04450;AT4G12020;AT4G18170;AT4G22070;AT4G23810;AT4G24240;AT4G26440;AT4G26640;AT4G30935;AT4G31550;AT4G31800;AT4G39410;AT5G07100;AT5G13080;AT5G15130;AT5G22570;AT5G24110;AT5G28650;AT5G45050;AT5G45260;AT5G46350;AT5G49520;AT5G52830;AT5G56270
270	TF_motif_seq_0275	(Motif sequence only)	+	1	TTGAC	WBOXATNPR1
271	TF_motif_s	Homeodomain;TALE	+	1	TGACT	AT1G23380;AT1G62360;AT1G70510;AT4G08150

	eq_0246					
271	TF_motif_seq_0270	WRKY	+	1	TGACT	AT1G13960;AT1G18860;AT1G29280;AT1G29860;AT1G30650;AT1G55600;AT1G62300;AT1G64000;AT1G66550;AT1G68150;AT1G69310;AT1G69810;AT1G80590;AT1G80840;AT2G03340;AT2G23320;AT2G24570;AT2G25000;AT2G30250;AT2G30590;AT2G34830;AT2G37260;AT2G38470;AT2G40740;AT2G40750;AT2G44745;AT2G46130;AT2G46400;AT2G47260;AT3G01080;AT3G01970;AT3G04670;AT3G56400;AT3G58710;AT4G01250;AT4G01720;AT4G04450;AT4G12020;AT4G18170;AT4G22070;AT4G23810;AT4G24240;AT4G26440;AT4G26640;AT4G30935;AT4G31550;AT4G31800;AT4G39410;AT5G07100;AT5G13080;AT5G15130;AT5G22570;AT5G24110;AT5G28650;AT5G45050;AT5G45260;AT5G46350;AT5G49520;AT5G52830;AT5G56270
271	TF_motif_seq_0271	bZIP	+	0.8	TGACT	AT1G77920;AT3G12250;AT5G06950;AT5G06960;AT5G10030;AT5G65210;AT1G22070
271	TF_motif_seq_0450	(Motif sequence only)	+	0.75	TGACTtaa	PALINDROMICCBOXGM
273	TFmatrixID_0412	Sox;YABBY	+	1	actTAATTac	AT1G23420
274	TFmatrixID_0628	Homeodomain;bZIP;HD-ZIP;WOX	+	0.96	ctTAATTact	AT4G35550
274	TFmatrixID_0628	Homeodomain;bZIP;HD-ZIP;WOX	-	0.96	cttAATTAct	AT4G35550
275	TF_motif_seq_0241	ZF-HD	-	1	TTAAT	AT1G75240
278	TF_motif_seq_0241	ZF-HD	+	1	ATTAC	AT1G75240
278	TF_motif_seq_0267	Trihelix	+	0.8	ATTAC	AT5G01380
282	TFmatrixID_0461	WRKY	-	0.99	ctagTTGACc	AT1G18860;AT1G29280;AT1G62300;AT1G64000;AT1G66550;AT1G66560;AT1G68150;AT1G80590;AT2G34830;AT2G40740;AT2G40750;AT2G44745;AT2G46400;AT3G01970;AT3G04670;AT3G56400;AT3G58710;AT3G62340;AT4G04450;AT4G11070;AT4G22070;AT4G23810;AT4G24240;AT4G39410;AT5G15130;AT5G22570;AT5G24110;AT5G26170;AT5G28650;AT5G41570;AT5G43290;AT5G45050;AT5G45260
283	TFmatrixID_0442	WRKY	-	0.99	tagTTGACca	AT1G18860;AT1G29280;AT1G29860;AT1G30650;AT1G55600;AT1G62300;AT1G64000;AT1G66550;AT1G66560;AT1G68150;AT1G69810;AT2G21900;AT2G34830;AT2G40740;AT2G40750;AT2G44745;AT2G46400;AT3G01970;AT3G04670;AT3G56400;AT3G58710;AT3G62340;AT4G04450;AT4G11070;AT4G18170;AT4G22070;AT4G23810;AT4G24240;AT4G39410;AT5G15130;AT5G22570;AT5G26170;AT5G28650;AT5G41570;AT5G43290;AT5G45050;AT5G45260
283	TFmatrixID_0446	WRKY	-	1	tagTTGACca	AT1G18860;AT1G29280;AT1G29860;AT1G55600;AT1G62300;AT1G64000;AT1G68150;AT1G69810;AT2G21900;AT2G23320;AT2G34830;AT2G40740;AT2G44745;AT3G01970;AT3G04670;AT3G58710;AT3G62340;AT4G04450;AT4G11070;AT4G18170;AT4G22070;AT4G23810;AT4G24240;AT4G39410;AT5G15130;AT5G22570;AT5G26170;AT5G28650;AT5G41570;AT5G43290;AT5G45050;AT5G45260
283	TFmatrixID_0448	WRKY	-	0.99	tagTTGACcaa	AT1G18860;AT1G29280;AT1G29860;AT1G55600;AT1G62300;AT1G64000;AT1G68150;AT1G69810;AT2G21900;AT2G25000;AT2G34830;AT2G44745;AT2G46400;AT3G01970;AT3G04670;AT3G58710;AT3G62340;AT4G04450;AT4G11070;AT4G18170;AT4G22070;AT4G24240;AT4G39410;AT5G15130;AT5G26170;AT5G28650;AT5G41570;AT5G43290;AT5G45050
283	TFmatrixID_0455	WRKY	-	0.98	tagTTGACcaa	AT1G18860;AT1G29280;AT1G29860;AT1G55600;AT1G62300;AT1G64000;AT1G66550;AT1G66560;AT1G68150;AT1G69810;AT2G21900;AT2G34830;AT2G40740;AT2G44745;AT2G46400;AT3G01970;AT3G04670;AT3G58710;AT3G62340;AT4G01720;AT4G04450;AT4G11070;AT4G18170;AT4G22070;AT4G23810;AT4G24240;AT4G39410;AT5G15130;AT5G26170;AT5G28650;AT5G41570;AT5G43290;AT5G45050;AT5G45260
283	TFmatrixID_0457	WRKY	-	0.99	tagTTGACca	AT1G18860;AT1G29280;AT1G29860;AT1G55600;AT1G62300;AT1G64000;AT1G66560;AT1G68150;AT1G69810;AT2G21900;AT2G34830;AT2G40740;AT2G44745;AT2G46400;AT3G01970;AT3G04670;AT3G56400;AT3G58710;AT3G62340;AT4G04450;AT4G11070;AT4G18170;AT4G22070;AT4G23810;AT4G24240;AT4G31550;AT4G39410;AT5G15130;AT5G22570;AT5G26170;AT5G28650;AT5G41570;AT5G43290;AT5G45050;AT5G45260
283	TFmatrixID_0629	WRKY	+	0.96	tagTTGACca	AT2G44745
283	TFmatrixID_0631	WRKY	+	0.97	tagTTGACca	AT5G22570
283	TFmatrixID_0632	WRKY	+	0.92	tagTTGACca	AT3G01970
283	TF_motif_seq_0254	AP2;ERF	-	0.8	TAGTT	AT3G14230
284	TFmatrixID_0382	NAC;NAM	-	1	agTTGACca	AT1G01720;AT1G52880;AT1G52890;AT1G69490;AT3G04070;AT3G15500;AT3G15510;AT4G27410
284	TFmatrixID_0444	WRKY	-	0.98	agTTGACcaa	AT1G18860;AT1G29280;AT1G29860;AT1G55600;AT1G62300;AT1G64000;AT1G66550;AT1G66560;AT1G68150;AT1G69310;AT1G69810;AT1G80590;AT2G21900;AT2G34830;AT2G40740;AT2G44745;AT2G46400;AT3G01970;AT3G04670;AT3G56400;AT3G58710;AT3G62340;AT4G04450;AT4G11070;AT4G18170;AT4G22070;AT4G23810;AT4G24240;AT4G39410;AT5G15130;AT5G22570;AT5G26170;AT5G28650;AT5G41570;AT5G43290;AT5G45050
284	TFmatrixID_0447	WRKY	-	0.99	agTTGACcaa	AT1G18860;AT1G29280;AT1G29860;AT1G55600;AT1G62300;AT1G64000;AT1G68150;AT1G69810;AT2G21900;AT2G24570;AT2G34830;AT2G40740;AT2G44745;AT3G01970;AT3G04670;AT3G58710;AT3G62340;AT4G04450;AT4G11070;AT4G18170;AT4G22070;AT4G23810;AT4G24240;AT4G39410;AT5G15130;AT5G22570;AT5G26170;AT5G28650;AT5G41570;AT5G43290;AT5G45050;AT5G45260
284	TFmatrixID_0450	WRKY	-	1	agTTGACcaa	AT1G18860;AT1G29280;AT1G29860;AT1G55600;AT1G62300;AT1G64000;AT1G68150;AT1G69810;AT2G21900;AT2G30590;AT2G34830;AT2G40740;AT2G44745;AT3G01970;AT3G04670;AT3G58710;AT3G62340;AT4G04450;AT4G11070;AT4G18170;AT4G22070;AT4G24240;AT4G39410;AT5G15130;AT5G22570;AT5G26170;AT5G28650;AT5G41570;AT5G43290;AT5G45050;AT5G45260
284	TFmatrixID_0451	WRKY	-	1	agTTGACcaa	AT1G13960;AT2G03340;AT2G37260;AT2G38470;AT3G01080;AT4G12020;AT4G26440;AT4G26640;AT4G30935;AT5G07100
284	TFmatrixID_0453	WRKY	-	0.92	agTTGACc	AT1G18860;AT1G29280;AT1G29860;AT1G55600;AT1G62300;AT1G64000;AT1G66550;AT1G66560;AT1G68150;AT1G69810;AT1G80590;AT2G21900;AT2G34830;AT2G40740;AT2G40750;AT2G44745;AT2G46400;AT2G47260;AT3G01970;AT3G04670;AT3G56400;AT3G58710;AT3G62340;AT4G04450;AT4G11070;AT4G18170;AT4G22070;AT4G23810;AT4G24240;AT4G39410;AT5G15130;AT5G22570;AT5G26170;AT5G28650;AT5G41570;AT5G43290;AT5G45050
284	TFmatrixID_0454	WRKY	-	1	agTTGACcaa	AT1G18860;AT1G29280;AT1G29860;AT1G55600;AT1G62300;AT1G64000;AT1G66550;AT1G66560;AT1G68150;AT1G69810;AT1G80590;AT2G21900;AT2G34830;AT2G40740;AT2G40750;AT2G44745;AT2G46400;AT3G01970;AT3G04670;AT3G56400;AT3G58710;AT3G62340;AT4G01250;AT4G04450;AT4G11070;AT4G18170;AT4G22070;AT4G23810;AT4G24240;AT4G39410;AT5G15130;AT5G22570;AT5G26170;AT5G28650;AT5G41570;AT5G43290;AT5G45050;AT5G45260
284	TFmatrixID_0456	WRKY	-	1	agTTGACcaa	AT1G18860;AT1G29280;AT1G29860;AT1G55600;AT1G62300;AT1G64000;AT1G66560;AT1G68150;AT1G69810;AT1G80590;AT2G21900;AT2G34830;AT2G40740;AT2G40750;AT2G44745;AT2G46400;AT3G01970;AT3G04670;AT3G56400;AT3G58710;AT3G62340;AT4G04450;AT4G11070;AT4G18170;AT4G22070;AT4G23550;AT4G23810;AT4G24240;AT4G39410;AT5G15130;AT5G22570;AT5G26170;AT5G28650;AT5G41570;AT5G43290;AT5G45050;AT5G45260
284	TFmatrixID_0458	WRKY	-	1	agTTGACcaa	AT1G18860;AT1G29280;AT1G29860;AT1G55600;AT1G62300;AT1G64000;AT1G68150;AT1G69810;AT2G21900;AT2G34830;AT2G40740;AT2G44745;AT2G46400;AT3G01970;AT3G04670;AT3G58710;AT3G62340;AT4G04450;AT4G11070;AT4G18170;AT4G22070;AT4G24240;AT4G31800;AT4G39410;AT5G15130;AT5G26170;AT5G28650;AT5G41570;AT5G43290;AT5G45050
284	TFmatrixID_0462	WRKY	-	1	agTTGACca	AT1G18860;AT1G29280;AT1G29860;AT1G55600;AT1G62300;AT1G64000;AT1G66550;AT1G66560;AT1G68150;AT1G69810;AT1G80590;AT2G21900;AT2G34830;AT2G40740;AT2G44745;AT3G01970;AT3G04670;AT3G58710;AT3G62340;AT4G04450;AT4G11070;AT4G18170;AT4G22070;AT4G23810;AT4G24240;AT4G39410;AT5G15130;AT5G22570;AT5G26170;AT5G28650;AT5G41570;AT5G43290;AT5G45050;AT5G45260;AT5G46350
284	TFmatrixID_0463	WRKY	-	1	agTTGACcaa	AT1G18860;AT1G29280;AT1G29860;AT1G55600;AT1G62300;AT1G64000;AT1G66550;AT1G66560;AT1G68150;AT1G69810;AT1G80590;AT2G21900;AT2G34830;AT2G40740;AT2G40750;AT2G44745;AT2G46400;AT3G01970;AT3G04670;AT3G56400;AT3G58710;AT3G62340;AT4G04450;AT4G11070;AT4G18170;AT4G22070;AT4G23810;AT4G24240;AT4G39410;AT5G15130;AT5G22570;AT5G26170;AT5G28650;AT5G41570;AT5G43290;AT5G45050;AT5G45260;AT5G49520
284	TFmatrixID_0464	WRKY	-	1	agTTGACca	AT1G18860;AT1G29280;AT1G29860;AT1G55600;AT1G62300;AT1G64000;AT1G66550;AT1G66560;AT1G68150;AT1G69810;AT1G80590;AT2G21900;AT2G34830;AT2G40740;AT2G40750;AT2G44745;AT2G46400;AT3G01970;AT3G04670;AT3G56400;AT3G58710;AT3G62340;AT4G04450;AT4G11070;AT4G18170;AT4G22070;AT4G23810;AT4G24240;AT4G39410;AT5G15130;AT5G22570;AT5G26170;AT5G28650;AT5G41570;AT5G43290;AT5G45050;AT5G45260;AT5G52830
284	TFmatrixID_0466	WRKY	-	1	agTTGACcaa	AT1G18860;AT1G29280;AT1G29860;AT1G55600;AT1G62300;AT1G64000;AT1G68150;AT1G69810;AT2G21900;AT2G34830;AT2G44745;AT3G01970;AT3G04670;AT3G58710;AT3G62340;AT4G04450;AT4G18170;AT4G22070;AT4G24240;AT4G39410;AT5G15130;AT5G26170;AT5G28650;AT5G41570;AT5G43290;AT5G45050;AT5G64810
284	TFmatrixID_0468	WRKY	-	1	agTTGACca	AT1G18860;AT1G29280;AT1G29860;AT1G55600;AT1G62300;AT1G64000;AT1G66550;AT1G66560;AT1G68150;AT1G69810;AT1G80590;AT2G21900;AT2G34830;AT2G40740;AT2G40750;AT2G44745;AT2G46400;AT3G01970;AT3G04670;AT3G56400;AT3G58710;AT3G62340;AT4G04450;AT4G11070;AT4G18170;AT4G22070;AT4G23810;AT4G24240;AT4G39410;AT5G15130;AT5G22570;AT5G26170;AT5G28650;AT5G41570;AT5G43290;AT5G45050;AT5G45260
284	TFmatrixID	WRKY	-	0.96	agTTGACcaa	AT4G31800

	_0630					
284	TF_motif_seq_0060	(Motif sequence only)	-	0.82	agttgaCCAAT	UPRE1AT
285	TFmatrixID_0443	WRKY	-	1	gTTGACca	AT1G29860;AT1G64000;AT1G66550;AT1G66560;AT1G66600;AT1G68150;AT1G69810;AT1G80590;AT2G40740;AT2G40750;AT2G44745;AT2G46400;AT3G01970;AT3G56400;AT3G62340;AT4G04450;AT4G11070;AT4G18170;AT4G23810;AT4G39410;AT5G22570;AT5G26170;AT5G41570;AT5G43290;AT5G45050;AT5G45260
285	TFmatrixID_0445	WRKY	-	1	gTTGACca	AT1G18860;AT1G29280;AT1G29860;AT1G55600;AT1G62300;AT1G64000;AT1G68150;AT1G69810;AT1G80840;AT2G21900;AT2G34830;AT2G44745;AT3G01970;AT3G04670;AT3G58710;AT3G62340;AT4G04450;AT4G18170;AT4G22070;AT4G24240;AT4G39410;AT5G15130;AT5G26170;AT5G28650;AT5G41570;AT5G43290;AT5G45050;AT5G45260
285	TFmatrixID_0449	WRKY	-	0.99	gTTGACca	AT1G13960;AT2G03340;AT2G30250;AT2G37260;AT3G01080;AT4G12020;AT4G26440;AT4G26640;AT4G30935;AT5G07100
285	TFmatrixID_0459	WRKY	-	1	gTTGACca	AT1G29280;AT1G29860;AT1G64000;AT1G66550;AT1G66560;AT1G69810;AT1G80590;AT2G40740;AT2G40750;AT2G44745;AT2G46400;AT3G01970;AT3G56400;AT3G62340;AT4G11070;AT4G18170;AT4G23810;AT4G24240;AT5G01900;AT5G22570;AT5G26170;AT5G41570;AT5G43290;AT5G45050;AT5G45260
285	TFmatrixID_0460	WRKY	-	1	gTTGACca	AT1G18860;AT1G29280;AT1G29860;AT1G55600;AT1G62300;AT1G64000;AT1G66550;AT1G66560;AT1G68150;AT1G69810;AT2G21900;AT2G34830;AT2G40740;AT2G40750;AT2G44745;AT3G01970;AT3G04670;AT3G56400;AT3G58710;AT3G62340;AT4G04450;AT4G11070;AT4G18170;AT4G22070;AT4G23810;AT4G24240;AT4G39410;AT5G13080;AT5G15130;AT5G22570;AT5G26170;AT5G28650;AT5G41570;AT5G43290;AT5G45050;AT5G45260
285	TFmatrixID_0465	WRKY	-	1	gTTGACca	AT1G13960;AT2G03340;AT2G37260;AT3G01080;AT4G12020;AT4G26440;AT4G26640;AT4G30935;AT5G07100;AT5G56270
285	TFmatrixID_0491	TBP	+	0.94	gttgaccaaTATATatattat	AT1G55520;AT3G13445
285	TFmatrixID_0572	TBP	+	0.94	gttgaccaaTATATatattat	AT1G55520;AT3G13445
286	TFmatrixID_0534	WRKY	-	0.88	TTGACcaatat	AT1G13960;AT2G03340;AT2G04880;AT2G37260;AT3G01080;AT4G12020;AT4G26440;AT4G26640;AT4G30935;AT5G07100
286	TF_motif_seq_0339	WRKY	+	1	TTGACc	AT1G13960;AT1G18860;AT1G29280;AT1G29860;AT1G30650;AT1G55600;AT1G62300;AT1G64000;AT1G66550;AT1G68150;AT1G69310;AT1G69810;AT1G80590;AT1G80840;AT2G03340;AT2G23320;AT2G24570;AT2G25000;AT2G30250;AT2G30590;AT2G34830;AT2G37260;AT2G38470;AT2G40740;AT2G40750;AT2G44745;AT2G46130;AT2G46400;AT2G47260;AT3G01080;AT3G01970;AT3G04670;AT3G56400;AT3G58710;AT4G01250;AT4G01720;AT4G04450;AT4G12020;AT4G18170;AT4G22070;AT4G23810;AT4G24240;AT4G26440;AT4G26640;AT4G30935;AT4G31550;AT4G31800;AT4G39410;AT5G07100;AT5G13080;AT5G15130;AT5G22570;AT5G24110;AT5G28650;AT5G45050;AT5G45260;AT5G46350;AT5G49520;AT5G52830;AT5G56270
286	TF_motif_seq_0275	(Motif sequence only)	+	1	TTGAC	WBOXATNPR1
287	TFmatrixID_0491	TBP	+	0.94	tgaccaataTATATattatta	AT1G55520;AT3G13445
287	TFmatrixID_0572	TBP	+	0.94	tgaccaataTATATattatta	AT1G55520;AT3G13445
287	TF_motif_seq_0246	Homeodomain;TALE	+	1	TGACC	AT1G23380;AT1G62360;AT1G70510;AT4G08150
287	TF_motif_seq_0270	WRKY	+	1	TGACC	AT1G13960;AT1G18860;AT1G29280;AT1G29860;AT1G30650;AT1G55600;AT1G62300;AT1G64000;AT1G66550;AT1G68150;AT1G69310;AT1G69810;AT1G80590;AT1G80840;AT2G03340;AT2G23320;AT2G24570;AT2G25000;AT2G30250;AT2G30590;AT2G34830;AT2G37260;AT2G38470;AT2G40740;AT2G40750;AT2G44745;AT2G46130;AT2G46400;AT2G47260;AT3G01080;AT3G01970;AT3G04670;AT3G56400;AT3G58710;AT4G01250;AT4G01720;AT4G04450;AT4G12020;AT4G18170;AT4G22070;AT4G23810;AT4G24240;AT4G26440;AT4G26640;AT4G30935;AT4G31550;AT4G31800;AT4G39410;AT5G07100;AT5G13080;AT5G15130;AT5G22570;AT5G24110;AT5G28650;AT5G45050;AT5G45260;AT5G46350;AT5G49520;AT5G52830;AT5G56270
287	TF_motif_seq_0271	bZIP	+	0.8	TGACC	AT1G77920;AT3G12250;AT5G06950;AT5G06960;AT5G10030;AT5G65210;AT1G22070
288	TFmatrixID_0491	TBP	-	0.95	gaccaatATATAtattattaa	AT1G55520;AT3G13445
288	TFmatrixID_0572	TBP	-	0.95	gaccaatATATAtattattaa	AT1G55520;AT3G13445
290	TFmatrixID_0491	TBP	-	0.95	ccaatatATATAttattaaaa	AT1G55520;AT3G13445
290	TFmatrixID_0572	TBP	-	0.95	ccaatatATATAttattaaaa	AT1G55520;AT3G13445
290	TF_motif_seq_0257	NF-YB;NF-YA;NF-YC	+	1	CCAAT	AT1G09030;AT1G17590;AT1G21970;AT1G30500;AT1G54160;AT1G54830;AT1G56170;AT1G72830;AT2G38880;AT2G47810;AT3G05690;AT3G14020;AT3G20910;AT3G53340;AT4G14540;AT5G06510;AT5G12840;AT5G27910;AT5G38140;AT5G47640;AT5G47670;AT5G50470;AT5G50480
290	TF_motif_seq_0363	(Motif sequence only)	+	0.86	CCAATat	LEAFYATAG
292	TFmatrixID_0003	AT-Hook	+	0.98	aATATAtata	AT1G63480
292	TFmatrixID_0003	AT-Hook	-	1	aataTATATa	AT1G63480
292	TFmatrixID_0419	TBP	+	1	aaTATAT	AT1G55520;AT3G13445
293	TF_motif_seq_0254	AP2;ERF	+	0.8	ATATA	AT3G14230
294	TFmatrixID_0003	AT-Hook	+	1	tATATAtatt	AT1G63480
294	TFmatrixID_0003	AT-Hook	-	0.98	tataTATATt	AT1G63480
294	TF_motif_seq_0254	AP2;ERF	-	0.8	TATAT	AT3G14230
295	TFmatrixID_0282	Homeodomain	+	1	atataTATTAtta	AT2G36610
295	TF_motif_seq_0254	AP2;ERF	+	0.8	ATATA	AT3G14230
296	TF_motif_seq_0254	AP2;ERF	-	0.8	TATAT	AT3G14230
297	TFmatrixID	TBP	-	1	ATATAtt	AT1G55520;AT3G13445

	_0419					
297	TF_motif_seq_0254	AP2;ERF	+	0.8	ATATA	AT3G14230
298	TF_motif_seq_0254	AP2;ERF	-	0.8	TATAT	AT3G14230
301	TF_motif_seq_0241	ZF-HD	+	1	ATTAT	AT1G75240
304	TF_motif_seq_0241	ZF-HD	+	1	ATTAA	AT1G75240
308	TF_motif_seq_0239	Dof	+	1	AAAGA	AT1G29160;AT1G64620;AT2G37590;AT3G21270;AT3G45610;AT3G47500;AT4G38000;AT5G39660;AT5G60200;AT5G60850;AT5G62940;AT2G46590;AT1G07640;AT1G21340;AT1G26790;AT1G47655;AT1G51700;AT1G69570;AT2G28510;AT2G28810;AT2G34140;AT3G50410;AT3G55370;AT3G61850;AT4G00940;AT4G21050;AT4G21080;AT4G24060;AT5G02460;AT5G62430;AT5G65590;AT5G66940
317	TF_motif_seq_0257	NF-YB;NF-YA;NF-YC	-	0.8	ATTGT	AT1G09030;AT1G17590;AT1G21970;AT1G30500;AT1G54160;AT1G54830;AT1G56170;AT1G72830;AT2G38880;AT2G47810;AT3G05690;AT3G14020;AT3G20910;AT3G53340;AT4G14540;AT5G06510;AT5G12840;AT5G27910;AT5G38140;AT5G47640;AT5G47670;AT5G50470;AT5G50480
320	TF_motif_seq_0243	GATA;tify	-	1	GTATC	AT1G51600;AT2G45050;AT3G06740;AT3G16870;AT3G21175;AT3G24050;AT3G54810;AT3G60530;AT4G17570;AT4G24470;AT4G26150;AT4G32890;AT4G34680;AT5G25830;AT5G26930;AT5G56860;AT5G66320;AT2G18380;AT3G50870;AT4G36620
320	TF_motif_seq_0267	Trihelix	-	0.8	GTATC	AT5G01380
320	TF_motif_seq_0261	(Motif sequence only)	-	0.8	GTATC	SURECOREATSULTR11
321	TF_motif_seq_0237	GATA;tify	-	1	TATCG	AT1G51600;AT2G45050;AT3G06740;AT3G16870;AT3G21175;AT3G24050;AT3G54810;AT3G60530;AT4G17570;AT4G24470;AT4G26150;AT4G32890;AT4G34680;AT5G25830;AT5G26930;AT5G56860;AT5G66320;AT2G18380;AT3G50870;AT4G36620
323	TF_motif_seq_0248	(Motif sequence only)	-	0.8	TCGTT	MYBCOREATCYCB1
324	TF_motif_seq_0066	WRKY	+	0.73	CGTTGaaagcg	AT2G04880
326	TF_motif_seq_0275	(Motif sequence only)	+	0.8	TTGAA	WBOXATNPR1
329	TF_motif_seq_0239	Dof	+	1	AAAGC	AT1G29160;AT1G64620;AT2G37590;AT3G21270;AT3G45610;AT3G47500;AT4G38000;AT5G39660;AT5G60200;AT5G60850;AT5G62940;AT2G46590;AT1G07640;AT1G21340;AT1G26790;AT1G47655;AT1G51700;AT1G69570;AT2G28510;AT2G28810;AT2G34140;AT3G50410;AT3G55370;AT3G61850;AT4G00940;AT4G21050;AT4G21080;AT4G24060;AT5G02460;AT5G62430;AT5G65590;AT5G66940
331	TF_motif_seq_0248	(Motif sequence only)	+	0.8	AGCGG	MYBCOREATCYCB1
332	TFmatrixID_0018	Myb/SANT;MYB;ARR-B	+	0.9	gcGGATCatc	AT2G01760
333	TFmatrixID_0262	GATA	-	1	cgGATCAtc	AT3G06740;AT3G16870;AT4G16141;AT4G26150;AT5G26930;AT5G49300;AT5G56860
334	TF_motif_seq_0237	GATA;tify	+	1	GGATC	AT1G51600;AT2G45050;AT3G06740;AT3G16870;AT3G21175;AT3G24050;AT3G54810;AT3G60530;AT4G17570;AT4G24470;AT4G26150;AT4G32890;AT4G34680;AT5G25830;AT5G26930;AT5G56860;AT5G66320;AT2G18380;AT3G50870;AT4G36620
335	TF_motif_seq_0237	GATA;tify	-	1	GATCA	AT1G51600;AT2G45050;AT3G06740;AT3G16870;AT3G21175;AT3G24050;AT3G54810;AT3G60530;AT4G17570;AT4G24470;AT4G26150;AT4G32890;AT4G34680;AT5G25830;AT5G26930;AT5G56860;AT5G66320;AT2G18380;AT3G50870;AT4G36620
338	TF_motif_seq_0237	GATA;tify	-	1	CATCG	AT1G51600;AT2G45050;AT3G06740;AT3G16870;AT3G21175;AT3G24050;AT3G54810;AT3G60530;AT4G17570;AT4G24470;AT4G26150;AT4G32890;AT4G34680;AT5G25830;AT5G26930;AT5G56860;AT5G66320;AT2G18380;AT3G50870;AT4G36620
339	TF_motif_seq_0257	NF-YB;NF-YA;NF-YC	-	0.8	ATCGG	AT1G09030;AT1G17590;AT1G21970;AT1G30500;AT1G54160;AT1G54830;AT1G56170;AT1G72830;AT2G38880;AT2G47810;AT3G05690;AT3G14020;AT3G20910;AT3G53340;AT4G14540;AT5G06510;AT5G12840;AT5G27910;AT5G38140;AT5G47640;AT5G47670;AT5G50470;AT5G50480
339	TF_motif_seq_0258	Dehydrin	-	0.8	ATCGG	U01377
339	TF_motif_seq_0248	(Motif sequence only)	+	0.8	ATCGG	MYBCOREATCYCB1
340	TF_motif_seq_0331	TCP	+	1	tCGGGT	AT3G27010
340	TF_motif_seq_0402	(Motif sequence only)	-	0.88	tcgGGTTT	UP2ATMSD
341	TF_motif_seq_0251	TCP	-	1	CGGGT	AT3G27010
350	TF_motif_seq_0239	Dof	+	1	AAAGA	AT1G29160;AT1G64620;AT2G37590;AT3G21270;AT3G45610;AT3G47500;AT4G38000;AT5G39660;AT5G60200;AT5G60850;AT5G62940;AT2G46590;AT1G07640;AT1G21340;AT1G26790;AT1G47655;AT1G51700;AT1G69570;AT2G28510;AT2G28810;AT2G34140;AT3G50410;AT3G55370;AT3G61850;AT4G00940;AT4G21050;AT4G21080;AT4G24060;AT5G02460;AT5G62430;AT5G65590;AT5G66940
353	TF_motif_seq_0321	(Motif sequence only)	+	1	GAAAAa	GT1CONSENSUS
356	TF_motif_seq_0343	(Motif sequence only)	+	0.86	AAACAca	ANAERO1CONSENSUS
359	TF_motif_seq_0249	(Motif sequence only)	-	0.8	CACAT	ABRELATERD1
360	TF_motif_seq_0009	(Motif sequence only)	+	0.7	ACATCgttga	LS7ATPR1
361	TF_motif_seq_0237	GATA;tify	-	1	CATCG	AT1G51600;AT2G45050;AT3G06740;AT3G16870;AT3G21175;AT3G24050;AT3G54810;AT3G60530;AT4G17570;AT4G24470;AT4G26150;AT4G32890;AT4G34680;AT5G25830;AT5G26930;AT5G56860;AT5G66320;AT2G18380;AT3G50870;AT4G36620
363	TF_motif_seq_0248	(Motif sequence only)	-	0.8	TCGTT	MYBCOREATCYCB1
366	TF_motif_s	(Motif sequence only)	+	0.8	TTGAA	WBOXATNPR1

	eq_0275					
368	TF_motif_seq_0267	Trihelix	-	0.8	GAAAC	AT5G01380
368	TF_motif_seq_0261	(Motif sequence only)	+	0.8	GAAAC	SURECOREATSULTR11
371	TF_motif_seq_0249	(Motif sequence only)	+	0.8	ACTTG	ABRELATERD1
373	TF_motif_seq_0275	(Motif sequence only)	+	0.8	TTGAA	WBOXATNPR1
374	TF_motif_seq_0421	AP2;ERF	-	0.88	tgaAAGTG	AT2G40220
376	TF_motif_seq_0239	Dof	+	1	AAAGT	AT1G29160;AT1G64620;AT2G37590;AT3G21270;AT3G45610;AT3G47500;AT4G38000;AT5G39660;AT5G60200;AT5G60850;AT5G62940;AT2G46590;AT1G07640;AT1G21340;AT1G26790;AT1G47655;AT1G51700;AT1G69570;AT2G28510;AT2G28810;AT2G34140;AT3G50410;AT3G55370;AT3G61850;AT4G00940;AT4G21050;AT4G21080;AT4G24060;AT5G02460;AT5G62430;AT5G65590;AT5G66940
377	TF_motif_seq_0249	(Motif sequence only)	+	0.8	AAGTG	ABRELATERD1
379	TF_motif_seq_0390	(Motif sequence only)	-	1	gtGATGA	ANAERO3CONSENSUS
379	TF_motif_seq_0435	(Motif sequence only)	+	0.88	GTGATgac	PIATGAPB
380	TF_motif_seq_0237	GATA;tify	+	1	TGATG	AT1G51600;AT2G45050;AT3G06740;AT3G16870;AT3G21175;AT3G24050;AT3G54810;AT3G60530;AT4G17570;AT4G24470;AT4G26150;AT4G32890;AT4G34680;AT5G25830;AT5G26930;AT5G56860;AT5G66320;AT2G18380;AT3G50870;AT4G36620
380	TF_motif_seq_0271	bZIP	+	0.8	TGATG	AT1G77920;AT3G12250;AT5G06950;AT5G06960;AT5G10030;AT5G65210;AT1G22070
382	TF_motif_seq_0275	(Motif sequence only)	+	0.8	ATGAC	WBOXATNPR1
383	TF_motif_seq_0246	Homeodomain;TALE	+	1	TGACT	AT1G23380;AT1G62360;AT1G70510;AT4G08150
383	TF_motif_seq_0270	WRKY	+	1	TGACT	AT1G13960;AT1G18860;AT1G29280;AT1G29860;AT1G30650;AT1G55600;AT1G62300;AT1G64000;AT1G66550;AT1G68150;AT1G69310;AT1G69810;AT1G80590;AT1G80840;AT2G03340;AT2G23320;AT2G24570;AT2G25000;AT2G30250;AT2G30590;AT2G34830;AT2G37260;AT2G38470;AT2G40740;AT2G40750;AT2G44745;AT2G46130;AT2G46400;AT2G47260;AT3G01080;AT3G01970;AT3G04670;AT3G56400;AT3G58710;AT4G01250;AT4G01720;AT4G04450;AT4G12020;AT4G18170;AT4G22070;AT4G23810;AT4G24240;AT4G26440;AT4G26640;AT4G30935;AT4G31550;AT4G31800;AT4G39410;AT5G07100;AT5G13080;AT5G15130;AT5G22570;AT5G24110;AT5G28650;AT5G45050;AT5G45260;AT5G46350;AT5G49520;AT5G52830;AT5G56270
383	TF_motif_seq_0271	bZIP	+	0.8	TGACT	AT1G77920;AT3G12250;AT5G06950;AT5G06960;AT5G10030;AT5G65210;AT1G22070
385	TFmatrixID_0131	AT-Hook	+	1	actaATAAA	AT1G19485;AT1G48610
386	TF_motif_seq_0241	ZF-HD	-	1	CTAAT	AT1G75240
386	TF_motif_seq_0257	NF-YB;NF-YA;NF-YC	+	0.8	CTAAT	AT1G09030;AT1G17590;AT1G21970;AT1G30500;AT1G54160;AT1G54830;AT1G56170;AT1G72830;AT2G38880;AT2G47810;AT3G05690;AT3G14020;AT3G20910;AT3G53340;AT4G14540;AT5G06510;AT5G12840;AT5G27910;AT5G38140;AT5G47640;AT5G47670;AT5G50470;AT5G50480
388	TFmatrixID_0222	CSD	+	1	aATAAAaa	AT2G21060;AT4G38680
391	TFmatrixID_0638	Dof	+	0.99	aaAAAGAtct	AT5G65590
392	TFmatrixID_0265	GATA;tify	-	0.98	aaaaGATCTa	AT2G45050;AT3G45170;AT3G51080;AT5G25830;AT5G66320
392	TFmatrixID_0269	GATA;tify	-	0.98	aaaAGATCtaa	AT2G28340;AT2G45050;AT4G32890;AT5G25830;AT5G66320
392	TFmatrixID_0270	GATA;tify	-	1	aaaaGATCTa	AT2G28340;AT2G45050;AT4G34680;AT5G25830;AT5G66320
393	TFmatrixID_0016	MYB;ARR-B	+	0.95	aaAGATCtaa	AT1G67710
393	TFmatrixID_0016	MYB;ARR-B	-	0.95	aaaGATCTaa	AT1G67710
393	TFmatrixID_0019	Myb/SANT;MYB;ARR-B	+	0.91	aaAGATCtaa	AT2G01760
393	TFmatrixID_0019	Myb/SANT;MYB;ARR-B	-	0.91	aaaGATCTaa	AT2G01760
393	TFmatrixID_0042	GATA;tify	+	0.99	aaAGATCtaa	AT5G25830
393	TFmatrixID_0042	GATA;tify	-	1	aaaGATCTaa	AT5G25830
393	TFmatrixID_0264	GATA;tify	+	1	aaAGATCtaa	AT2G45050;AT3G24050;AT5G25830;AT5G66320
393	TFmatrixID_0264	GATA;tify	-	1	aaaGATCTaa	AT2G45050;AT3G24050;AT5G25830;AT5G66320
393	TFmatrixID_0266	GATA;tify	-	0.99	aaAGATCta	AT2G28340;AT2G45050;AT3G54810;AT5G25830;AT5G66320
393	TFmatrixID_0267	GATA;tify	+	1	aaAGATCtaa	AT2G28340;AT2G45050;AT3G60530;AT5G25830;AT5G66320
393	TFmatrixID	GATA;tify	-	1	aaaGATCTaa	AT2G28340;AT2G45050;AT3G60530;AT5G25830;AT5G66320

	_0267					
393	TFmatrixID_0269	GATA;tify	+	0.99	aaaGATCTaaa	AT2G28340;AT2G45050;AT4G32890;AT5G25830;AT5G66320
393	TFmatrixID_0271	GATA;tify	+	0.99	aaaGATCTaa	AT2G45050;AT3G45170;AT4G36240;AT5G25830;AT5G66320
393	TFmatrixID_0271	GATA;tify	-	0.99	aaAGATCTaa	AT2G45050;AT3G45170;AT4G36240;AT5G25830;AT5G66320
393	TF_motif_seq_0239	Dof	+	1	AAAGA	AT1G29160;AT1G64620;AT2G37590;AT3G21270;AT3G45610;AT3G47500;AT4G38000;AT5G39660;AT5G60200;AT5G60850;AT5G62940;AT2G46590;AT1G07640;AT1G21340;AT1G26790;AT1G47655;AT1G51700;AT1G69570;AT2G28510;AT2G28810;AT2G34140;AT3G50410;AT3G55370;AT3G61850;AT4G00940;AT4G21050;AT4G21080;AT4G24060;AT5G02460;AT5G62430;AT5G65590;AT5G66940
394	TFmatrixID_0259	GATA;tify	+	0.95	aaGATCTa	AT1G08000;AT2G28340;AT2G45050;AT5G25830;AT5G66320
394	TFmatrixID_0259	GATA;tify	-	0.92	aAGATCta	AT1G08000;AT2G28340;AT2G45050;AT5G25830;AT5G66320
394	TFmatrixID_0260	GATA;tify	+	0.97	aAGATCta	AT1G08010;AT2G28340;AT2G45050;AT5G25830;AT5G66320
394	TFmatrixID_0260	GATA;tify	-	0.94	aaGATCTa	AT1G08010;AT2G28340;AT2G45050;AT5G25830;AT5G66320
394	TFmatrixID_0265	GATA;tify	+	1	aAGATCtaaa	AT2G45050;AT3G45170;AT3G51080;AT5G25830;AT5G66320
394	TFmatrixID_0266	GATA;tify	+	1	aaGATCTaa	AT2G28340;AT2G45050;AT3G54810;AT5G25830;AT5G66320
394	TF_motif_seq_0254	AP2;ERF	-	0.8	AAGAT	AT3G14230
395	TFmatrixID_0261	GATA	-	1	aGATCTa	AT1G51600;AT4G24470
395	TF_motif_seq_0237	GATA;tify	+	1	AGATC	AT1G51600;AT2G45050;AT3G06740;AT3G16870;AT3G21175;AT3G24050;AT3G54810;AT3G60530;AT4G17570;AT4G24470;AT4G26150;AT4G32890;AT4G34680;AT5G25830;AT5G26930;AT5G56860;AT5G66320;AT2G18380;AT3G50870;AT4G36620
396	TF_motif_seq_0237	GATA;tify	-	1	GATCT	AT1G51600;AT2G45050;AT3G06740;AT3G16870;AT3G21175;AT3G24050;AT3G54810;AT3G60530;AT4G17570;AT4G24470;AT4G26150;AT4G32890;AT4G34680;AT5G25830;AT5G26930;AT5G56860;AT5G66320;AT2G18380;AT3G50870;AT4G36620
397	TF_motif_seq_0254	AP2;ERF	+	1	ATCTA	AT3G14230
398	TFmatrixID_0495	BES1	-	0.87	tctaaACGTGtccg	AT1G75080
400	TFmatrixID_0182	bZIP	+	0.95	taaACGTGtccgg	AT1G45249;AT3G19290
400	TFmatrixID_0183	bZIP	-	0.93	taaACGTGtcc	AT1G49720;AT3G19290
400	TFmatrixID_0184	bZIP	+	0.94	taaACGTGtc	AT1G49720;AT3G19290
400	TF_motif_seq_0029	(Motif sequence only)	-	0.8	taaacGTGTC	ACEATCHS
401	TFmatrixID_0187	bZIP	+	0.96	aaACGTGtcc	AT2G36270
401	TFmatrixID_0193	bZIP	+	0.88	AAACGtgt	AT3G19290;AT4G34000
401	TFmatrixID_0193	bZIP	-	0.88	aaaCGTGT	AT3G19290;AT4G34000
401	TFmatrixID_0194	bZIP	-	0.95	aaACGTGtcc	AT2G35530;AT4G36730
401	TFmatrixID_0202	bZIP	-	0.85	aaACGTGt	AT1G03970;AT5G44080
401	TF_motif_seq_0410	bHLH	+	0.88	AAACGtgt	AT1G32640
401	TF_motif_seq_0410	bHLH	-	0.75	aaaCGTGT	AT1G32640
402	TF_motif_seq_0240	bZIP	-	1	AACGT	AT3G54620;AT4G02640
402	TF_motif_seq_0300	bHLH	+	0.83	AACGTg	AT1G09530;AT2G20180;AT4G17880;AT5G46760
402	TF_motif_seq_0300	bHLH	-	0.83	aACGTG	AT1G09530;AT2G20180;AT4G17880;AT5G46760
402	TF_motif_seq_0248	(Motif sequence only)	+	0.8	AACGT	MYBCOREATCYCB1
402	TF_motif_seq_0249	(Motif sequence only)	-	0.8	AACGT	ABRELATERD1
402	TF_motif_seq_0279	(Motif sequence only)	+	1	AACGTg	T/GBOXATPIN2
402	TF_motif_	(Motif sequence only)	+	1	aACGTGt	ABRERATCAL

	eq_0374					
403	TF_motif_seq_0240	bZIP	+	1	ACGTG	AT3G54620;AT4G02640
403	TF_motif_seq_0249	(Motif sequence only)	+	1	ACGTG	ABRELATERD1
403	TF_motif_seq_0353	(Motif sequence only)	+	1	ACGTGtc	ACGTABREMOTIFA2OSEM
403	TF_motif_seq_0354	(Motif sequence only)	+	1	ACGTGtc	GADOWNAT
405	TF_motif_seq_0261	(Motif sequence only)	-	0.8	GTGTC	SURECOREATSULTR11
405	TF_motif_seq_0263	(Motif sequence only)	-	0.8	GTGTC	SORLIP1AT
407	TF_motif_seq_0258	Dehydrin	-	0.8	GTCCG	U01377
409	TF_motif_seq_0248	(Motif sequence only)	-	0.8	CCGGT	MYBCOREATCYCB1
411	TF_motif_seq_0246	Homeodomain;TALE	-	1	GGTCA	AT1G23380;AT1G62360;AT1G70510;AT4G08150
411	TF_motif_seq_0270	WRKY	-	1	GGTCA	AT1G13960;AT1G18860;AT1G29280;AT1G29860;AT1G30650;AT1G55600;AT1G62300;AT1G64000;AT1G66550;AT1G68150;AT1G69310;AT1G69810;AT1G80590;AT1G80840;AT2G03340;AT2G23320;AT2G24570;AT2G25000;AT2G30250;AT2G30590;AT2G34830;AT2G37260;AT2G38470;AT2G40740;AT2G40750;AT2G44745;AT2G46130;AT2G46400;AT2G47260;AT3G01080;AT3G01970;AT3G04670;AT3G56400;AT3G58710;AT4G01250;AT4G01720;AT4G04450;AT4G12020;AT4G18170;AT4G22070;AT4G23810;AT4G24240;AT4G26440;AT4G26640;AT4G30935;AT4G31550;AT4G31800;AT4G39410;AT5G07100;AT5G13080;AT5G15130;AT5G22570;AT5G24110;AT5G28650;AT5G45050;AT5G45260;AT5G46350;AT5G49520;AT5G52830;AT5G56270
411	TF_motif_seq_0271	bZIP	-	0.8	GGTCA	AT1G77920;AT3G12250;AT5G06950;AT5G06960;AT5G10030;AT5G65210;AT1G22070
412	TFmatrixID_0336	Myb/SANT;MYB	-	0.98	gtcACCTAcca	AT1G22640;AT2G16720;AT4G09460
412	TF_motif_seq_0267	Trihelix	+	0.8	GTCAC	AT5G01380
412	TF_motif_seq_0267	Trihelix	-	0.8	GTCAC	AT5G01380
412	TF_motif_seq_0261	(Motif sequence only)	-	0.8	GTCAC	SURECOREATSULTR11
412	TF_motif_seq_0263	(Motif sequence only)	+	0.8	GTCAC	SORLIP1AT
412	TF_motif_seq_0275	(Motif sequence only)	-	0.8	GTCAC	WBOXATNPR1
413	TFmatrixID_0322	Myb/SANT;MYB	-	0.93	tcACCTAcca	AT5G49330
413	TFmatrixID_0519	Myb/SANT	-	0.89	tcacCTACCaatg	AT3G23250
413	TFmatrixID_0521	Myb/SANT;MYB	-	0.85	tcacCTACCaatg	AT3G49690;AT5G57620;AT5G65790;O49746_ARATH
413	TFmatrixID_0586	Myb/SANT;MYB	-	0.98	tcACCTAcca	AT5G49330
413	TFmatrixID_0587	Myb/SANT;MYB	-	0.97	tcacCTACCa	AT5G49330
413	TFmatrixID_0588	MYB	-	0.96	tcACCTAcca	AT5G12870
414	TFmatrixID_0352	Myb/SANT;MYB	-	1	cACCTAcc	AT2G16720;AT4G09460;AT4G34990;AT4G38620
414	TFmatrixID_0592	MYB	+	0.95	cACCTAccaa	AT4G01680
414	TF_motif_seq_0249	(Motif sequence only)	-	0.8	CACCT	ABRELATERD1
414	TF_motif_seq_0440	(Motif sequence only)	+	1	cACCTAcc	MYBPLANT
415	TF_motif_seq_0254	AP2;ERF	+	0.8	ACCTA	AT3G14230
416	TF_motif_seq_0258	Dehydrin	+	0.8	CCTAC	U01377
420	TF_motif_seq_0257	NF-YB;NF-YA;NF-YC	+	1	CCAAT	AT1G09030;AT1G17590;AT1G21970;AT1G30500;AT1G54160;AT1G54830;AT1G56170;AT1G72830;AT2G38880;AT2G47810;AT3G05690;AT3G14020;AT3G20910;AT3G53340;AT4G14540;AT5G06510;AT5G12840;AT5G27910;AT5G38140;AT5G47640;AT5G47670;AT5G50470;AT5G50480
420	TF_motif_seq_0363	(Motif sequence only)	+	1	CCAATgt	LEAFYATAG
423	TF_motif_seq_0249	(Motif sequence only)	+	0.8	ATGTG	ABRELATERD1
425	TF_motif_seq_0263	(Motif sequence only)	-	0.8	GTGGT	SORLIP1AT
426	TF_motif_	(Motif sequence only)	-	1	TGGTTt	MYB1AT

	eq_0341					
427	TF_motif_seq_0053	(Motif sequence only)	-	0.7	ggtttTGCAA	SORLREP5AT
428	TF_motif_seq_0490	(Motif sequence only)	+	1	GTTTTgcaa	ANAERO4CONSENSUS
431	TFmatrixID_0484	Homeodomain;HD-ZIP;bZIP	-	0.92	ttgcaaaTTATTg	AT1G26960;AT1G69780;AT3G01220;AT5G15150;AT5G65310
432	TFmatrixID_0058	Homeodomain;bZIP;HD-ZIP	+	0.96	tgcaaATTATtgtc	AT3G01470
432	TFmatrixID_0540	Homeodomain;HD-ZIP;bZIP	-	0.95	tgcaaaTTATTgtc	AT1G69780;AT3G01220;AT3G01470;AT5G15150
433	TFmatrixID_0517	Homeodomain;HD-ZIP;bZIP	-	0.97	gcaaaTTATTgt	AT1G69780;AT3G01220;AT3G01470;AT5G15150
434	TF_motif_seq_0257	NF-YB;NF-YA;NF-YC	+	0.8	CAAAT	AT1G09030;AT1G17590;AT1G21970;AT1G30500;AT1G54160;AT1G54830;AT1G56170;AT1G72830;AT2G38880;AT2G47810;AT3G05690;AT3G14020;AT3G20910;AT3G53340;AT4G14540;AT5G06510;AT5G12840;AT5G27910;AT5G38140;AT5G47640;AT5G47670;AT5G50470;AT5G50480
434	TF_motif_seq_0027	(Motif sequence only)	+	1	CAAATtattg	CARGCW8GAT
434	TF_motif_seq_0027	(Motif sequence only)	-	1	caaatTATTG	CARGCW8GAT
435	TFmatrixID_0026	bZIP;Homeodomain;HD-ZIP	+	1	aaATTATtgt	AT5G03790
435	TFmatrixID_0116	Homeodomain;bZIP;HD-ZIP	+	0.93	aaaTTATTg	AT5G65310
435	TFmatrixID_0471	Homeodomain;HD-ZIP;bZIP	-	0.99	aaATTATt	AT1G69780;AT3G01220;AT3G01470;AT5G15150
435	TFmatrixID_0541	Homeodomain;HD-ZIP;bZIP	-	0.94	aaaTTATTg	AT1G26960;AT1G69780;AT3G01220;AT5G15150;AT5G65310
435	TF_motif_seq_0472	Homeodomain;bZIP;HD-ZIP	-	0.88	aaatTATTG	AT5G65310
436	TFmatrixID_0281	Homeodomain;HD-ZIP	+	1	aaTTATTgt	AT1G26960;AT1G69780;AT2G22430;AT3G01220;AT5G15150
436	TFmatrixID_0292	Homeodomain;HD-ZIP	+	0.96	aATTATtg	AT1G26960;AT1G69780;AT3G01220;AT4G40060;AT5G15150
437	TF_motif_seq_0241	ZF-HD	+	1	ATTAT	AT1G75240
440	TF_motif_seq_0257	NF-YB;NF-YA;NF-YC	-	0.8	ATTGT	AT1G09030;AT1G17590;AT1G21970;AT1G30500;AT1G54160;AT1G54830;AT1G56170;AT1G72830;AT2G38880;AT2G47810;AT3G05690;AT3G14020;AT3G20910;AT3G53340;AT4G14540;AT5G06510;AT5G12840;AT5G27910;AT5G38140;AT5G47640;AT5G47670;AT5G50470;AT5G50480
441	TF_motif_seq_0275	(Motif sequence only)	+	0.8	TTGTC	WBOXATNPR1
442	TF_motif_seq_0246	Homeodomain;TALE	-	1	TGTCA	AT1G23380;AT1G62360;AT1G70510;AT4G08150
442	TF_motif_seq_0271	bZIP	-	0.8	TGTCA	AT1G77920;AT3G12250;AT5G06950;AT5G06960;AT5G10030;AT5G65210;AT1G22070
442	TF_motif_seq_0339	WRKY	-	0.95	tGTCAA	AT1G13960;AT1G18860;AT1G29280;AT1G29860;AT1G30650;AT1G55600;AT1G62300;AT1G64000;AT1G66550;AT1G68150;AT1G69310;AT1G69810;AT1G80590;AT1G80840;AT2G03340;AT2G23320;AT2G24570;AT2G25000;AT2G30250;AT2G30590;AT2G34830;AT2G37260;AT2G38470;AT2G40740;AT2G40750;AT2G44745;AT2G46130;AT2G46400;AT2G47260;AT3G01080;AT3G01970;AT3G04670;AT3G56400;AT3G58710;AT4G01250;AT4G01720;AT4G04450;AT4G12020;AT4G18170;AT4G22070;AT4G23810;AT4G24240;AT4G26440;AT4G26640;AT4G30935;AT4G31550;AT4G31800;AT4G39410;AT5G07100;AT5G13080;AT5G15130;AT5G22570;AT5G24110;AT5G28650;AT5G45050;AT5G45260;AT5G46350;AT5G49520;AT5G52830;AT5G56270
443	TF_motif_seq_0275	(Motif sequence only)	-	1	GTCAA	WBOXATNPR1
445	TF_motif_seq_0249	(Motif sequence only)	-	0.8	CAAGT	ABRELATERD1
447	TF_motif_seq_0244	SBP	-	1	AGTAC	AT2G33810;AT2G47070
448	TF_motif_seq_0244	SBP	+	1	GTACC	AT2G33810;AT2G47070
448	TF_motif_seq_0267	Trihelix	-	0.8	GTACC	AT5G01380
450	TFmatrixID_0455	WRKY	-	0.91	accTTGACtat	AT1G18860;AT1G29280;AT1G29860;AT1G55600;AT1G62300;AT1G64000;AT1G66550;AT1G66560;AT1G68150;AT1G69810;AT2G21900;AT2G34830;AT2G40740;AT2G44745;AT2G46400;AT3G01970;AT3G04670;AT3G58710;AT3G62340;AT4G01720;AT4G04450;AT4G11070;AT4G18170;AT4G22070;AT4G23810;AT4G24240;AT4G39410;AT5G15130;AT5G26170;AT5G28650;AT5G41570;AT5G43290;AT5G45050;AT5G45260
450	TFmatrixID_0632	WRKY	+	0.89	accTTGACta	AT3G01970
450	TF_motif_seq_0239	Dof	-	1	ACCTT	AT1G29160;AT1G64620;AT2G37590;AT3G21270;AT3G45610;AT3G47500;AT4G38000;AT5G39660;AT5G60200;AT5G60850;AT5G62940;AT2G46590;AT1G07640;AT1G21340;AT1G26790;AT1G47655;AT1G51700;AT1G69570;AT2G28510;AT2G28810;AT2G34140;AT3G50410;AT3G55370;AT3G61850;AT4G00940;AT4G21050;AT4G21080;AT4G24060;AT5G02460;AT5G62430;AT5G65590;AT5G66940
451	TFmatrixID_0382	NAC;NAM	-	1	ccTTGACta	AT1G01720;AT1G52880;AT1G52890;AT1G69490;AT3G04070;AT3G15500;AT3G15510;AT4G27410
451	TFmatrixID_0453	WRKY	-	0.91	ccTTGACt	AT1G18860;AT1G29280;AT1G29860;AT1G55600;AT1G62300;AT1G64000;AT1G66550;AT1G66560;AT1G68150;AT1G69810;AT1G80590;AT2G21900;AT2G34830;AT2G40740;AT2G40750;AT2G44745;AT2G46400;AT2G47260;AT3G01970;AT3G04670;AT3G56400;AT3G58710;AT3G62340;AT4G04450;AT4G11070;AT4G18170;AT4G22070;AT4G23810;AT4G24240;AT4G39410;AT5G15130;AT5G22570;AT5G26170;AT5G28650;AT5G41570;AT5G43290;AT5G45050
452	TFmatrixID_0445	WRKY	-	1	cTTGACta	AT1G18860;AT1G29280;AT1G29860;AT1G55600;AT1G62300;AT1G64000;AT1G68150;AT1G69810;AT1G80840;AT2G21900;AT2G34830;AT2G44745;AT3G01970;AT3G04670;AT3G58710;AT3G62340;AT4G04450;AT4G18170;AT4G22070;AT4G24240;AT4G39410;AT5G15130;AT5G26170;AT5G28650;AT5G41570;AT5G43290;AT5G45050;AT5G45260
453	TF_motif_s	WRKY	+	1	TTGACt	AT1G13960;AT1G18860;AT1G29280;AT1G29860;AT1G30650;AT1G55600;AT1G62300;AT1G64000;AT1G66550;AT1G68150;AT1G69310;AT1G69810;AT1G80590;AT1G80840;AT2G03340;AT2G23320;AT2G24570;AT2G25000;AT2G30250;AT2G30590;AT2G34830;AT2G37260;AT2G38470;AT2G40740;AT2G40750;AT2G44745;AT2G46130;AT2G46400;AT2G47260;AT3G01080;AT3G01970;AT3G04670;AT3G56400;AT3G58710;AT4G01250;A

	eq_0339					T4G01720;AT4G04450;AT4G12020;AT4G18170;AT4G22070;AT4G23810;AT4G24240;AT4G26440;AT4G26640;AT4G30935;AT4G31550;AT4G31800;AT4G39410;AT5G07100;AT5G13080;AT5G15130;AT5G22570;AT5G24110;AT5G28650;AT5G45050;AT5G45260;AT5G46350;AT5G49520;AT5G52830;AT5G56270
453	TF_motif_seq_0275	(Motif sequence only)	+	1	TTGAC	WBOXATNPR1
454	TF_motif_seq_0246	Homeodomain;TALE	+	1	TGACT	AT1G23380;AT1G62360;AT1G70510;AT4G08150
454	TF_motif_seq_0270	WRKY	+	1	TGACT	AT1G13960;AT1G18860;AT1G29280;AT1G29860;AT1G30650;AT1G55600;AT1G62300;AT1G64000;AT1G66550;AT1G68150;AT1G69310;AT1G69810;AT1G80590;AT1G80840;AT2G03340;AT2G23320;AT2G24570;AT2G25000;AT2G30250;AT2G30590;AT2G34830;AT2G37260;AT2G38470;AT2G40740;AT2G40750;AT2G44745;AT2G46130;AT2G46400;AT2G47260;AT3G01080;AT3G01970;AT3G04670;AT3G56400;AT3G58710;AT4G01250;AT4G01720;AT4G04450;AT4G12020;AT4G18170;AT4G22070;AT4G23810;AT4G24240;AT4G26440;AT4G26640;AT4G30935;AT4G31550;AT4G31800;AT4G39410;AT5G07100;AT5G13080;AT5G15130;AT5G22570;AT5G24110;AT5G28650;AT5G45050;AT5G45260;AT5G46350;AT5G49520;AT5G52830;AT5G56270
454	TF_motif_seq_0271	bZIP	+	0.8	TGACT	AT1G77920;AT3G12250;AT5G06950;AT5G06960;AT5G10030;AT5G65210;AT1G22070
456	TFmatrixID_0144	AT-Hook	+	0.93	actaTATTAaat	AT4G21895;AT5G62260
458	TF_motif_seq_0254	AP2;ERF	-	0.8	TATAT	AT3G14230
459	TFmatrixID_0005	AT-Hook	+	0.92	atATTAAata	AT4G14465
460	TFmatrixID_0476	AT-Hook	+	0.91	tattaaataaAAAAAt	AT1G48610
461	TF_motif_seq_0241	ZF-HD	+	1	ATTAA	AT1G75240
463	TF_motif_seq_0254	AP2;ERF	-	0.8	TAAAT	AT3G14230
465	TFmatrixID_0222	CSD	+	1	aATAAAaa	AT2G21060;AT4G38680
468	TFmatrixID_0129	AT-Hook	+	1	aaaaAAATT	AT1G14900;AT1G48610
468	TFmatrixID_0140	AT-Hook	+	1	aaaAAAAT	AT4G21895;AT5G62260
469	TFmatrixID_0148	AT-Hook	+	1	aaAAAATt	AT1G19485;AT1G48610
470	TFmatrixID_0152	AT-Hook	+	1	aaAAATT	AT1G19485;AT1G48610
475	TF_motif_seq_0275	(Motif sequence only)	+	0.8	TTCAC	WBOXATNPR1
479	TF_motif_seq_0248	(Motif sequence only)	-	0.8	CCGTA	MYBCOREATCYCB1
480	TF_motif_seq_0271	bZIP	-	0.8	CGTAA	AT1G77920;AT3G12250;AT5G06950;AT5G06960;AT5G10030;AT5G65210;AT1G22070
481	TF_motif_seq_0267	Trihelix	+	0.8	GTAAC	AT5G01380
481	TF_motif_seq_0267	Trihelix	-	1	GTAAC	AT5G01380
482	TF_motif_seq_0377	(Motif sequence only)	+	0.84	TAACAca	GAREAT
485	TF_motif_seq_0249	(Motif sequence only)	-	0.8	CACAT	ABRELATERD1
488	TFmatrixID_0610	MYB-related	-	0.98	attGATATtc	AT5G17300
488	TF_motif_seq_0257	NF-YB;NF-YA;NF-YC	-	0.8	ATTGA	AT1G09030;AT1G17590;AT1G21970;AT1G30500;AT1G54160;AT1G54830;AT1G56170;AT1G72830;AT2G38880;AT2G47810;AT3G05690;AT3G14020;AT3G20910;AT3G53340;AT4G14540;AT5G06510;AT5G12840;AT5G27910;AT5G38140;AT5G47640;AT5G47670;AT5G50470;AT5G50480
489	TF_motif_seq_0254	AP2;ERF	-	0.8	TTGAT	AT3G14230
489	TF_motif_seq_0275	(Motif sequence only)	+	0.8	TTGAT	WBOXATNPR1
490	TFmatrixID_0334	Myb/SANT;MYB-related	-	0.97	tGATATtca	AT1G18330;AT3G10113
490	TF_motif_seq_0237	GATA;tify	+	1	TGATA	AT1G51600;AT2G45050;AT3G06740;AT3G16870;AT3G21175;AT3G24050;AT3G54810;AT3G60530;AT4G17570;AT4G24470;AT4G26150;AT4G32890;AT4G34680;AT5G25830;AT5G26930;AT5G56860;AT5G66320;AT2G18380;AT3G50870;AT4G36620
490	TF_motif_seq_0434	(Motif sequence only)	-	0.83	tgaTATTC	P1BS
491	TF_motif_seq_0243	GATA;tify	+	1	GATAT	AT1G51600;AT2G45050;AT3G06740;AT3G16870;AT3G21175;AT3G24050;AT3G54810;AT3G60530;AT4G17570;AT4G24470;AT4G26150;AT4G32890;AT4G34680;AT5G25830;AT5G26930;AT5G56860;AT5G66320;AT2G18380;AT3G50870;AT4G36620
495	TF_motif_seq_0275	(Motif sequence only)	-	0.8	TTCAA	WBOXATNPR1
497	TF_motif_seq_0302	bHLH	+	1	CAACTg	AT5G08130;AT3G26744
497	TF_motif_seq_0302	bHLH	-	1	cAACTG	AT5G08130;AT3G26744
497	TF_motif_s	(Others)	-	1	cAACTG	D14712

	eq_0313					
497	TF_motif_seq_0342	(Motif sequence only)	+	1	cAACTG	MYB2CONSENSUSAT
498	TF_motif_seq_0248	(Motif sequence only)	+	0.8	AACTG	MYBCOREATCYCB1
500	TFmatrixID_0345	Myb/SANT;G2-like	-	1	ctGATTCcta	AT1G79430;AT3G12730;AT3G24120;AT4G13640
501	TFmatrixID_0342	Myb/SANT	-	1	tGATTCcta	AT3G04030
501	TFmatrixID_0358	Myb/SANT	-	0.99	tGATTCctaa	AT5G18240
501	TF_motif_seq_0237	GATA;tify	+	1	TGATT	AT1G51600;AT2G45050;AT3G06740;AT3G16870;AT3G21175;AT3G24050;AT3G54810;AT3G60530;AT4G17570;AT4G24470;AT4G26150;AT4G32890;AT4G34680;AT5G25830;AT5G26930;AT5G56860;AT5G66320;AT2G18380;AT3G50870;AT4G36620
501	TF_motif_seq_0268	(Motif sequence only)	+	1	TGATT	ARR1AT
509	TFmatrixID_0140	AT-Hook	+	1	aaaAAAAT	AT4G21895;AT5G62260
510	TFmatrixID_0148	AT-Hook	+	1	aaAAAATa	AT1G19485;AT1G48610
511	TFmatrixID_0137	AT-Hook	+	1	aaaAATAT	AT4G21895;AT5G62260
513	TF_motif_seq_0434	(Motif sequence only)	-	0.83	aaaTATAC	P1BS
515	TF_motif_seq_0254	AP2;ERF	+	0.8	ATATA	AT3G14230
522	TF_motif_seq_0254	AP2;ERF	+	0.8	AACTA	AT3G14230
525	TF_motif_seq_0131	AP2	-	0.85	tattgggagTTGTG	AT4G37750
526	TF_motif_seq_0257	NF-YB;NF-YA;NF-YC	-	1	ATTGG	AT1G09030;AT1G17590;AT1G21970;AT1G30500;AT1G54160;AT1G54830;AT1G56170;AT1G72830;AT2G38880;AT2G47810;AT3G05690;AT3G14020;AT3G20910;AT3G53340;AT4G14540;AT5G06510;AT5G12840;AT5G27910;AT5G38140;AT5G47640;AT5G47670;AT5G50470;AT5G50480
537	TFmatrixID_0569	TBP	-	0.98	tgagattTTTATat	AT1G55520;AT3G13445
538	TF_motif_seq_0254	AP2;ERF	-	0.8	GAGAT	AT3G14230
538	TF_motif_seq_0261	(Motif sequence only)	+	0.8	GAGAT	SURECOREATSULTR11
539	TF_motif_seq_0237	GATA;tify	+	1	AGATT	AT1G51600;AT2G45050;AT3G06740;AT3G16870;AT3G21175;AT3G24050;AT3G54810;AT3G60530;AT4G17570;AT4G24470;AT4G26150;AT4G32890;AT4G34680;AT5G25830;AT5G26930;AT5G56860;AT5G66320;AT2G18380;AT3G50870;AT4G36620
539	TF_motif_seq_0252	Myb/SANT;MYB;ARR-B	+	1	AGATT	AT2G01760;AT3G16857;AT4G16110;AT4G18020;AT4G31920;AT5G58080;AT1G67710;AT1G49190;AT2G25180;AT5G49240
539	TF_motif_seq_0268	(Motif sequence only)	+	1	AGATT	ARR1AT
539	TF_motif_seq_0403	(Motif sequence only)	-	1	AGATTttt	CCA1ATLHCB1
540	TFmatrixID_0148	AT-Hook	-	0.99	gATTTTtt	AT1G19485;AT1G48610
542	TFmatrixID_0585	TBP	-	0.98	tttTTTATatc	AT1G55520;AT3G13445
545	TFmatrixID_0418	TBP	-	1	ttTATAT	AT1G55520;AT3G13445
547	TF_motif_seq_0254	AP2;ERF	-	0.8	TATAT	AT3G14230
548	TF_motif_seq_0243	GATA;tify	-	1	ATATC	AT1G51600;AT2G45050;AT3G06740;AT3G16870;AT3G21175;AT3G24050;AT3G54810;AT3G60530;AT4G17570;AT4G24470;AT4G26150;AT4G32890;AT4G34680;AT5G25830;AT5G26930;AT5G56860;AT5G66320;AT2G18380;AT3G50870;AT4G36620
549	TF_motif_seq_0237	GATA;tify	-	1	TATCA	AT1G51600;AT2G45050;AT3G06740;AT3G16870;AT3G21175;AT3G24050;AT3G54810;AT3G60530;AT4G17570;AT4G24470;AT4G26150;AT4G32890;AT4G34680;AT5G25830;AT5G26930;AT5G56860;AT5G66320;AT2G18380;AT3G50870;AT4G36620
552	TFmatrixID_0211	C2H2	-	1	cAGTGTt	AT1G27730;AT3G49930;AT3G60580;AT5G04340;AT5G43170
552	TFmatrixID_0213	C2H2	-	1	cAGTGTt	AT1G02030;AT2G45120;AT3G19580;AT3G49930;AT3G60580;AT5G04340;AT5G43170
555	TF_motif_seq_0255	AP2;RAV;B3	-	1	TGTTG	AT1G25560;AT1G13260
555	TF_motif_seq_0349	(Others)	-	0.86	tgTTGGT	X67670;X67671
556	TF_motif_seq_0257	NF-YB;NF-YA;NF-YC	-	0.8	GTTGG	AT1G09030;AT1G17590;AT1G21970;AT1G30500;AT1G54160;AT1G54830;AT1G56170;AT1G72830;AT2G38880;AT2G47810;AT3G05690;AT3G14020;AT3G20910;AT3G53340;AT4G14540;AT5G06510;AT5G12840;AT5G27910;AT5G38140;AT5G47640;AT5G47670;AT5G50470;AT5G50480
556	TF_motif_s	Dehydrin	-	0.8	GTTGG	U01377

	eq_0258					
560	TFmatrixID_0638	Dof	-	0.98	gtcTCTTTac	AT5G65590
560	TF_motif_seq_0261	(Motif sequence only)	-	1	GTCTC	SURECOREATSULTR11
563	TF_motif_seq_0239	Dof	-	1	TCTTT	AT1G29160;AT1G64620;AT2G37590;AT3G21270;AT3G45610;AT3G47500;AT4G38000;AT5G39660;AT5G60200;AT5G60850;AT5G62940;AT2G46590;AT1G07640;AT1G21340;AT1G26790;AT1G47655;AT1G51700;AT1G69570;AT2G28510;AT2G28810;AT2G34140;AT3G50410;AT3G55370;AT3G61850;AT4G00940;AT4G21050;AT4G21080;AT4G24060;AT5G02460;AT5G62430;AT5G65590;AT5G66940
565	TF_motif_seq_0267	Trihelix	+	0.8	TTTAC	AT5G01380
565	TF_motif_seq_0275	(Motif sequence only)	+	0.8	TTTAC	WBOXATNPR1
567	TF_motif_seq_0254	AP2;ERF	-	0.8	TACAT	AT3G14230
569	TF_motif_seq_0302	bHLH	+	1	CATTTg	AT5G08130;AT3G26744
569	TF_motif_seq_0302	bHLH	-	1	cATTTG	AT5G08130;AT3G26744
570	TF_motif_seq_0257	NF-YB;NF-YA;NF-YC	-	0.8	ATTTG	AT1G09030;AT1G17590;AT1G21970;AT1G30500;AT1G54160;AT1G54830;AT1G56170;AT1G72830;AT2G38880;AT2G47810;AT3G05690;AT3G14020;AT3G20910;AT3G53340;AT4G14540;AT5G06510;AT5G12840;AT5G27910;AT5G38140;AT5G47640;AT5G47670;AT5G50470;AT5G50480
571	TF_motif_seq_0009	(Motif sequence only)	-	0.7	tttgtGATGT	LS7ATPR1
575	TF_motif_seq_0237	GATA;tify	+	1	TGATG	AT1G51600;AT2G45050;AT3G06740;AT3G16870;AT3G21175;AT3G24050;AT3G54810;AT3G60530;AT4G17570;AT4G24470;AT4G26150;AT4G32890;AT4G34680;AT5G25830;AT5G26930;AT5G56860;AT5G66320;AT2G18380;AT3G50870;AT4G36620
575	TF_motif_seq_0271	bZIP	+	0.8	TGATG	AT1G77920;AT3G12250;AT5G06950;AT5G06960;AT5G10030;AT5G65210;AT1G22070
577	TF_motif_seq_0249	(Motif sequence only)	+	0.8	ATGTG	ABRELATERD1
579	TF_motif_seq_0263	(Motif sequence only)	-	0.8	GTGGT	SORLIP1AT
584	TFmatrixID_0491	TBP	+	0.91	gttatagcaTATATagtaata	AT1G55520;AT3G13445
584	TFmatrixID_0572	TBP	+	0.91	gttatagcaTATATagtaata	AT1G55520;AT3G13445
584	TF_motif_seq_0267	Trihelix	+	0.8	GTTAT	AT5G01380
590	TF_motif_seq_0434	(Motif sequence only)	+	0.83	GCATAtat	P1BS
592	TF_motif_seq_0254	AP2;ERF	+	0.8	ATATA	AT3G14230
593	TF_motif_seq_0254	AP2;ERF	-	0.8	TATAT	AT3G14230
594	TF_motif_seq_0254	AP2;ERF	+	0.8	ATATA	AT3G14230
598	TFmatrixID_0131	AT-Hook	+	1	agtaATAAA	AT1G19485;AT1G48610
599	TF_motif_seq_0241	ZF-HD	-	1	GTAAT	AT1G75240
599	TF_motif_seq_0267	Trihelix	-	0.8	GTAAT	AT5G01380
602	TFmatrixID_0500	MADS box;MIKC	+	0.82	ataaactcaaaaGGAAAtta	AT4G22950;AT4G24540;AT4G37940;AT5G23260;AT5G51860;AT5G51870;AT5G62165;AT2G14210;AT2G22540;AT2G45650;AT3G57390;AT4G11880
604	TFmatrixID_0493	MADS box;MIKC	+	0.86	aaactcaaaaGGAAA	AT4G22950;AT4G24540;AT5G13790;AT5G51860;AT5G51870;AT5G60910;AT5G62165;AT1G26310;AT2G14210;AT2G45650;AT3G30260;AT3G57230;AT3G57390;AT3G61120;AT4G09960;AT4G11880
606	TF_motif_seq_0399	(Motif sequence only)	-	0.84	acTCAAA	WBBOXPCWRKY1
607	TF_motif_seq_0275	(Motif sequence only)	-	0.8	CTCAA	WBOXATNPR1
611	TF_motif_seq_0239	Dof	+	1	AAAGG	AT1G29160;AT1G64620;AT2G37590;AT3G21270;AT3G45610;AT3G47500;AT4G38000;AT5G39660;AT5G60200;AT5G60850;AT5G62940;AT2G46590;AT1G07640;AT1G21340;AT1G26790;AT1G47655;AT1G51700;AT1G69570;AT2G28510;AT2G28810;AT2G34140;AT3G50410;AT3G55370;AT3G61850;AT4G00940;AT4G21050;AT4G21080;AT4G24060;AT5G02460;AT5G62430;AT5G65590;AT5G66940
611	TF_motif_seq_0248	(Motif sequence only)	+	0.8	AAAGG	MYBCOREATCYCB1
612	TF_motif_seq_0239	Dof	+	1	AAGGA	AT1G29160;AT1G64620;AT2G37590;AT3G21270;AT3G45610;AT3G47500;AT4G38000;AT5G39660;AT5G60200;AT5G60850;AT5G62940;AT2G46590;AT1G07640;AT1G21340;AT1G26790;AT1G47655;AT1G51700;AT1G69570;AT2G28510;AT2G28810;AT2G34140;AT3G50410;AT3G55370;AT3G61850;AT4G00940;AT4G21050;AT4G21080;AT4G24060;AT5G02460;AT5G62430;AT5G65590;AT5G66940
614	TF_motif_seq_0321	(Motif sequence only)	+	1	GGAAAt	GT1CONSENSUS
618	TF_motif_seq_0241	ZF-HD	+	1	ATTAG	AT1G75240
618	TF_motif_s	NF-YB;NF-YA;NF-YC	-	0.8	ATTAG	AT1G09030;AT1G17590;AT1G21970;AT1G30500;AT1G54160;AT1G54830;AT1G56170;AT1G72830;AT2G38880;AT2G47810;AT3G05690;AT3G14020;AT3G20910;AT3G53340;AT4G14540;AT5G06510;AT5G12840;AT5G27910;AT5G38140;AT5G47640;AT5G47670;AT5G50470;AT5G50480

	eq_0257					
620	TF_motif_seq_0254	AP2;ERF	-	1	TAGAT	AT3G14230
621	TFmatrixID_0193	bZIP	-	0.75	agaTGTGT	AT3G19290;AT4G34000
621	TF_motif_seq_0237	GATA;tify	+	1	AGATG	AT1G51600;AT2G45050;AT3G06740;AT3G16870;AT3G21175;AT3G24050;AT3G54810;AT3G60530;AT4G17570;AT4G24470;AT4G26150;AT4G32890;AT4G34680;AT5G25830;AT5G26930;AT5G56860;AT5G66320;AT2G18380;AT3G50870;AT4G36620
623	TF_motif_seq_0249	(Motif sequence only)	+	0.8	ATGTG	ABRELATERD1
624	TF_motif_seq_0343	(Motif sequence only)	-	0.86	tgTGTTT	ANAERO1CONSENSUS
625	TF_motif_seq_0415	(Motif sequence only)	-	0.88	gtgTTTG	CDA1ATCAB2
627	TFmatrixID_0446	WRKY	-	0.99	gttTTGACca	AT1G18860;AT1G29280;AT1G29860;AT1G55600;AT1G62300;AT1G64000;AT1G68150;AT1G69810;AT2G21900;AT2G23320;AT2G34830;AT2G40740;AT2G44745;AT3G01970;AT3G04670;AT3G58710;AT3G62340;AT4G04450;AT4G11070;AT4G18170;AT4G22070;AT4G23810;AT4G24240;AT4G39410;AT5G15130;AT5G22570;AT5G26170;AT5G28650;AT5G41570;AT5G43290;AT5G45050;AT5G45260
627	TFmatrixID_0448	WRKY	-	0.98	gttTTGACcat	AT1G18860;AT1G29280;AT1G29860;AT1G55600;AT1G62300;AT1G64000;AT1G68150;AT1G69810;AT2G21900;AT2G25000;AT2G34830;AT2G44745;AT2G46400;AT3G01970;AT3G04670;AT3G58710;AT3G62340;AT4G04450;AT4G11070;AT4G18170;AT4G22070;AT4G24240;AT4G39410;AT5G15130;AT5G26170;AT5G28650;AT5G41570;AT5G43290;AT5G45050
628	TFmatrixID_0382	NAC;NAM	-	1	ttTTGACca	AT1G01720;AT1G52880;AT1G52890;AT1G69490;AT3G04070;AT3G15500;AT3G15510;AT4G27410
628	TFmatrixID_0451	WRKY	-	1	ttTTGACcat	AT1G13960;AT2G03340;AT2G37260;AT2G38470;AT3G01080;AT4G12020;AT4G26440;AT4G26640;AT4G30935;AT5G07100
628	TFmatrixID_0458	WRKY	-	1	ttTTGACcat	AT1G18860;AT1G29280;AT1G29860;AT1G55600;AT1G62300;AT1G64000;AT1G68150;AT1G69810;AT2G21900;AT2G34830;AT2G40740;AT2G44745;AT2G46400;AT3G01970;AT3G04670;AT3G58710;AT3G62340;AT4G04450;AT4G11070;AT4G18170;AT4G22070;AT4G24240;AT4G31800;AT4G39410;AT5G15130;AT5G26170;AT5G28650;AT5G41570;AT5G43290;AT5G45050
628	TFmatrixID_0462	WRKY	-	0.99	ttTTGACca	AT1G18860;AT1G29280;AT1G29860;AT1G55600;AT1G62300;AT1G64000;AT1G66550;AT1G66560;AT1G68150;AT1G69810;AT1G80590;AT2G21900;AT2G34830;AT2G44745;AT3G01970;AT3G04670;AT3G58710;AT3G62340;AT4G04450;AT4G11070;AT4G18170;AT4G22070;AT4G23810;AT4G24240;AT4G39410;AT5G15130;AT5G22570;AT5G26170;AT5G28650;AT5G41570;AT5G43290;AT5G45050;AT5G45260;ATSG46350
628	TFmatrixID_0463	WRKY	-	1	ttTTGACcat	AT1G18860;AT1G29280;AT1G29860;AT1G55600;AT1G62300;AT1G64000;AT1G66550;AT1G66560;AT1G68150;AT1G69810;AT1G80590;AT2G21900;AT2G34830;AT2G40740;AT2G44745;AT2G46400;AT3G01970;AT3G04670;AT3G56400;AT3G58710;AT3G62340;AT4G04450;AT4G11070;AT4G18170;AT4G22070;AT4G23810;AT4G24240;AT4G39410;AT5G15130;AT5G22570;AT5G26170;AT5G28650;AT5G41570;AT5G43290;AT5G45050;AT5G45260;AT5G49520
628	TFmatrixID_0464	WRKY	-	1	ttTTGACca	AT1G18860;AT1G29280;AT1G29860;AT1G55600;AT1G62300;AT1G64000;AT1G66550;AT1G66560;AT1G68150;AT1G69810;AT1G80590;AT2G21900;AT2G34830;AT2G40740;AT2G40750;AT2G44745;AT2G46400;AT3G01970;AT3G04670;AT3G56400;AT3G58710;AT3G62340;AT4G04450;AT4G11070;AT4G18170;AT4G22070;AT4G23810;AT4G24240;AT4G39410;AT5G15130;AT5G22570;AT5G26170;AT5G28650;AT5G41570;AT5G43290;AT5G45050;AT5G45260;AT5G52830
628	TFmatrixID_0466	WRKY	-	1	ttTTGACcat	AT1G18860;AT1G29280;AT1G29860;AT1G55600;AT1G62300;AT1G64000;AT1G68150;AT1G69810;AT2G21900;AT2G34830;AT2G44745;AT3G01970;AT3G04670;AT3G58710;AT3G62340;AT4G04450;AT4G18170;AT4G22070;AT4G24240;AT4G39410;AT5G15130;AT5G26170;AT5G28650;AT5G41570;AT5G43290;AT5G45050;AT5G64810
628	TFmatrixID_0468	WRKY	-	0.99	ttTTGACca	AT1G18860;AT1G29280;AT1G29860;AT1G55600;AT1G62300;AT1G64000;AT1G66550;AT1G66560;AT1G68150;AT1G69810;AT1G80590;AT2G21900;AT2G34830;AT2G40740;AT2G40750;AT2G44745;AT2G46400;AT3G01970;AT3G04670;AT3G56400;AT3G58710;AT3G62340;AT4G04450;AT4G11070;AT4G18170;AT4G22070;AT4G23810;AT4G24240;AT4G39410;AT5G15130;AT5G22570;AT5G26170;AT5G28650;AT5G41570;AT5G43290;AT5G45050;AT5G45260
628	TFmatrixID_0630	WRKY	-	0.95	ttTTGACcat	AT4G31800
629	TFmatrixID_0443	WRKY	-	0.99	tTTGACca	AT1G29860;AT1G64000;AT1G66550;AT1G66560;AT1G66600;AT1G68150;AT1G69810;AT1G80590;AT2G40740;AT2G40750;AT2G44745;AT2G46400;AT3G01970;AT3G56400;AT3G62340;AT4G04450;AT4G11070;AT4G18170;AT4G22070;AT4G23810;AT4G39410;AT5G22570;AT5G26170;AT5G41570;AT5G43290;AT5G45050;AT5G45260
629	TFmatrixID_0445	WRKY	-	1	tTTGACca	AT1G18860;AT1G29280;AT1G29860;AT1G55600;AT1G62300;AT1G64000;AT1G68150;AT1G69810;AT1G80840;AT2G21900;AT2G34830;AT2G44745;AT3G01970;AT3G04670;AT3G58710;AT3G62340;AT4G04450;AT4G18170;AT4G22070;AT4G24240;AT4G39410;AT5G15130;AT5G26170;AT5G28650;AT5G41570;AT5G43290;AT5G45050;AT5G45260
629	TFmatrixID_0449	WRKY	-	0.97	tTTGACca	AT1G13960;AT2G03340;AT2G30250;AT2G37260;AT3G01080;AT4G12020;AT4G26440;AT4G26640;AT4G30935;AT5G07100
629	TFmatrixID_0459	WRKY	-	0.96	tTTGACca	AT1G29280;AT1G29860;AT1G64000;AT1G66550;AT1G66560;AT1G69810;AT1G80590;AT2G40740;AT2G40750;AT2G44745;AT2G46400;AT3G01970;AT3G56400;AT3G62340;AT4G11070;AT4G18170;AT4G23810;AT4G24240;AT5G01900;AT5G22570;AT5G26170;AT5G41570;AT5G43290;AT5G45050;AT5G45260
629	TFmatrixID_0465	WRKY	-	0.99	tTTGACca	AT1G13960;AT2G03340;AT2G37260;AT3G01080;AT4G12020;AT4G26440;AT4G26640;AT4G30935;AT5G07100;AT5G56270
629	TF_motif_seq_0399	(Motif sequence only)	+	1	TTTGAcc	WBBOXPCWRKY1
630	TFmatrixID_0534	WRKY	-	0.87	TTGACcattta	AT1G13960;AT2G03340;AT2G04880;AT2G37260;AT3G01080;AT4G12020;AT4G26440;AT4G26640;AT4G30935;AT5G07100
630	TF_motif_seq_0339	WRKY	+	1	TTGACc	AT1G13960;AT1G18860;AT1G29280;AT1G29860;AT1G30650;AT1G55600;AT1G62300;AT1G64000;AT1G66550;AT1G68150;AT1G69310;AT1G69810;AT1G80590;AT1G80840;AT2G03340;AT2G23320;AT2G24570;AT2G25000;AT2G30250;AT2G30590;AT2G34830;AT2G37260;AT2G38470;AT2G40740;AT2G40750;AT2G44745;AT2G46130;AT2G46400;AT2G47260;AT3G01080;AT3G01970;AT3G04670;AT3G56400;AT3G58710;AT4G01250;AT4G01720;AT4G04450;AT4G12020;AT4G18170;AT4G22070;AT4G23810;AT4G24240;AT4G26440;AT4G26640;AT4G30935;AT4G31550;AT4G31800;AT4G39410;AT5G07100;AT5G13080;AT5G15130;AT5G22570;AT5G24110;AT5G28650;AT5G45050;AT5G45260;AT5G46350;AT5G49520;AT5G52830;AT5G56270
630	TF_motif_seq_0275	(Motif sequence only)	+	1	TTGAC	WBOXATNPR1
631	TF_motif_seq_0246	Homeodomain;TALE	+	1	TGACC	AT1G23380;AT1G62360;AT1G70510;AT4G08150
631	TF_motif_seq_0270	WRKY	+	1	TGACC	AT1G13960;AT1G18860;AT1G29280;AT1G29860;AT1G30650;AT1G55600;AT1G62300;AT1G64000;AT1G66550;AT1G68150;AT1G69310;AT1G69810;AT1G80590;AT1G80840;AT2G03340;AT2G23320;AT2G24570;AT2G25000;AT2G30250;AT2G30590;AT2G34830;AT2G37260;AT2G38470;AT2G40740;AT2G40750;AT2G44745;AT2G46130;AT2G46400;AT2G47260;AT3G01080;AT3G01970;AT3G04670;AT3G56400;AT3G58710;AT4G01250;AT4G01720;AT4G04450;AT4G12020;AT4G18170;AT4G22070;AT4G23810;AT4G24240;AT4G26440;AT4G26640;AT4G30935;AT4G31550;AT4G31800;AT4G39410;AT5G07100;AT5G13080;AT5G15130;AT5G22570;AT5G24110;AT5G28650;AT5G45050;AT5G45260;AT5G46350;AT5G49520;AT5G52830;AT5G56270
631	TF_motif_seq_0271	bZIP	+	0.8	TGACC	AT1G77920;AT3G12250;AT5G06950;AT5G06960;AT5G10030;AT5G65210;AT1G22070
634	TF_motif_seq_0257	NF-YB;NF-YA;NF-YC	+	0.8	CCATT	AT1G09030;AT1G17590;AT1G21970;AT1G30500;AT1G54160;AT1G54830;AT1G56170;AT1G72830;AT2G38880;AT2G47810;AT3G05690;AT3G14020;AT3G20910;AT3G53340;AT4G14540;AT5G06510;AT5G12840;AT5G27910;AT5G38140;AT5G47640;AT5G47670;AT5G50470;AT5G50480
634	TF_motif_seq_0248	(Motif sequence only)	-	0.8	CCATT	MYBCOREATCYCB1
636	TF_motif_seq_0254	AP2;ERF	+	0.8	ATTTA	AT3G14230
640	TF_motif_seq_0241	ZF-HD	+	1	ATTAA	AT1G75240
650	TF_motif_	Dof	-	1	ACCTT	AT1G29160;AT1G64620;AT2G37590;AT3G21270;AT3G45610;AT3G47500;AT4G38000;AT5G39660;AT5G60200;AT5G60850;AT5G62940;AT2G46590;AT1G07640;AT1G21340;AT1G26790;AT1G47655;AT1G51700;AT1G69570;AT2G28510;AT2G28810;AT2G34140;AT3G50410;AT3G55370;AT3G61850;AT4G00940;AT4G21050;AT4G21080;AT4G24060;AT5G02460;AT5G62430;AT5G65590;AT5G66940

	eq_0239					
651	TF_motif_seq_0239	Dof	-	1	CCTTT	AT1G29160;AT1G64620;AT2G37590;AT3G21270;AT3G45610;AT3G47500;AT4G38000;AT5G39660;AT5G60200;AT5G60850;AT5G62940;AT2G46590;AT1G07640;AT1G21340;AT1G26790;AT1G47655;AT1G51700;AT1G69570;AT2G28510;AT2G28810;AT2G34140;AT3GS0410;AT3GS5370;AT3G61850;AT4G00940;AT4G21050;AT4G21080;AT4G24060;AT5G02460;AT5G62430;AT5G65590;AT5G66940
651	TF_motif_seq_0248	(Motif sequence only)	-	0.8	CCTTT	MYBCOREATCYCB1
658	TF_motif_seq_0275	(Motif sequence only)	+	0.8	TTGTC	WBOXATNPR1
659	TF_motif_seq_0246	Homeodomain;TALE	-	1	TGTCA	AT1G23380;AT1G62360;AT1G70510;AT4G08150
659	TF_motif_seq_0271	bZIP	-	0.8	TGTCA	AT1G77920;AT3G12250;AT5G06950;AT5G06960;AT5G10030;AT5G65210;AT1G22070
659	TF_motif_seq_0339	WRKY	-	0.95	tGTCAA	AT1G13960;AT1G18860;AT1G29280;AT1G29860;AT1G30650;AT1GS5600;AT1G62300;AT1G64000;AT1G66550;AT1G68150;AT1G69310;AT1G69810;AT1G80590;AT1G80840;AT2G03340;AT2G23320;AT2G24570;AT2G25000;AT2G30250;AT2G30590;AT2G34830;AT2G37260;AT2G38470;AT2G40740;AT2G40750;AT2G44745;AT2G46130;AT2G46400;AT2G47260;AT3G01080;AT3G01970;AT3G04670;AT3GS6400;AT3GS8710;AT4G01250;AT4G01720;AT4G04450;AT4G12020;AT4G18170;AT4G22070;AT4G23810;AT4G24240;AT4G26440;AT4G26640;AT4G30935;AT4G31550;AT4G31800;AT4G39410;AT5G07100;AT5G13080;AT5G15130;AT5G22570;AT5G24110;AT5G28650;AT5G45050;AT5G45260;AT5G46350;AT5G49520;AT5G52830;AT5G56270
659	TF_motif_seq_0399	(Motif sequence only)	-	0.96	tgTCAAA	WBBOXPCWRKY1
660	TF_motif_seq_0275	(Motif sequence only)	-	1	GTCAA	WBOXATNPR1
666	TFmatrixID_0227	TCR;CPP	+	0.97	caTTTGAaaa	AT4G29000
666	TF_motif_seq_0302	bHLH	+	1	CATTTg	AT5G08130;AT3G26744
666	TF_motif_seq_0302	bHLH	-	1	cATTTG	AT5G08130;AT3G26744
667	TF_motif_seq_0257	NF-YB;NF-YA;NF-YC	-	0.8	ATTTG	AT1G09030;AT1G17590;AT1G21970;AT1G30500;AT1G54160;AT1GS4830;AT1GS6170;AT1G72830;AT2G38880;AT2G47810;AT3G05690;AT3G14020;AT3G20910;AT3G53340;AT4G14540;AT5G06510;AT5G12840;AT5G27910;AT5G38140;AT5G47640;AT5G47670;AT5GS0470;AT5GS0480
669	TF_motif_seq_0275	(Motif sequence only)	+	0.8	TTGAA	WBOXATNPR1
671	TF_motif_seq_0321	(Motif sequence only)	+	1	GAAAAa	GT1CONSENSUS
676	TF_motif_seq_0410	bHLH	+	0.75	ATACTagt	AT1G32640
680	TF_motif_seq_0254	AP2;ERF	-	0.8	TAGTT	AT3G14230
685	TFmatrixID_0508	MADS box;MIKC	-	0.91	tttttTTTTGg	AT4G22950;AT4G24540;AT5G51860;AT5G60910;AT5G62165;AT1G24260;AT1G26310;AT2G45650;AT3G30260;AT3G57230;AT3G57390;AT3G61120;AT4G09960;AT4G11880
691	TF_motif_seq_0257	NF-YB;NF-YA;NF-YC	-	0.8	TTTGG	AT1G09030;AT1G17590;AT1G21970;AT1G30500;AT1G54160;AT1GS4830;AT1GS6170;AT1G72830;AT2G38880;AT2G47810;AT3G05690;AT3G14020;AT3G20910;AT3G53340;AT4G14540;AT5G06510;AT5G12840;AT5G27910;AT5G38140;AT5G47640;AT5G47670;AT5GS0470;AT5GS0480
692	TF_motif_seq_0263	(Motif sequence only)	-	0.8	TTGGC	SORLIP1AT
692	TF_motif_seq_0275	(Motif sequence only)	+	0.8	TTGGC	WBOXATNPR1
693	TFmatrixID_0242	Dof	+	0.97	tggcAACGTtg	AT5G60850
694	TF_motif_seq_0275	(Motif sequence only)	-	0.8	GGCAA	WBOXATNPR1
695	TFmatrixID_0125	AP2;B3	+	0.99	gcAACGTtgt	AT1G50680;AT1G51120
695	TFmatrixID_0125	AP2;B3	-	0.99	gcaACGTTgt	AT1G50680;AT1G51120
695	TF_motif_seq_0267	Trihelix	-	0.8	GCAAC	AT5G01380
695	TF_motif_seq_0263	(Motif sequence only)	+	0.8	GCAAC	SORLIP1AT
696	TFmatrixID_0242	Dof	-	0.97	caACGTTgtaa	AT5G60850
697	TF_motif_seq_0240	bZIP	-	1	AACGT	AT3G54620;AT4G02640
697	TF_motif_seq_0248	(Motif sequence only)	+	0.8	AACGT	MYBCOREATCYCB1
697	TF_motif_seq_0249	(Motif sequence only)	-	0.8	AACGT	ABRELATERD1
698	TF_motif_seq_0240	bZIP	+	1	ACGTT	AT3G54620;AT4G02640
698	TF_motif_seq_0009	(Motif sequence only)	+	0.7	ACGTTgtaaa	LS7ATPR1
698	TF_motif_seq_0248	(Motif sequence only)	-	0.8	ACGTT	MYBCOREATCYCB1
698	TF_motif_s	(Motif sequence only)	+	0.8	ACGTT	ABRELATERD1

	eq_0249					
703	TFmatrixID_0146	AT-Hook	+	1	gtaaATAAT	AT4G21895;AT5G62260
703	TF_motif_seq_0267	Trihelix	-	0.8	GTAAA	AT5G01380
703	TF_motif_seq_0275	(Motif sequence only)	-	0.8	GTAAA	WBOXATNPR1
704	TF_motif_seq_0254	AP2;ERF	-	0.8	TAAAT	AT3G14230
706	TFmatrixID_0471	Homeodomain;HD-ZIP;bZIP	+	0.92	aATAATag	AT1G69780;AT3G01220;AT3G01470;AT5G15150
707	TF_motif_seq_0241	ZF-HD	-	1	ATAAT	AT1G75240
711	TF_motif_seq_0254	AP2;ERF	-	0.8	TAGTT	AT3G14230
713	TF_motif_seq_0267	Trihelix	+	0.8	GTTAA	AT5G01380
713	TF_motif_seq_0275	(Motif sequence only)	-	0.8	GTTAA	WBOXATNPR1
720	TFmatrixID_0044	MYB;G2-like	-	0.91	atAGATTtta	AT2G20570
721	TF_motif_seq_0254	AP2;ERF	-	1	TAGAT	AT3G14230
722	TF_motif_seq_0237	GATA;tify	+	1	AGATT	AT1G51600;AT2G45050;AT3G06740;AT3G16870;AT3G21175;AT3G24050;AT3G54810;AT3G60530;AT4G17570;AT4G24470;AT4G26150;AT4G32890;AT4G34680;AT5G25830;AT5G26930;AT5G56860;AT5G66320;AT2G18380;AT3G50870;AT4G36620
722	TF_motif_seq_0252	Myb/SANT;MYB;ARR-B	+	1	AGATT	AT2G01760;AT3G16857;AT4G16110;AT4G18020;AT4G31920;AT5G58080;AT1G67710;AT1G49190;AT2G25180;AT5G49240
722	TF_motif_seq_0268	(Motif sequence only)	+	1	AGATT	ARR1AT
722	TF_motif_seq_0403	(Motif sequence only)	-	0.86	AGATTtta	CCA1ATLHCB1
731	TF_motif_seq_0261	(Motif sequence only)	-	1	GTCTC	SURECOREATSULTR11
733	TF_motif_seq_0249	(Motif sequence only)	-	0.8	CTCGT	ABRELATERD1
734	TF_motif_seq_0248	(Motif sequence only)	-	0.8	TCGTT	MYBCOREATCYCB1
741	TFmatrixID_0131	AT-Hook	-	1	TTTATgcat	AT1G19485;AT1G48610
742	TFmatrixID_0256	EIN3;EIL	+	0.99	ttATGCAtat	AT3G20770;AT5G21120;AT5G65100
742	TFmatrixID_0256	EIN3;EIL	-	0.99	ttaTGCATat	AT3G20770;AT5G21120;AT5G65100
746	TF_motif_seq_0434	(Motif sequence only)	+	0.83	GCATAtag	P1BS
748	TF_motif_seq_0254	AP2;ERF	+	0.8	ATATA	AT3G14230
751	TF_motif_seq_0254	AP2;ERF	-	0.8	TAGTT	AT3G14230
753	TF_motif_seq_0267	Trihelix	+	0.8	GTTTC	AT5G01380
753	TF_motif_seq_0261	(Motif sequence only)	-	0.8	GTTTC	SURECOREATSULTR11
758	TF_motif_seq_0257	NF-YB;NF-YA;NF-YC	-	0.8	ATTCG	AT1G09030;AT1G17590;AT1G21970;AT1G30500;AT1G54160;AT1G54830;AT1G56170;AT1G72830;AT2G38880;AT2G47810;AT3G05690;AT3G14020;AT3G20910;AT3G53340;AT4G14540;AT5G06510;AT5G12840;AT5G27910;AT5G38140;AT5G47640;AT5G47670;AT5G50470;AT5G50480
762	TF_motif_seq_0239	Dof	-	1	GCTTT	AT1G29160;AT1G64620;AT2G37590;AT3G21270;AT3G45610;AT3G47500;AT4G38000;AT5G39660;AT5G60200;AT5G60850;AT5G62940;AT2G46590;AT1G07640;AT1G21340;AT1G26790;AT1G47655;AT1G51700;AT1G69570;AT2G28510;AT2G28810;AT2G34140;AT3G50410;AT3G55370;AT3G61850;AT4G00940;AT4G21050;AT4G21080;AT4G24060;AT5G02460;AT5G62430;AT5G65590;AT5G66940
764	TFmatrixID_0131	AT-Hook	-	1	TTTATtaga	AT1G19485;AT1G48610
767	TF_motif_seq_0241	ZF-HD	+	1	ATTAG	AT1G75240
767	TF_motif_seq_0257	NF-YB;NF-YA;NF-YC	-	0.8	ATTAG	AT1G09030;AT1G17590;AT1G21970;AT1G30500;AT1G54160;AT1G54830;AT1G56170;AT1G72830;AT2G38880;AT2G47810;AT3G05690;AT3G14020;AT3G20910;AT3G53340;AT4G14540;AT5G06510;AT5G12840;AT5G27910;AT5G38140;AT5G47640;AT5G47670;AT5G50470;AT5G50480
769	TF_motif_seq_0254	AP2;ERF	-	0.8	TAGAC	AT3G14230
769	TF_motif_seq_0261	(Motif sequence only)	+	0.8	TAGAC	SURECOREATSULTR11
769	TF_motif_s	(Motif sequence only)	+	0.8	TAGAC	WBOXATNPR1

	eq_0275					
771	TF_motif_seq_0261	(Motif sequence only)	-	0.8	GACTC	SURECOREATSULTR11
772	TF_motif_seq_0399	(Motif sequence only)	-	0.84	acTCAAA	WBBOXPCWRKY1
773	TF_motif_seq_0275	(Motif sequence only)	-	0.8	CTCAA	WBOXATNPR1
775	TF_motif_seq_0257	NF-YB;NF-YA;NF-YC	+	0.8	CAAAT	AT1G09030;AT1G17590;AT1G21970;AT1G30500;AT1G54160;AT1G54830;AT1G56170;AT1G72830;AT2G38880;AT2G47810;AT3G05690;AT3G14020;AT3G20910;AT3G53340;AT4G14540;AT5G06510;AT5G12840;AT5G27910;AT5G38140;AT5G47640;AT5G47670;AT5G50470;AT5G50480
776	TF_motif_seq_0434	(Motif sequence only)	-	0.83	aaaTATAC	P1BS
778	TF_motif_seq_0254	AP2;ERF	+	0.8	ATATA	AT3G14230
780	TFmatrixID_0233	Dof	-	1	ataCTTTTaa	AT1G64620
780	TFmatrixID_0237	Dof	-	0.99	ataCTTTTa	AT3G47500
780	TF_motif_seq_0410	bHLH	+	0.75	ATACTttt	AT1G32640
782	TFmatrixID_0235	Dof	-	1	aCTTTTaa	AT3G21270
782	TFmatrixID_0238	Dof	-	1	aCTTTTaat	AT4G38000
782	TFmatrixID_0243	Dof	-	1	aCTTTTaa	AT5G62940
782	TF_motif_seq_0239	Dof	-	1	ACTTT	AT1G29160;AT1G64620;AT2G37590;AT3G21270;AT3G45610;AT3G47500;AT4G38000;AT5G39660;AT5G60200;AT5G60850;AT5G62940;AT2G46590;AT1G07640;AT1G21340;AT1G26790;AT1G47655;AT1G51700;AT1G69570;AT2G28510;AT2G28810;AT2G34140;AT3G50410;AT3G55370;AT3G61850;AT4G00940;AT4G21050;AT4G21080;AT4G24060;AT5G02460;AT5G62430;AT5G65590;AT5G66940
784	TFmatrixID_0412	Sox;YABBY	+	1	tttTAATTaa	AT1G23420
785	TFmatrixID_0628	Homeodomain;bZIP;HD-ZIP;WOX	+	1	ttTAATTaaa	AT4G35550
785	TFmatrixID_0628	Homeodomain;bZIP;HD-ZIP;WOX	-	1	tttAATTAaa	AT4G35550
786	TFmatrixID_0412	Sox;YABBY	-	1	ttAATTAaat	AT1G23420
786	TF_motif_seq_0241	ZF-HD	-	1	TTAAT	AT1G75240
787	TFmatrixID_0005	AT-Hook	+	0.98	taATTAAatt	AT4G14465
787	TFmatrixID_0007	AT-Hook	+	0.97	tAATTAaatt	AT4G35390
787	TFmatrixID_0223	TCR;CPP	-	0.97	taattAAATTttg	AT4G14770
789	TF_motif_seq_0241	ZF-HD	+	1	ATTAA	AT1G75240
791	TF_motif_seq_0254	AP2;ERF	-	0.8	TAAAT	AT3G14230
802	TF_motif_seq_0261	(Motif sequence only)	+	0.8	GAGAA	SURECOREATSULTR11
806	TF_motif_seq_0241	ZF-HD	+	1	ATTAA	AT1G75240
809	TFmatrixID_0108	bZIP;Homeodomain;HD-ZIP	-	0.84	aaaggtaATCATttgccaa	AT1G30490
809	TFmatrixID_0518	bZIP;Homeodomain;HD-ZIP	-	0.82	aaaggtaATCATttgccaa	AT1G30490;AT1G52150;AT2G34710;AT4G32880;AT5G60690
809	TFmatrixID_0542	bZIP;Homeodomain;HD-ZIP	-	0.82	aaaggtaATCATttgccaa	AT1G30490;AT1G52150;AT2G34710;AT4G32880;AT5G60690
809	TF_motif_seq_0239	Dof	+	1	AAAGG	AT1G29160;AT1G64620;AT2G37590;AT3G21270;AT3G45610;AT3G47500;AT4G38000;AT5G39660;AT5G60200;AT5G60850;AT5G62940;AT2G46590;AT1G07640;AT1G21340;AT1G26790;AT1G47655;AT1G51700;AT1G69570;AT2G28510;AT2G28810;AT2G34140;AT3G50410;AT3G55370;AT3G61850;AT4G00940;AT4G21050;AT4G21080;AT4G24060;AT5G02460;AT5G62430;AT5G65590;AT5G66940
809	TF_motif_seq_0248	(Motif sequence only)	+	0.8	AAAGG	MYBCOREATCYCB1
810	TF_motif_seq_0239	Dof	+	1	AAGGT	AT1G29160;AT1G64620;AT2G37590;AT3G21270;AT3G45610;AT3G47500;AT4G38000;AT5G39660;AT5G60200;AT5G60850;AT5G62940;AT2G46590;AT1G07640;AT1G21340;AT1G26790;AT1G47655;AT1G51700;AT1G69570;AT2G28510;AT2G28810;AT2G34140;AT3G50410;AT3G55370;AT3G61850;AT4G00940;AT4G21050;AT4G21080;AT4G24060;AT5G02460;AT5G62430;AT5G65590;AT5G66940
812	TF_motif_seq_0321	(Motif sequence only)	+	1	GGTAAt	GT1CONSENSUS
813	TFmatrixID_0283	Homeodomain;HD-ZIP	-	0.98	gtAATCAttt	AT2G22800;AT2G44910;AT4G16780;AT4G37790;AT5G06710;AT5G47370
813	TFmatrixID	Homeodomain;HD-ZIP	-	0.93	gtAATCAttt	AT2G46680

	_0284					
813	TFmatrixID_0286	Homeodomain;HD-ZIP	-	0.98	gtAATCAt	AT2G22800;AT3G60390;AT4G16780;AT4G37790;AT5G06710;AT5G47370
813	TFmatrixID_0289	Homeodomain;HD-ZIP	-	0.99	gtAATCAttt	AT2G22800;AT4G16780;AT4G17460;AT4G37790;AT5G06710;AT5G47370
813	TFmatrixID_0634	Sox;YABBY	-	1	gtaATCATtt	AT2G26580
813	TF_motif_seq_0075	bZIP;Homeodomain;HD-ZIP	+	0.81	GTAATcatttg	AT1G30490
813	TF_motif_seq_0241	ZF-HD	-	1	GTAAT	AT1G75240
813	TF_motif_seq_0267	Trihelix	-	0.8	GTAAT	AT5G01380
813	TF_motif_seq_0076	(Motif sequence only)	+	0.81	GTAATcatttg	HDZIPIIIAT
814	TFmatrixID_0298	Homeodomain;HD-ZIP	-	0.99	tAATCAtttg	AT1G69780;AT2G18550;AT3G01220;AT5G15150
814	TFmatrixID_0413	Sox;YABBY	+	1	taATCAT	AT2G26580;AT4G00180
815	TF_motif_seq_0237	GATA;tify	-	1	AATCA	AT1G51600;AT2G45050;AT3G06740;AT3G16870;AT3G21175;AT3G24050;AT3G54810;AT3G60530;AT4G17570;AT4G24470;AT4G26150;AT4G32890;AT4G34680;AT5G25830;AT5G26930;AT5G56860;AT5G66320;AT2G18380;AT3G50870;AT4G36620
815	TF_motif_seq_0268	(Motif sequence only)	-	1	AATCA	ARR1AT
818	TF_motif_seq_0302	bHLH	+	1	CATTTg	AT5G08130;AT3G26744
818	TF_motif_seq_0302	bHLH	-	1	cATTTG	AT5G08130;AT3G26744
819	TF_motif_seq_0257	NF-YB;NF-YA;NF-YC	-	0.8	ATTTG	AT1G09030;AT1G17590;AT1G21970;AT1G30500;AT1G54160;AT1G54830;AT1G56170;AT1G72830;AT2G38880;AT2G47810;AT3G05690;AT3G14020;AT3G20910;AT3G53340;AT4G14540;AT5G06510;AT5G12840;AT5G27910;AT5G38140;AT5G47640;AT5G47670;AT5G50470;AT5G50480
821	TF_motif_seq_0275	(Motif sequence only)	+	0.8	TTGCC	WBOXATNPR1
823	TF_motif_seq_0263	(Motif sequence only)	+	0.8	GCCAA	SORLIP1AT
823	TF_motif_seq_0275	(Motif sequence only)	-	0.8	GCCAA	WBOXATNPR1
824	TF_motif_seq_0257	NF-YB;NF-YA;NF-YC	+	0.8	CCAAG	AT1G09030;AT1G17590;AT1G21970;AT1G30500;AT1G54160;AT1G54830;AT1G56170;AT1G72830;AT2G38880;AT2G47810;AT3G05690;AT3G14020;AT3G20910;AT3G53340;AT4G14540;AT5G06510;AT5G12840;AT5G27910;AT5G38140;AT5G47640;AT5G47670;AT5G50470;AT5G50480
826	TF_motif_seq_0239	Dof	+	1	AAGGA	AT1G29160;AT1G64620;AT2G37590;AT3G21270;AT3G45610;AT3G47500;AT4G38000;AT5G39660;AT5G60200;AT5G60850;AT5G62940;AT2G46590;AT1G07640;AT1G21340;AT1G26790;AT1G47655;AT1G51700;AT1G69570;AT2G28510;AT2G28810;AT2G34140;AT3G50410;AT3G55370;AT3G61850;AT4G00940;AT4G21050;AT4G21080;AT4G24060;AT5G02460;AT5G62430;AT5G65590;AT5G66940
828	TF_motif_seq_0321	(Motif sequence only)	+	1	GGAAAa	GT1CONSENSUS
829	TF_motif_seq_0321	(Motif sequence only)	+	1	GAAAAa	GT1CONSENSUS
832	TF_motif_seq_0341	(Motif sequence only)	+	1	aAACCA	MYB1AT
833	TF_motif_seq_0053	(Motif sequence only)	-	0.8	aaccaTGCAA	SORLREP5AT
834	TFmatrixID_0526	B3	+	1	acCATGCaaat	AT1G28300
840	TF_motif_seq_0257	NF-YB;NF-YA;NF-YC	+	0.8	CAAAT	AT1G09030;AT1G17590;AT1G21970;AT1G30500;AT1G54160;AT1G54830;AT1G56170;AT1G72830;AT2G38880;AT2G47810;AT3G05690;AT3G14020;AT3G20910;AT3G53340;AT4G14540;AT5G06510;AT5G12840;AT5G27910;AT5G38140;AT5G47640;AT5G47670;AT5G50470;AT5G50480
841	TF_motif_seq_0053	(Motif sequence only)	-	0.7	aaataTGCAA	SORLREP5AT
841	TF_motif_seq_0434	(Motif sequence only)	-	0.83	aaaTATGC	P1BS
843	TFmatrixID_0503	MADS box;MIKC	+	0.86	atatgcaataagtAGAAAtaa	AT4G22950;AT5G10140;AT5G65050;AT5G65060;AT5G65070;AT5G65080;AT1G77080;AT2G45650;AT3G57390;AT4G11880
845	TF_motif_seq_0169	(Others)	-	0.83	atgcaataagtAGAAA	U81368;U81369;U81370
847	TF_motif_seq_0257	NF-YB;NF-YA;NF-YC	+	0.8	GCAAT	AT1G09030;AT1G17590;AT1G21970;AT1G30500;AT1G54160;AT1G54830;AT1G56170;AT1G72830;AT2G38880;AT2G47810;AT3G05690;AT3G14020;AT3G20910;AT3G53340;AT4G14540;AT5G06510;AT5G12840;AT5G27910;AT5G38140;AT5G47640;AT5G47670;AT5G50470;AT5G50480
855	TF_motif_seq_0254	AP2;ERF	-	0.8	TAGAA	AT3G14230
856	TFmatrixID_0146	AT-Hook	+	1	agaaATAAT	AT4G21895;AT5G62260
860	TF_motif_seq_0241	ZF-HD	-	1	ATAAT	AT1G75240
865	TF_motif_s	Trihelix	+	0.8	GTTAA	AT5G01380

	eq_0267					
865	TF_motif_seq_0275	(Motif sequence only)	-	0.8	GTTAA	WBOXATNPR1
866	TF_motif_seq_0241	ZF-HD	-	1	TTAAT	AT1G75240
871	TF_motif_seq_0261	(Motif sequence only)	+	0.8	GAGAG	SURECOREATSULTR11
875	TF_motif_seq_0267	Trihelix	-	0.8	GTAAG	AT5G01380
878	TFmatrixID_0461	WRKY	-	0.98	agcgTTGACa	AT1G18860;AT1G29280;AT1G62300;AT1G64000;AT1G66550;AT1G66560;AT1G68150;AT1G80590;AT2G34830;AT2G40740;AT2G40750;AT2G44745;AT2G46400;AT3G01970;AT3G04670;AT3G56400;AT3G58710;AT3G62340;AT4G04450;AT4G11070;AT4G22070;AT4G23810;AT4G24240;AT4G39410;AT5G15130;AT5G22570;AT5G24110;AT5G26170;AT5G28650;AT5G41570;AT5G43290;AT5G45050;AT5G45260
879	TFmatrixID_0442	WRKY	-	0.98	gcgTTGACat	AT1G18860;AT1G29280;AT1G29860;AT1G30650;AT1G55600;AT1G62300;AT1G64000;AT1G66550;AT1G66560;AT1G68150;AT1G69810;AT2G21900;AT2G34830;AT2G40740;AT2G40750;AT2G44745;AT2G46400;AT3G01970;AT3G04670;AT3G58710;AT3G62340;AT3G56400;AT3G58710;AT3G62340;AT4G04450;AT4G11070;AT4G18170;AT4G22070;AT4G23810;AT4G24240;AT4G39410;AT5G15130;AT5G22570;AT5G26170;AT5G28650;AT5G41570;AT5G43290;AT5G45050;AT5G45260
879	TFmatrixID_0455	WRKY	-	0.97	gcgTTGACata	AT1G18860;AT1G29280;AT1G29860;AT1G55600;AT1G62300;AT1G64000;AT1G66550;AT1G66560;AT1G68150;AT1G69810;AT2G21900;AT2G34830;AT2G40740;AT2G44745;AT2G46400;AT3G01970;AT3G04670;AT3G58710;AT3G62340;AT4G01720;AT4G04450;AT4G11070;AT4G18170;AT4G22070;AT4G23810;AT4G24240;AT4G39410;AT5G15130;AT5G26170;AT5G28650;AT5G41570;AT5G43290;AT5G45050;AT5G45260
879	TFmatrixID_0457	WRKY	-	0.99	gcgTTGACat	AT1G18860;AT1G29280;AT1G29860;AT1G55600;AT1G62300;AT1G64000;AT1G66560;AT1G68150;AT1G69810;AT2G21900;AT2G34830;AT2G40740;AT2G44745;AT2G46400;AT3G01970;AT3G04670;AT3G56400;AT3G58710;AT3G62340;AT4G04450;AT4G11070;AT4G18170;AT4G22070;AT4G23810;AT4G24240;AT4G31550;AT4G39410;AT5G15130;AT5G22570;AT5G26170;AT5G28650;AT5G41570;AT5G43290;AT5G45050;AT5G45260
879	TFmatrixID_0629	WRKY	+	0.94	gcgTTGACat	AT2G44745
879	TFmatrixID_0631	WRKY	+	0.93	gcgTTGACat	AT5G22570
879	TFmatrixID_0632	WRKY	+	0.94	gcgTTGACat	AT3G01970
879	TF_motif_seq_0248	(Motif sequence only)	-	0.8	GCGTT	MYBCOREATCYCB1
880	TFmatrixID_0447	WRKY	-	0.99	cgTTGACata	AT1G18860;AT1G29280;AT1G29860;AT1G55600;AT1G62300;AT1G64000;AT1G68150;AT1G69810;AT2G21900;AT2G24570;AT2G34830;AT2G40740;AT2G44745;AT3G01970;AT3G04670;AT3G58710;AT3G62340;AT4G04450;AT4G11070;AT4G18170;AT4G22070;AT4G23810;AT4G24240;AT4G39410;AT5G15130;AT5G22570;AT5G26170;AT5G28650;AT5G41570;AT5G43290;AT5G45050;AT5G45260
880	TFmatrixID_0450	WRKY	-	0.99	cgTTGACata	AT1G18860;AT1G29280;AT1G29860;AT1G55600;AT1G62300;AT1G64000;AT1G68150;AT1G69810;AT2G21900;AT2G30590;AT2G34830;AT2G40740;AT2G44745;AT3G01970;AT3G04670;AT3G58710;AT3G62340;AT4G04450;AT4G11070;AT4G18170;AT4G22070;AT4G24240;AT4G39410;AT5G15130;AT5G22570;AT5G26170;AT5G28650;AT5G41570;AT5G43290;AT5G45050;AT5G45260
880	TFmatrixID_0453	WRKY	-	0.94	cgTTGACa	AT1G18860;AT1G29280;AT1G29860;AT1G55600;AT1G62300;AT1G64000;AT1G66550;AT1G66560;AT1G68150;AT1G69810;AT1G80590;AT2G21900;AT2G34830;AT2G40740;AT2G40750;AT2G44745;AT2G46400;AT2G47260;AT3G01080;AT3G01970;AT3G04670;AT3G56400;AT3G58710;AT3G62340;AT4G04450;AT4G11070;AT4G18170;AT4G22070;AT4G23810;AT4G24240;AT4G39410;AT5G15130;AT5G22570;AT5G26170;AT5G28650;AT5G41570;AT5G43290;AT5G45050
880	TFmatrixID_0456	WRKY	-	1	cgTTGACata	AT1G18860;AT1G29280;AT1G29860;AT1G55600;AT1G62300;AT1G64000;AT1G66560;AT1G68150;AT1G69810;AT1G80590;AT2G21900;AT2G34830;AT2G40740;AT2G40750;AT2G44745;AT2G46400;AT3G01970;AT3G04670;AT3G56400;AT3G58710;AT3G62340;AT4G04450;AT4G11070;AT4G18170;AT4G22070;AT4G23550;AT4G23810;AT4G24240;AT4G39410;AT5G15130;AT5G22570;AT5G26170;AT5G28650;AT5G41570;AT5G43290;AT5G45050;AT5G45260
880	TF_motif_seq_0066	WRKY	+	0.73	CGTTGacatat	AT2G04880
882	TF_motif_seq_0339	WRKY	+	0.95	TTGACa	AT1G13960;AT1G18860;AT1G29280;AT1G29860;AT1G30650;AT1G55600;AT1G62300;AT1G64000;AT1G66550;AT1G68150;AT1G69310;AT1G69810;AT1G80590;AT1G80840;AT2G03340;AT2G23320;AT2G24570;AT2G25000;AT2G30250;AT2G30590;AT2G34830;AT2G37260;AT2G38470;AT2G40740;AT2G40750;AT2G44745;AT2G46130;AT2G46400;AT2G47260;AT3G01080;AT3G01970;AT3G04670;AT3G56400;AT3G58710;AT4G01250;AT4G01720;AT4G04450;AT4G12020;AT4G18170;AT4G22070;AT4G23810;AT4G24240;AT4G26440;AT4G26640;AT4G30935;AT4G31550;AT4G31800;AT4G39410;AT5G07100;AT5G13080;AT5G15130;AT5G22570;AT5G24110;AT5G28650;AT5G45050;AT5G45260;AT5G46350;AT5G49520;AT5G52830;AT5G56270
882	TF_motif_seq_0275	(Motif sequence only)	+	1	TTGAC	WBOXATNPR1
883	TF_motif_seq_0246	Homeodomain;TALE	+	1	TGACA	AT1G23380;AT1G62360;AT1G70510;AT4G08150
883	TF_motif_seq_0271	bZIP	+	0.8	TGACA	AT1G77920;AT3G12250;AT5G06950;AT5G06960;AT5G10030;AT5G65210;AT1G22070
887	TFmatrixID_0419	TBP	-	1	ATATAtt	AT1G55520;AT3G13445
887	TF_motif_seq_0254	AP2;ERF	+	0.8	ATATA	AT3G14230
888	TF_motif_seq_0254	AP2;ERF	-	0.8	TATAT	AT3G14230
888	TF_motif_seq_0009	(Motif sequence only)	-	0.8	tatatTACGT	LS7ATPR1
891	TFmatrixID_0012	NAC;NAM	+	0.86	atTACGTcct	AT3G15500
891	TF_motif_seq_0241	ZF-HD	+	1	ATTAC	AT1G75240
891	TF_motif_seq_0267	Trihelix	+	0.8	ATTAC	AT5G01380
892	TF_motif_seq_0271	bZIP	+	0.8	TTACG	AT1G77920;AT3G12250;AT5G06950;AT5G06960;AT5G10030;AT5G65210;AT1G22070
892	TF_motif_seq_0450	(Motif sequence only)	+	0.75	TTACGtcc	PALINDROMICCBOXGM
892	TF_motif_seq_0450	(Motif sequence only)	-	0.75	ttaCGTCC	PALINDROMICCBOXGM
893	TF_motif_seq_0240	bZIP	-	1	TACGT	AT3G54620;AT4G02640
893	TF_motif_seq_0249	(Motif sequence only)	-	0.8	TACGT	ABRELATERD1
894	TF_motif_s	bZIP	+	1	ACGTC	AT3G54620;AT4G02640

	eq_0240					
894	TF_motif_seq_0009	(Motif sequence only)	+	0.7	ACGTCctggt	LS7ATPR1
894	TF_motif_seq_0249	(Motif sequence only)	+	0.8	ACGTC	ABRELATERD1
895	TF_motif_seq_0271	bZIP	-	0.8	CGTCC	AT1G77920;AT3G12250;AT5G06950;AT5G06960;AT5G10030;AT5G65210;AT1G22070
900	TF_motif_seq_0508	SBP	-	0.75	tgGTCCGaa	AT1G20980;AT1G27360;AT1G27370;AT1G53160;AT1G69170;AT1G76580;AT2G33810;AT2G42200;AT2G47070;AT3G15270;AT3G57920;AT3G60030;AT5G18830;AT5G43270
901	TF_motif_seq_0265	(Motif sequence only)	+	0.8	GGTCC	SORLIP2AT
901	TF_motif_seq_0265	(Motif sequence only)	-	0.8	GGTCC	SORLIP2AT
902	TF_motif_seq_0258	Dehydrin	-	0.8	GTCCG	U01377
903	TF_motif_seq_0508	SBP	+	0.75	tcCGAACat	AT1G20980;AT1G27360;AT1G27370;AT1G53160;AT1G69170;AT1G76580;AT2G33810;AT2G42200;AT2G47070;AT3G15270;AT3G57920;AT3G60030;AT5G18830;AT5G43270
904	TF_motif_seq_0258	Dehydrin	+	0.8	CCGAA	U01377
905	TF_motif_seq_0010	HSF	-	0.88	cgaacATTCT	AT3G24520;AT1G32330;AT1G46264;AT1G67970;AT2G26150;AT2G41690;AT3G02990;AT3G22830;AT3G51910;AT3G63350;AT4G11660;AT4G13980;AT4G17750;AT4G18880;AT5G03720;AT5G16820;AT5G43840;AT5G45710;AT5G54070;AT5G62020
910	TF_motif_seq_0281	bZIP	-	1	aTTCTT	AT1G68640
912	TFmatrixID_0238	Dof	+	1	tctTAAAGt	AT4G38000
916	TF_motif_seq_0239	Dof	+	1	AAAGT	AT1G29160;AT1G64620;AT2G37590;AT3G21270;AT3G45610;AT3G47500;AT4G38000;AT5G39660;AT5G60200;AT5G60850;AT5G62940;AT2G46590;AT1G07640;AT1G21340;AT1G26790;AT1G47655;AT1G51700;AT1G69570;AT2G28510;AT2G28810;AT2G34140;AT3G50410;AT3G55370;AT3G61850;AT4G00940;AT4G21050;AT4G21080;AT4G24060;AT5G02460;AT5G62430;AT5G65590;AT5G66940
917	TFmatrixID_0394	NAC;NAM	+	0.94	aagTTGCGtaa	AT1G76420;AT2G24430;AT3G04060;AT3G15170;AT3G18400;AT3G29035;AT5G18270;AT5G53950
918	TFmatrixID_0387	NAC;NAM	+	1	agTTGCGtaa	AT2G33480;AT5G13180
919	TFmatrixID_0013	NAC;NAM	-	0.93	gtTGCGTaac	AT3G18400
919	TFmatrixID_0396	NAC;NAM	+	0.98	gtTGCGTaac	AT1G76420;AT2G24430;AT3G04060;AT3G15170;AT3G18400;AT3G29035;AT5G18270;AT5G53950
919	TFmatrixID_0397	NAC;NAM	+	0.99	gttGCGTAac	AT1G12260;AT1G32770;AT1G33280;AT1G62700;AT1G71930;AT1G79580;AT2G18060;AT3G61910;AT4G10350;AT4G36160;AT5G62380;AT5G66300
919	TF_motif_seq_0267	Trihelix	+	0.8	GTTGC	AT5G01380
919	TF_motif_seq_0263	(Motif sequence only)	-	0.8	GTTGC	SORLIP1AT
920	TFmatrixID_0392	NAC;NAM	+	1	tTGCGTaaca	AT1G12260;AT1G32770;AT1G33280;AT1G62700;AT1G71930;AT1G79580;AT2G18060;AT3G61910;AT4G10350;AT4G36160;AT5G62380;AT5G66300
921	TF_motif_seq_0508	SBP	+	0.75	tgCGTAAca	AT1G20980;AT1G27360;AT1G27370;AT1G53160;AT1G69170;AT1G76580;AT2G33810;AT2G42200;AT2G47070;AT3G15270;AT3G57920;AT3G60030;AT5G18830;AT5G43270
923	TF_motif_seq_0271	bZIP	-	0.8	CGTAA	AT1G77920;AT3G12250;AT5G06950;AT5G06960;AT5G10030;AT5G65210;AT1G22070
924	TFmatrixID_0637	C2H2	+	1	gtaaCACTAa	AT5G04340
924	TF_motif_seq_0267	Trihelix	+	0.8	GTAAC	AT5G01380
924	TF_motif_seq_0267	Trihelix	-	1	GTAAC	AT5G01380
926	TFmatrixID_0211	C2H2	+	1	aACACTa	AT1G27730;AT3G49930;AT3G60580;AT5G04340;AT5G43170
926	TFmatrixID_0213	C2H2	+	1	aACACTa	AT1G02030;AT2G45120;AT3G19580;AT3G49930;AT3G60580;AT5G04340;AT5G43170
930	TF_motif_seq_0241	ZF-HD	-	1	CTAAT	AT1G75240
930	TF_motif_seq_0257	NF-YB;NF-YA;NF-YC	+	0.8	CTAAT	AT1G09030;AT1G17590;AT1G21970;AT1G30500;AT1G54160;AT1G54830;AT1G56170;AT1G72830;AT2G38880;AT2G47810;AT3G05690;AT3G14020;AT3G20910;AT3G53340;AT4G14540;AT5G06510;AT5G12840;AT5G27910;AT5G38140;AT5G47640;AT5G47670;AT5G50470;AT5G50480
933	TF_motif_seq_0267	Trihelix	-	0.8	ATAAC	AT5G01380
934	TFmatrixID_0623	AP2	+	0.91	taaCCTTAga	AT2G28550
934	TFmatrixID_0626	AP2	+	0.91	taaCCTTAga	AT5G60120
936	TF_motif_s	Dof	-	1	ACCTT	AT1G29160;AT1G64620;AT2G37590;AT3G21270;AT3G45610;AT3G47500;AT4G38000;AT5G39660;AT5G60200;AT5G60850;AT5G62940;AT2G46590;AT1G07640;AT1G21340;AT1G26790;AT1G47655;AT1G51700;AT1G69570;AT2G28510;AT2G28810;AT2G34140;AT3G50410;AT3G55370;AT3G61850;AT4G00940;AT4G21050;AT4G21080;AT4G24060;AT5G02460;AT5G62430;AT5G65590;AT5G66940

	eq_0239					
940	TF_motif_seq_0254	AP2;ERF	-	0.8	TAGAA	AT3G14230
943	TF_motif_seq_0254	AP2;ERF	-	0.8	AAGAT	AT3G14230
944	TFmatrixID_0589	MYB	-	0.94	agaTGGTTgg	AT5G12870
944	TF_motif_seq_0237	GATA;tify	+	1	AGATG	AT1G51600;AT2G45050;AT3G06740;AT3G16870;AT3G21175;AT3G24050;AT3G54810;AT3G60530;AT4G17570;AT4G24470;AT4G26150;AT4G32890;AT4G34680;AT5G25830;AT5G26930;AT5G56860;AT5G66320;AT2G18380;AT3G50870;AT4G36620
947	TF_motif_seq_0341	(Motif sequence only)	-	0.95	TGGTTg	MYB1AT
948	TFmatrixID_0589	MYB	-	0.96	ggtTGGTTga	AT5G12870
948	TFmatrixID_0593	MYB	+	0.92	ggtTGGTTga	AT4G01680
948	TF_motif_seq_0440	(Motif sequence only)	-	1	ggTTGGTt	MYBPLANT
949	TF_motif_seq_0257	NF-YB;NF-YA;NF-YC	-	0.8	GTTGG	AT1G09030;AT1G17590;AT1G21970;AT1G30500;AT1G54160;AT1G54830;AT1G56170;AT1G72830;AT2G38880;AT2G47810;AT3G05690;AT3G14020;AT3G20910;AT3G53340;AT4G14540;AT5G06510;AT5G12840;AT5G27910;AT5G38140;AT5G47640;AT5G47670;AT5G50470;AT5G50480
949	TF_motif_seq_0258	Dehydrin	-	0.8	GTTGG	U01377
950	TFmatrixID_0461	WRKY	-	0.99	ttggTTGACt	AT1G18860;AT1G29280;AT1G62300;AT1G64000;AT1G66550;AT1G66560;AT1G68150;AT1G80590;AT2G34830;AT2G40740;AT2G40750;AT2G44745;AT2G46400;AT3G01970;AT3G04670;AT3G56400;AT3G58710;AT3G62340;AT4G00450;AT4G11070;AT4G22070;AT4G23810;AT4G24240;AT4G39410;AT5G15130;AT5G22570;AT5G24110;AT5G26170;AT5G28650;AT5G41570;AT5G43290;AT5G45050;AT5G45260
951	TFmatrixID_0442	WRKY	-	0.99	tggTTGACta	AT1G18860;AT1G29280;AT1G29860;AT1G30650;AT1G55600;AT1G62300;AT1G64000;AT1G66550;AT1G66560;AT1G68150;AT1G69810;AT2G21900;AT2G34830;AT2G40740;AT2G40750;AT2G44745;AT2G46400;AT3G01970;AT3G04670;AT3G56400;AT3G58710;AT3G62340;AT4G00450;AT4G11070;AT4G18170;AT4G22070;AT4G23810;AT4G24240;AT4G39410;AT5G15130;AT5G22570;AT5G26170;AT5G28650;AT5G41570;AT5G43290;AT5G45050;AT5G45260
951	TFmatrixID_0446	WRKY	-	0.99	tggTTGACta	AT1G18860;AT1G29280;AT1G29860;AT1G55600;AT1G62300;AT1G64000;AT1G68150;AT1G69810;AT2G21900;AT2G23320;AT2G34830;AT2G40740;AT2G44745;AT3G01970;AT3G04670;AT3G58710;AT3G62340;AT4G00450;AT4G11070;AT4G18170;AT4G22070;AT4G23810;AT4G24240;AT4G39410;AT5G15130;AT5G22570;AT5G26170;AT5G28650;AT5G41570;AT5G43290;AT5G45050;AT5G45260
951	TFmatrixID_0448	WRKY	-	0.93	tggTTGACtat	AT1G18860;AT1G29280;AT1G29860;AT1G55600;AT1G62300;AT1G64000;AT1G68150;AT1G69810;AT2G21900;AT2G25000;AT2G34830;AT2G44745;AT2G46400;AT3G01970;AT3G04670;AT3G58710;AT3G62340;AT4G00450;AT4G11070;AT4G18170;AT4G22070;AT4G24240;AT4G39410;AT5G15130;AT5G26170;AT5G28650;AT5G41570;AT5G43290;AT5G45050
951	TFmatrixID_0452	WRKY	-	1	tggTTGACta	AT1G18860;AT1G29280;AT1G29860;AT1G55600;AT1G62300;AT1G64000;AT1G66550;AT1G66560;AT1G68150;AT1G69810;AT2G21900;AT2G34830;AT2G40740;AT2G40750;AT2G44745;AT2G46130;AT2G46400;AT3G01970;AT3G04670;AT3G56400;AT3G58710;AT3G62340;AT4G00450;AT4G11070;AT4G18170;AT4G22070;AT4G23810;AT4G24240;AT4G39410;AT5G15130;AT5G22570;AT5G26170;AT5G28650;AT5G41570;AT5G43290;AT5G45050;AT5G45260
951	TFmatrixID_0455	WRKY	-	0.98	tggTTGACtat	AT1G18860;AT1G29280;AT1G29860;AT1G55600;AT1G62300;AT1G64000;AT1G66550;AT1G66560;AT1G68150;AT1G69810;AT2G21900;AT2G34830;AT2G40740;AT2G44745;AT2G46400;AT3G01970;AT3G04670;AT3G58710;AT3G62340;AT4G01720;AT4G00450;AT4G11070;AT4G18170;AT4G22070;AT4G23810;AT4G24240;AT4G39410;AT5G15130;AT5G26170;AT5G28650;AT5G41570;AT5G43290;AT5G45050;AT5G45260
951	TFmatrixID_0457	WRKY	-	0.99	tggTTGACta	AT1G18860;AT1G29280;AT1G29860;AT1G55600;AT1G62300;AT1G64000;AT1G66560;AT1G68150;AT1G69810;AT2G21900;AT2G34830;AT2G40740;AT2G44745;AT2G46400;AT3G01970;AT3G04670;AT3G56400;AT3G58710;AT3G62340;AT4G00450;AT4G11070;AT4G18170;AT4G22070;AT4G23810;AT4G24240;AT4G31550;AT4G39410;AT5G15130;AT5G22570;AT5G26170;AT5G28650;AT5G41570;AT5G43290;AT5G45050;AT5G45260
951	TFmatrixID_0629	WRKY	+	0.9	tggTTGACta	AT2G44745
951	TFmatrixID_0631	WRKY	+	0.92	tggTTGACta	AT5G22570
951	TFmatrixID_0632	WRKY	+	0.91	tggTTGACta	AT3G01970
951	TF_motif_seq_0341	(Motif sequence only)	-	0.95	TGGTTg	MYB1AT
952	TFmatrixID_0382	NAC;NAM	-	1	ggTTGACta	AT1G01720;AT1G52880;AT1G52890;AT1G69490;AT3G04070;AT3G15500;AT3G15510;AT4G27410
952	TFmatrixID_0444	WRKY	-	1	ggTTGACtat	AT1G18860;AT1G29280;AT1G29860;AT1G55600;AT1G62300;AT1G64000;AT1G66550;AT1G66560;AT1G68150;AT1G69310;AT1G69810;AT1G80590;AT2G21900;AT2G34830;AT2G40740;AT2G44745;AT2G46400;AT3G01970;AT3G04670;AT3G56400;AT3G58710;AT3G62340;AT4G00450;AT4G11070;AT4G18170;AT4G22070;AT4G23810;AT4G24240;AT4G39410;AT5G15130;AT5G22570;AT5G26170;AT5G28650;AT5G41570;AT5G43290;AT5G45050
952	TFmatrixID_0447	WRKY	-	0.99	ggTTGACtat	AT1G18860;AT1G29280;AT1G29860;AT1G55600;AT1G62300;AT1G64000;AT1G68150;AT1G69810;AT2G21900;AT2G24570;AT2G34830;AT2G40740;AT2G44745;AT3G01970;AT3G04670;AT3G58710;AT3G62340;AT4G00450;AT4G11070;AT4G18170;AT4G22070;AT4G23810;AT4G24240;AT4G39410;AT5G15130;AT5G22570;AT5G26170;AT5G28650;AT5G41570;AT5G43290;AT5G45050;AT5G45260
952	TFmatrixID_0450	WRKY	-	1	ggTTGACtat	AT1G18860;AT1G29280;AT1G29860;AT1G55600;AT1G62300;AT1G64000;AT1G68150;AT1G69810;AT2G21900;AT2G30590;AT2G34830;AT2G40740;AT2G44745;AT3G01970;AT3G04670;AT3G58710;AT3G62340;AT4G00450;AT4G11070;AT4G18170;AT4G22070;AT4G24240;AT4G39410;AT5G15130;AT5G22570;AT5G26170;AT5G28650;AT5G41570;AT5G43290;AT5G45050;AT5G45260
952	TFmatrixID_0451	WRKY	-	1	ggTTGACtat	AT1G13960;AT2G03340;AT2G37260;AT2G38470;AT3G01080;AT4G12020;AT4G26440;AT4G26640;AT4G30935;AT5G07100
952	TFmatrixID_0453	WRKY	-	0.96	ggTTGACt	AT1G18860;AT1G29280;AT1G29860;AT1G55600;AT1G62300;AT1G64000;AT1G66550;AT1G66560;AT1G68150;AT1G69810;AT1G80590;AT2G21900;AT2G34830;AT2G40740;AT2G40750;AT2G44745;AT2G46400;AT2G47260;AT3G01970;AT3G04670;AT3G56400;AT3G58710;AT3G62340;AT4G00450;AT4G11070;AT4G18170;AT4G22070;AT4G23810;AT4G24240;AT4G39410;AT5G15130;AT5G22570;AT5G26170;AT5G28650;AT5G41570;AT5G43290;AT5G45050
952	TFmatrixID_0454	WRKY	-	1	ggTTGACtat	AT1G18860;AT1G29280;AT1G29860;AT1G55600;AT1G62300;AT1G64000;AT1G66550;AT1G66560;AT1G68150;AT1G69810;AT1G80590;AT2G21900;AT2G34830;AT2G40740;AT2G40750;AT2G44745;AT2G46400;AT3G01970;AT3G04670;AT3G56400;AT3G58710;AT3G62340;AT4G01250;AT4G00450;AT4G11070;AT4G18170;AT4G22070;AT4G23810;AT4G24240;AT4G39410;AT5G15130;AT5G22570;AT5G26170;AT5G28650;AT5G41570;AT5G43290;AT5G45050;AT5G45260
952	TFmatrixID_0456	WRKY	-	1	ggTTGACtat	AT1G18860;AT1G29280;AT1G29860;AT1G55600;AT1G62300;AT1G64000;AT1G66560;AT1G68150;AT1G69810;AT1G80590;AT2G21900;AT2G34830;AT2G40740;AT2G40750;AT2G44745;AT2G46400;AT3G01970;AT3G04670;AT3G56400;AT3G58710;AT3G62340;AT4G00450;AT4G11070;AT4G18170;AT4G22070;AT4G23550;AT4G23810;AT4G24240;AT4G39410;AT5G15130;AT5G22570;AT5G26170;AT5G28650;AT5G41570;AT5G43290;AT5G45050;AT5G45260
952	TFmatrixID_0462	WRKY	-	1	ggTTGACta	AT1G18860;AT1G29280;AT1G29860;AT1G55600;AT1G62300;AT1G64000;AT1G66550;AT1G66560;AT1G68150;AT1G69810;AT1G80590;AT2G21900;AT2G34830;AT2G44745;AT3G01970;AT3G04670;AT3G58710;AT3G62340;AT4G00450;AT4G11070;AT4G18170;AT4G22070;AT4G23810;AT4G24240;AT4G39410;AT5G15130;AT5G22570;AT5G26170;AT5G28650;AT5G41570;AT5G43290;AT5G45050;AT5G45260;AT5G46350
952	TFmatrixID_0463	WRKY	-	1	ggTTGACtat	AT1G18860;AT1G29280;AT1G29860;AT1G55600;AT1G62300;AT1G64000;AT1G66550;AT1G66560;AT1G68150;AT1G69810;AT1G80590;AT2G21900;AT2G34830;AT2G40740;AT2G40750;AT2G44745;AT2G46400;AT3G01970;AT3G04670;AT3G56400;AT3G58710;AT3G62340;AT4G00450;AT4G11070;AT4G18170;AT4G22070;AT4G23810;AT4G24240;AT4G39410;AT5G15130;AT5G22570;AT5G26170;AT5G28650;AT5G41570;AT5G43290;AT5G45050;AT5G45260;AT5G49520
952	TFmatrixID_0464	WRKY	-	1	ggTTGACta	AT1G18860;AT1G29280;AT1G29860;AT1G55600;AT1G62300;AT1G64000;AT1G66550;AT1G66560;AT1G68150;AT1G69810;AT1G80590;AT2G21900;AT2G34830;AT2G40740;AT2G40750;AT2G44745;AT2G46400;AT3G01970;AT3G04670;AT3G56400;AT3G58710;AT3G62340;AT4G00450;AT4G11070;AT4G18170;AT4G22070;AT4G23810;AT4G24240;AT4G39410;AT5G15130;AT5G22570;AT5G26170;AT5G28650;AT5G41570;AT5G43290;AT5G45050;AT5G45260;AT5G52830
952	TFmatrixID_0466	WRKY	-	1	ggTTGACtat	AT1G18860;AT1G29280;AT1G29860;AT1G55600;AT1G62300;AT1G64000;AT1G68150;AT1G69810;AT2G21900;AT2G34830;AT2G44745;AT3G01970;AT3G04670;AT3G58710;AT3G62340;AT4G00450;AT4G18170;AT4G22070;AT4G24240;AT4G39410;AT5G15130;AT5G26170;AT5G28650;AT5G41570;AT5G43290;AT5G45050;AT5G64810
953	TFmatrixID	WRKY	-	1	gTTGACta	AT1G18860;AT1G29280;AT1G29860;AT1G55600;AT1G62300;AT1G64000;AT1G68150;AT1G69810;AT1G80840;AT2G21900;AT2G34830;AT2G44745;AT3G01970;AT3G04670;AT3G58710;AT3G62340;AT4G00450;AT4G18170;AT4G22070;AT4G24240;AT4G39410;AT5G15130;AT5G26170;AT5G28650;AT5G41570;AT5G43290;AT5G45050;AT5G45260

	_0445					
953	TFmatrixID_0459	WRKY	-	0.97	gTTGACta	AT1G29280;AT1G29860;AT1G64000;AT1G66550;AT1G66560;AT1G69810;AT1G80590;AT2G40740;AT2G40750;AT2G44745;AT2G46400;AT3G01970;AT3G56400;AT3G62340;AT4G11070;AT4G18170;AT4G23810;AT4G24240;AT5G01900;AT5G22570;AT5G26170;AT5G41570;AT5G43290;AT5G45050;AT5G45260
953	TFmatrixID_0460	WRKY	-	1	gTTGACta	AT1G18860;AT1G29280;AT1G29860;AT1G55600;AT1G62300;AT1G64000;AT1G66550;AT1G66560;AT1G68150;AT1G69810;AT2G21900;AT2G34830;AT2G40740;AT2G40750;AT2G44745;AT3G01970;AT3G04670;AT3G56400;AT3G58710;AT3G62340;AT4G04450;AT4G11070;AT4G18170;AT4G22070;AT4G23810;AT4G24240;AT4G39410;AT5G13080;AT5G15130;AT5G22570;AT5G26170;AT5G28650;AT5G41570;AT5G43290;AT5G45050;AT5G45260
954	TF_motif_seq_0339	WRKY	+	1	TTGACt	AT1G13960;AT1G18860;AT1G29280;AT1G29860;AT1G30650;AT1G55600;AT1G62300;AT1G64000;AT1G66550;AT1G68150;AT1G69310;AT1G69810;AT1G80590;AT1G80840;AT2G03340;AT2G23320;AT2G24570;AT2G25000;AT2G30250;AT2G30590;AT2G34830;AT2G37260;AT2G38470;AT2G40740;AT2G40750;AT2G44745;AT2G46130;AT2G46400;AT2G47260;AT3G01080;AT3G01970;AT3G04670;AT3G56400;AT3G58710;AT4G01250;AT4G01720;AT4G04450;AT4G12020;AT4G18170;AT4G22070;AT4G23810;AT4G24240;AT4G26440;AT4G26640;AT4G30935;AT4G31550;AT4G31800;AT4G39410;AT5G07100;AT5G13080;AT5G15130;AT5G22570;AT5G24110;AT5G28650;AT5G45050;AT5G45260;AT5G46350;AT5G49520;AT5G52830;AT5G56270
954	TF_motif_seq_0275	(Motif sequence only)	+	1	TTGAC	WBOXATNPR1
955	TF_motif_seq_0246	Homeodomain;TALE	+	1	TGACT	AT1G23380;AT1G62360;AT1G70510;AT4G08150
955	TF_motif_seq_0270	WRKY	+	1	TGACT	AT1G13960;AT1G18860;AT1G29280;AT1G29860;AT1G30650;AT1G55600;AT1G62300;AT1G64000;AT1G66550;AT1G68150;AT1G69310;AT1G69810;AT1G80590;AT1G80840;AT2G03340;AT2G23320;AT2G24570;AT2G25000;AT2G30250;AT2G30590;AT2G34830;AT2G37260;AT2G38470;AT2G40740;AT2G40750;AT2G44745;AT2G46130;AT2G46400;AT2G47260;AT3G01080;AT3G01970;AT3G04670;AT3G56400;AT3G58710;AT4G01250;AT4G01720;AT4G04450;AT4G12020;AT4G18170;AT4G22070;AT4G23810;AT4G24240;AT4G26440;AT4G26640;AT4G30935;AT4G31550;AT4G31800;AT4G39410;AT5G07100;AT5G13080;AT5G15130;AT5G22570;AT5G24110;AT5G28650;AT5G45050;AT5G45260;AT5G46350;AT5G49520;AT5G52830;AT5G56270
955	TF_motif_seq_0271	bZIP	+	0.8	TGACT	AT1G77920;AT3G12250;AT5G06950;AT5G06960;AT5G10030;AT5G65210;AT1G22070
958	TF_motif_seq_0243	GATA;tify	-	1	CTATC	AT1G51600;AT2G45050;AT3G06740;AT3G16870;AT3G21175;AT3G24050;AT3G54810;AT3G60530;AT4G17570;AT4G24470;AT4G26150;AT4G32890;AT4G34680;AT5G25830;AT5G26930;AT5G56860;AT5G66320;AT2G18380;AT3G50870;AT4G36620
959	TF_motif_seq_0237	GATA;tify	-	1	TATCA	AT1G51600;AT2G45050;AT3G06740;AT3G16870;AT3G21175;AT3G24050;AT3G54810;AT3G60530;AT4G17570;AT4G24470;AT4G26150;AT4G32890;AT4G34680;AT5G25830;AT5G26930;AT5G56860;AT5G66320;AT2G18380;AT3G50870;AT4G36620
960	TF_motif_seq_0254	AP2;ERF	+	0.8	ATCAA	AT3G14230
960	TF_motif_seq_0275	(Motif sequence only)	-	0.8	ATCAA	WBOXATNPR1
962	TF_motif_seq_0255	AP2;RAV;B3	+	1	CAACA	AT1G25560;AT1G13260
965	TF_motif_seq_0237	GATA;tify	-	1	CATCT	AT1G51600;AT2G45050;AT3G06740;AT3G16870;AT3G21175;AT3G24050;AT3G54810;AT3G60530;AT4G17570;AT4G24470;AT4G26150;AT4G32890;AT4G34680;AT5G25830;AT5G26930;AT5G56860;AT5G66320;AT2G18380;AT3G50870;AT4G36620
966	TF_motif_seq_0254	AP2;ERF	+	0.8	ATCTT	AT3G14230
969	TFmatrixID_0448	WRKY	-	0.97	ttaTTGACcaa	AT1G18860;AT1G29280;AT1G29860;AT1G55600;AT1G62300;AT1G64000;AT1G68150;AT1G69810;AT2G21900;AT2G25000;AT2G34830;AT2G44745;AT2G46400;AT3G01970;AT3G04670;AT3G58710;AT3G62340;AT4G04450;AT4G11070;AT4G18170;AT4G22070;AT4G24240;AT4G39410;AT5G15130;AT5G26170;AT5G28650;AT5G41570;AT5G43290;AT5G45050
970	TFmatrixID_0382	NAC;NAM	-	1	taTTGACca	AT1G01720;AT1G52880;AT1G52890;AT1G69490;AT3G04070;AT3G15500;AT3G15510;AT4G27410
970	TFmatrixID_0451	WRKY	-	1	taTTGACcaa	AT1G13960;AT2G03340;AT2G37260;AT2G38470;AT3G01080;AT4G12020;AT4G26440;AT4G26640;AT4G30935;AT5G07100
970	TFmatrixID_0458	WRKY	-	1	taTTGACcaa	AT1G18860;AT1G29280;AT1G29860;AT1G55600;AT1G62300;AT1G64000;AT1G68150;AT1G69810;AT2G21900;AT2G34830;AT2G40740;AT2G44745;AT2G46400;AT3G01970;AT3G04670;AT3G58710;AT3G62340;AT4G04450;AT4G11070;AT4G18170;AT4G22070;AT4G24240;AT4G31800;AT4G39410;AT5G15130;AT5G26170;AT5G28650;AT5G41570;AT5G43290;AT5G45050
970	TFmatrixID_0463	WRKY	-	1	taTTGACcaa	AT1G18860;AT1G29280;AT1G29860;AT1G55600;AT1G62300;AT1G64000;AT1G66550;AT1G66560;AT1G68150;AT1G69810;AT1G80590;AT2G21900;AT2G34830;AT2G40740;AT2G40750;AT2G44745;AT2G46400;AT3G01970;AT3G04670;AT3G56400;AT3G58710;AT3G62340;AT4G04450;AT4G18170;AT4G22070;AT4G24240;AT4G39410;AT5G15130;AT5G26170;AT5G28650;AT5G41570;AT5G43290;AT5G45050;AT5G45260;AT5G49520
970	TFmatrixID_0466	WRKY	-	0.99	taTTGACcaa	AT1G18860;AT1G29280;AT1G29860;AT1G55600;AT1G62300;AT1G64000;AT1G68150;AT1G69810;AT2G21900;AT2G34830;AT2G44745;AT3G01970;AT3G04670;AT3G58710;AT3G62340;AT4G04450;AT4G18170;AT4G22070;AT4G24240;AT4G39410;AT5G15130;AT5G26170;AT5G28650;AT5G41570;AT5G43290;AT5G45050;AT5G64810
970	TFmatrixID_0468	WRKY	-	0.99	taTTGACca	AT1G18860;AT1G29280;AT1G29860;AT1G55600;AT1G62300;AT1G64000;AT1G66550;AT1G66560;AT1G68150;AT1G69810;AT1G80590;AT2G21900;AT2G34830;AT2G40740;AT2G40750;AT2G44745;AT2G46400;AT3G01970;AT3G04670;AT3G56400;AT3G58710;AT3G62340;AT4G04450;AT4G18170;AT4G22070;AT4G24240;AT4G39410;AT5G15130;AT5G26170;AT5G28650;AT5G41570;AT5G43290;AT5G45050;AT5G45260
970	TFmatrixID_0630	WRKY	-	0.96	taTTGACcaa	AT4G31800
971	TFmatrixID_0443	WRKY	-	0.99	aTTGACca	AT1G29860;AT1G64000;AT1G66550;AT1G66560;AT1G66600;AT1G68150;AT1G69810;AT1G80590;AT2G40740;AT2G40750;AT2G44745;AT2G46400;AT3G01970;AT3G56400;AT3G62340;AT4G04450;AT4G11070;AT4G18170;AT4G23810;AT4G39410;AT5G22570;AT5G26170;AT5G41570;AT5G43290;AT5G45050;AT5G45260
971	TFmatrixID_0445	WRKY	-	1	aTTGACca	AT1G18860;AT1G29280;AT1G29860;AT1G55600;AT1G62300;AT1G64000;AT1G68150;AT1G69810;AT1G80840;AT2G21900;AT2G34830;AT2G44745;AT3G01970;AT3G04670;AT3G58710;AT3G62340;AT4G04450;AT4G18170;AT4G22070;AT4G24240;AT4G39410;AT5G15130;AT5G26170;AT5G28650;AT5G41570;AT5G43290;AT5G45050;AT5G45260
971	TFmatrixID_0449	WRKY	-	0.97	aTTGACca	AT1G13960;AT2G03340;AT2G30250;AT2G37260;AT3G01080;AT4G12020;AT4G26440;AT4G26640;AT4G30935;AT5G07100
971	TFmatrixID_0459	WRKY	-	0.93	aTTGACca	AT1G29280;AT1G29860;AT1G64000;AT1G66550;AT1G66560;AT1G69810;AT1G80590;AT2G40740;AT2G40750;AT2G44745;AT2G46400;AT3G01970;AT3G56400;AT3G62340;AT4G11070;AT4G18170;AT4G23810;AT4G24240;AT5G01900;AT5G22570;AT5G26170;AT5G41570;AT5G43290;AT5G45050;AT5G45260
971	TFmatrixID_0465	WRKY	-	0.98	aTTGACca	AT1G13960;AT2G03340;AT2G37260;AT3G01080;AT4G12020;AT4G26440;AT4G26640;AT4G30935;AT5G07100;AT5G56270
971	TF_motif_seq_0257	NF-YB;NF-YA;NF-YC	-	0.8	ATTGA	AT1G09030;AT1G17590;AT1G21970;AT1G30500;AT1G54160;AT1G54830;AT1G56170;AT1G72830;AT2G38880;AT2G47810;AT3G05690;AT3G14020;AT3G20910;AT3G53340;AT4G14540;AT5G06510;AT5G12840;AT5G27910;AT5G38140;AT5G47640;AT5G47670;AT5G50470;AT5G50480
972	TFmatrixID_0534	WRKY	-	0.89	TTGACcaaatg	AT1G13960;AT2G03340;AT2G04880;AT2G37260;AT3G01080;AT4G12020;AT4G26440;AT4G26640;AT4G30935;AT5G07100
972	TF_motif_seq_0339	WRKY	+	1	TTGACc	AT1G13960;AT1G18860;AT1G29280;AT1G29860;AT1G30650;AT1G55600;AT1G62300;AT1G64000;AT1G66550;AT1G68150;AT1G69310;AT1G69810;AT1G80590;AT1G80840;AT2G03340;AT2G23320;AT2G24570;AT2G25000;AT2G30250;AT2G30590;AT2G34830;AT2G37260;AT2G38470;AT2G40740;AT2G40750;AT2G44745;AT2G46130;AT2G46400;AT2G47260;AT3G01080;AT3G01970;AT3G04670;AT3G56400;AT3G58710;AT4G01250;AT4G01720;AT4G04450;AT4G12020;AT4G18170;AT4G22070;AT4G23810;AT4G24240;AT4G26440;AT4G26640;AT4G30935;AT4G31550;AT4G31800;AT4G39410;AT5G07100;AT5G13080;AT5G15130;AT5G22570;AT5G24110;AT5G28650;AT5G45050;AT5G45260;AT5G46350;AT5G49520;AT5G52830;AT5G56270
972	TF_motif_seq_0275	(Motif sequence only)	+	1	TTGAC	WBOXATNPR1
973	TF_motif_seq_0246	Homeodomain;TALE	+	1	TGACC	AT1G23380;AT1G62360;AT1G70510;AT4G08150
973	TF_motif_seq_0270	WRKY	+	1	TGACC	AT1G13960;AT1G18860;AT1G29280;AT1G29860;AT1G30650;AT1G55600;AT1G62300;AT1G64000;AT1G66550;AT1G68150;AT1G69310;AT1G69810;AT1G80590;AT1G80840;AT2G03340;AT2G23320;AT2G24570;AT2G25000;AT2G30250;AT2G30590;AT2G34830;AT2G37260;AT2G38470;AT2G40740;AT2G40750;AT2G44745;AT2G46130;AT2G46400;AT2G47260;AT3G01080;AT3G01970;AT3G04670;AT3G56400;AT3G58710;AT4G01250;AT4G01720;AT4G04450;AT4G12020;AT4G18170;AT4G22070;AT4G23810;AT4G24240;AT4G26440;AT4G26640;AT4G30935;AT4G31550;AT4G31800;AT4G39410;AT5G07100;AT5G13080;AT5G15130;AT5G22570;AT5G24110;AT5G28650;AT5G45050;AT5G45260;AT5G46350;AT5G49520;AT5G52830;AT5G56270
973	TF_motif_s	bZIP	+	0.8	TGACC	AT1G77920;AT3G12250;AT5G06950;AT5G06960;AT5G10030;AT5G65210;AT1G22070

	eq_0271					
976	TF_motif_seq_0146	C2H2	+	0.73	CCAAAtgttttttt	AT1G30970
976	TF_motif_seq_0257	NF-YB;NF-YA;NF-YC	+	0.8	CCAAA	AT1G09030;AT1G17590;AT1G21970;AT1G30500;AT1G54160;AT1G54830;AT1G56170;AT1G72830;AT2G38880;AT2G47810;AT3G05690;AT3G14020;AT3G20910;AT3G53340;AT4G14540;AT5G06510;AT5G12840;AT5G27910;AT5G38140;AT5G47640;AT5G47670;AT5G50470;AT5G50480
977	TF_motif_seq_0257	NF-YB;NF-YA;NF-YC	+	0.8	CAAAT	AT1G09030;AT1G17590;AT1G21970;AT1G30500;AT1G54160;AT1G54830;AT1G56170;AT1G72830;AT2G38880;AT2G47810;AT3G05690;AT3G14020;AT3G20910;AT3G53340;AT4G14540;AT5G06510;AT5G12840;AT5G27910;AT5G38140;AT5G47640;AT5G47670;AT5G50470;AT5G50480
977	TF_motif_seq_0302	bHLH	+	1	CAAATg	AT5G08130;AT3G26744
977	TF_motif_seq_0302	bHLH	-	1	cAAATG	AT5G08130;AT3G26744
982	TFmatrixID_0476	AT-Hook	-	0.94	gTTTTTttttttttaa	AT1G48610
992	TFmatrixID_0412	Sox;YABBY	+	1	tttTAATTat	AT1G23420
993	TFmatrixID_0628	Homeodomain;bZIP;HD-ZIP;WOX	+	0.97	ttTAATTata	AT4G35550
993	TFmatrixID_0628	Homeodomain;bZIP;HD-ZIP;WOX	-	0.97	tttAATTAta	AT4G35550
994	TFmatrixID_0412	Sox;YABBY	-	1	ttAATTAtaa	AT1G23420
994	TF_motif_seq_0241	ZF-HD	-	1	TTAAT	AT1G75240
997	TFmatrixID_0585	TBP	+	0.95	attATAAAaca	AT1G55520;AT3G13445
997	TF_motif_seq_0241	ZF-HD	+	1	ATTAT	AT1G75240
998	TFmatrixID_0569	TBP	+	0.97	ttATAAAacagttgc	AT1G55520;AT3G13445
1004	TF_motif_seq_0248	(Motif sequence only)	+	0.8	AACAG	MYBCOREATCYCB1
1006	TF_motif_seq_0302	bHLH	+	1	CAGTTg	AT5G08130;AT3G26744
1006	TF_motif_seq_0302	bHLH	-	1	cAGTTG	AT5G08130;AT3G26744
1006	TF_motif_seq_0313	(Others)	+	1	CAGTTg	D14712
1006	TF_motif_seq_0248	(Motif sequence only)	-	0.8	CAGTT	MYBCOREATCYCB1
1006	TF_motif_seq_0342	(Motif sequence only)	-	1	CAGTTg	MYB2CONSENSUSAT
1008	TF_motif_seq_0267	Trihelix	+	0.8	GTTGC	AT5G01380
1008	TF_motif_seq_0263	(Motif sequence only)	-	0.8	GTTGC	SORLIP1AT
1015	TF_motif_seq_0257	NF-YB;NF-YA;NF-YC	-	0.8	ATTGC	AT1G09030;AT1G17590;AT1G21970;AT1G30500;AT1G54160;AT1G54830;AT1G56170;AT1G72830;AT2G38880;AT2G47810;AT3G05690;AT3G14020;AT3G20910;AT3G53340;AT4G14540;AT5G06510;AT5G12840;AT5G27910;AT5G38140;AT5G47640;AT5G47670;AT5G50470;AT5G50480
1019	TF_motif_seq_0254	AP2;ERF	+	0.8	CTCTA	AT3G14230
1023	TF_motif_seq_0265	(Motif sequence only)	-	0.8	AGCCC	SORLIP2AT
1023	TF_motif_seq_0334	(Motif sequence only)	-	1	aGCCCA	SITEIIATCYTC
1029	TF_motif_seq_0261	(Motif sequence only)	+	0.8	GAGAA	SURECOREATSULTR11
1032	TF_motif_seq_0239	Dof	+	1	AAAGC	AT1G29160;AT1G64620;AT2G37590;AT3G21270;AT3G45610;AT3G47500;AT4G38000;AT5G39660;AT5G60200;AT5G60850;AT5G62940;AT2G46590;AT1G07640;AT1G21340;AT1G26790;AT1G47655;AT1G51700;AT1G69570;AT2G28510;AT2G28810;AT2G34140;AT3G50410;AT3G55370;AT3G61850;AT4G00940;AT4G21050;AT4G21080;AT4G24060;AT5G02460;AT5G62430;AT5G65590;AT5G66940
1034	TFmatrixID_0021	C2H2	+	0.91	agCAGCTcaa	AT4G35610
1034	TF_motif_seq_0291	(Motif sequence only)	+	1	AGCAGc	ANAERO2CONSENSUS
1039	TF_motif_seq_0275	(Motif sequence only)	-	0.8	CTCAA	WBOXATNPR1
1040	TF_motif_seq_0257	NF-YB;NF-YA;NF-YC	+	0.8	TCAAT	AT1G09030;AT1G17590;AT1G21970;AT1G30500;AT1G54160;AT1G54830;AT1G56170;AT1G72830;AT2G38880;AT2G47810;AT3G05690;AT3G14020;AT3G20910;AT3G53340;AT4G14540;AT5G06510;AT5G12840;AT5G27910;AT5G38140;AT5G47640;AT5G47670;AT5G50470;AT5G50480
1041	TFmatrixID_0005	AT-Hook	+	0.92	caATTAAgta	AT4G14465
10	TF_motif_s	ZF-HD	+	1	ATTAA	AT1G75240

43	eq_0241					
1044	TFmatrixID_0384	NAC;NAM	-	0.9	ttaAGTAAa	AT1G33060;AT3G49530;AT4G35580;AT5G24590
1048	TF_motif_seq_0267	Trihelix	-	0.8	GTAAA	AT5G01380
1048	TF_motif_seq_0275	(Motif sequence only)	-	0.8	GTAAA	WBOXATNPR1
1049	TF_motif_seq_0254	AP2;ERF	-	0.8	TAAAT	AT3G14230
1051	TF_motif_seq_0257	NF-YB;NF-YA;NF-YC	-	0.8	AATGG	AT1G09030;AT1G17590;AT1G21970;AT1G30500;AT1G54160;AT1G54830;AT1G56170;AT1G72830;AT2G38880;AT2G47810;AT3G05690;AT3G14020;AT3G20910;AT3G53340;AT4G14540;AT5G06510;AT5G12840;AT5G27910;AT5G38140;AT5G47640;AT5G47670;AT5G50470;AT5G50480
1051	TF_motif_seq_0248	(Motif sequence only)	+	0.8	AATGG	MYBCOREATCYCB1
1052	TF_motif_seq_0263	(Motif sequence only)	-	0.8	ATGGC	SORLIP1AT
1053	TF_motif_seq_0271	bZIP	+	0.8	TGGCG	AT1G77920;AT3G12250;AT5G06950;AT5G06960;AT5G10030;AT5G65210;AT1G22070
1056	TF_motif_seq_0237	GATA;tify	+	1	CGATG	AT1G51600;AT2G45050;AT3G06740;AT3G16870;AT3G21175;AT3G24050;AT3G54810;AT3G60530;AT4G17570;AT4G24470;AT4G26150;AT4G32890;AT4G34680;AT5G25830;AT5G26930;AT5G56860;AT5G66320;AT2G18380;AT3G50870;AT4G36620
1060	TF_motif_seq_0267	Trihelix	+	0.8	GTTAA	AT5G01380
1060	TF_motif_seq_0275	(Motif sequence only)	-	0.8	GTTAA	WBOXATNPR1
1062	TF_motif_seq_0403	(Motif sequence only)	+	0.86	taaAATCT	CCA1ATLHCB1
1065	TF_motif_seq_0237	GATA;tify	-	1	AATCT	AT1G51600;AT2G45050;AT3G06740;AT3G16870;AT3G21175;AT3G24050;AT3G54810;AT3G60530;AT4G17570;AT4G24470;AT4G26150;AT4G32890;AT4G34680;AT5G25830;AT5G26930;AT5G56860;AT5G66320;AT2G18380;AT3G50870;AT4G36620
1065	TF_motif_seq_0252	Myb/SANT;MYB;ARR-B	-	1	AATCT	AT2G01760;AT3G16857;AT4G16110;AT4G18020;AT4G31920;AT5G58080;AT1G67710;AT1G49190;AT2G25180;AT5G49240
1065	TF_motif_seq_0268	(Motif sequence only)	-	1	AATCT	ARR1AT
1066	TF_motif_seq_0254	AP2;ERF	+	0.8	ATCTC	AT3G14230
1066	TF_motif_seq_0261	(Motif sequence only)	-	0.8	ATCTC	SURECOREATSULTR11
1069	TF_motif_seq_0239	Dof	-	1	TCTTT	AT1G29160;AT1G64620;AT2G37590;AT3G21270;AT3G45610;AT3G47500;AT4G38000;AT5G39660;AT5G60200;AT5G60850;AT5G62940;AT2G46590;AT1G07640;AT1G21340;AT1G26790;AT1G47655;AT1G51700;AT1G69570;AT2G28510;AT2G28810;AT2G34140;AT3G50410;AT3G55370;AT3G61850;AT4G00940;AT4G21050;AT4G21080;AT4G24060;AT5G02460;AT5G62430;AT5G65590;AT5G66940
1074	TF_motif_seq_0237	GATA;tify	-	1	CATCG	AT1G51600;AT2G45050;AT3G06740;AT3G16870;AT3G21175;AT3G24050;AT3G54810;AT3G60530;AT4G17570;AT4G24470;AT4G26150;AT4G32890;AT4G34680;AT5G25830;AT5G26930;AT5G56860;AT5G66320;AT2G18380;AT3G50870;AT4G36620
1075	TF_motif_seq_0254	AP2;ERF	+	0.8	ATCGA	AT3G14230
1076	TF_motif_seq_0254	AP2;ERF	-	0.8	TCGAT	AT3G14230
1077	TF_motif_seq_0237	GATA;tify	+	1	CGATT	AT1G51600;AT2G45050;AT3G06740;AT3G16870;AT3G21175;AT3G24050;AT3G54810;AT3G60530;AT4G17570;AT4G24470;AT4G26150;AT4G32890;AT4G34680;AT5G25830;AT5G26930;AT5G56860;AT5G66320;AT2G18380;AT3G50870;AT4G36620
1077	TF_motif_seq_0268	(Motif sequence only)	+	1	CGATT	ARR1AT
1081	TFmatrixID_0131	AT-Hook	-	1	TTTATtcac	AT1G19485;AT1G48610
1085	TF_motif_seq_0275	(Motif sequence only)	+	0.8	TTCAC	WBOXATNPR1
1092	TF_motif_seq_0239	Dof	-	1	GCTTT	AT1G29160;AT1G64620;AT2G37590;AT3G21270;AT3G45610;AT3G47500;AT4G38000;AT5G39660;AT5G60200;AT5G60850;AT5G62940;AT2G46590;AT1G07640;AT1G21340;AT1G26790;AT1G47655;AT1G51700;AT1G69570;AT2G28510;AT2G28810;AT2G34140;AT3G50410;AT3G55370;AT3G61850;AT4G00940;AT4G21050;AT4G21080;AT4G24060;AT5G02460;AT5G62430;AT5G65590;AT5G66940

Supplementary table 2: Primer efficiencies of the qPCR runs

	Primer	Efficiency
Bio rep. 1	FRK1	97.14%
	Actin2	91.38%
Bio rep. 2	FRK1	84.12%
	Actin2	86.03%
Bio rep. 3	FRK1	88.33%
	Actin2	92.64%

Supplementary table 3: Identified Peptides of dTALE ChAP Repetition 1, 2 & 3

	dTALE-ChAP trial 1			
	Gene	Peptide number with flg22 and DEX	peptide number control	
	AT5G60390.3	105	13	
	TALE369	105	3	
	AT3G09260.1	46	1	
	AT5G59970.1	45	12	
	AT1G20620.1	25		
	AT1G54270.1	25		
	AT2G34420.1	21	3	
	AT3G18080.1	20		
	AT5G44340.1	20		
	AT3G08580.2	19		
	AT2G30620.2	18	2	
	AT3G44310.3	18		
	AT1G07790.1	16	25	
	AT1G78830.1	16		
	AT3G14310.1	15		
	AT1G43170.9	14		
	AT2G41840.1	14	1	
	AT2G16600.2	13		
	AT5G09810.1	13		
	AT4G14960.2	12		
	AT5G26260.1	12		
	AT5G02560.1	11		
	AT3G04920.1	11		
	AT1G66280.1	11		
	AT3G17390.1	10		
	AT5G27670.1	9	3	
	AT1G48920.1	9	1	
	AT2G21660.1	8		
	AT5G47210.1	8		
	AT5G52470.1	8		
	AT3G09630.2	7	1	
	AT4G01700.1	7		
	AT1G76010.1	7		
	AT3G49010.5	7		
	AT1G20580.1	7		
	AT1G33140.1	7		
	AT3G20370.1	7		
	AT1G78850.1	6		
	AT5G59870.1	6		

	ATCG00680.1	6		
	AT1G56070.1	6		
	ATCG00020.1	6		
	AT1G19880.1	6		
	AT1G26630.1	6		
	AT3G18780.2	6		
	AT5G65360.1	6	1	
	AT5G26280.2	5		
	AT5G56030.1	5		
	AT5G44500.2	5		
	AT3G04120.1	5	1	
	AT4G27090.1	5	1	
	AT2G31880.1	5		
	AT5G44020.1	5		
	AT2G34040.2	5		
	AT5G54640.1	5	4	
	AT1G52740.1	5		
	AT3G55280.3	5		
	AT4G17390.1	5		
	AT3G59540.1	5		
	AT4G00100.1	5		
	AT4G13940.1	5	1	
	AT5G38420.1	4		
	ATCG00490.1	4		
	AT2G19730.3	4	1	
	AT4G11010.1	4		
	AT2G05100.1	4		
	AT1G74060.1	4		
	AT1G48600.1	4		
	AT2G27530.2	4		
	AT3G62290.3	4		
	AT4G34555.1	4		
	AT5G03350.1	4		
	AT5G15200.1	4		
	AT1G20696.3	3		
	AT3G44110.2	3		
	AT4G34870.1	3		
	AT1G80490.1	3		
	AT5G52040.1	3	1	
	AT2G04160.1	3		
	AT5G59850.1	3		
	AT5G10980.1	3	6	
	AT5G02500.1	3		

	AT1G29930.1	3		
	AT3G10610.1	3		
	AT5G17920.2	3		
	AT4G09800.1	3		
	AT2G41475.1	3		
	AT2G22170.1	3		
	AT2G45220.1	3		
	AT1G59359.1	3		
	AT2G05380.1	3	8	
	AT3G62870.1	3		
	AT4G19410.1	3		
	AT2G01250.1	3		
	AT3G25520.2	3		
	AT3G49910.1	3		
	AT4G38680.1	2		
	AT4G20360.1	2		
	AT1G14320.1	2		
	AT1G31330.1	2		
	AT4G31580.2	2		
	AT3G07590.2	2		
	AT5G42020.2	2		
	AT3G61240.2	2		
	AT5G45775.1	2		
	AT5G07090.2	2		
	AT3G04840.1	2		
	AT5G08690.1	2		
	AT1G16300.1	2		
	AT5G09510.2	2		
	AT4G39200.2	2		
	AT1G03220.1	2		
	AT3G01290.1	2		
	AT1G03880.1	2		
	AT1G68560.1	2		
	AT5G11200.1	2		
	AT1G02780.1	2	1	
	AT2G05830.1	2		
	AT4G26630.2	2		
	AT3G16420.3	2		
	AT4G27170.1	2		
	AT5G19780.1	2		
	ATCG01060.1	2		
	AT1G67090.1	2		
	ATMG01190.1	2		

	AT4G10340.1	2		
	AT4G38740.1	2		
	AT1G79930.2	2		
	AT4G39260.3	2		
	AT1G67430.2	2		
	AT3G53430.1	2		
	AT1G17860.1	2		
	AT5G36890.2	1		
	AT2G24590.1	1		
	AT1G08360.1	1		
	AT2G45640.2	1		
	AT5G22650.2	1		
	AT1G75280.1	1		
	AT5G46070.1	1		
	AT1G26110.2	1		
	AT1G22060.1	1		
	AT4G14320.1	1		
	AT5G18380.3	1		
	AT2G16700.2	1		
	AT3G26060.1	1		
	AT4G15160.2	1		
	AT2G32700.6	1		
	AT2G17720.1	1		
	AT2G02470.2	1		
	AT3G06720.2	1		
	AT3G61440.3	1		
	AT2G19520.1	1		
	AT2G45180.1	1		
	AT4G22140.2	1		
	AT5G17270.1	1		
	AT4G22485.1	1		
	AT5G20290.1	1		
	AT4G23680.1	1		
	AT5G26210.1	1		
	AT4G23990.1	1		
	AT5G27850.1	1		
	AT1G09770.1	1		
	AT3G46000.1	1		
	AT4G27000.1	1		
	AT5G45280.2	1		
	AT1G10200.1	1		
	AT5G48760.2	1		
	AT4G27160.1	1	2	

	AT3G55460.1	1		
	AT3G09440.2	1		
	AT2G39880.1	1		
	AT4G27500.1	1		
	AT5G60790.1	1		
	AT4G29040.1	1		
	ATCG00280.1	1		
	AT4G30290.1	1		
	AT4G02520.1	1		
	AT4G31500.1	1		
	AT3G19390.1	1		
	AT1G33590.1	1		
	AT3G19760.1	1		
	AT4G31880.2	1		
	AT1G26550.1	1		
	AT4G33865.1	1		
	AT5G22010.1	1		
	AT2G21060.1	1		
	AT5G24550.1	1	1	
	AT3G11630.1	1		
	AT2G27830.1	1	5	
	AT4G35310.1	1		
	AT1G18080.1	1		
	AT4G36690.2	1		
	AT5G35760.1	1		
	AT4G38600.2	1		
	AT1G27650.2	1		
	AT3G12860.1	1		
	AT2G32080.2	1		
	AT3G13790.2	1		
	AT3G53020.1	1		
	AT3G13920.3	1		
	AT2G33040.1	1		
	AT3G14210.1	1		
	AT1G17370.2	1		
	AT3G14220.1	1		
	AT3G54400.1	1		
	AT2G21580.2	1		
	AT5G54270.1	1		
	AT5G02960.1	1		
	AT5G55190.1	1		
	AT3G15730.1	1		
	AT3G59620.1	1		

	AT5G03850.1	1		
	AT5G59910.1	1		
	AT5G06870.1	1		
	AT1G16610.2	1		
	AT1G66270.2	1		
	AT5G62300.2	1		
	AT3G16460.2	1		
	AT1G73260.1	1		
	AT5G09440.1	1		
	AT2G43920.2	1		
	AT1G79330.1	1		
	AT4G01880.1	1		
	AT1G12090.1	1		
	AT1G24310.1	1		
	AT3G18740.1	1		
	AT3G53740.1	1		
	AT1G80550.1		1	
	AT5G35530.1		1	
	AT2G37470.1		1	
	dTALE-ChAP trial 2	peptide number sample N14 induced / N15 uninduced		
		biorep. 1	biorep 2	biorep 3
	AT1G07930.2			
	AT1G11190.1			1
	AT1G20580.1			
	AT1G43170.4			
	AT1G48920.1	6		
	AT1G52740.1			
	AT1G54270.2	4		
	AT1G57860.1			
	AT1G62070.1	1		
	AT1G67430.2			
	AT1G68470.1			1
	AT1G80550.1		4	6
	AT2G01210.1	1		
	AT2G24590.1			
	AT2G30620.2			
	AT2G32240.1			
	AT2G41475.1		1	
	AT2G45970.1		2	1
	AT3G02880.1	1	1	7
	AT3G09260.1			
	AT3G18080.1			

	AT3G25520.2	7		
	AT3G46030.1	18		
	AT4G03080.1			
	AT4G09800.1	2		
	AT4G27610.3	1		
	AT4G39260.3			
	AT5G07090.2			
	AT5G10980.1	18		
	AT5G16590.1		8	14
	AT5G27670.1			
	AT5G36890.2			
	AT5G44500.2			
	AT5G50410.1			
	AT5G54640.1	6		
	AT5G59970.1	90		
	AT5G65360.1	5		
	dTALE C	103	19	18
		peptide number sample N15 induced / N14 uninduced		
		biorep. 1	biorep 2	biorep 3
	AT1G07930.2	22		
	AT1G11190.1			
	AT1G20580.1	5		
	AT1G43170.4	1		
	AT1G48920.1	7		
	AT1G52740.1	7		
	AT1G54270.2	1		
	AT1G57860.1	1		
	AT1G62070.1			
	AT1G67430.2	2		
	AT1G68470.1			
	AT1G80550.1	3		6
	AT2G01210.1			
	AT2G24590.1	4		
	AT2G30620.2	2		
	AT2G32240.1	1		
	AT2G41475.1			
	AT2G45970.1		1	
	AT3G02880.1		6	
	AT3G09260.1	4		
	AT3G18080.1	2		
	AT3G25520.2	3		
	AT3G46030.1	30		

	AT4G03080.1	2		
	AT4G09800.1	7		
	AT4G27610.3			
	AT4G39260.3	10		
	AT5G07090.2	5		
	AT5G10980.1	36		
	AT5G16590.1		14	8
	AT5G27670.1	2		
	AT5G36890.2	4		
	AT5G44500.2	1		
	AT5G50410.1	2		
	AT5G54640.1	28		
	AT5G59970.1	153		
	AT5G65360.1	36		
	dTALE C	71	13	1
	dTALE ChAP trial 3			
	peptide number sample N14 induced / N15 uninduced	sum of 3 bioreplicates		
	dTALE C	6		
	AT5G59970.1	7		
	AT5G02570.1	3		
	AT5G54640.1	2		
	AT1G11190.1	1		
	AT4G09800.1	2		
	AT1G48920.1	1		
	AT1G49730.4	1		
	AT3G14220.1	1		
	AT3G13920.3	1		
	AT1G64550.1	1		
	AT1G68470.1	1		
	AT5G10980.1	3		
	AT1G78830.1	2		
	AT1G80550.1	1		
	AT2G01210.1	1		
	AT2G01850.1	1		
	AT2G17360.2	1		
	AT2G27830.1	1		
	AT2G37230.1	1		
	AT2G41475.1	2		
	AT2G45970.1	1		
	AT3G02880.1	2		
	AT5G27770.1	1		
	AT3G14950.1	1		

	AT3G25520.2	1		
	AT3G63140.1	1		
	AT4G09780.1	1		
	AT4G12070.1	1		
	AT4G26690.1	1		
	AT4G27610.3	1		
	AT5G16590.1	1		
	AT5G25475.4	2		
	peptide number sample N15 induced / N14 uninduced	sum of 3 bioreplicaes		
	dTALE C	6		
	AT5G59970.1	10		
	AT1G07930.2	4		
	AT5G65360.1	5		
	AT1G20580.1	2		
	AT4G09800.1	4		
	AT1G28960.4	2		
	AT1G48920.1	2		
	AT5G54640.1	3		
	AT1G52740.1	2		
	AT2G05520.5	1		
	AT2G24590.1;	1		
	AT3G02880.1	1		
	AT3G04460.1	1		
	AT3G09260.1	2		
	AT3G18070.2	1		
	AT3G46030.1	6		
	AT4G39260.3	2		
	AT5G16590.1	1		
	AT5G27670.1	3		

Supplementary table 4: Over-representation Tests of identified Peptides in dTALE-ChAP Repetition 1, 2 & 3

dTALE ChAP trial 1 no treshold	trial 1 no treshold	Analysis Type:	PANTHER Overrepresentation Test (Released 20171205)						
		Annotation Version and Release Date:	GO Ontology database Released 2018-06-01						
		Analyzed List:	upload_1 (Arabidopsis thaliana)						
		Reference List:	Arabidopsis thaliana (all genes in database)						
		Test Type:	FISHER						
		GO cellular component complete	Arabidopsis thaliana - REFLIST (27502)	upload_1 (235)	upload_1 (expected)	upload_1 (over/under)	upload_1 (fold Enrichment)	upload_1 (raw P-value)	upload_1 (FDR)
		chloroplast ribulose bisphosphate carboxylase complex (GO:0009573)	3	2	0.03	+	78.02	7.03E-04	7.78E-03
		ribulose bisphosphate carboxylase complex (GO:0048492)	3	2	0.03	+	78.02	7.03E-04	7.70E-03
		chloroplast stromal thylakoid (GO:0009533)	10	4	0.09	+	46.81	4.70E-06	7.04E-05
		PSII associated light-harvesting complex II (GO:0009517)	6	2	0.05	+	39.01	1.94E-03	1.98E-02
		thylakoid light-harvesting complex (GO:0009503)	6	2	0.05	+	39.01	1.94E-03	1.96E-02
		pICln-Sm protein complex (GO:0034715)	6	2	0.05	+	39.01	1.94E-03	1.94E-02
		tubulin complex (GO:0045298)	13	4	0.11	+	36.01	1.10E-05	1.51E-04
		SMN-Sm protein complex (GO:0034719)	7	2	0.06	+	33.44	2.47E-03	2.39E-02
		nucleosome (GO:0000786)	47	12	0.4	+	29.88	8.13E-14	2.47E-12
		U2AF (GO:0089701)	8	2	0.07	+	29.26	3.08E-03	2.95E-02
		DNA packaging complex (GO:0044815)	51	12	0.44	+	27.54	1.88E-13	5.26E-12
		U4 snRNP (GO:0005687)	13	3	0.11	+	27.01	3.10E-04	3.92E-03
		proton-transporting ATP synthase complex, catalytic core F(1) (GO:0045261)	14	3	0.12	+	25.08	3.74E-04	4.62E-03
		cytosolic small ribosomal subunit (GO:0022627)	108	22	0.92	+	23.84	1.86E-22	7.08E-21
		heterochromatin (GO:0000792)	15	3	0.13	+	23.41	4.46E-04	5.27E-03
		light-harvesting complex (GO:0030076)	25	5	0.21	+	23.41	5.02E-06	7.40E-05
		cytosolic large ribosomal subunit (GO:0022625)	147	28	1.26	+	22.29	1.35E-27	6.50E-26
		commitment complex (GO:0000243)	16	3	0.14	+	21.94	5.26E-04	6.08E-03
		box C/D snoRNP complex (GO:0031428)	11	2	0.09	+	21.28	5.24E-03	4.80E-02
		cytosolic ribosome (GO:0022626)	324	58	2.77	+	20.95	1.06E-55	3.76E-53
		photosystem I (GO:0009522)	41	7	0.35	+	19.98	1.57E-07	2.83E-06
		small ribosomal subunit (GO:0015935)	134	22	1.15	+	19.21	1.18E-20	4.33E-19

		cytosolic part (GO:0044445)	372	59	3.18	+	18.56	6.04E-54	1.60E-51
		ribosomal subunit (GO:0044391)	340	50	2.91	+	17.21	4.43E-44	3.14E-42
		protein-DNA complex (GO:0032993)	83	12	0.71	+	16.92	3.04E-11	7.87E-10
		U5 snRNP (GO:0005682)	21	3	0.18	+	16.72	1.07E-03	1.14E-02
		large ribosomal subunit (GO:0015934)	204	28	1.74	+	16.06	4.28E-24	1.75E-22
		proton-transporting two-sector ATPase complex, catalytic domain (GO:0033178)	22	3	0.19	+	15.96	1.20E-03	1.28E-02
		nucleolus (GO:0005730)	445	60	3.8	+	15.78	3.95E-51	6.00E-49
		plastoglobule (GO:0010287)	80	10	0.68	+	14.63	4.98E-09	1.08E-07
		ribosome (GO:0005840)	469	58	4.01	+	14.47	1.97E-47	2.62E-45
		photosystem II (GO:0009523)	67	8	0.57	+	13.97	2.44E-07	4.32E-06
		small nucleolar ribonucleoprotein complex (GO:0005732)	43	5	0.37	+	13.61	5.32E-05	6.99E-04
		U1 snRNP (GO:0005685)	27	3	0.23	+	13	2.06E-03	2.05E-02
		photosystem (GO:0009521)	92	10	0.79	+	12.72	1.70E-08	3.47E-07
		mitochondrial proton-transporting ATP synthase complex (GO:0005753)	28	3	0.24	+	12.54	2.27E-03	2.21E-02
		nuclear speck (GO:0016607)	84	9	0.72	+	12.54	1.00E-07	1.90E-06
		endoplasmic reticulum lumen (GO:0005788)	38	4	0.32	+	12.32	4.37E-04	5.22E-03
		ribonucleoprotein complex (GO:1990904)	811	73	6.93	+	10.53	2.39E-51	4.23E-49
		nuclear body (GO:0016604)	113	10	0.97	+	10.36	1.02E-07	1.91E-06
		chromatin (GO:0000785)	170	14	1.45	+	9.64	6.57E-10	1.59E-08
		proton-transporting ATP synthase complex (GO:0045259)	37	3	0.32	+	9.49	4.71E-03	4.39E-02
		U2 snRNP (GO:0005686)	37	3	0.32	+	9.49	4.71E-03	4.35E-02
		nuclear chromatin (GO:0000790)	79	6	0.68	+	8.89	8.68E-05	1.13E-03
		plasmodesma (GO:0009506)	1011	75	8.64	+	8.68	2.92E-47	3.45E-45
		symplast (GO:0055044)	1011	75	8.64	+	8.68	2.92E-47	3.10E-45
		cell-cell junction (GO:0005911)	1013	75	8.66	+	8.66	3.33E-47	3.22E-45
		cell junction (GO:0030054)	1013	75	8.66	+	8.66	3.33E-47	2.95E-45
		spliceosomal complex (GO:0005681)	151	11	1.29	+	8.53	1.49E-07	2.72E-06
		U2-type spliceosomal complex (GO:0005684)	57	4	0.49	+	8.21	1.80E-03	1.89E-02
		intracellular non-membrane-bounded organelle (GO:0043232)	1670	112	14.27	+	7.85	1.17E-69	1.24E-66
		non-membrane-bounded organelle (GO:0043228)	1670	112	14.27	+	7.85	1.17E-69	6.22E-67
		nuclear lumen (GO:0031981)	1053	68	9	+	7.56	5.70E-39	3.57E-37
		apoplast (GO:0048046)	496	32	4.24	+	7.55	3.05E-18	1.05E-16
		external encapsulating structure (GO:0030312)	777	47	6.64	+	7.08	1.84E-25	8.15E-24
		cell wall (GO:0005618)	777	47	6.64	+	7.08	1.84E-25	7.82E-24

		intracellular organelle lumen (GO:0070013)	1279	72	10.93	+	6.59	1.09E-37	6.43E-36
		membrane-enclosed lumen (GO:0031974)	1279	72	10.93	+	6.59	1.09E-37	6.09E-36
		organelle lumen (GO:0043233)	1279	72	10.93	+	6.59	1.09E-37	5.79E-36
		vacuolar membrane (GO:0005774)	650	34	5.55	+	6.12	1.04E-16	3.44E-15
		vacuolar part (GO:0044437)	652	34	5.57	+	6.1	1.13E-16	3.64E-15
		nuclear part (GO:0044428)	1396	69	11.93	+	5.78	1.14E-32	5.75E-31
		vacuole (GO:0005773)	1114	55	9.52	+	5.78	9.68E-26	4.47E-24
		cytosol (GO:0005829)	2261	108	19.32	+	5.59	1.18E-52	2.50E-50
		chromosomal part (GO:0044427)	333	15	2.85	+	5.27	3.29E-07	5.74E-06
		chromosome (GO:0005694)	386	15	3.3	+	4.55	1.94E-06	3.17E-05
		nuclear chromosome part (GO:0044454)	161	6	1.38	+	4.36	3.08E-03	2.92E-02
		chloroplast thylakoid membrane (GO:0009535)	407	15	3.48	+	4.31	3.61E-06	5.73E-05
		plastid thylakoid membrane (GO:0055035)	408	15	3.49	+	4.3	3.71E-06	5.72E-05
		protein-containing complex (GO:0032991)	3150	112	26.92	+	4.16	1.20E-42	7.94E-41
		thylakoid (GO:0009579)	591	21	5.05	+	4.16	7.02E-08	1.36E-06
		thylakoid membrane (GO:0042651)	428	15	3.66	+	4.1	6.47E-06	9.29E-05
		photosynthetic membrane (GO:0034357)	429	15	3.67	+	4.09	6.65E-06	9.42E-05
		nuclear chromosome (GO:0000228)	174	6	1.49	+	4.04	4.44E-03	4.18E-02
		whole membrane (GO:0098805)	994	34	8.49	+	4	1.18E-11	3.14E-10
		thylakoid part (GO:0044436)	470	16	4.02	+	3.98	4.52E-06	6.87E-05
		chloroplast thylakoid (GO:0009534)	517	17	4.42	+	3.85	3.54E-06	5.70E-05
		plastid thylakoid (GO:0031976)	518	17	4.43	+	3.84	3.63E-06	5.67E-05
		chloroplast stroma (GO:0009570)	749	22	6.4	+	3.44	7.87E-07	1.35E-05
		plastid stroma (GO:0009532)	772	22	6.6	+	3.34	1.28E-06	2.12E-05
		bounding membrane of organelle (GO:0098588)	1317	36	11.25	+	3.2	1.13E-09	2.61E-08
		nucleoplasm part (GO:0044451)	410	11	3.5	+	3.14	9.97E-04	1.08E-02
		intracellular organelle part (GO:0044446)	5417	145	46.29	+	3.13	2.08E-44	1.70E-42
		organelle part (GO:0044422)	5424	145	46.35	+	3.13	2.43E-44	1.85E-42
		plant-type cell wall (GO:0009505)	380	10	3.25	+	3.08	1.92E-03	1.98E-02
		nucleoplasm (GO:0005654)	511	12	4.37	+	2.75	1.80E-03	1.87E-02
		chloroplast envelope (GO:0009941)	684	16	5.84	+	2.74	3.39E-04	4.24E-03
		plastid envelope (GO:0009526)	703	16	6.01	+	2.66	4.54E-04	5.31E-03
		organelle membrane (GO:0031090)	1891	42	16.16	+	2.6	1.58E-08	3.29E-07
		membrane protein complex (GO:0098796)	670	14	5.73	+	2.45	2.23E-03	2.19E-02
		chloroplast part (GO:0044434)	1429	29	12.21	+	2.37	2.12E-05	2.88E-04

		chloroplast (GO:0009507)	3975	80	33.97	+	2.36	6.37E-14	1.99E-12
		plastid part (GO:0044435)	1457	29	12.45	+	2.33	2.81E-05	3.78E-04
		plastid (GO:0009536)	4034	80	34.47	+	2.32	1.65E-13	4.75E-12
		extracellular region (GO:0005576)	2926	58	25	+	2.32	1.08E-09	2.55E-08
		envelope (GO:0031975)	1210	23	10.34	+	2.22	3.74E-04	4.57E-03
		organelle envelope (GO:0031967)	1210	23	10.34	+	2.22	3.74E-04	4.52E-03
		cell periphery (GO:0071944)	4525	86	38.67	+	2.22	1.59E-13	4.69E-12
		plasma membrane (GO:0005886)	3881	67	33.16	+	2.02	1.55E-08	3.29E-07
		cytoplasmic part (GO:0044444)	10752	168	91.87	+	1.83	2.23E-23	8.77E-22
		membrane (GO:0016020)	8459	126	72.28	+	1.74	5.00E-13	1.36E-11
		cytoplasm (GO:0005737)	13219	182	112.95	+	1.61	7.36E-20	2.61E-18
		nucleus (GO:0005634)	9826	110	83.96	+	1.31	6.04E-04	6.91E-03
		intracellular organelle (GO:0043229)	17998	199	153.79	+	1.29	7.14E-11	1.81E-09
		organelle (GO:0043226)	18037	199	154.12	+	1.29	7.35E-11	1.82E-09
		intracellular part (GO:0044424)	20009	209	170.97	+	1.22	2.22E-09	5.01E-08
		intracellular (GO:0005622)	20022	209	171.08	+	1.22	2.24E-09	4.95E-08
		intracellular membrane-bounded organelle (GO:0043231)	17644	180	150.77	+	1.19	5.10E-05	6.77E-04
		membrane-bounded organelle (GO:0043227)	17746	180	151.64	+	1.19	8.71E-05	1.12E-03
		cell part (GO:0044464)	22024	219	188.19	+	1.16	3.59E-08	7.07E-07
		cell (GO:0005623)	22025	219	188.2	+	1.16	3.59E-08	7.20E-07
		cellular_component (GO:0005575)	25076	228	214.27	+	1.06	6.77E-04	7.57E-03
		membrane part (GO:0044425)	5608	22	47.92	-	0.46	8.93E-06	1.25E-04
		integral component of membrane (GO:0016021)	4853	17	41.47	-	0.41	6.13E-06	8.93E-05
		intrinsic component of membrane (GO:0031224)	5102	17	43.6	-	0.39	1.16E-06	1.96E-05
		Unclassified (UNCLASSIFIED)	2426	7	20.73	-	0.34	6.77E-04	7.65E-03
trial 1 treshold = at least 5 found peptides	**Cellular Component**	Analysis Type:	PANTHER Overrepresentation Test (Released 20171205)						
		Annotation Version and Release Date:	GO Ontology database Released 2018-06-01						
		Analyzed List:	upload_1 (Arabidopsis thaliana)						
		Reference List:	Arabidopsis thaliana (all genes in database)						
		Test Type:	FISHER						
		GO cellular component complete	Arabidopsis thaliana - REFLIST (27502)	upload_1 (64)	upload_1 (expected)	upload_1 (over/under)	upload_1 (fold Enrichment)	upload_1 (raw P-value)	upload_1 (FDR)

		heterochromatin (GO:0000792)	15	3	0.03	+	85.94	9.50E-06	2.20E-04
		nucleosome (GO:0000786)	47	9	0.11	+	82.29	7.58E-15	4.48E-13
		DNA packaging complex (GO:0044815)	51	9	0.12	+	75.83	1.47E-14	8.22E-13
		tubulin complex (GO:0045298)	13	2	0.03	+	66.11	5.46E-04	9.84E-03
		U4 snRNP (GO:0005687)	13	2	0.03	+	66.11	5.46E-04	9.68E-03
		protein-DNA complex (GO:0032993)	83	9	0.19	+	46.6	8.15E-13	3.77E-11
		U5 snRNP (GO:0005682)	21	2	0.05	+	40.93	1.30E-03	2.13E-02
		U1 snRNP (GO:0005685)	27	2	0.06	+	31.83	2.07E-03	3.19E-02
		small nucleolar ribonucleoprotein complex (GO:0005732)	43	3	0.1	+	29.98	1.69E-04	3.38E-03
		nuclear chromatin (GO:0000790)	79	5	0.18	+	27.2	1.54E-06	3.81E-05
		cytosolic large ribosomal subunit (GO:0022625)	147	9	0.34	+	26.31	9.96E-11	4.07E-09
		nucleolus (GO:0005730)	445	24	1.04	+	23.18	2.58E-26	2.74E-23
		chromatin (GO:0000785)	170	9	0.4	+	22.75	3.40E-10	1.25E-08
		chromosome, centromeric region (GO:0000775)	59	3	0.14	+	21.85	4.09E-04	7.50E-03
		photosystem II (GO:0009523)	67	3	0.16	+	19.24	5.85E-04	1.02E-02
		large ribosomal subunit (GO:0015934)	204	9	0.47	+	18.96	1.58E-09	5.60E-08
		cytosolic ribosome (GO:0022626)	324	14	0.75	+	18.57	3.66E-14	1.94E-12
		chromosomal region (GO:0098687)	101	4	0.24	+	17.02	1.06E-04	2.17E-03
		cytosolic part (GO:0044445)	372	14	0.87	+	16.17	2.24E-13	1.13E-11
		plastoglobule (GO:0010287)	80	3	0.19	+	16.11	9.61E-04	1.60E-02
		ribosomal subunit (GO:0044391)	340	12	0.79	+	15.17	2.82E-11	1.20E-09
		photosystem (GO:0009521)	92	3	0.21	+	14.01	1.42E-03	2.29E-02
		nuclear chromosome part (GO:0044454)	161	5	0.37	+	13.35	4.27E-05	9.65E-04
		ribosome (GO:0005840)	469	14	1.09	+	12.83	4.59E-12	2.03E-10
		plasmodesma (GO:0009506)	1011	30	2.35	+	12.75	6.48E-26	3.44E-23
		symplast (GO:0055044)	1011	30	2.35	+	12.75	6.48E-26	2.30E-23
		cell-cell junction (GO:0005911)	1013	30	2.36	+	12.73	6.85E-26	1.82E-23
		cell junction (GO:0030054)	1013	30	2.36	+	12.73	6.85E-26	1.46E-23
		nuclear chromosome (GO:0000228)	174	5	0.4	+	12.35	6.10E-05	1.35E-03
		cytosolic small ribosomal subunit (GO:0022627)	108	3	0.25	+	11.94	2.21E-03	3.36E-02
		chromosomal part (GO:0044427)	333	9	0.77	+	11.61	9.48E-08	2.72E-06
		nuclear lumen (GO:0031981)	1053	26	2.45	+	10.61	2.77E-20	2.68E-18
		chromosome (GO:0005694)	386	9	0.9	+	10.02	3.20E-07	8.28E-06
		ribonucleoprotein complex (GO:1990904)	811	18	1.89	+	9.54	3.32E-13	1.60E-11
		apoplast (GO:0048046)	496	11	1.15	+	9.53	2.26E-08	7.06E-07

		intracellular organelle lumen (GO:0070013)	1279	28	2.98	+	9.41	1.37E-20	1.82 E-18
		membrane-enclosed lumen (GO:0031974)	1279	28	2.98	+	9.41	1.37E-20	1.62 E-18
		organelle lumen (GO:0043233)	1279	28	2.98	+	9.41	1.37E-20	1.46 E-18
		vacuolar membrane (GO:0005774)	650	14	1.51	+	9.26	3.05E-10	1.20 E-08
		vacuolar part (GO:0044437)	652	14	1.52	+	9.23	3.17E-10	1.20 E-08
		intracellular non-membrane-bounded organelle (GO:0043232)	1670	35	3.89	+	9.01	8.54E-26	1.51 E-23
		non-membrane-bounded organelle (GO:0043228)	1670	35	3.89	+	9.01	8.54E-26	1.30 E-23
		vacuole (GO:0005773)	1114	22	2.59	+	8.49	4.27E-15	2.84 E-13
		nuclear part (GO:0044428)	1396	26	3.25	+	8	2.43E-17	2.15 E-15
		external encapsulating structure (GO:0030312)	777	14	1.81	+	7.74	2.90E-09	9.95 E-08
		cell wall (GO:0005618)	777	14	1.81	+	7.74	2.90E-09	9.64 E-08
		whole membrane (GO:0098805)	994	14	2.31	+	6.05	6.08E-08	1.80 E-06
		cytosol (GO:0005829)	2261	31	5.26	+	5.89	3.14E-17	2.57 E-15
		bounding membrane of organelle (GO:0098588)	1317	14	3.06	+	4.57	1.73E-06	4.09 E-05
		protein-containing complex (GO:0032991)	3150	33	7.33	+	4.5	4.62E-15	2.89 E-13
		intracellular organelle part (GO:0044446)	5417	43	12.61	+	3.41	2.36E-16	1.79 E-14
		organelle part (GO:0044422)	5424	43	12.62	+	3.41	2.48E-16	1.76 E-14
		organelle membrane (GO:0031090)	1891	14	4.4	+	3.18	9.72E-05	2.11 E-03
		plasma membrane (GO:0005886)	3881	26	9.03	+	2.88	1.95E-07	5.31 E-06
		chloroplast (GO:0009507)	3975	25	9.25	+	2.7	1.26E-06	3.18 E-05
		plastid (GO:0009536)	4034	25	9.39	+	2.66	1.66E-06	4.00 E-05
		cell periphery (GO:0071944)	4525	28	10.53	+	2.66	2.70E-07	7.17 E-06
		extracellular region (GO:0005576)	2926	17	6.81	+	2.5	2.93E-04	5.56 E-03
		membrane (GO:0016020)	8459	40	19.68	+	2.03	1.94E-07	5.41 E-06
		cytoplasmic part (GO:0044444)	10752	48	25.02	+	1.92	7.85E-09	2.53 E-07
		cytoplasm (GO:0005737)	13219	52	30.76	+	1.69	5.61E-08	1.70 E-06
		nucleus (GO:0005634)	9826	37	22.87	+	1.62	3.59E-04	6.70 E-03
		intracellular organelle (GO:0043229)	17998	56	41.88	+	1.34	1.01E-04	2.14 E-03
		organelle (GO:0043226)	18037	56	41.97	+	1.33	1.02E-04	2.14 E-03
		intracellular membrane-bounded organelle (GO:0043231)	17644	53	41.06	+	1.29	1.54E-03	2.44 E-02
		membrane-bounded organelle (GO:0043227)	17746	53	41.3	+	1.28	1.60E-03	2.50 E-02
		intracellular part (GO:0044424)	20009	59	46.56	+	1.27	1.91E-04	3.75 E-03
		intracellular (GO:0005622)	20022	59	46.59	+	1.27	1.91E-04	3.69 E-03
		cell part (GO:0044464)	22024	61	51.25	+	1.19	8.45E-04	1.45 E-02
		cell (GO:0005623)	22025	61	51.25	+	1.19	8.45E-04	1.43 E-02

	Protein Class	Analysis Type:	PANTHER Overrepresentation Test (Released 20171205)						
		Annotation Version and Release Date:	PANTHER version 13.1 Released 2018-02-03						
		Analyzed List:	upload_1 (Arabidopsis thaliana)						
		Reference List:	Arabidopsis thaliana (all genes in database)						
		Test Type:	FISHER						
		PANTHER Protein Class	Arabidopsis thaliana - REFLIST (27502)	upload_1 (64)	upload_1 (expected)	upload_1 (over/under)	upload_1 (fold Enrichment)	upload_1 (raw P-value)	upload_1 (FDR)
		histone (PC00118)	11	4	0.03	+	>100	3.54E-08	1.56E-06
		tubulin (PC00228)	17	2	0.04	+	50.56	8.85E-04	1.56E-02
		translation elongation factor (PC00222)	44	5	0.1	+	48.83	1.01E-07	3.57E-06
		actin and actin related protein (PC00039)	19	2	0.04	+	45.23	1.08E-03	1.73E-02
		translation initiation factor (PC00224)	96	6	0.22	+	26.86	1.39E-07	4.09E-06
		G-protein (PC00020)	95	5	0.22	+	22.62	3.65E-06	8.04E-05
		translation factor (PC00223)	138	6	0.32	+	18.68	1.07E-06	2.69E-05
		ribosomal protein (PC00202)	322	10	0.75	+	13.35	4.78E-09	2.80E-07
		RNA binding protein (PC00031)	1115	19	2.59	+	7.32	6.06E-12	5.34E-10
		nucleic acid binding (PC00171)	1771	24	4.12	+	5.82	5.75E-13	1.01E-10
		Unclassified (UNCLASSIFIED)	19939	31	46.4	-	0.67	5.75E-05	1.13E-03
	Molecular Function	Analysis Type:	PANTHER Overrepresentation Test (Released 20171205)						
		Annotation Version and Release Date:	GO Ontology database Released 2018-06-01						
		Analyzed List:	upload_1 (Arabidopsis thaliana)						
		Reference List:	Arabidopsis thaliana (all genes in database)						
		Test Type:	FISHER						
		GO molecular function complete	Arabidopsis thaliana - REFLIST (27502)	upload_1 (64)	upload_1 (expected)	upload_1 (over/under)	upload_1 (fold Enrichment)	upload_1 (raw P-value)	upload_1 (FDR)
		translation elongation factor activity (GO:0003746)	55	6	0.13	+	46.88	6.19E-09	1.95E-06
		chlorophyll binding (GO:0016168)	36	3	0.08	+	35.81	1.03E-04	2.02E-02
		structural constituent of cytoskeleton (GO:0005200)	50	4	0.12	+	34.38	7.66E-06	1.61E-03
		scopolin beta-glucosidase activity (GO:0102483)	42	3	0.1	+	30.69	1.58E-04	2.93E-02

		protein heterodimerization activity (GO:0046982)	118	8	0.27	+	29.13	5.44E-10	1.90E-07
		translation factor activity, RNA binding (GO:0008135)	165	7	0.38	+	18.23	1.50E-07	4.30E-05
		mRNA binding (GO:0003729)	418	17	0.97	+	17.48	1.20E-16	1.88E-13
		GTPase activity (GO:0003924)	180	7	0.42	+	16.71	2.65E-07	6.95E-05
		structural constituent of ribosome (GO:0003735)	360	12	0.84	+	14.32	5.34E-11	2.41E-08
		structural molecule activity (GO:0005198)	530	16	1.23	+	12.97	9.18E-14	4.82E-11
		copper ion binding (GO:0005507)	240	5	0.56	+	8.95	2.65E-04	4.64E-02
		RNA binding (GO:0003723)	1457	26	3.39	+	7.67	6.70E-17	2.11E-13
		protein dimerization activity (GO:0046983)	551	9	1.28	+	7.02	5.64E-06	1.27E-03
		nucleic acid binding (GO:0003676)	4005	36	9.32	+	3.86	1.31E-14	1.38E-11
		heterocyclic compound binding (GO:1901363)	6970	45	16.22	+	2.77	6.36E-14	5.01E-11
		organic cyclic compound binding (GO:0097159)	6991	45	16.27	+	2.77	7.14E-14	4.50E-11
		protein binding (GO:0005515)	4369	26	10.17	+	2.56	1.98E-06	4.81E-04
		binding (GO:0005488)	11350	52	26.41	+	1.97	9.29E-11	3.66E-08
	Biological Process	Analysis Type:	PANTHER Overrepresentation Test (Released 20171205)						
		Annotation Version and Release Date:	GO Ontology database Released 2018-06-01						
		Analyzed List:	upload_1 (Arabidopsis thaliana)						
		Reference List:	Arabidopsis thaliana (all genes in database)						
		Test Type:	FISHER						
		GO biological process complete	Arabidopsis thaliana - REFLIST (27502)	upload_1 (64)	upload_1 (expected)	upload_1 (over/under)	upload_1 (fold Enrichment)	upload_1 (raw P-value)	upload_1 (FDR)
		heterochromatin organization (GO:0070828)	11	3	0.03	+	100	4.27E-06	1.05E-03
		S-adenosylmethionine metabolic process (GO:0046500)	10	2	0.02	+	85.94	3.45E-04	3.51E-02
		photosynthetic electron transport in photosystem II (GO:0009772)	10	2	0.02	+	85.94	3.45E-04	3.45E-02
		chromatin silencing (GO:0006342)	54	6	0.13	+	47.75	5.59E-09	3.66E-06
		negative regulation of gene expression, epigenetic (GO:0045814)	58	6	0.13	+	44.45	8.31E-09	4.90E-06
		translational elongation (GO:0006414)	73	6	0.17	+	35.32	3.00E-08	1.36E-05
		nucleosome assembly (GO:0006334)	40	3	0.09	+	32.23	1.38E-04	1.73E-02
		protein-chromophore linkage (GO:0018298)	44	3	0.1	+	29.3	1.80E-04	2.08E-02
		chromatin assembly (GO:0031497)	48	3	0.11	+	26.86	2.30E-04	2.60E-02
		sulfur compound catabolic process (GO:0044273)	52	3	0.12	+	24.79	2.87E-04	3.08E-02
		nucleosome organization (GO:0034728)	53	3	0.12	+	24.32	3.03E-04	3.13E-02

		glycosyl compound catabolic process (GO:1901658)	60	3	0.14	+	21.49	4.29E-04	4.22 E-02
		chromatin assembly or disassembly (GO:0006333)	61	3	0.14	+	21.13	4.49E-04	4.14 E-02
		DNA packaging (GO:0006323)	63	3	0.15	+	20.46	4.92E-04	4.46 E-02
		carbohydrate derivative catabolic process (GO:1901136)	97	4	0.23	+	17.72	9.11E-05	1.28 E-02
		regulation of gene expression, epigenetic (GO:0040029)	149	6	0.35	+	17.3	1.64E-06	5.38 E-04
		gene silencing (GO:0016458)	161	6	0.37	+	16.01	2.53E-06	7.11 E-04
		DNA conformation change (GO:0071103)	115	4	0.27	+	14.95	1.72E-04	2.02 E-02
		response to cytokinin (GO:0009735)	251	7	0.58	+	11.98	2.29E-06	6.74 E-04
		chromatin organization (GO:0006325)	359	10	0.84	+	11.97	1.30E-08	6.99 E-06
		translation (GO:0006412)	612	17	1.42	+	11.94	5.07E-14	2.99 E-10
		peptide biosynthetic process (GO:0043043)	617	17	1.44	+	11.84	5.77E-14	1.70 E-10
		negative regulation of transcription, DNA-templated (GO:0045892)	239	6	0.56	+	10.79	2.26E-05	4.30 E-03
		negative regulation of RNA biosynthetic process (GO:1902679)	240	6	0.56	+	10.74	2.31E-05	4.26 E-03
		negative regulation of nucleic acid-templated transcription (GO:1903507)	240	6	0.56	+	10.74	2.31E-05	4.13 E-03
		amide biosynthetic process (GO:0043604)	693	17	1.61	+	10.54	3.57E-13	7.02 E-10
		negative regulation of RNA metabolic process (GO:0051253)	248	6	0.58	+	10.4	2.77E-05	4.80 E-03
		peptide metabolic process (GO:0006518)	707	17	1.65	+	10.33	4.88E-13	7.19 E-10
		negative regulation of nucleobase-containing compound metabolic process (GO:0045934)	275	6	0.64	+	9.38	4.86E-05	7.74 E-03
		chromosome organization (GO:0051276)	529	11	1.23	+	8.94	4.29E-08	1.81 E-05
		cellular amide metabolic process (GO:0043603)	847	17	1.97	+	8.62	8.07E-12	9.51 E-09
		negative regulation of cellular macromolecule biosynthetic process (GO:2000113)	305	6	0.71	+	8.45	8.50E-05	1.25 E-02
		negative regulation of macromolecule biosynthetic process (GO:0010558)	306	6	0.71	+	8.43	8.65E-05	1.24 E-02
		ribosome biogenesis (GO:0042254)	423	8	0.98	+	8.13	6.89E-06	1.56 E-03
		negative regulation of cellular biosynthetic process (GO:0031327)	326	6	0.76	+	7.91	1.22E-04	1.59 E-02
		negative regulation of biosynthetic process (GO:0009890)	331	6	0.77	+	7.79	1.32E-04	1.69 E-02
		ribonucleoprotein complex biogenesis (GO:0022613)	512	9	1.19	+	7.55	3.14E-06	8.42 E-04
		response to cadmium ion (GO:0046686)	342	6	0.8	+	7.54	1.57E-04	1.89 E-02
		response to cold (GO:0009409)	411	7	0.96	+	7.32	5.17E-05	8.03 E-03
		cellular protein-containing complex assembly (GO:0034622)	495	8	1.15	+	6.94	2.10E-05	4.13 E-03
		negative regulation of nitrogen compound metabolic process (GO:0051172)	383	6	0.89	+	6.73	2.86E-04	3.12 E-02
		response to temperature stimulus (GO:0009266)	600	9	1.4	+	6.45	1.10E-05	2.32 E-03

		protein-containing complex assembly (GO:0065003)	541	8	1.26	+	6.35	3.91E-05	6.58 E-03
		negative regulation of cellular metabolic process (GO:0031324)	415	6	0.97	+	6.21	4.35E-04	4.07 E-02
		protein-containing complex subunit organization (GO:0043933)	632	8	1.47	+	5.44	1.14E-04	1.53 E-02
		organonitrogen compound biosynthetic process (GO:1901566)	1573	19	3.66	+	5.19	1.90E-09	1.60 E-06
		organelle organization (GO:0006996)	1617	18	3.76	+	4.78	1.97E-08	9.70 E-06
		cellular component assembly (GO:0022607)	772	8	1.8	+	4.45	4.33E-04	4.12 E-02
		cellular component biogenesis (GO:0044085)	1268	13	2.95	+	4.41	6.38E-06	1.50 E-03
		cellular component organization or biogenesis (GO:0071840)	3101	28	7.22	+	3.88	5.59E-11	5.49 E-08
		cellular component organization (GO:0016043)	2752	24	6.4	+	3.75	4.86E-09	3.58 E-06
		response to abiotic stimulus (GO:0009628)	2070	15	4.82	+	3.11	6.62E-05	1.00 E-02
		cellular protein metabolic process (GO:0044267)	3253	23	7.57	+	3.04	5.40E-07	1.87 E-04
		gene expression (GO:0010467)	3226	22	7.51	+	2.93	1.95E-06	6.04 E-04
		cellular nitrogen compound biosynthetic process (GO:0044271)	3032	20	7.06	+	2.83	1.12E-05	2.28 E-03
		protein metabolic process (GO:0019538)	3618	23	8.42	+	2.73	3.44E-06	8.83 E-04
		organonitrogen compound metabolic process (GO:1901564)	4851	30	11.29	+	2.66	7.45E-08	2.93 E-05
		cellular macromolecule biosynthetic process (GO:0034645)	2983	18	6.94	+	2.59	1.14E-04	1.56 E-02
		macromolecule biosynthetic process (GO:0009059)	3030	18	7.05	+	2.55	1.39E-04	1.70 E-02
		cellular nitrogen compound metabolic process (GO:0034641)	4694	26	10.92	+	2.38	7.68E-06	1.68 E-03
		nitrogen compound metabolic process (GO:0006807)	7880	34	18.34	+	1.85	4.24E-05	6.95 E-03
		macromolecule metabolic process (GO:0043170)	7094	30	16.51	+	1.82	2.83E-04	3.15 E-02
		cellular process (GO:0009987)	12311	50	28.65	+	1.75	8.34E-08	3.07 E-05
		primary metabolic process (GO:0044238)	9047	35	21.05	+	1.66	4.30E-04	4.16 E-02
		cellular metabolic process (GO:0044237)	9346	36	21.75	+	1.66	2.98E-04	3.14 E-02
	Reactome Pathway	Analysis Type:	PANTHER Overrepresentation Test (Released 20171205)						
		Annotation Version and Release Date:	Reactome version 58 Released 2016-12-07						
		Analyzed List:	upload_1 (Arabidopsis thaliana)						
		Reference List:	Arabidopsis thaliana (all genes in database)						
		Test Type:	FISHER						
		Reactome pathways	Arabidopsis thaliana - REFLIST (27502)	upload_1 (64)	upload_1 (expected)	upload_1 (over/under)	upload_1 (fold Enrichment)	upload_1 (raw P-value)	upload_1 (FDR)

		Eukaryotic Translation Elongation (R-ATH-156842)	12	5	0.03	+	> 100	3.48E-10	6.60E-08
		Gamma carboxylation, hypusine formation and arylsulfatase activation (R-ATH-163841)	12	2	0.03	+	71.62	4.74E-04	2.00E-02
		Methylation (R-ATH-156581)	13	2	0.03	+	66.11	5.46E-04	2.18E-02
		HSF1 activation (R-ATH-3371511)	49	5	0.11	+	43.85	1.67E-07	8.42E-06
		Translation (R-ATH-72766)	276	14	0.64	+	21.8	4.44E-15	3.37E-12
		GTP hydrolysis and joining of the 60S ribosomal subunit (R-ATH-72706)	201	9	0.47	+	19.24	1.39E-09	2.11E-07
		Cellular response to heat stress (R-ATH-3371556)	114	5	0.27	+	18.85	8.57E-06	3.82E-04
		SRP-dependent cotranslational protein targeting to membrane (R-ATH-1799339)	206	9	0.48	+	18.77	1.72E-09	2.17E-07
		Nonsense Mediated Decay (NMD) independent of the Exon Junction Complex (EJC) (R-ATH-975956)	210	9	0.49	+	18.42	2.02E-09	2.18E-07
		Formation of a pool of free 40S subunits (R-ATH-72689)	220	9	0.51	+	17.58	2.98E-09	2.83E-07
		Nonsense Mediated Decay (NMD) enhanced by the Exon Junction Complex (EJC) (R-ATH-975957)	227	9	0.53	+	17.04	3.88E-09	3.27E-07
		Nonsense-Mediated Decay (NMD) (R-ATH-927802)	227	9	0.53	+	17.04	3.88E-09	2.94E-07
		L13a-mediated translational silencing of Ceruloplasmin expression (R-ATH-156827)	233	9	0.54	+	16.6	4.83E-09	3.33E-07
		Cap-dependent Translation Initiation (R-ATH-72737)	241	9	0.56	+	16.05	6.41E-09	4.05E-07
		Eukaryotic Translation Initiation (R-ATH-72613)	247	9	0.57	+	15.66	7.88E-09	4.59E-07
		Cellular responses to stress (R-ATH-2262752)	192	6	0.45	+	13.43	6.75E-06	3.20E-04
		Gene Expression (R-ATH-74160)	741	18	1.72	+	10.44	7.47E-14	2.83E-11
		Metabolism of proteins (R-ATH-392499)	696	15	1.62	+	9.26	6.35E-11	1.61E-08
		Unclassified (UNCLASSIFIED)	24272	39	56.48	-	0.69	2.25E-08	1.22E-06
dTALE-ChAP trial 2	**Cellular Component**	Analysis Type:	PANTHER Overrepresentation Test (Released 20171205)						
		Annotation Version and Release Date:	GO Ontology database Released 2018-06-01						
		Analyzed List:	upload_1 (Arabidopsis thaliana)						
		Reference List:	Arabidopsis thaliana (all genes in database)						
		Test Type:	FISHER						
		GO cellular component complete	Arabidopsis thaliana - REFLIST (27502)	upload_1 (41)	upload_1 (expected)	upload_1 (over/under)	upload_1 (fold Enrichment)	upload_1 (raw P-value)	upload_1 (FDR)
		nucleosome (GO:0000786)	47	8	0.07	+	> 100	1.35E-14	3.58E-12
		DNA packaging complex (GO:0044815)	51	8	0.08	+	> 100	2.45E-14	5.20E-12
		U4 snRNP (GO:0005687)	13	2	0.02	+	> 100	2.24E-04	6.62E-03

		protein-DNA complex (GO:0032993)	83	8	0.12	+	64.65	9.06E-13	1.60E-10
		U5 snRNP (GO:0005682)	21	2	0.03	+	63.88	5.36E-04	1.39E-02
		U1 snRNP (GO:0005685)	27	2	0.04	+	49.69	8.56E-04	2.17E-02
		U2 snRNP (GO:0005686)	37	2	0.06	+	36.26	1.55E-03	3.82E-02
		nuclear chromatin (GO:0000790)	79	4	0.12	+	33.96	7.13E-06	2.53E-04
		spliceosomal tri-snRNP complex (GO:0097526)	42	2	0.06	+	31.94	1.97E-03	4.64E-02
		chromatin (GO:0000785)	170	8	0.25	+	31.57	2.07E-10	1.37E-08
		small nucleolar ribonucleoprotein complex (GO:0005732)	43	2	0.06	+	31.2	2.06E-03	4.75E-02
		cytosolic large ribosomal subunit (GO:0022625)	147	5	0.22	+	22.82	3.06E-06	1.12E-04
		nucleolus (GO:0005730)	445	15	0.66	+	22.61	7.46E-17	7.93E-14
		nuclear chromosome part (GO:0044454)	161	4	0.24	+	16.67	1.06E-04	3.51E-03
		cytosolic ribosome (GO:0022626)	324	8	0.48	+	16.56	2.77E-08	1.40E-06
		large ribosomal subunit (GO:0015934)	204	5	0.3	+	16.44	1.44E-05	4.93E-04
		chromosomal part (GO:0044427)	333	8	0.5	+	16.11	3.40E-08	1.64E-06
		nuclear chromosome (GO:0000228)	174	4	0.26	+	15.42	1.42E-04	4.56E-03
		cytosolic part (GO:0044445)	372	8	0.55	+	14.43	7.83E-08	3.47E-06
		chromosome (GO:0005694)	386	8	0.58	+	13.9	1.03E-07	4.39E-06
		ribosomal subunit (GO:0044391)	340	7	0.51	+	13.81	7.38E-07	2.80E-05
		spliceosomal complex (GO:0005681)	151	3	0.23	+	13.33	1.56E-03	3.78E-02
		ribosome (GO:0005840)	469	8	0.7	+	11.44	4.42E-07	1.74E-05
		nuclear lumen (GO:0031981)	1053	16	1.57	+	10.19	9.82E-13	1.49E-10
		plasmodesma (GO:0009506)	1011	15	1.51	+	9.95	8.54E-12	8.25E-10
		symplast (GO:0055044)	1011	15	1.51	+	9.95	8.54E-12	7.56E-10
		cell-cell junction (GO:0005911)	1013	15	1.51	+	9.93	8.78E-12	7.18E-10
		cell junction (GO:0030054)	1013	15	1.51	+	9.93	8.78E-12	6.66E-10
		ribonucleoprotein complex (GO:1990904)	811	12	1.21	+	9.93	1.67E-09	9.84E-08
		intracellular organelle lumen (GO:0070013)	1279	17	1.91	+	8.92	1.27E-12	1.69E-10
		membrane-enclosed lumen (GO:0031974)	1279	17	1.91	+	8.92	1.27E-12	1.50E-10
		organelle lumen (GO:0043233)	1279	17	1.91	+	8.92	1.27E-12	1.35E-10
		intracellular non-membrane-bounded organelle (GO:0043232)	1670	22	2.49	+	8.84	1.53E-16	8.12E-14
		non-membrane-bounded organelle (GO:0043228)	1670	22	2.49	+	8.84	1.53E-16	5.42E-14
		nuclear part (GO:0044428)	1396	16	2.08	+	7.69	6.38E-11	4.52E-09
		vacuole (GO:0005773)	1114	12	1.66	+	7.23	5.41E-08	2.50E-06
		vacuolar membrane (GO:0005774)	650	6	0.97	+	6.19	3.94E-04	1.10E-02
		vacuolar part (GO:0044437)	652	6	0.97	+	6.17	4.01E-04	1.09E-02

		external encapsulating structure (GO:0030312)	777	7	1.16	+	6.04	1.43E-04	4.46 E-03
		cell wall (GO:0005618)	777	7	1.16	+	6.04	1.43E-04	4.33 E-03
		protein-containing complex (GO:0032991)	3150	21	4.7	+	4.47	4.86E-10	3.04 E-08
		cytosol (GO:0005829)	2261	15	3.37	+	4.45	4.37E-07	1.79 E-05
		intracellular organelle part (GO:0044446)	5417	25	8.08	+	3.1	8.58E-09	4.80 E-07
		organelle part (GO:0044422)	5424	25	8.09	+	3.09	8.82E-09	4.69 E-07
		plasma membrane (GO:0005886)	3881	15	5.79	+	2.59	2.91E-04	8.37 E-03
		cell periphery (GO:0071944)	4525	16	6.75	+	2.37	4.67E-04	1.24 E-02
	Protein Class	Analysis Type:	PANTHER Overrepresentation Test (Released 20171205)						
		Annotation Version and Release Date:	PANTHER version 13.1 Released 2018-02-03						
		Analyzed List:	upload_1 (Arabidopsis thaliana)						
		Reference List:	Arabidopsis thaliana (all genes in database)						
		Test Type:	FISHER						
		PANTHER Protein Class	Arabidopsis thaliana - REFLIST (27502)	upload_1 (41)	upload_1 (expected)	upload_1 (over/under)	upload_1 (fold Enrichment)	upload_1 (raw P-value)	upload_1 (FDR)
		histone (PC00118)	11	3	0.02	+	> 100	1.10E-06	4.85 E-05
		translation elongation factor (PC00222)	44	4	0.07	+	60.98	7.84E-07	4.60 E-05
		G-protein (PC00020)	95	4	0.14	+	28.24	1.44E-05	5.05 E-04
		translation initiation factor (PC00224)	96	4	0.14	+	27.95	1.49E-05	4.38 E-04
		translation factor (PC00223)	138	4	0.21	+	19.44	5.91E-05	1.49 E-03
		mRNA splicing factor (PC00148)	150	3	0.22	+	13.42	1.53E-03	3.00 E-02
		ribosomal protein (PC00202)	322	5	0.48	+	10.42	1.21E-04	2.66 E-03
		RNA binding protein (PC00031)	1115	12	1.66	+	7.22	5.46E-08	4.81 E-06
		nucleic acid binding (PC00171)	1771	15	2.64	+	5.68	1.80E-08	3.17 E-06
	Molecular function	Analysis Type:	PANTHER Overrepresentation Test (Released 20171205)						
		Annotation Version and Release Date:	GO Ontology database Released 2018-06-01						
		Analyzed List:	upload_1 (Arabidopsis thaliana)						
		Reference List:	Arabidopsis thaliana (all genes in database)						
		Test Type:	FISHER						

		GO molecular function complete	Arabidopsis thaliana - REFLIST (27502)	upload_1 (41)	upload_1 (expected)	upload_1 (over/under)	upload_1 (fold Enrichment)	upload_1 (raw P-value)	upload_1 (FDR)
		nucleosomal DNA binding (GO:0031492)	9	2	0.01	+	> 100	1.18E-04	2.32E-02
		translation elongation factor activity (GO:0003746)	55	4	0.08	+	48.78	1.81E-06	7.14E-04
		scopolin beta-glucosidase activity (GO:0102483)	42	3	0.06	+	47.91	4.16E-05	1.09E-02
		protein heterodimerization activity (GO:0046982)	118	7	0.18	+	39.79	6.62E-10	2.09E-06
		beta-glucosidase activity (GO:0008422)	80	3	0.12	+	25.15	2.59E-04	4.53E-02
		translation factor activity, RNA binding (GO:0008135)	165	5	0.25	+	20.33	5.29E-06	1.67E-03
		rRNA binding (GO:0019843)	156	4	0.23	+	17.2	9.39E-05	1.97E-02
		GTPase activity (GO:0003924)	180	4	0.27	+	14.91	1.61E-04	2.98E-02
		structural constituent of ribosome (GO:0003735)	360	7	0.54	+	13.04	1.07E-06	5.63E-04
		mRNA binding (GO:0003729)	418	7	0.62	+	11.23	2.83E-06	9.92E-04
		protein dimerization activity (GO:0046983)	551	8	0.82	+	9.74	1.45E-06	6.53E-04
		structural molecule activity (GO:0005198)	530	7	0.79	+	8.86	1.30E-05	3.73E-03
		RNA binding (GO:0003723)	1457	13	2.17	+	5.99	1.17E-07	1.23E-04
		nucleic acid binding (GO:0003676)	4005	22	5.97	+	3.68	5.80E-09	9.14E-06
		protein binding (GO:0005515)	4369	17	6.51	+	2.61	8.39E-05	1.89E-02
		heterocyclic compound binding (GO:1901363)	6970	26	10.39	+	2.5	3.15E-07	2.48E-04
		organic cyclic compound binding (GO:0097159)	6991	26	10.42	+	2.49	3.36E-07	2.12E-04
		binding (GO:0005488)	11350	30	16.92	+	1.77	4.49E-05	1.09E-02
	Biological Process	Analysis Type:	PANTHER Overrepresentation Test (Released 20171205)						
		Annotation Version and Release Date:	GO Ontology database Released 2018-06-01						
		Analyzed List:	upload_1 (Arabidopsis thaliana)						
		Reference List:	Arabidopsis thaliana (all genes in database)						
		Test Type:	FISHER						
		GO biological process complete	Arabidopsis thaliana - REFLIST (27502)	upload_1 (41)	upload_1 (expected)	upload_1 (over/under)	upload_1 (fold Enrichment)	upload_1 (raw P-value)	upload_1 (FDR)
		response to symbiotic fungus (GO:0009610)	12	2	0.02	+	> 100	1.95E-04	3.95E-02
		response to symbiont (GO:0009608)	14	2	0.02	+	95.83	2.56E-04	4.57E-02
		nucleosome assembly (GO:0006334)	40	4	0.06	+	67.08	5.49E-07	5.40E-04
		chromatin assembly (GO:0031497)	48	4	0.07	+	55.9	1.09E-06	8.00E-04
		nucleosome organization (GO:0034728)	53	4	0.08	+	50.62	1.58E-06	1.03E-03

		chromatin assembly or disassembly (GO:0006333)	61	4	0.09	+	43.99	2.68E-06	1.58E-03
		DNA packaging (GO:0006323)	63	4	0.09	+	42.59	3.03E-06	1.62E-03
		chromatin silencing (GO:0006342)	54	3	0.08	+	37.27	8.47E-05	2.17E-02
		translational elongation (GO:0006414)	73	4	0.11	+	36.76	5.29E-06	2.60E-03
		protein-DNA complex assembly (GO:0065004)	75	4	0.11	+	35.77	5.86E-06	2.66E-03
		negative regulation of gene expression, epigenetic (GO:0045814)	58	3	0.09	+	34.7	1.04E-04	2.55E-02
		protein-DNA complex subunit organization (GO:0071824)	93	4	0.14	+	28.85	1.32E-05	4.88E-03
		DNA conformation change (GO:0071103)	115	4	0.17	+	23.33	2.96E-05	8.74E-03
		mRNA splicing, via spliceosome (GO:0000398)	180	4	0.27	+	14.91	1.61E-04	3.51E-02
		RNA splicing, via transesterification reactions with bulged adenosine as nucleophile (GO:0000377)	197	4	0.29	+	13.62	2.26E-04	4.29E-02
		RNA splicing, via transesterification reactions (GO:0000375)	197	4	0.29	+	13.62	2.26E-04	4.16E-02
		chromatin organization (GO:0006325)	359	7	0.54	+	13.08	1.05E-06	8.87E-04
		translation (GO:0006412)	612	10	0.91	+	10.96	1.92E-08	1.13E-04
		peptide biosynthetic process (GO:0043043)	617	10	0.92	+	10.87	2.07E-08	6.09E-05
		amide biosynthetic process (GO:0043604)	693	10	1.03	+	9.68	6.04E-08	1.19E-04
		peptide metabolic process (GO:0006518)	707	10	1.05	+	9.49	7.26E-08	1.07E-04
		cellular protein-containing complex assembly (GO:0034622)	495	7	0.74	+	9.49	8.42E-06	3.55E-03
		chromosome organization (GO:0051276)	529	7	0.79	+	8.88	1.29E-05	5.06E-03
		protein-containing complex assembly (GO:0065003)	541	7	0.81	+	8.68	1.49E-05	4.87E-03
		cellular amide metabolic process (GO:0043603)	847	10	1.26	+	7.92	3.77E-07	4.45E-04
		protein-containing complex subunit organization (GO:0043933)	632	7	0.94	+	7.43	3.96E-05	1.06E-02
		cellular component assembly (GO:0022607)	772	7	1.15	+	6.08	1.37E-04	3.11E-02
		organonitrogen compound biosynthetic process (GO:1901566)	1573	11	2.35	+	4.69	1.40E-05	4.85E-03
		organelle organization (GO:0006996)	1617	10	2.41	+	4.15	1.04E-04	2.46E-02
		gene expression (GO:0010467)	3226	15	4.81	+	3.12	3.50E-05	9.84E-03
		cellular protein metabolic process (GO:0044267)	3253	14	4.85	+	2.89	1.64E-04	3.46E-02
		cellular nitrogen compound metabolic process (GO:0034641)	4694	17	7	+	2.43	2.08E-04	4.08E-02
		cellular process (GO:0009987)	12311	32	18.35	+	1.74	2.27E-05	7.04E-03
	Reactome Pathway	Analysis Type:	PANTHER Overrepresentation Test (Released 20171205)						
		Annotation Version and Release Date:	Reactome version 58 Released 2016-12-07						

		Analyzed List:	upload_1 (Arabidopsis thaliana)						
		Reference List:	Arabidopsis thaliana (all genes in database)						
		Test Type:	FISHER						
		Reactome pathways	Arabidopsis thaliana - REFLIST (27502)	upload_1 (41)	upload_1 (expected)	upload_1 (over/under)	upload_1 (fold Enrichment)	upload_1 (raw P-value)	upload_1 (FDR)
		Eukaryotic Translation Elongation (R-ATH-156842)	12	4	0.02	+	> 100	7.59E-09	5.75E-06
		HSF1 activation (R-ATH-3371511)	49	4	0.07	+	54.76	1.17E-06	2.22E-04
		mRNA Splicing - Minor Pathway (R-ATH-72165)	77	3	0.11	+	26.13	2.32E-04	2.20E-02
		Cellular response to heat stress (R-ATH-3371556)	114	4	0.17	+	23.54	2.87E-05	3.62E-03
		Translation (R-ATH-72766)	276	8	0.41	+	19.44	8.24E-09	3.12E-06
		Cellular responses to stress (R-ATH-2262752)	192	4	0.29	+	13.97	2.05E-04	2.22E-02
		GTP hydrolysis and joining of the 60S ribosomal subunit (R-ATH-72706)	201	4	0.3	+	13.35	2.43E-04	2.05E-02
		SRP-dependent cotranslational protein targeting to membrane (R-ATH-1799339)	206	4	0.31	+	13.02	2.67E-04	2.02E-02
		Nonsense Mediated Decay (NMD) independent of the Exon Junction Complex (EJC) (R-ATH-975956)	210	4	0.31	+	12.78	2.86E-04	1.97E-02
		Formation of a pool of free 40S subunits (R-ATH-72689)	220	4	0.33	+	12.2	3.41E-04	2.15E-02
		Nonsense Mediated Decay (NMD) enhanced by the Exon Junction Complex (EJC) (R-ATH-975957)	227	4	0.34	+	11.82	3.83E-04	2.23E-02
		Nonsense-Mediated Decay (NMD) (R-ATH-927802)	227	4	0.34	+	11.82	3.83E-04	2.07E-02
		L13a-mediated translational silencing of Ceruloplasmin expression (R-ATH-156827)	233	4	0.35	+	11.52	4.22E-04	2.13E-02
		Cap-dependent Translation Initiation (R-ATH-72737)	241	4	0.36	+	11.13	4.78E-04	2.26E-02
		Eukaryotic Translation Initiation (R-ATH-72613)	247	4	0.37	+	10.86	5.23E-04	2.33E-02
		Gene Expression (R-ATH-74160)	741	11	1.1	+	9.96	8.75E-09	2.21E-06
		Metabolism of proteins (R-ATH-392499)	696	8	1.04	+	7.71	7.93E-06	1.20E-03
dTALE ChAP trial 3	**Cellular component**	Analysis Type:	PANTHER Overrepresentation Test (Released 20171205)						
		Annotation Version and Release Date:	GO Ontology database Released 2018-06-01						
		Analyzed List:	upload_1 (Arabidopsis thaliana)						
		Reference List:	Arabidopsis thaliana (all genes in database)						
		Test Type:	FISHER						
		GO cellular component complete	Arabidopsis thaliana - REFLIST (27502)	upload_1 (45)	upload_1 (expected)	upload_1 (over/under)	upload_1 (fold Enrichment)	upload_1 (raw P-value)	upload_1 (FDR)

		nucleosome (GO:0000786)	47	6	0.08	+	78.02	2.91E-10	1.55 E-07
		DNA packaging complex (GO:0044815)	51	6	0.08	+	71.9	4.58E-10	1.62 E-07
		protein-DNA complex (GO:0032993)	83	6	0.14	+	44.18	7.05E-09	1.87 E-06
		nuclear chromatin (GO:0000790)	79	3	0.13	+	23.21	3.30E-04	1.40 E-02
		chromatin (GO:0000785)	170	6	0.28	+	21.57	4.14E-07	2.93 E-05
		nucleolus (GO:0005730)	445	11	0.73	+	15.11	1.39E-10	1.47 E-07
		chromosomal part (GO:0044427)	333	6	0.54	+	11.01	1.81E-05	1.13 E-03
		chromosome (GO:0005694)	386	6	0.63	+	9.5	4.07E-05	2.16 E-03
		plant-type cell wall (GO:0009505)	380	5	0.62	+	8.04	4.01E-04	1.52 E-02
		plasmodesma (GO:0009506)	1011	12	1.65	+	7.25	5.98E-08	9.08 E-06
		symplast (GO:0055044)	1011	12	1.65	+	7.25	5.98E-08	7.94 E-06
		cell-cell junction (GO:0005911)	1013	12	1.66	+	7.24	6.11E-08	7.21 E-06
		cell junction (GO:0030054)	1013	12	1.66	+	7.24	6.11E-08	6.49 E-06
		nuclear lumen (GO:0031981)	1053	12	1.72	+	6.96	9.26E-08	7.03 E-06
		external encapsulating structure (GO:0030312)	777	8	1.27	+	6.29	3.56E-05	2.10 E-03
		cell wall (GO:0005618)	777	8	1.27	+	6.29	3.56E-05	1.99 E-03
		intracellular organelle lumen (GO:0070013)	1279	13	2.09	+	6.21	8.97E-08	8.67 E-06
		membrane-enclosed lumen (GO:0031974)	1279	13	2.09	+	6.21	8.97E-08	7.95 E-06
		organelle lumen (GO:0043233)	1279	13	2.09	+	6.21	8.97E-08	7.34 E-06
		intracellular non-membrane-bounded organelle (GO:0043232)	1670	15	2.73	+	5.49	3.55E-08	7.54 E-06
		non-membrane-bounded organelle (GO:0043228)	1670	15	2.73	+	5.49	3.55E-08	6.28 E-06
		ribonucleoprotein complex (GO:1990904)	811	7	1.33	+	5.28	3.37E-04	1.38 E-02
		nuclear part (GO:0044428)	1396	12	2.28	+	5.25	1.81E-06	1.20 E-04
		vacuole (GO:0005773)	1114	9	1.82	+	4.94	7.09E-05	3.59 E-03
		protein-containing complex (GO:0032991)	3150	14	5.15	+	2.72	3.53E-04	1.39 E-02
		plasma membrane (GO:0005886)	3881	16	6.35	+	2.52	2.71E-04	1.20 E-02
		cell periphery (GO:0071944)	4525	17	7.4	+	2.3	7.90E-04	2.90 E-02
		intracellular organelle part (GO:0044446)	5417	20	8.86	+	2.26	1.94E-04	9.38 E-03
		organelle part (GO:0044422)	5424	20	8.87	+	2.25	1.96E-04	9.06 E-03
	Protein Class	Analysis Type:	PANTHER Overrepresentation Test (Released 20171205)						
		Annotation Version and Release Date:	PANTHER version 13.1 Released 2018-02-03						
		Analyzed List:	upload_1 (Arabidopsis thaliana)						

		Reference List:	Arabidopsis thaliana (all genes in database)						
		Test Type:	FISHER						
		PANTHER Protein Class	Arabidopsis thaliana - REFLIST (27502)	upload_1 (45)	upload_1 (expected)	upload_1 (over/under)	upload_1 (fold Enrichment)	upload_1 (raw P-value)	upload_1 (FDR)
		histone (PC00118)	11	2	0.02	+	> 100	2.01E-04	5.06E-03
		translation elongation factor (PC00222)	44	5	0.07	+	69.45	1.67E-08	2.94E-06
		G-protein (PC00020)	95	4	0.16	+	25.73	2.09E-05	7.35E-04
		translation initiation factor (PC00224)	96	4	0.16	+	25.46	2.17E-05	6.37E-04
		translation factor (PC00223)	138	5	0.23	+	22.14	3.63E-06	3.20E-04
		RNA binding protein (PC00031)	1115	10	1.82	+	5.48	1.07E-05	6.30E-04
		nucleic acid binding (PC00171)	1771	12	2.9	+	4.14	2.02E-05	8.88E-04
	Molecular Function	Analysis Type:	PANTHER Overrepresentation Test (Released 20171205)						
		Annotation Version and Release Date:	GO Ontology database Released 2018-06-01						
		Analyzed List:	upload_1 (Arabidopsis thaliana)						
		Reference List:	Arabidopsis thaliana (all genes in database)						
		Test Type:	FISHER						
		GO molecular function complete	Arabidopsis thaliana - REFLIST (27502)	upload_1 (45)	upload_1 (expected)	upload_1 (over/under)	upload_1 (fold Enrichment)	upload_1 (raw P-value)	upload_1 (FDR)
		nucleosomal DNA binding (GO:0031492)	9	2	0.01	+	> 100	1.42E-04	4.07E-02
		translation elongation factor activity (GO:0003746)	55	4	0.09	+	44.45	2.65E-06	1.39E-03
		protein heterodimerization activity (GO:0046982)	118	6	0.19	+	31.08	5.20E-08	8.19E-05
		rRNA binding (GO:0019843)	156	5	0.26	+	19.59	6.48E-06	2.55E-03
		translation factor activity, RNA binding (GO:0008135)	165	4	0.27	+	14.82	1.67E-04	4.40E-02
		mRNA binding (GO:0003729)	418	7	0.68	+	10.23	5.42E-06	2.44E-03
		protein dimerization activity (GO:0046983)	551	7	0.9	+	7.76	3.14E-05	9.89E-03
		RNA binding (GO:0003723)	1457	14	2.38	+	5.87	5.04E-08	1.59E-04
		nucleic acid binding (GO:0003676)	4005	22	6.55	+	3.36	5.36E-08	5.63E-05
		heterocyclic compound binding (GO:1901363)	6970	28	11.4	+	2.46	1.99E-07	1.57E-04
		organic cyclic compound binding (GO:0097159)	6991	28	11.44	+	2.45	2.13E-07	1.34E-04
		binding (GO:0005488)	11350	33	18.57	+	1.78	2.30E-05	8.04E-03
	Biological	Analysis Type:	PANTHER Overrepresentatio						

	Process		n Test (Released 20171205)						
		Annotation Version and Release Date:	GO Ontology database Released 2018-06-01						
		Analyzed List:	upload_1 (Arabidopsis thaliana)						
		Reference List:	Arabidopsis thaliana (all genes in database)						
		Test Type:	FISHER						
		GO biological process complete	Arabidopsis thaliana - REFLIST (27502)	upload_1 (45)	upload_1 (expected)	upload_1 (over/under)	upload_1 (fold Enrichment)	upload_1 (raw P-value)	upload_1 (FDR)
		translational elongation (GO:0006414)	73	4	0.12	+	33.49	7.71E-06	7.57E-03
		response to cytokinin (GO:0009735)	251	5	0.41	+	12.17	6.01E-05	4.43E-02
		translation (GO:0006412)	612	9	1	+	8.99	6.10E-07	3.59E-03
		peptide biosynthetic process (GO:0043043)	617	9	1.01	+	8.91	6.52E-07	1.92E-03
		amide biosynthetic process (GO:0043604)	693	9	1.13	+	7.94	1.68E-06	2.48E-03
		peptide metabolic process (GO:0006518)	707	9	1.16	+	7.78	1.98E-06	2.33E-03
		cellular amide metabolic process (GO:0043603)	847	10	1.39	+	7.22	9.58E-07	1.88E-03
		organonitrogen compound biosynthetic process (GO:1901566)	1573	11	2.57	+	4.27	3.63E-05	3.06E-02
	Reactome Pathway	Analysis Type:	PANTHER Overrepresentation Test (Released 20171205)						
		Annotation Version and Release Date:	Reactome version 58 Released 2016-12-07						
		Analyzed List:	upload_1 (Arabidopsis thaliana)						
		Reference List:	Arabidopsis thaliana (all genes in database)						
		Test Type:	FISHER						
		Reactome pathways	Arabidopsis thaliana - REFLIST (27502)	upload_1 (45)	upload_1 (expected)	upload_1 (over/under)	upload_1 (fold Enrichment)	upload_1 (raw P-value)	upload_1 (FDR)
		Eukaryotic Translation Elongation (R-ATH-156842)	12	4	0.02	+	> 100	1.11E-08	8.45E-06
		HSF1 activation (R-ATH-3371511)	49	4	0.08	+	49.89	1.72E-06	3.25E-04
		Cellular response to heat stress (R-ATH-3371556)	114	4	0.19	+	21.44	4.16E-05	5.26E-03
		Translation (R-ATH-72766)	276	8	0.45	+	17.71	1.79E-08	6.79E-06
		Cellular responses to stress (R-ATH-2262752)	192	4	0.31	+	12.73	2.95E-04	3.19E-02
		GTP hydrolysis and joining of the 60S ribosomal subunit (R-ATH-72706)	201	4	0.33	+	12.16	3.49E-04	3.31E-02
		SRP-dependent cotranslational protein targeting to membrane (R-ATH-1799339)	206	4	0.34	+	11.87	3.83E-04	3.22E-02

		Nonsense Mediated Decay (NMD) independent of the Exon Junction Complex (EJC) (R-ATH-975956)	210	4	0.34	+	11.64	4.11E-04	3.12 E-02
		Formation of a pool of free 40S subunits (R-ATH-72689)	220	4	0.36	+	11.11	4.88E-04	3.36 E-02
		Nonsense Mediated Decay (NMD) enhanced by the Exon Junction Complex (EJC) (R-ATH-975957)	227	4	0.37	+	10.77	5.48E-04	3.46 E-02
		Nonsense-Mediated Decay (NMD) (R-ATH-927802)	227	4	0.37	+	10.77	5.48E-04	3.20 E-02
		L13a-mediated translational silencing of Ceruloplasmin expression (R-ATH-156827)	233	4	0.38	+	10.49	6.03E-04	3.27 E-02
		Cap-dependent Translation Initiation (R-ATH-72737)	241	4	0.39	+	10.14	6.83E-04	3.45 E-02
		Eukaryotic Translation Initiation (R-ATH-72613)	247	4	0.4	+	9.9	7.48E-04	3.54 E-02
		Gene Expression (R-ATH-74160)	741	10	1.21	+	8.25	2.88E-07	7.27 E-05
		Metabolism of proteins (R-ATH-392499)	696	8	1.14	+	7.02	1.63E-05	2.48 E-03

Danksagungen

Ich möchte mich zuallererst bei Klaus Harter bedanken, der mir die Möglichkeit gegeben hat, in seiner Arbeitsgruppe meine Doktorarbeit zu schreiben. Ich möchte mich für das entgegen gebrachte Vertrauen, die Unterstützung und die vielen aufmunternden Worte bedanken. Vor allem, dass er nach wie vor an das Projekt geglaubt hat, egal welcher Stein über den Weg gerollt kam. Des weiteren möchte ich mich bei Thomas Lahaye, sowie dem anderen Mitglied meines Promotionskomitees Frederic Brunner bedanken, für die großartige Unterstützung und hilfreichen Hinweise.

Ich danke Allen, die mit ihrer Expertise während des Projektes zugearbeitet haben und hervorragende Kollaborationspartner waren. Insbesondere seien hier Waltraud Schulze und Xuna Wu für ihre Hilfe bei den MS Experimenten, sowie Robert Morbitzer für die Klonierung der dTALEs erwähnt.

Ein riesen Dankeschön gilt einer Person, ohne die dieses Projekt nicht möglich gewesen wäre: Luise Brand. Luise, ohne dich wäre ich jetzt nicht da wo ich jetzt bin. Du warst ein hervorragender Gegenpol, hast mich immer wieder in Spur gebracht und auf Kurs gehalten. Ohne dich hätte ich das nicht geschafft!

Ich möchte mich bei allen Kollegen des ZMBPs, der Pflanzenphysiologie vor Allem bei den aktuellen und alten Mitgliedern von Bay 6-8 bedanken. Ihr habt meine Zeit hier unvergesslich gemacht. Vielen Dank an Brigitte und das Gärtnerei Team. Anne und Rebecca, nun hat es auch der letzte der alten Riege fast geschafft, vielen Dank euch zwei. Danke Juan, Nina klein, Nina groß, Andi, Sachie, Heunes (Quallenmann), Üner, Fredi, Nata, Angela, Claudi, Nilles, Thomas, Rosa, Lydia, Sabine und Lisa. Ich hatte viel Spaß mit euch.

Der letzte Absatz gilt meiner Familie, meinen Eltern und Großeltern und natürlich auch meinen Freunden. Vielen Dank für fortwährende Unterstützung, das Ertragen schlechter Launen und die ein oder andere finanzielle Spritze.

Mama & Papa danke, dass ihr mir immer den Rücken freigehalten habt und mich immer in meinen Vorhaben unterstützt habt.

Und jetzt von ganzem Herzen: Endlich fertig!